



Engaging the Immune System in the Fight Against Cancer

Lisanne Noordam

Engaging the Immune System in the Fight Against Cancer

Benutten van het immuunsysteem bij de strijd tegen
kanker

Lisanne Noordam

The work described in this thesis was conducted at the Department of Gastroenterology and Hepatology, Erasmus MC Rotterdam, the Netherlands.

Erasmus MC provided financial support for the printing of this thesis.

Layout: Lianne Noordam

Printing: ProefschriftMaken | www.proefschriftmaken.nl

ISBN: 978-94-6469-345-4

© Lianne Noordam. 2023. All rights reserved. No part of this thesis may be reproduced in any form without prior written permission of the author.

Engaging the Immune System in the Fight Against Cancer

Benutten van het immuunsysteem bij de strijd tegen
kanker

Proefschrift

ter verkrijging van de graad van doctor aan de
Erasmus Universiteit Rotterdam
op gezag van de
rector magnificus

Prof. dr. A.L. Bredenoord

en volgens het besluit van het College voor Promoties.

De openbare verdediging zal plaatsvinden op
dinsdag 20 juni 2023 om 13.00 uur

door

Lisanne Noordam
geboren te 's-Gravenhage

Promotiecomissie

Promotor Prof. dr. M.J. Bruno

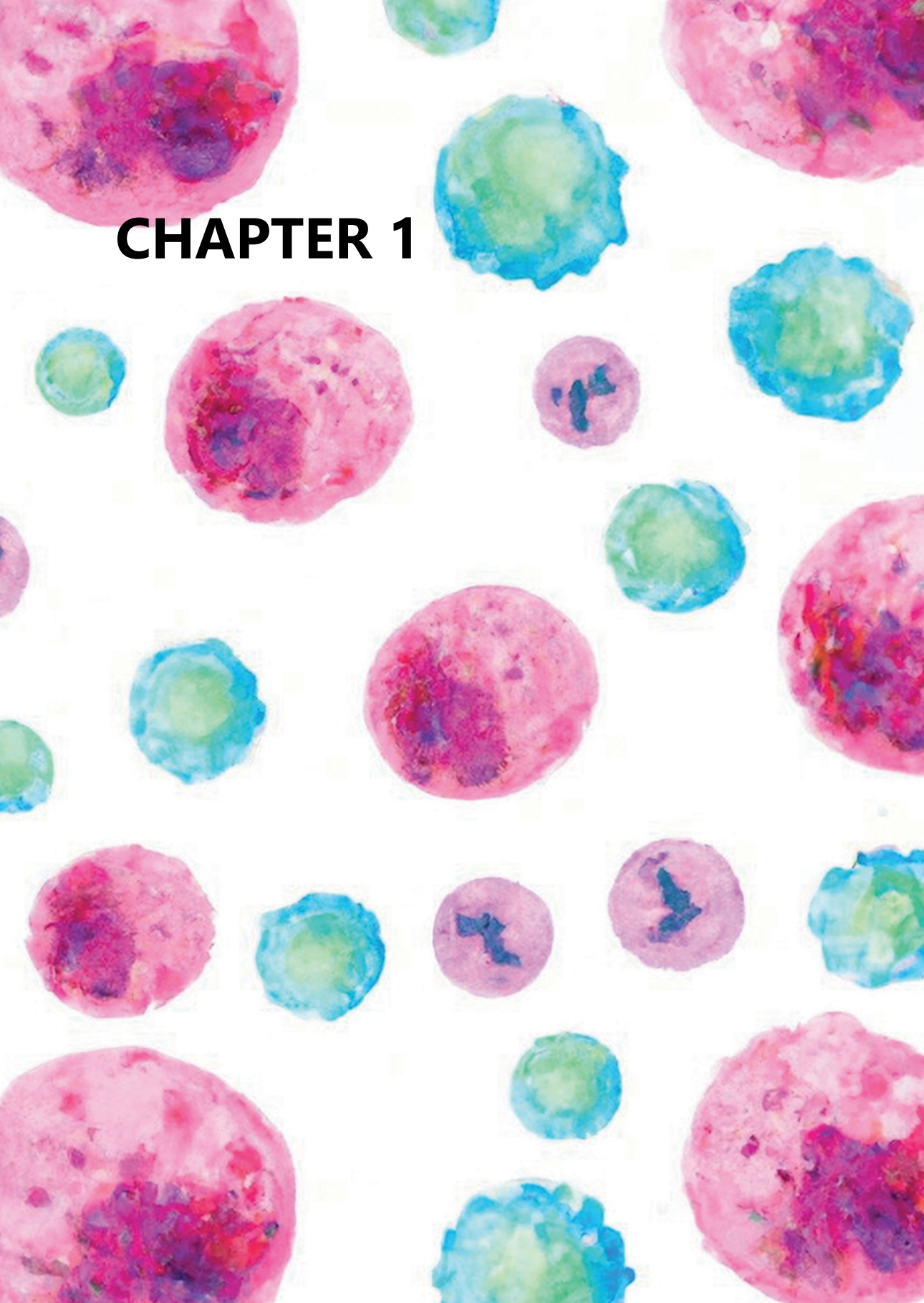
Overige leden Prof. dr. M.P. Peppelenbosch
Prof. dr. L.J.W. van der Laan
Dr. L.L. Kodach

Copromotor Dr. J. Kwekkeboom

TABLE OF CONTENTS

Chapter 1	Introduction	6
Targeting Immune Checkpoints in Cancer		
Chapter 2	Blockade of LAG3 enhances responses of tumor-infiltrating T cells in mismatch repair-proficient liver metastases of colorectal cancer	30
Chapter 3	A bispecific antibody targeting CD137 and PD-L1 boosts in vitro responses of T cells derived from gastro-intestinal carcinomas	66
Enhancing Tumor-Specific Immune Responses		
Chapter 4	Expression of Cancer Testis Antigens in tumor-adjacent normal liver is associated with post-resection recurrence of hepatocellular carcinoma	88
Chapter 5	Systemic T-cell and antibody responses against tumor-restricted cancer testis antigens in hepatocellular carcinoma patients	132
Tumor Microenvironment		
Chapter 6	Low-dose cyclophosphamide depletes circulating naïve and activated regulatory T cells in malignant pleural mesothelioma patients synergistically treated with dendritic-cell based immunotherapy	182
Chapter 7	Summary and Discussion	208
Chapter 8	Nederlandse samenvatting	220
Chapter 9	Abbreviations	228
	Word of thanks	232
	List of publications	236
	PhD portfolio	240
	Curriculum Vitae	242

CHAPTER 1



INTRODUCTION

Immunotherapie en het hepatocellulair carcinoom

L. Noordam, J. Kwekkeboom, R.A. de Man, D. Sprengers
NED TIJDSCHR ONCOL, Sept 2018, Vol. 15, No. 6: 210–17

*Parts of this chapter have been published as a review in Nederlands
Tijdschrift voor Oncologie.*

INTRODUCTION

I. Cancer

As of 2007, cancer is the leading cause of death in the Netherlands and, with 46,627 fatalities, it accounted for 30.4% of all deaths in 2018.¹ In the USA, cancer is the second leading cause of death with approximately 600,000 deaths annually.² Globally, non-communicable diseases (NCDs) are responsible for the majority of deaths, and cancer is expected to rank as the leading cause in the 21st century.³ The epidemiology of cancer is continually changing due to demographic changes including aging and population growth, changes in risk factors such as smoking and obesity, and the improvement in the detection and treatment of cancer. The changes in incidence and prevalence are unique for every histological subtype of cancer and vary substantially. Generally, the total number of cancer cases and deaths continues to increase due an aging and growing population, even for those cancers with declining age-standardized incidences and death rates.²

I a. Hepatocellular carcinoma

Globally, liver cancer is the sixth most diagnosed cancer type and the fourth leading cause of cancer related death. In the past 20 years the incidence has increased by 62% to over 750,000 new cases a year.³ Hepatocellular carcinoma (HCC) accounts for approximately 80% of liver cancer cases, intrahepatic cholangiocarcinoma for 10-15%, and other rare types account for the rest. The current treatment of HCC only leads to a modest survival benefit, manifested by the small difference between the annual incidence and mortality rate of liver cancer, globally 841,000 and 782,000 cases respectively.³ This is partially caused by the limited treatment modalities; classical chemotherapeutics have no effect and the use of radiotherapy is restricted by liver toxicity.⁴ Furthermore, most HCC patients are diagnosed with advanced disease and only a small percentage of patients qualifies for the potential curative treatments such as liver transplantation, surgical resection or radiofrequency ablation (RFA). Patients with advanced HCC are only eligible for locoregional or systemic therapies.⁴ Sorafenib, a tyrosine kinase inhibitor, and regorafenib, a multi-kinase inhibitor, are currently the only systemic treatments for HCC that have shown an effect extending patient survival with an average of 3 months.⁵

I b. Colorectal carcinoma

Colorectal carcinoma (CRC) is the third most common cause of cancer worldwide, with 1.8 million new cases each year. It is the second most common cause of cancer related death, with close to 900,000 deaths annually and is therefore accountable for 1 in 10 cancer-related deaths.³ The incidence is 3-fold higher in developed areas, however survival is also better, causing low variation in mortality rates among the world. Europe ranks in the top regions regarding incidence rates. Age is a major risk factor for sporadic CRC, as it is uncommon in people under 40. The incidence increases significantly between the ages of 40 and 50, after which it further increases in each succeeding decade.^{6,7}

Over the course of disease, more than 50% of CRC patients will develop metastatic disease in their liver, which eventually results in death for more than two thirds of these patients.^{8,9} Currently, hepatic

resection of liver metastases of CRC (LM-CRC) is the only curative treatment option for patients with isolated liver metastasis. However, even with adjuvant treatment, resection is curative in only 20% of patients.⁹

I c. Malignant Mesothelioma

Malignant mesothelioma is a rare and aggressive form of cancer. In 2018, 30,443 new cases were diagnosed and 25,576 deaths were reported worldwide.³ It arises from mesothelial surfaces of the pleural cavity, the peritoneal cavity, tunica vaginalis of the testes or the pericardium. Malignant pleural mesothelioma (MPM) is the most common type and is associated with asbestos exposure, usually after a long latency period.¹⁰ Global incidence has risen over the past decades and is predicted to have its peak in 2020. The prognosis is unfavorable. The median survival is 4-13 months without treatment¹¹ and 6-18 months for treated patients, regardless of the therapeutic approach.¹²⁻¹⁴ Due to its rarity there have been few prospective clinical trials and most knowledge has been gained from case series and pre-clinical research. In the last ten years no major breakthroughs have been reported and consequently systemic therapy has remained unchanged.¹⁵ Extensive investigations of the effects of implementation of radiotherapy and/or debulking surgery in standard treatment revealed variable success, but only when applied to select patient subgroups.¹⁶⁻¹⁸

Since traditional therapies yield unsatisfactory results in these three cancers, there is an urgent need for more effective therapies. Immunotherapy, in which a tumor-specific immune response is induced or stimulated, has gained momentum in the recent years and has been proven effective in the treatment of melanoma and lung cancer, amongst others,¹⁹ but research concerning its suitability for HCC, CRC and MPM is still in its infancy. Anti-tumor immune responses can be enhanced by stimulation of the tumor-specific immune response or by overcoming the immunosuppressive microenvironment. Besides immunotherapy, new molecular targeted therapies may potentially improve outcomes. Several targeted therapies, such as anti-angiogenic antibodies and small molecules, are currently under investigation.²⁰ In this thesis the focus is upon improving immunotherapeutic strategies and finding new targets for targeted therapies for these cancer types.

II. Tumor immune micro environment

Tumors are complex environments, composed of tumor cells, extracellular matrix (ECM), and supporting, non-malignant cells, such as stromal cells, endothelial cells and infiltrating immune cells. The tumor microenvironment is largely orchestrated by the immune cells, and is indispensable in tumor formation, as it promotes and contributes to survival, angiogenesis, genomic instability, proliferation and eventually migration of tumor cells.^{21, 22} Chronic inflammation is a hallmark of cancer, and at least 25% of cancers develop in chronically inflamed tissues caused by autoimmunity or viral infections.^{21, 23} For example, hepatitis B and C virus infections induce chronic liver inflammation which can eventually lead to development of HCC, with lifetime risk being as high as 38% in men infected with both hepatitis B and C.^{24, 25} Patients with a chronic inflammatory bowel disease (IBD), and thus chronic inflammation, have

an increased risk for CRC development,²⁶ accounting for approximately 15% of deaths in IBD patients.²⁷ Similarly, mesothelioma is caused by chronic inflammation induced by persistent asbestos fibers, and exposure to asbestos leads to a 4.5-10% lifetime risk of developing malignant mesothelioma.^{14, 28}

Once tumors have formed, the immune system tries to combat tumor growth. High numbers of tumor-infiltrating lymphocytes, particularly CD8⁺ cytotoxic T cells (CTLs), are associated with improved disease outcome in various histological subtypes of cancer. However, accumulation of immunosuppressive cells, such as MDSCs and Tregs, in the tumors disrupt the capacity of CTLs to effectively control cancer growth.²⁹⁻³¹ Moreover, tumor cells appropriate some of the signaling molecules of both the innate and adaptive immune system, such as co-inhibitory immune checkpoints, chemokines and their receptors for immune resistance, tissue invasion, migration and metastasis. During tumor formation, the tissue architecture evolves into a highly specialized microenvironment characterized by chronic inflammation and a corrupted ECM and chronic inflammation.²¹

In the next paragraphs, after detailing the function of immune checkpoint pathways, the immunosuppressive mechanisms exploited by the tumor micro environment of the three tumors studied will be described.

Ila. Immune checkpoint pathways

Inhibitory immune checkpoint pathways play a role in the prevention of undesired T cell activation. They maintain immune responses within a physiological range and protect the host against autoimmunity. Stimulatory immune checkpoints have the opposite effect and activation of these molecules leads to T cell activation and differentiation to induce an effective T cell response.³² After T cell receptor (TCR) signaling, induced by recognition of an antigenic peptide in a Major Histocompatibility Complex (MHC) molecule on an antigen presenting cell (APC), interactions between co-stimulatory and co-inhibitory receptors on T cells and their ligands on the APC play critical roles in T cell priming and activation, and in modulation of T cell differentiation, effector function and survival (**Figure 1A**).³³

The most well-known co-stimulatory receptors on T cells are CD28, 4-1BB (CCD137), OX40 (CD134) and glucocorticoid-induced TNFR-related protein (GITR). Activation of these molecules leads to proliferation, differentiation, survival, cytotoxic function and cytokine production of T cells. The most well-known inhibitory receptors include programmed death receptor-1 (PD-1), cytotoxic T-lymphocyte-associated protein-4 (CTLA-4), lymphocyte-activation gene 3 (LAG3) and T cell immunoglobulin and mucin-domain containing 3 (TIM3), which cause inhibition of the T cell cycle and effector function, immune tolerance, exhaustion and apoptosis upon binding to their respective ligands (**Figure 1A**).³⁴

Ilb. The immunosuppressive tumor micro environment of HCC

The majority of HCC tumors arise in an inflamed liver, either due to chronic infection with hepatitis B or C virus or alcoholic or non-alcoholic steatohepatitis (NASH). HCC, therefore, can be considered a classical inflammation-induced cancer with some exceptions.³⁵ The intra-hepatic chronic inflammatory processes promote hepatocarcinogenesis, as has been shown in mice with NASH.³⁶ Prevention of HBV infection

by vaccination has shown to dramatically decrease the number of HCC diagnoses in Taiwan.³⁷ Once a tumor has established itself in the liver, it induces complementary immunosuppressive mechanisms to evade immune control. By downregulation of MHC class I molecules on the tumor cells and reduced efficacy of antigen procession by APCs, the chance of T cell recognition is diminished.³⁸ The tumor also attracts or induces intra-tumoral differentiation of immune suppressive cell populations, such as Tregs and myeloid derived suppressor cells (MDSCs), that, in turn, limit the anti-tumor responses of natural killer (NK) cells, CD4⁺ T helper (Th) cells and CTL in the tumor micro-environment.³⁵ Additionally the co-inhibitory pathways are reinforced; expression of CTLA-4, PD-1, LAG-3 and TIM-3 on tumor-infiltrating T cells and their ligands on APC and tumor cells are induced and play an important role in the inhibition of T cell reactivity in liver tumors³⁹

Ilc. The immunosuppressive tumor micro environment of CRC

Colorectal carcinogenesis is a multi-step process involving the accumulation of genetic alterations over time that ultimately leads to neoplastic growth. Immune cells are less involved in the initial oncogenesis.⁴⁰ Genetic mutations in the adenomatous polyposis coli (APC)/ β -catenin pathway are a key event and drive the development of sporadic CRC.⁴¹ Consecutive abnormal Wnt signaling leads to early adenomas and eventually mutations in oncogenes and tumor suppressors leading to the formation of advanced adenomas and CRC.⁴¹ This process promotes immune infiltration of cells of both the innate and adaptive immune system.⁴² The initial anti-tumor immune responses are then converted into an immunosuppressive response, which leads to tumor escape.⁴² This immunosuppressive environment is characterized by Tregs and MDSCs and the activation of the PD-1 and CTLA-4 pathway.⁴³

Approximately 15% of CRCs are mismatch repair (MMR) deficient.^{44, 45} These tumors are characterized by a high mutational load due to a defective mismatch repair mechanism, display higher infiltration of activated CTLs and Th1 cells, and show increased intra-tumoral interferon-gamma (IFN γ) production compared to MMR-proficient CRCs. This immune activation is counterbalanced by upregulation of immune checkpoint pathways, including PD-1, PD-L1, PD-L2, CTLA-4, TIM-3, LAG3, B and T lymphocyte attenuator (BTLA) and indoleamine 2,3-dioxygenase (IDO).⁴⁶⁻⁴⁸

Compared to the primary tumors, LM-CRC are less frequently MMR deficient.⁴⁹ They are generally characterized by more CTL infiltration compared to primary CRC, especially at the invasive margin of the tumor, but the numbers of T-cells surrounding the tumors and in the tumor centers are strongly variable between individual patients.⁵⁰⁻⁵² Additionally, we have previously shown that both CTL and Th are functionally impaired.⁵³ The role of immune checkpoint pathways in LM-CRC has not been studied yet.

IId. The immunosuppressive tumor micro-environment of MPM

Asbestos carcinogenesis is driven by a chronic inflammation, induced by the deposition and persistence of the asbestos fibers.⁵⁴ Inflammatory cells, in particular macrophages, play an important role in this process: promoting inflammation by releasing mutagenic reactive oxygen species and various

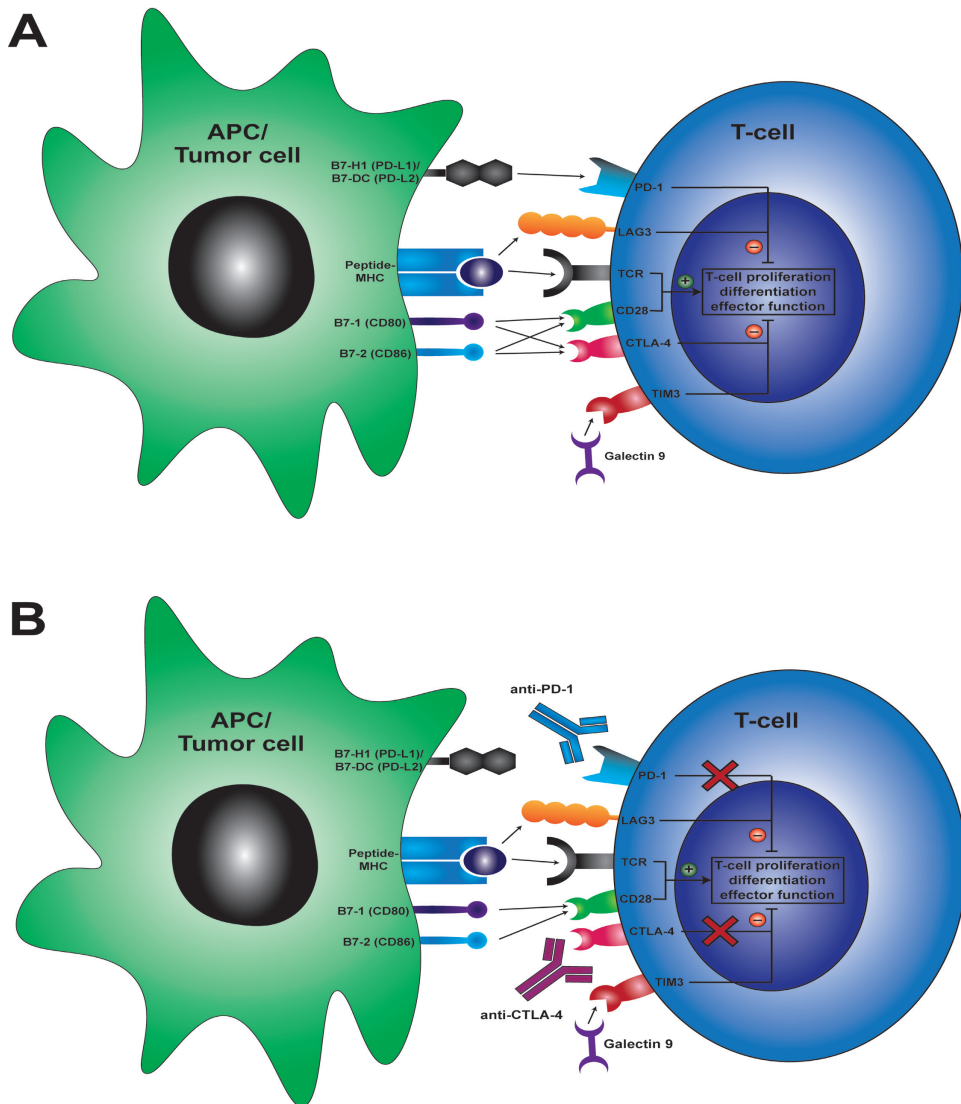


Figure 1. Co-inhibitory molecules inhibit T cell proliferation, differentiation and function, which can be blocked by checkpoint blockade.

A. Overview of the most well-known co-inhibitory receptors, expressed by T cells, and their corresponding ligands, expressed by APCs or tumor cells. These molecules inhibit the T cell response after antigen recognition (by binding of the TCR to a peptide-MHC complex). **B.** Checkpoint inhibitors are monoclonal antibodies that inhibit the interaction between the co-inhibitory receptor and their corresponding ligand, which allows initiation of anti-tumor T cell responses and may lead to long-lasting clinical responses.

APC, antigen-presenting cell; CTLA-4, cytotoxic T-lymphocyte-associated antigen 4; LAG3, lymphocyte activation gene 3; MHC, Major Histocompatibility Complex; PD-1, programmed cell death protein 1; PDL1, PD-1 ligand; TCR, T cell Receptor; TIM3, T cell membrane protein 3.

cytokines.^{55, 56} The chronic inflammation, in turn, causes necrosis and more secretion of cytokines, sustaining inflammation.⁵⁷ This vicious cycle of chronic cell death and inflammation can lead to MPM.⁵⁸ Malignant pleural mesothelioma is a heterogeneous disease, which is also reflected in the tumor micro-environment. The inflammatory component often found in mesothelioma has shown to be associated with survival.^{59, 60} Generally, intra-tumoral macrophages seem to be associated with worse patient outcome; in a cohort of 230 patients those with high intra-tumoral numbers of macrophages and low CTL numbers had a bad outcome, whereas patients with low macrophage and high B cell numbers had a better prognosis.⁵⁹ Inhibitory immune checkpoint pathways also play a role in suppression of intra-tumoral immunity, as it was shown that PD-L1 is expressed by tumor cells in 40% of patients, and is associated with poor survival.⁶¹

III. Tumor-specific immunity

As malignant cells differ from their normal counterparts and they often express aberrant proteins that can be presented by MHC class I molecules, they can act as a target for the immune system, CTL in particular.

IIIA. Tumor associated antigens

These proteins are known as tumor-associated antigens (TAAs) and can be classified as follows; oncofetal (typically expressed during fetal development and in tumors), oncoviral (encoded by tumorigenic transforming viruses), overexpressed (expressed in both healthy and tumor tissues, but increased expression in tumors), cancer/testis (typically expressed in germ cells and tumors), lineage-restricted (typically expressed by one histological cancer type), mutated (only expressed in tumors, as a result of a mutation or alteration in transcription), posttranslationally altered (tumor-associated alteration in glycosylation, etc.) or idiotypic (present in malignancies of lymphocytic origin).⁶² Well-known examples are of oncofetal antigens are carcinoembryonic antigen (CEA), used for diagnosis and monitoring of CRC patients,⁶³ and alpha-fetoprotein (AFP) and Glypican3 (GPC3) expressed in HCC.⁶⁴ Human papilloma virus E6 and E7 proteins are oncoviral antigens, associated with cervical carcinoma.⁶⁵ Examples of overexpressed antigens include mesothelin, overexpressed in mesothelioma,⁶⁶ EpCam, overexpressed in CRC and HCC,^{67, 68} and human telomerase reverse transcriptase (hTERT), overexpressed in more than 85% of human cancers, including the three histological tumor types studied in this thesis.⁶⁹⁻⁷¹ The melanoma associated antigen (MAGE) family and New York esophageal squamous cell carcinoma 1 (NY-ESO-1), both expressed in a multitude of cancers, including HCC, CRC and mesothelioma, are part of the cancer/testis antigen family.⁷²⁻⁷⁴ Most lineage-restricted antigens are expressed in melanoma, and include Melan-A and Gp100.^{75, 76} β -catenin and p53 are mutated antigens, the former expressed in HCC and CRC and the latter in all three studied malignancies.⁷⁷⁻⁸⁰ Neo-antigens are another example of mutated antigens, and can either be shared between patients or patient-specific.⁸¹

IIIb. Tumor-specific T-cell responses

Previous research has shown that the presence of tumor-infiltrating lymphocytes is associated with improved disease outcome in various histological subtypes of cancer, however, together with the inhibitory checkpoint pathway, the presence of MDSCs and Tregs disrupts the capacity of CTLs to control cancer.²⁹⁻³¹ In various types of cancer, it has been shown that the tumor-infiltrating lymphocytes (TIL) contain tumor-reactive T cells that specifically recognize TAAs. In HCC, various TAA-specific T cells have been detected, both by our group and by other research groups. We have detected MAGE-C2 and GPC3-specific intratumoral T cells.³⁹ In blood of HCC patients, a wide variety TAA-specific T cells have been detected, including T cells directed against AFP, cyclophorin B (Cyp-B), NY-ESO-1, several MAGE-A antigens, hTERT, squamous cell carcinoma antigen recognized by T cells (SART), GPC3, p53 and multiresistance protein 3 (MRP3).⁸² It was also shown that local ablative therapies, such as RFA and transarterial chemoablation (TACE), can enhance or induce these responses.^{35, 83, 84} The same effect was also seen in LM-CRC patients treated with RFA in whom increased cytokine T cell responses against a CRC cell line were observed.⁸⁵ Thus, in CRC, tumor-specific T cells are also present, however, few spontaneous TAA-specific T cell responses have been described; one study found CEA, EpCam and her-2/neu-specific T cells in blood and others found peripheral tumor-reactive T cells by stimulating with autologous tumor lysate.^{86, 87} In mesothelioma, little is known regarding tumor-specificity of T cells, however, recently a CTL response against a neo-antigen was detected.⁸⁸

IV. Cancer Immunotherapy

Identification of tumor-specific immune responses has led to the development of cancer immunotherapy. However, once tumors have formed, these tumor-specific immune responses are generally not sufficient to eradicate the tumor, as spontaneous tumor clearance is rare.⁸⁹ In HCC, it has been shown that the TAA-specific T cells are lower in frequency, are present in fewer patients, and have decreased cytokine-producing and cytotoxic capacity compared to virus-specific T cells.^{83, 90, 91} Furthermore, as discussed previously, the tumor harnesses several mechanisms to suppress the immune system including immune checkpoint pathways and attraction of immunosuppressive cells. Immune therapy is based on modifying the immune system to regain control of tumor growth, which can either be achieved by inhibiting immune suppression, activating the immune system or enhancing or inducing tumor-specific responses. As adoptive cell therapy, another type of cancer immunotherapy, falls beyond the scope of this thesis, it is not discussed here.

IVa. Therapeutic cancer vaccination

Vaccinations are widely used for prevention of infections, and have had a major global healthy impact. Just as vaccinations can be used to prevent infections with bacteria or viruses, they can also be used in oncology. Either preventive, by preventing infection with oncogenic viruses such as hepatitis B virus, or human papilloma virus (HPV), or therapeutically, by enhancing or inducing tumor-specific T cells that can then recognize and kill cancer cells. Until now, therapeutic cancer vaccines alone have shown to be not very effective, leading only to moderate antitumor responses. This is probably due to both suboptimal

target selection, also expressed by non-malignant tissues, and the immunosuppressive tumor micro-environment preventing a successful immune response. However, advances have been made in target selection, vaccine technology and reversing the tumor micro-environment, by either debulking surgery or immune checkpoint inhibition. Moreover, as historically vaccines were used to prevent microbial infections, at first the principles of microbial vaccines were applied to cancer vaccine development. This may have caused the first vaccines to be less successful, as in contrast to microbial infections, which function primarily via antibody responses, T cells are the most important factor in anti-tumor responses. Using recently improved understanding of the principles of T cell activation and function, advances are being made in cancer vaccine development.⁸¹ By these new evolutions, therapeutic vaccination could become a valuable addition to cancer immunotherapy. A theoretical advantage of this therapy would be that memory T cells could reside and thereby would prevent new tumor formation.⁹²

There are three major categories of therapeutic cancer vaccines; molecular vaccines, in which tumor cell components, such as proteins or ribonucleic acid (RNA), are included in the vaccine; cellular vaccines, in which either autologous or allogeneic cells are used for the vaccination; and virus vector vaccines, in which a virus is exploited as the vaccine carrier. According to the framework of this thesis, we will highlight and discuss only the first two categories.

IVa1. Molecular vaccines

IVa.1-1 Peptide vaccines

Classical peptide vaccines consist of one or more short peptides of 8-11 amino acids which are antigenic epitopes that are recognized by CTLs in the context of specific human leukocyte antigens (HLA)-class I types. Even though treatment with short peptide vaccines induced T-cell responses in many clinical trials, no clear clinical benefits were achieved.^{93, 94} CRC vaccination with short peptides derived from TAAs ring finger protein 43 (RNF43) and translocase of outer mitochondrial membrane 34 (TOMM34) led to some CTL responses, but no clinical responses.⁹⁵ In another trial, vaccination with short-peptides from RNF43, TOMM34, KOC1, vascular endothelial growth factor receptor (VEGFR)1 and VEGFR2 in metastatic CRC patients led to a complete response in 1 out of 18 patients, whereas 6 other patients had stable disease.⁹⁶ A phase II trial, in which this treatment was combined with chemotherapy and compared to vaccination and chemotherapy in HLA-mismatched patients, did not show a benefit of the peptide vaccination.⁹⁷ The most promising study in CRC included advanced CRC patients which were treated with a personalized vaccine, in which maximally four HLA-matched short peptides were included, based on pre-existing host immunity. Immunological responses were observed, and they were significantly predictive of improved survival.⁹⁸ Several short peptide vaccination studies have been performed in HCC, of which AFP was the first TAA to be targeted. AFP peptide vaccination in HLA-A2+ patients led to transient immunological responses, but no clinical effects.⁹⁹ GPC3 peptide vaccinations, either HLA-A24:02- or HLA-A02:01-restricted, led to detectable GPC-3 specific CTL responses and a positive correlation of these responses with patient survival, both in early HCC patients treated in an adjuvant setting after curative treatment as in HCC patients with advanced disease.^{100, 101}

Most of these clinical trials used single short-peptides, which may not be able to overcome antigen loss, antigen heterogeneity or induce robust cytotoxic T cell and memory T-cell responses.^{93, 94} The short peptides can bind directly into the groove on the MHC class I molecules of all nucleated cells, and can therefore be presented by other cells than professional APCs. These cells cannot co-stimulate T cells, which lead to tolerogenic signals and T cell dysfunction.¹⁰² Moreover, these peptides are not presented by MHC class II and therefore do not activate Th cells, which are required for full activation of CTLs. Moreover, they are restricted to certain HLA-types and can therefore not be applied to all patients. This had led to the development of synthetic long peptides (SLPs), which are typically 20-30 amino acids in length and contain both CD4 and CD8 T cell epitopes and circumvent HLA-restriction. In addition, as they are too long to fit directly in the MHC molecules, they require uptake and processing by professional APCs, leading to more effective T cell priming and induction of memory T cell responses.^{102, 103} In mesothelioma, a phase II peptide vaccination study, using both short and long WT1 peptides, capable of stimulating both Th and CTLs in a HLA-unrestricted manner, showed induction of Wilms tumor protein (WT1)-specific CD4 and CD8 T cell responses, and moderate clinical efficacy.¹⁰⁴ In CRC a p53-SLP vaccine led to p53-specific T cell responses, but with a suboptimal CD4 T cell polarization.¹⁰⁵ Addition of IFN α to the p53-SLP vaccine, induced significantly more IFN γ -producing CD4 T cells, but no data on clinical effects were shown.¹⁰⁶ SLP vaccines have not yet been evaluated in HCC patients.

IVa.1-2 RNA vaccines

RNA vaccines consist of RNA that encodes for TAA proteins and have several advantages over peptide vaccines; they are not HLA-restricted and are less dependent on adjuvants, as RNA itself can act as an adjuvant by providing costimulatory signals via toll-like receptor (TLR) activation, and thereby minimize the risk of inducing tolerogenic signals.¹⁰⁷ The drawback of RNA vaccines is the relative instability of RNA and the low efficiency of RNA uptake by APCs. RNA degradation can be prevented by chemical modification and incorporation of modified nucleosides.¹⁰⁸ To improve RNA uptake, different delivery methods have been tested, such as nanoparticles or liposomes. In addition, by adding either a MHC Class I or II trafficking signal, the presentation of MHC class I and II epitopes can be strongly improved, and leads to increased Th and CTL expansion and effector functions.^{109, 110} A recent clinical trial in which personalized poly-neo-epitope RNA vaccines were administered to advanced melanoma patients, led to immunological responses in all patients and sustained progression-free survival.¹¹¹ Interestingly, vaccination with RNA encoding CTAs also induced robust CTA-specific T cell responses.¹¹¹ In HCC, CRC and mesothelioma no clinical trials with naked RNA vaccinations have been performed.¹¹²

IVa2. Cellular vaccines

Cellular vaccines can comprise either immune cells presenting cancer antigens, or (killed) tumor cells themselves, and both can be either autologous or allogeneic.⁸¹ An advantage of this type of vaccination is that TAAs do not need to be identified and all possible relevant antigens are included.

Dendritic cell vaccines, in which autologous dendritic cells (DCs) are loaded with TAAs (either known peptide antigens, proteins or tumor lysate), have been studied extensively.¹¹³ Generally, they are characterized by their low complication rates and good tolerance.¹¹⁴ The sipuleucel-T treatment, consisting of autologous DCs activated *ex vivo* with a chimeric protein in which granulocyte-macrophage colony-stimulating factor (GM-CSF) is fused to the TAA prostate acid phosphatase (PAP), is the first Food and Drug Administration (FDA) approved cancer vaccine, and is used to treat metastatic prostate carcinoma patients.¹¹⁵ In mesothelioma, DC vaccines, consisting of autologous DCs loaded with either autologous tumor lysate or allogeneic tumor lysates, have also proven to be feasible and safe.¹¹⁶ Currently a phase II/III randomized clinical trial is ongoing, in which therapeutic DC vaccination is compared with best supportive care (BSC). Also in HCC, various clinical trials have studied vaccinations with DCs loaded with HCC-specific antigens, and it seems that these vaccines can promote antitumor responses.¹¹⁷⁻¹¹⁹ Both AFP-peptide vaccination and vaccination with DCs loaded with the same AFP-peptides induced transient immune responses, but failed to lead to clinical efficacy.^{99, 119} DCs loaded with autologous tumor lysate showed better clinical response rates, especially in patients treated with monthly boost vaccinations.^{120, 121} However, none of these vaccination strategies have advanced into phase III trials yet. In CRC a few phase I clinical trials with DC vaccines loaded with CEA peptides have been performed. All studies showed that the strategy is safe, and also some tumor regression was observed, correlating to the number of tumor-specific CTLs induced by the treatment.¹²²⁻¹²⁵ Of note, all these trials date from at least 15 years ago and no further advances have been made.

Iva3. Optimization of cancer vaccination therapies

The results discussed in the preceding paragraphs highlight the potential of therapeutic cancer vaccination strategies to elicit immunological and clinical anti-tumor responses. The development of multi-antigen vaccinations, targeting TAAs with oncogenic functions, may lead to superior tumor control, as antigen loss will not lead to tumor escape.⁹¹ Computer-guided HLA-epitope optimization may also lead to maximization of anti-tumor responses.¹²⁶ Moreover, certain adjuvants can potentially enhance the efficacy of therapeutic vaccination including the induction of cytokine and chemokine production, recruitment of immune cells, promotion of antigen transport to lymph nodes and improvement of antigen stability, delivery, and processing and presentation to T cells.¹²⁷ Certain adjuvants, such as tumor necrosis factor receptor (TNFR) ligands, TLR agonists like CpG oligodeoxynucleotides (CpG ODN) and GM-CSF aim at enhancing costimulatory signals for T cell activation. Another method is combining a molecular vaccine with TriMix, a mix of mRNA encoding for CD40 ligand, constitutive active TLR4 and CD70, which modifies and matures the DCs taking up the vaccine components *in vivo*.¹²⁸ Besides enhancing T cell activation, vaccination therapy can also be optimized by altering the tumor microenvironment (TME), for example by co-treating the patients with checkpoint inhibitors (CPIs), which has shown promising results when combined with a tumor-specific vaccine in HPV-related cancer.¹²⁹ Another strategy is a combination with low dose cyclophosphamide, which should selectively deplete Tregs, and thereby promote anti-tumor responses.¹³⁰ Lastly, the TME can be removed by debulking surgery or tumor resection, and vaccination

therapy can be given as adjuvant treatment to clear the last tumor cells and prevent metastasis. In HCC, adjuvant treatment with a GPC3-peptide vaccination in patients who had received curative treatment, improved the recurrence rates in patients with GPC3-positive tumors.¹³¹

IVb. Immune checkpoint-targeting therapies

Immune checkpoint inhibition therapy has revolutionized cancer therapy paradigms in the past decade, as it has shown to completely eradicate tumors in patients deemed incurable.¹³² By targeting co-inhibitory pathways with antagonistic antibodies, inhibitory signals are removed and existing anti-tumor T cell responses can be unleashed (**Figure 1B**). Alternatively, the co-stimulatory receptors can be targeted with agonistic antibodies, which provide the second signal necessary for T cell activation.

In the past decade the FDA has approved several different immune checkpoint blockade therapies for a variety of tumor types, targeting either the co-inhibitory PD-1/PD-L1 pathway or the co-inhibitory receptor CTLA-4.¹³³ Likely, more checkpoint therapies for additional indications will be approved in the near future, including antibodies agonistically targeting costimulatory molecules.¹³⁴

Nivolumab, pembrolizumab (both anti-PD-1) and ipilimumab (anti-CTLA4) are the most well-known CPIs and have currently been approved by the FDA for treatment of melanoma, non-small cell lung cancer (NSCLC), renal cell carcinoma (RCC), Hodgkin lymphoma, head and neck squamous cell carcinoma (HNSCC), urothelial carcinoma, MMR deficient tumors of any origin, HCC and gastric and gastroesophageal carcinoma.¹³³ So far, agonistic antibodies targeting co-stimulatory molecules have not been approved by the FDA for cancer treatment. Agonistically targeting CD137 demonstrated strong anti-tumor responses in murine studies.¹³⁵ Unfortunately, clinical trials so far revealed lethal hepatotoxicity or lacked clinical efficacy.^{136, 137} Currently several trials are ongoing, either with adjusted dosing, or in combination with other immunotherapies. Preclinical studies with GITR and OX40 targeting antibodies showed promising results and are currently being tested in the clinic.¹³⁸⁻¹⁴¹

Despite FDA approval of nivolumab for treatment of advanced HCC patients and the initial promising results,¹⁴² randomized phase III trials of anti-PD1 monotherapy did not demonstrate statistically significant improvements in overall survival.^{143, 144} Therefore, as for other cancers, combination therapies are now explored in several phase III trials.^{145, 146} Either dual CPI therapy, or a combination of a CPI with anti-angiogenic therapies, which are considered critical for antitumor efficacy in HCC as they enhance DC maturation, decrease the numbers of tumor-associated macrophages, Tregs and MDSCs and enhance T cell function and migration.¹⁴⁶⁻¹⁵⁰ The first results of such combination therapies are promising, as the combination of atezolizumab (anti-PDL1) and bevacizumab (anti-VEGF) led to better overall and progression-free survival than sorafenib in advanced HCC patients.¹⁵¹

Even though there is a strong correlation between TIL infiltration and overall prognosis in CRC, CPIs are only successful in a subset of CRC patients.^{48, 152-156} CPIs have shown to be especially favorable in the treatment of patients with tumors with a high tumor mutational burden (TMB).^{157, 158} As MMR deficient CRC, representing 10-20% of CRC patients, have a high mutational load, these tumors respond well to

CPI therapy.¹⁵⁹ However, in MMR proficient CRC patients, CPI monotherapy barely has any effect.^{154, 156} Nevertheless, there is a small percentage of MMR proficient patients with a high TMB, which may respond to CPI therapy.¹⁶⁰ In addition, as LM-CRC are immunologically different from primary CRC in terms of immune infiltration, combined with the distinct immune environment in the liver, these tumors may respond differently to CPI.^{161, 162}

In mesothelioma, clinical trials using CTLA-4 inhibitors failed to improve survival.¹⁶³ As patients with PD-L1 expression on their tumors had worse survival, it is thought PD-L1 blockade may benefit these patients.⁶¹ Several trials are currently ongoing combining blockade of the PD-1 pathway with CTLA-4 inhibitors or chemotherapy, however, most studies are still recruiting patients.^{14, 163} In a phase II trial, it was shown that the combination of ipilimumab and nivolumab led to a better disease control rate than nivolumab alone, but the results have to be confirmed in a phase III trial.¹⁶⁴

AIMS AND OUTLINE OF THE THESIS

The immune system is essential in fighting against foreign compounds and protects the body against infectious diseases caused by bacteria, viruses, fungi, parasites and their toxins. However anti-tumor immunity is hindered by the immunosuppressive tumor micro environment.

In this thesis, we aim to find targets to stimulate and modulate the immune system, making use of its specific and inherent qualities, so it can regain control of tumor growth. The first approach investigated is stimulation of tumor-infiltrating T-cells by targeting of inhibitory and stimulatory immune checkpoint receptors, described in **Chapters 2 and 3**. In **Chapter 2** we explore which checkpoint inhibitors are able to stimulate tumor-infiltrating T cells isolated from liver metastases of MMR-proficient CRC patients. In a pilot study, described in **Chapter 3**, we present preliminary data on the effects of a novel bispecific antibody, which co-targets a stimulatory and an inhibitory immune checkpoint, on ex vivo functions of tumor-infiltrating T cells from patients with HCC, primary CRC and liver metastasis of CRC.

The second approach studied is the stimulation of systemic anti-tumor T cell responses. To stimulate systemic anti-tumor T cells responses by therapeutic cancer vaccination, identification of targets uniquely expressed in the tumor and not in other tissues is critical for two reasons; it prevents auto-immunity upon vaccination and enables induction of potent T-cells, as TCRs specific for self-antigens are negatively selected in the thymus. Therefore, in **Chapter 4** we aim to find TAAs specifically expressed in HCC and not in other healthy tissues by performing an extensive analysis of CTA expression in HCC, healthy livers and other healthy tissues.

Once targets have been selected, the capacity of the immune system to recognize these TAAs needs to be assessed. Thus, in **Chapter 5** we aim to investigate the immunogenicity of the CTAs found in **Chapter 4**, by determining responses of both cellular and humoral responses against these CTAs in HCC patients.

Another approach to improve the effect of therapeutic cancer vaccination on systemic anti-vaccine T-cell responses is described in **Chapter 6**. Here, we investigate the effect of low-dose cyclophosphamide on its ability to decrease the number of circulating Tregs, as a synergistic treatment to therapeutic DC-vaccination in malignant pleural mesothelioma patients.

Finally, the implications of our findings are put into perspective in **Chapter 7**.

REFERENCES

1. CBS. Doordoorzakenstatistiek, 2018.
2. Siegel RL, Miller KD, Jemal A. Cancer statistics, 2020. *CA Cancer J Clin* 2020;70:7-30.
3. Bray F, Ferlay J, Soerjomataram I, et al. Global cancer statistics 2018: GLOBOCAN estimates of incidence and mortality worldwide for 36 cancers in 185 countries. *CA Cancer J Clin* 2018;68:394-424.
4. Villanueva A, Hernandez-Gea V, Llovet JM. Medical therapies for hepatocellular carcinoma: a critical view of the evidence. *Nat Rev Gastroenterol Hepatol* 2013;10:34-42.
5. Allaire M, Nault JC. Advances in management of hepatocellular carcinoma. *Curr Opin Oncol* 2017;29:288-295.
6. Brenner DR, Heer E, Sutherland RL, et al. National Trends in Colorectal Cancer Incidence Among Older and Younger Adults in Canada. *JAMA Netw Open* 2019;2:e198090.
7. Abualkhair WH, Zhou M, Ahnen D, et al. Trends in Incidence of Early-Onset Colorectal Cancer in the United States Among Those Approaching Screening Age. *JAMA Netw Open* 2020;3:e1920407.
8. House MG, Kemeny NE, Gonen M, et al. Comparison of adjuvant systemic chemotherapy with or without hepatic arterial infusional chemotherapy after hepatic resection for metastatic colorectal cancer. *Ann Surg* 2011;254:851-6.
9. Tomlinson JS, Jarnagin WR, DeMatteo RP, et al. Actual 10-year survival after resection of colorectal liver metastases defines cure. *J Clin Oncol* 2007;25:4575-80.
10. Sekido Y. Molecular pathogenesis of malignant mesothelioma. *Carcinogenesis* 2013;34:1413-9.
11. Ong ST, Vogelzang NJ. Chemotherapy in malignant pleural mesothelioma. A review. *J Clin Oncol* 1996;14:1007-17.
12. Antman KH. Natural history and epidemiology of malignant mesothelioma. *Chest* 1993;103:373S- 376S.
13. Aisner J. Current approach to malignant mesothelioma of the pleura. *Chest* 1995;107:332S-344S.
14. Carbone M, Adusumilli PS, Alexander HR, Jr., et al. Mesothelioma: Scientific clues for prevention, diagnosis, and therapy. *CA Cancer J Clin* 2019;69:402-429.
15. Yap TA, Aerts JG, Popat S, et al. Novel insights into mesothelioma biology and implications for therapy. *Nat Rev Cancer* 2017;17:475-488.
16. Raja S, Murthy SC, Mason DP. Malignant pleural mesothelioma. *Curr Oncol Rep* 2011;13:259-64.
17. Haas AR, Sterman DH. Malignant pleural mesothelioma: update on treatment options with a focus on novel therapies. *Clin Chest Med* 2013;34:99-111.
18. Treasure T, Lang-Lazdunski L, Waller D, et al. Extra-pleural pneumonectomy versus no extra-pleural pneumonectomy for patients with malignant pleural mesothelioma: clinical outcomes of the Mesothelioma and Radical Surgery (MARS) randomised feasibility study. *Lancet Oncol* 2011;12:763-72.
19. La-Beck NM, Jean GW, Huynh C, et al. Immune Checkpoint Inhibitors: New Insights and Current Place in Cancer Therapy. *Pharmacotherapy* 2015;35:963-76.
20. Lee YT, Tan YJ, Oon CE. Molecular targeted therapy: Treating cancer with specificity. *Eur J Pharmacol* 2018;834:188-196.
21. Coussens LM, Werb Z. Inflammation and cancer. *Nature* 2002;420:860-7.
22. Hanahan D, Weinberg RA. Hallmarks of cancer: the next generation. *Cell* 2011;144:646-74.
23. Beaugerie L, Svrcek M, Seksik P, et al. Risk of colorectal high-grade dysplasia and cancer in a prospective observational cohort of patients with inflammatory bowel disease. *Gastroenterology* 2013;145:166-175 e8.
24. Prieto J, Melero I, Sangro B. Immunological landscape and immunotherapy of hepatocellular carcinoma. *Nat Rev Gastroenterol Hepatol* 2015;12:681-700.

25. Huang YT, Jen CL, Yang HI, et al. Lifetime risk and sex difference of hepatocellular carcinoma among patients with chronic hepatitis B and C. *J Clin Oncol* 2011;29:3643-50.
26. Lakatos PL, Lakatos L. Risk for colorectal cancer in ulcerative colitis: changes, causes and management strategies. *World J Gastroenterol* 2008;14:3937-47.
27. Munkholm P. Review article: the incidence and prevalence of colorectal cancer in inflammatory bowel disease. *Aliment Pharmacol Ther* 2003;18 Suppl 2:1-5.
28. Delgermaa V, Takahashi K, Park EK, et al. Global mesothelioma deaths reported to the World Health Organization between 1994 and 2008. *Bull World Health Organ* 2011;89:716-24, 724A-724C.
29. Barnes TA, Amir E. HYPE or HOPE: the prognostic value of infiltrating immune cells in cancer. *Br J Cancer* 2017;117:451-460.
30. Idos GE, Kwok J, Bonthala N, et al. The Prognostic Implications of Tumor Infiltrating Lymphocytes in Colorectal Cancer: A Systematic Review and Meta-Analysis. *Sci Rep* 2020;10:3360.
31. Wada Y, Nakashima O, Kutami R, et al. Clinicopathological study on hepatocellular carcinoma with lymphocytic infiltration. *Hepatology* 1998;27:407-14.
32. Donini C, D'Ambrosio L, Grignani G, et al. Next generation immune-checkpoints for cancer therapy. *J Thorac Dis* 2018;10:S1581-S1601.
33. Sharpe AH. Introduction to checkpoint inhibitors and cancer immunotherapy. *Immunol Rev* 2017;276:5-8.
34. Chen L, Flies DB. Molecular mechanisms of T cell co-stimulation and co-inhibition. *Nat Rev Immunol* 2013;13:227-42.
35. Greten TF, Duffy AG, Korangy F. Hepatocellular carcinoma from an immunologic perspective. *Clin Cancer Res* 2013;19:6678-85.
36. Park EJ, Lee JH, Yu GY, et al. Dietary and genetic obesity promote liver inflammation and tumorigenesis by enhancing IL-6 and TNF expression. *Cell* 2010;140:197-208.
37. Chang MH, Chen CJ, Lai MS, et al. Universal hepatitis B vaccination in Taiwan and the incidence of hepatocellular carcinoma in children. Taiwan Childhood Hepatoma Study Group. *N Engl J Med* 1997;336:1855-9.
38. Matsui M, Machida S, Itani-Yohda T, et al. Downregulation of the proteasome subunits, transporter, and antigen presentation in hepatocellular carcinoma, and their restoration by interferon-gamma. *J Gastroenterol Hepatol* 2002;17:897-907.
39. Zhou G, Sprengers D, Boor PPC, et al. Antibodies Against Immune Checkpoint Molecules Restore Functions of Tumor-Infiltrating T Cells in Hepatocellular Carcinomas. *Gastroenterology* 2017;153:1107-1119 e10.
40. Raskov H, Pommergaard HC, Burcharth J, et al. Colorectal carcinogenesis--update and perspectives. *World J Gastroenterol* 2014;20:18151-64.
41. Ott PA, Hu Z, Keskin DB, et al. An immunogenic personal neoantigen vaccine for patients with melanoma. *Nature* 2017;547:217-221.
42. Fletcher R, Wang YJ, Schoen RE, et al. Colorectal cancer prevention: Immune modulation taking the stage. *Biochim Biophys Acta Rev Cancer* 2018;1869:138-148.
43. Fingleton B, Carter KJ, Matrisian LM. Loss of functional Fas ligand enhances intestinal tumorigenesis in the Min mouse model. *Cancer Res* 2007;67:4800-6.
44. Poynter JN, Siegmund KD, Weisenberger DJ, et al. Molecular characterization of MSI-H colorectal cancer by MLH1 promoter methylation, immunohistochemistry, and mismatch repair germline mutation screening. *Cancer Epidemiol Biomarkers Prev* 2008;17:3208-15.
45. Ionov Y, Peinado MA, Malkhosyan S, et al. Ubiquitous somatic mutations in simple repeated sequences reveal a new mechanism for clonal carcinogenesis. *Nature* 1993;363:558-61.
46. Arora SP, Mahalingam D. Immunotherapy in colorectal cancer: for the select few or all? *J Gastrointest Oncol* 2018;9:170-179.

47. Jacobs J, Smits E, Lardon F, et al. Immune Checkpoint Modulation in Colorectal Cancer: What's New and What to Expect. *J Immunol Res* 2015;2015:158038.
48. Llosa NJ, Cruise M, Tam A, et al. The vigorous immune microenvironment of microsatellite instable colon cancer is balanced by multiple counter-inhibitory checkpoints. *Cancer Discov* 2015;5:43-51.
49. Nordholm-Carstensen A, Krarup PM, Morton D, et al. Mismatch repair status and synchronous metastases in colorectal cancer: A nationwide cohort study. *Int J Cancer* 2015;137:2139-48.
50. Ledys F, Klopfenstein Q, Truntzer C, et al. RAS status and neoadjuvant chemotherapy impact CD8+ cells and tumor HLA class I expression in liver metastatic colorectal cancer. *J Immunother Cancer* 2018;6:123.
51. Halama N, Spille A, Lerchl T, et al. Hepatic metastases of colorectal cancer are rather homogeneous but differ from primary lesions in terms of immune cell infiltration. *Oncoimmunology* 2013;2:e24116.
52. Van den Eynde M, Mlecnik B, Bindea G, et al. The Link between the Multiverse of Immune Microenvironments in Metastases and the Survival of Colorectal Cancer Patients. *Cancer Cell* 2018;34:1012-1026 e3.
53. Pedroza-Gonzalez A, Verhoef C, Ijzermans JN, et al. Activated tumor-infiltrating CD4+ regulatory T cells restrain antitumor immunity in patients with primary or metastatic liver cancer. *Hepatology* 2013;57:183-94.
54. Hillegass JM, Shukla A, Lathrop SA, et al. Inflammation precedes the development of human malignant mesotheliomas in a SCID mouse xenograft model. *Ann N Y Acad Sci* 2010;1203:7-14.
55. Quinlan TR, Marsh JP, Janssen YM, et al. Oxygen radicals and asbestos-mediated disease. *Environ Health Perspect* 1994;102 Suppl 10:107-10.
56. Acencio MM, Soares B, Marchi E, et al. Inflammatory Cytokines Contribute to Asbestos-Induced Injury of Mesothelial Cells. *Lung* 2015;193:831-7.
57. Yang H, Rivera Z, Jube S, et al. Programmed necrosis induced by asbestos in human mesothelial cells causes high-mobility group box 1 protein release and resultant inflammation. *Proc Natl Acad Sci U S A* 2010;107:12611-6.
58. Carbone M, Yang H. Molecular pathways: targeting mechanisms of asbestos and erionite carcinogenesis in mesothelioma. *Clin Cancer Res* 2012;18:598-604.
59. Ujiie H, Kadota K, Nitadori JI, et al. The tumoral and stromal immune microenvironment in malignant pleural mesothelioma: A comprehensive analysis reveals prognostic immune markers. *Oncoimmunology* 2015;4:e1009285.
60. Chene AL, d'Almeida S, Blondy T, et al. Pleural Effusions from Patients with Mesothelioma Induce Recruitment of Monocytes and Their Differentiation into M2 Macrophages. *J Thorac Oncol* 2016;11:1765-73.
61. Mansfield AS, Roden AC, Peikert T, et al. B7-H1 expression in malignant pleural mesothelioma is associated with sarcomatoid histology and poor prognosis. *J Thorac Oncol* 2014;9:1036-1040.
62. Kufe D, Pollock R, Weichselbaum R, et al. *Holland-Frei Cancer Medicine*, 6th edition. Hamilton (ON): BC Decker, 2003.
63. Shively JE, Beatty JD. CEA-related antigens: molecular biology and clinical significance. *Crit Rev Oncol Hematol* 1985;2:355-99.
64. Sideras K, Bots SJ, Biermann K, et al. Tumour antigen expression in hepatocellular carcinoma in a low-endemic western area. *Br J Cancer* 2015;112:1911-20.
65. Breitburd F, Coursaget P. Human papillomavirus vaccines. *Semin Cancer Biol* 1999;9:431-44.
66. Creaney J, Robinson BWS. Malignant Mesothelioma Biomarkers: From Discovery to Use in Clinical Practice for Diagnosis, Monitoring, Screening, and Treatment. *Chest* 2017;152:143-149.
67. Han S, Zong S, Shi Q, et al. Is Ep-CAM Expression a Diagnostic and Prognostic Biomarker for Colorectal Cancer? A Systematic Meta-Analysis. *EBioMedicine* 2017;20:61-69.

68. Yamashita T, Ji J, Budhu A, et al. EpCAM-positive hepatocellular carcinoma cells are tumor-initiating cells with stem/progenitor cell features. *Gastroenterology* 2009;136:1012-24.
69. Liu JP, Chen W, Schwarzer AP, et al. Telomerase in cancer immunotherapy. *Biochim Biophys Acta* 2010;1805:35-42.
70. Zhang N, Zhang R, Zou K, et al. Keratin 23 promotes telomerase reverse transcriptase expression and human colorectal cancer growth. *Cell Death Dis* 2017;8:e2961.
71. Tallet A, Nault JC, Renier A, et al. Overexpression and promoter mutation of the TERT gene in malignant pleural mesothelioma. *Oncogene* 2014;33:3748-52.
72. Weon JL, Potts PR. The MAGE protein family and cancer. *Curr Opin Cell Biol* 2015;37:1-8.
73. Raza A, Merhi M, Inchakalody VP, et al. Unleashing the immune response to NY-ESO-1 cancer testis antigen as a potential target for cancer immunotherapy. *J Transl Med* 2020;18:140.
74. Sigalotti L, Coral S, Altomonte M, et al. Cancer testis antigens expression in mesothelioma: role of DNA methylation and bioimmunotherapeutic implications. *Br J Cancer* 2002;86:979-82.
75. Kawakami Y, Eliyahu S, Sakaguchi K, et al. Identification of the immunodominant peptides of the MART-1 human melanoma antigen recognized by the majority of HLA-A2-restricted tumor infiltrating lymphocytes. *J Exp Med* 1994;180:347-52.
76. Bakker AB, Schreurs MW, de Boer AJ, et al. Melanocyte lineage-specific antigen gp100 is recognized by melanoma-derived tumor-infiltrating lymphocytes. *J Exp Med* 1994;179:1005-9.
77. Bhattacharya I, Barman N, Maiti M, et al. Assessment of beta-catenin expression by immunohistochemistry in colorectal neoplasms and its role as an additional prognostic marker in colorectal adenocarcinoma. *Med Pharm Rep* 2019;92:246-252.
78. Robbins PF, El-Gamil M, Li YF, et al. A mutated beta-catenin gene encodes a melanoma-specific antigen recognized by tumor infiltrating lymphocytes. *J Exp Med* 1996;183:1185-92.
79. DeLeo AB. p53-based immunotherapy of cancer. *Crit Rev Immunol* 1998;18:29-35.
80. Kafiri G, Thomas DM, Shepherd NA, et al. p53 expression is common in malignant mesothelioma. *Histopathology* 1992;21:331-4.
81. Hollingsworth RE, Jansen K. Turning the corner on therapeutic cancer vaccines. *NPJ Vaccines* 2019;4:7.
82. Mizukoshi E, Kaneko S. Immune cell therapy for hepatocellular carcinoma. *J Hematol Oncol* 2019;12:52.
83. Mizukoshi E, Nakamoto Y, Arai K, et al. Comparative analysis of various tumor-associated antigen-specific t-cell responses in patients with hepatocellular carcinoma. *Hepatology* 2011;53:1206-16.
84. Mizukoshi E, Yamashita T, Arai K, et al. Enhancement of tumor-associated antigen-specific T cell responses by radiofrequency ablation of hepatocellular carcinoma. *Hepatology* 2013;57:1448-57.
85. Hansler J, Wissniowski TT, Schuppan D, et al. Activation and dramatically increased cytolytic activity of tumor specific T lymphocytes after radio-frequency ablation in patients with hepatocellular carcinoma and colorectal liver metastases. *World J Gastroenterol* 2006;12:3716-21.
86. Nagorsen D, Scheibenbogen C, Letsch A, et al. T cell responses against tumor associated antigens and prognosis in colorectal cancer patients. *J Transl Med* 2005;3:3.
87. Reissfelder C, Stamova S, Gossmann C, et al. Tumor-specific cytotoxic T lymphocyte activity determines colorectal cancer patient prognosis. *J Clin Invest* 2015;125:739-51.
88. Sneddon S, Rive CM, Ma S, et al. Identification of a CD8+ T-cell response to a predicted neoantigen in malignant mesothelioma. *Oncoimmunology* 2020;9:1684713.
89. Zou W. Immunosuppressive networks in the tumour environment and their therapeutic relevance. *Nat Rev Cancer* 2005;5:263-74.

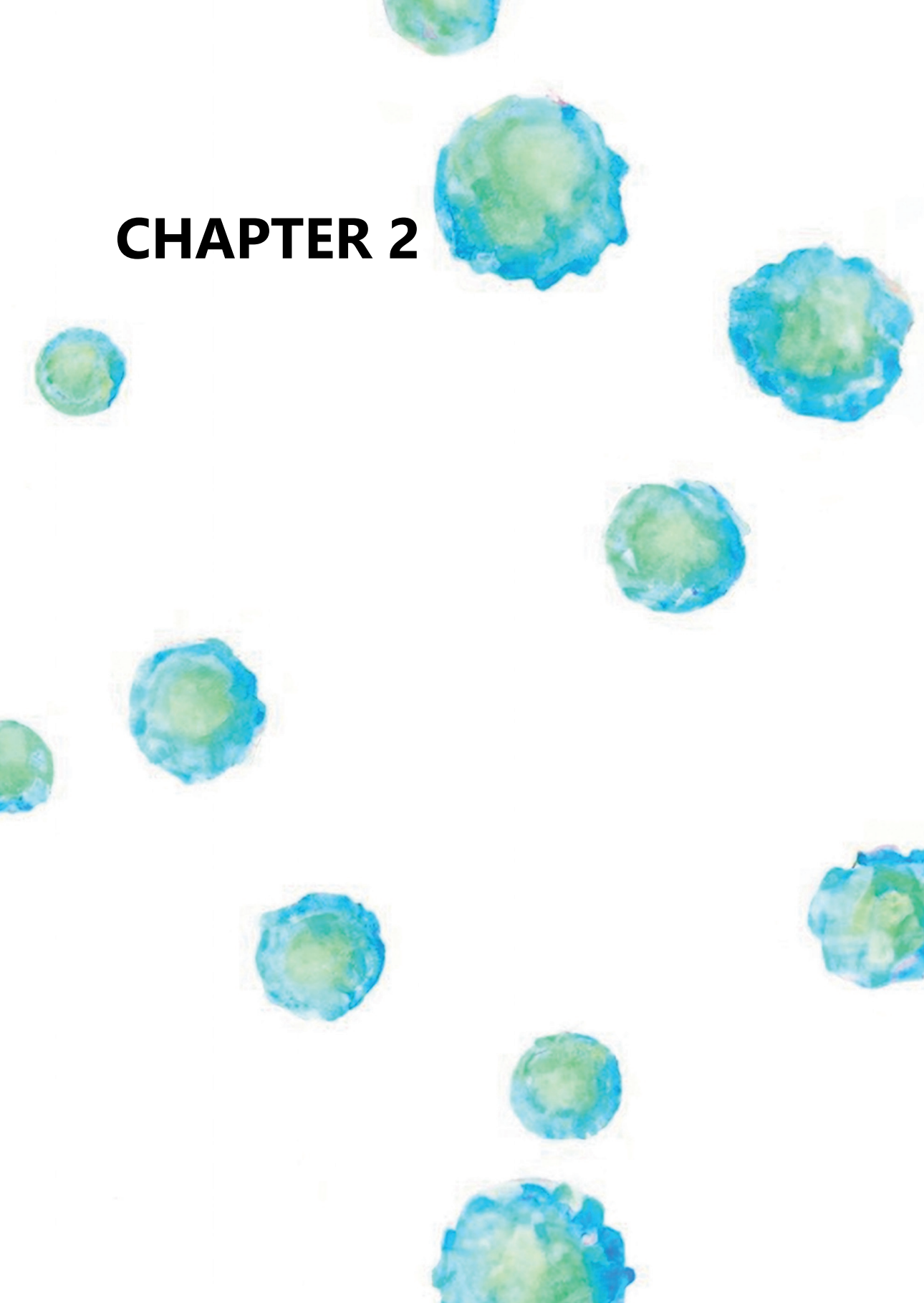
90. Mizukoshi E, Honda M, Arai K, et al. Expression of multidrug resistance-associated protein 3 and cytotoxic T cell responses in patients with hepatocellular carcinoma. *J Hepatol* 2008;49:946-54.
91. Flecken T, Schmidt N, Hild S, et al. Immunodominance and functional alterations of tumor-associated antigen-specific CD8+ T-cell responses in hepatocellular carcinoma. *Hepatology* 2014;59:1415-26.
92. Dobosz P, Dzieciatkowski T. The Intriguing History of Cancer Immunotherapy. *Front Immunol* 2019;10:2965.
93. Cecco S, Muraro E, Giacomini E, et al. Cancer vaccines in phase II/III clinical trials: state of the art and future perspectives. *Curr Cancer Drug Targets* 2011;11:85-102.
94. Lesterhuis WJ, Haanen JB, Punt CJ. Cancer immunotherapy--revisited. *Nat Rev Drug Discov* 2011;10:591-600.
95. Okuno K, Sugiura F, Hida JI, et al. Phase I clinical trial of a novel peptide vaccine in combination with UFT/LV for metastatic colorectal cancer. *Exp Ther Med* 2011;2:73-79.
96. Hazama S, Nakamura Y, Takenouchi H, et al. A phase I study of combination vaccine treatment of five therapeutic epitope-peptides for metastatic colorectal cancer; safety, immunological response, and clinical outcome. *J Transl Med* 2014;12:63.
97. Hazama S, Nakamura Y, Tanaka H, et al. A phase I study of five peptides combination with oxaliplatin-based chemotherapy as a first-line therapy for advanced colorectal cancer (FXV study). *J Transl Med* 2014;12:108.
98. Kibe S, Yutani S, Motoyama S, et al. Phase II study of personalized peptide vaccination for previously treated advanced colorectal cancer. *Cancer Immunol Res* 2014;2:1154-62.
99. Butterfield LH, Ribas A, Meng WS, et al. T-cell responses to HLA-A*0201 immunodominant peptides derived from alpha-fetoprotein in patients with hepatocellular cancer. *Clin Cancer Res* 2003;9:5902-8.
100. Sawada Y, Yoshikawa T, Nobuoka D, et al. Phase I trial of a glypican-3-derived peptide vaccine for advanced hepatocellular carcinoma: immunologic evidence and potential for improving overall survival. *Clin Cancer Res* 2012;18:3686-96.
101. Taniguchi M, Mizuno S, Yoshikawa T, et al. Peptide vaccine as an adjuvant therapy for glypican-3-positive hepatocellular carcinoma induces peptide-specific CTLs and improves long prognosis. *Cancer Sci* 2020.
102. Bijker MS, van den Eeden SJ, Franken KL, et al. Superior induction of anti-tumor CTL immunity by extended peptide vaccines involves prolonged, DC-focused antigen presentation. *Eur J Immunol* 2008;38:1033-42.
103. Rosalia RA, Quakkelaar ED, Redeker A, et al. Dendritic cells process synthetic long peptides better than whole protein, improving antigen presentation and T-cell activation. *Eur J Immunol* 2013;43:2554-65.
104. Zauderer MG, Tsao AS, Dao T, et al. A Randomized Phase II Trial of Adjuvant Galinpepimut-S, WT-1 Analogue Peptide Vaccine, After Multimodality Therapy for Patients with Malignant Pleural Mesothelioma. *Clin Cancer Res* 2017;23:7483-7489.
105. Speetjens FM, Kuppen PJ, Welters MJ, et al. Induction of p53-specific immunity by a p53 synthetic long peptide vaccine in patients treated for metastatic colorectal cancer. *Clin Cancer Res* 2009;15:1086-95.
106. Zeestraten EC, Speetjens FM, Welters MJ, et al. Addition of interferon-alpha to the p53-SLP(R) vaccine results in increased production of interferon-gamma in vaccinated colorectal cancer patients: a phase I/II clinical trial. *Int J Cancer* 2013;132:1581-91.
107. Eisenacher K, Steinberg C, Reindl W, et al. The role of viral nucleic acid recognition in dendritic cells for innate and adaptive antiviral immunity. *Immunobiology* 2007;212:701-14.

108. Kariko K, Muramatsu H, Welsh FA, et al. Incorporation of pseudouridine into mRNA yields superior nonimmunogenic vector with increased translational capacity and biological stability. *Mol Ther* 2008;16:1833-40.
109. Kreiter S, Selmi A, Diken M, et al. Increased antigen presentation efficiency by coupling antigens to MHC class I trafficking signals. *J Immunol* 2008;180:309-18.
110. Bonehill A, Heirman C, Tuyaerts S, et al. Messenger RNA-electroporated dendritic cells presenting MAGE-A3 simultaneously in HLA class I and class II molecules. *J Immunol* 2004;172:6649-57.
111. Sahin U, Derhovanessian E, Miller M, et al. Personalized RNA mutanome vaccines mobilize poly-specific therapeutic immunity against cancer. *Nature* 2017;547:222-226.
112. Pardi N, Hogan MJ, Porter FW, et al. mRNA vaccines - a new era in vaccinology. *Nat Rev Drug Discov* 2018;17:261-279.
113. Cannon MJ, Block MS, Morehead LC, et al. The evolving clinical landscape for dendritic cell vaccines and cancer immunotherapy. *Immunotherapy* 2019;11:75-79.
114. Gardner A, Ruffell B. Dendritic Cells and Cancer Immunity. *Trends Immunol* 2016;37:855-865.
115. Cheever MA, Higano CS. PROVENGE (Sipuleucel-T) in prostate cancer: the first FDA-approved therapeutic cancer vaccine. *Clin Cancer Res* 2011;17:3520-6.
116. Cornelissen R, Hegmans JP, Maat AP, et al. Extended Tumor Control after Dendritic Cell Vaccination with Low-Dose Cyclophosphamide as Adjuvant Treatment in Patients with Malignant Pleural Mesothelioma. *Am J Respir Crit Care Med* 2016;193:1023-31.
117. El Ansary M, Mogawer S, Elhamid SA, et al. Immunotherapy by autologous dendritic cell vaccine in patients with advanced HCC. *J Cancer Res Clin Oncol* 2013;139:39-48.
118. Tada F, Abe M, Hirooka M, et al. Phase I/II study of immunotherapy using tumor antigen-pulsed dendritic cells in patients with hepatocellular carcinoma. *Int J Oncol* 2012;41:1601-9.
119. Butterfield LH, Ribas A, Dissette VB, et al. A phase I/II trial testing immunization of hepatocellular carcinoma patients with dendritic cells pulsed with four alpha-fetoprotein peptides. *Clin Cancer Res* 2006;12:2817-25.
120. Lee WC, Wang HC, Hung CF, et al. Vaccination of advanced hepatocellular carcinoma patients with tumor lysate-pulsed dendritic cells: a clinical trial. *J Immunother* 2005;28:496-504.
121. Palmer DH, Midgley RS, Mirza N, et al. A phase II study of adoptive immunotherapy using dendritic cells pulsed with tumor lysate in patients with hepatocellular carcinoma. *Hepatology* 2009;49:124-32.
122. Fong L, Hou Y, Rivas A, et al. Altered peptide ligand vaccination with Flt3 ligand expanded dendritic cells for tumor immunotherapy. *Proc Natl Acad Sci U S A* 2001;98:8809-14.
123. Itoh T, Ueda Y, Kawashima I, et al. Immunotherapy of solid cancer using dendritic cells pulsed with the HLA-A24-restricted peptide of carcinoembryonic antigen. *Cancer Immunol Immunother* 2002;51:99-106.
124. Morse MA, Deng Y, Coleman D, et al. A Phase I study of active immunotherapy with carcinoembryonic antigen peptide (CAP-1)-pulsed, autologous human cultured dendritic cells in patients with metastatic malignancies expressing carcinoembryonic antigen. *Clin Cancer Res* 1999;5:1331-8.
125. Lesterhuis WJ, de Vries IJ, Schuurhuis DH, et al. Vaccination of colorectal cancer patients with CEA-loaded dendritic cells: antigen-specific T cell responses in DTH skin tests. *Ann Oncol* 2006;17:974-80.
126. Hong Y, Peng Y, Guo ZS, et al. Epitope-optimized alpha-fetoprotein genetic vaccines prevent carcinogen-induced murine autochthonous hepatocellular carcinoma. *Hepatology* 2014;59:1448-58.
127. Awate S, Babiuk LA, Mutwiri G. Mechanisms of action of adjuvants. *Front Immunol* 2013;4:114.
128. Van Lint S, Goyvaerts C, Maenhout S, et al. Preclinical evaluation of TriMix and antigen mRNA-based antitumor therapy. *Cancer Res* 2012;72:1661-71.

129. Massarelli E, William W, Johnson F, et al. Combining Immune Checkpoint Blockade and Tumor-Specific Vaccine for Patients With Incurable Human Papillomavirus 16-Related Cancer: A Phase 2 Clinical Trial. *JAMA Oncol* 2019;5:67-73.
130. Scurr M, Pembroke T, Bloom A, et al. Low-Dose Cyclophosphamide Induces Antitumor T-Cell Responses, which Associate with Survival in Metastatic Colorectal Cancer. *Clin Cancer Res* 2017;23:6771-6780.
131. Sawada Y, Yoshikawa T, Ofuji K, et al. Phase II study of the GPC3-derived peptide vaccine as an adjuvant therapy for hepatocellular carcinoma patients. *Oncoimmunology* 2016;5:e1129483.
132. McDermott D, Lebbe C, Hodi FS, et al. Durable benefit and the potential for long-term survival with immunotherapy in advanced melanoma. *Cancer Treat Rev* 2014;40:1056-64.
133. Wei SC, Duffy CR, Allison JP. Fundamental Mechanisms of Immune Checkpoint Blockade Therapy. *Cancer Discov* 2018;8:1069-1086.
134. Marhelava K, Pilch Z, Bajor M, et al. Targeting Negative and Positive Immune Checkpoints with Monoclonal Antibodies in Therapy of Cancer. *Cancers (Basel)* 2019;11.
135. Melero I, Shuford WW, Newby SA, et al. Monoclonal antibodies against the 4-1BB T-cell activation molecule eradicate established tumors. *Nat Med* 1997;3:682-5.
136. Segal NH, He AR, Doi T, et al. Phase I Study of Single-Agent Utomilumab (PF-05082566), a 4-1BB/CD137 Agonist, in Patients with Advanced Cancer. *Clin Cancer Res* 2018;24:1816-1823.
137. Segal NH, Logan TF, Hodi FS, et al. Results from an Integrated Safety Analysis of Urelumab, an Agonist Anti-CD137 Monoclonal Antibody. *Clin Cancer Res* 2017;23:1929-1936.
138. Cohen AD, Diab A, Perales MA, et al. Agonist anti-GITR antibody enhances vaccine-induced CD8(+) T-cell responses and tumor immunity. *Cancer Res* 2006;66:4904-12.
139. Piconese S, Valzasina B, Colombo MP. OX40 triggering blocks suppression by regulatory T cells and facilitates tumor rejection. *J Exp Med* 2008;205:825-39.
140. Curti BD, Kovacsocovics-Bankowski M, Morris N, et al. OX40 is a potent immune-stimulating target in late-stage cancer patients. *Cancer Res* 2013;73:7189-7198.
141. Knee DA, Hewes B, Brogdon JL. Rationale for anti-GITR cancer immunotherapy. *Eur J Cancer* 2016;67:1-10.
142. El-Khoueiry AB, Sangro B, Yau T, et al. Nivolumab in patients with advanced hepatocellular carcinoma (CheckMate 040): an open-label, non-comparative, phase 1/2 dose escalation and expansion trial. *Lancet* 2017;389:2492-2502.
143. Yau T, Park JW, Finn RS, et al. CHECKMATE 459: A randomized, multi-center phase 3 study of nivolumab (NIVO) vs sorafenib (SOR) as first-line (1L) treatment in patients (pts) with advanced hepatocellular carcinoma (aHCC). *Annals of Oncology* 2019;30 (suppl_5):v851-v934.
144. Finn RS, Ryoo BY, Merle P, et al. Pembrolizumab As Second-Line Therapy in Patients With Advanced Hepatocellular Carcinoma in KEYNOTE-240: A Randomized, Double-Blind, Phase III Trial. *J Clin Oncol* 2020;38:193-202.
145. Cheng AL, Hsu C, Chan SL, et al. Challenges of combination therapy with immune checkpoint inhibitors for hepatocellular carcinoma. *J Hepatol* 2020;72:307-319.
146. Greten TF, Lai CW, Li G, et al. Targeted and Immune-Based Therapies for Hepatocellular Carcinoma. *Gastroenterology* 2019;156:510-524.
147. Finn RS, Ryoo B-Y, Merle P, et al. Results of KEYNOTE-240: phase 3 study of pembrolizumab vs. best supportive care for second-line therapy in advanced hepatocellular carcinoma. *J Clin Oncol* 2019;37(suppl):4004.
148. Hegde PS, Wallin JJ, Mancao C. Predictive markers of anti-VEGF and emerging role of angiogenesis inhibitors as immunotherapeutics. *Semin Cancer Biol* 2018;52:117-124.

149. Ramjiawan RR, Griffioen AW, Duda DG. Anti-angiogenesis for cancer revisited: Is there a role for combinations with immunotherapy? *Angiogenesis* 2017;20:185-204.
150. Kwilas AR, Donahue RN, Tsang KY, et al. Immune consequences of tyrosine kinase inhibitors that synergize with cancer immunotherapy. *Cancer Cell Microenviron* 2015;2.
151. Finn RS, Qin S, Ikeda M, et al. Atezolizumab plus Bevacizumab in Unresectable Hepatocellular Carcinoma. *N Engl J Med* 2020;382:1894-1905.
152. Kim ST, Klempler SJ, Park SH, et al. Correlating programmed death ligand 1 (PD-L1) expression, mismatch repair deficiency, and outcomes across tumor types: implications for immunotherapy. *Oncotarget* 2017;8:77415-77423.
153. Topalian SL, Hodi FS, Brahmer JR, et al. Safety, activity, and immune correlates of anti-PD-1 antibody in cancer. *N Engl J Med* 2012;366:2443-54.
154. Brahmer JR, Tykodi SS, Chow LQ, et al. Safety and activity of anti-PD-L1 antibody in patients with advanced cancer. *N Engl J Med* 2012;366:2455-65.
155. Brahmer JR, Drake CG, Wollner I, et al. Phase I study of single-agent anti-programmed death-1 (MDX-1106) in refractory solid tumors: safety, clinical activity, pharmacodynamics, and immunologic correlates. *J Clin Oncol* 2010;28:3167-75.
156. O'Neil BH, Wallmark JM, Lorente D, et al. Safety and antitumor activity of the anti-PD-1 antibody pembrolizumab in patients with advanced colorectal carcinoma. *PLoS One* 2017;12:e0189848.
157. Goodman AM, Kato S, Bazhenova L, et al. Tumor Mutational Burden as an Independent Predictor of Response to Immunotherapy in Diverse Cancers. *Mol Cancer Ther* 2017;16:2598-2608.
158. Le DT, Durham JN, Smith KN, et al. Mismatch repair deficiency predicts response of solid tumors to PD-1 blockade. *Science* 2017;357:409-413.
159. Hermel DJ, Sigal D. The Emerging Role of Checkpoint Inhibition in Microsatellite Stable Colorectal Cancer. *J Pers Med* 2019;9.
160. Fabrizio DA, George TJ, Jr., Dunne RF, et al. Beyond microsatellite testing: assessment of tumor mutational burden identifies subsets of colorectal cancer who may respond to immune checkpoint inhibition. *J Gastrointest Oncol* 2018;9:610-617.
161. Halama N, Michel S, Kloor M, et al. Localization and density of immune cells in the invasive margin of human colorectal cancer liver metastases are prognostic for response to chemotherapy. *Cancer Res* 2011;71:5670-7.
162. Crispe IN. Immune tolerance in liver disease. *Hepatology* 2014;60:2109-17.
163. Mutti L, Peikert T, Robinson BWS, et al. Scientific Advances and New Frontiers in Mesothelioma Therapeutics. *J Thorac Oncol* 2018;13:1269-1283.
164. Scherpereel A, Mazieres J, Greillier L, et al. Nivolumab or nivolumab plus ipilimumab in patients with relapsed malignant pleural mesothelioma (IFCT-1501 MAPS2): a multicentre, open-label, randomised, non-comparative, phase 2 trial. *Lancet Oncol* 2019;20:239-253.

CHAPTER 2



BLOCKADE OF LAG3 ENHANCES RESPONSES OF TUMOR-INFILTRATING T CELLS IN MISMATCH REPAIR-PROFICIENT LIVER METASTASES OF COLORECTAL CANCER

Blockade of LAG3 enhances responses of tumor-infiltrating T cells in mismatch repair-proficient liver metastases of colorectal cancer

G. Zhou, L. Noordam, D. Sprengers, M. Doukas, P.P.C. Boor, A.A. van Beek, R. Erkens, S. Mancham, D. Grünhagen, A.G. Menon, J.F. Lange, P.J.W.A. Burger, A. Brandt, B. Galjart, C. Verhoef, J. Kwekkeboom, M.J. Bruno
Oncolmmunology, Apr 2018, Vol. 7, No. 7: e1448332

*This chapter has been published in *Oncolmmunology*.*

Purpose

Liver metastasis develops in >50% of patients with colorectal cancer (CRC), and is a leading cause of CRC-related mortality. We aimed to identify which inhibitory immune checkpoint pathways can be targeted to enhance functionality of intra-tumoral T-cells in mismatch repair-proficient liver metastases of colorectal cancer (LM-CRC).

Methodology

Intra-tumoral expression of multiple inhibitory molecules was compared among mismatch repair-proficient LM-CRC, peritoneal metastases of colorectal cancer (PM-CRC) and primary CRC. Expression of inhibitory molecules was also analyzed on leukocytes isolated from paired resected metastatic liver tumors, tumor-free liver tissues, and blood of patients with mismatch repair-proficient LM-CRC. The effects of blocking inhibitory pathways on tumor-infiltrating T-cell responses were studied in *ex vivo* functional assays.

Results

Mismatch repair-proficient LM-CRC showed higher expression of inhibitory receptors on intra-tumoral T-cells and contained higher proportions of CD8⁺ T-cells, dendritic cells and monocytes than mismatch repair-proficient primary CRC and/or PM-CRC. Inhibitory receptors LAG3, PD-1, TIM3 and CTLA4 were higher expressed on CD8⁺ T-cells, CD4⁺ T-helper and/or regulatory T-cells in LM-CRC tumors compared with tumor-free liver and blood. Antibody blockade of LAG3 or PD-L1 increased proliferation and effector cytokine production of intra-tumoral T-cells isolated from LM-CRC in response to both polyclonal and autologous tumor-specific stimulations. Higher LAG3 expression on intra-tumoral CD8⁺ T-cells associated with longer progression-free survival of LM-CRC patients.

Conclusion

Mismatch repair-proficient LM-CRC may be more sensitive to immune checkpoint inhibitors than mismatch repair-proficient primary CRC. Blocking LAG3 enhances tumor-infiltrating T-cell responses of mismatch repair-proficient LM-CRC, and therefore may be a new promising immunotherapeutic target for LM-CRC.

INTRODUCTION

Colorectal cancer (CRC) is the third most common cause of cancer-related mortality worldwide.¹⁻³ More than 50% of CRC patients develop metastatic disease to their liver over the course of their life,⁴ and liver metastasis is a leading cause of death from CRC.⁵⁻⁷ Unfortunately, surgical resection of isolated liver metastases of CRC (LM-CRC) is curative in only 20%-30% of patients,^{8, 9} and systemic therapy provides limited survival benefit.¹⁰ Patients with unresectable LM-CRC have a poor prognosis with a median survival of only two years.¹¹ Therefore, there is a pressing need for more effective therapeutic strategies for LM-CRC.

The immune system plays a crucial role in cancer surveillance and elimination, and antibody blockade of inhibitory immune checkpoint pathways that suppress anti-tumor T-cell immunity and assist tumor immune evasion,¹²⁻¹⁶ has recently emerged as an attractive treatment option for multiple types of malignancies.¹⁷⁻²¹ Targeting the PD-1/PD-L1 inhibitory pathway has resulted in objective responses in 17%-28% of advanced melanoma patients, 12%-27% of renal cell cancer patients, 10%-18% of non-small cell lung cancer patients and 20% of advanced hepatocellular carcinoma patients.²²⁻²⁵ In contrast, CRC patients hardly respond to PD-1 and PD-L1 blocking antibodies²³⁻²⁶, except for the minority of patients who are with mismatch repair (MMR)-deficient CRC.^{27, 28} A defective MMR enzyme system occurs in 10%-20% of CRC tumors and results in microsatellite instability, which is used as a molecular marker of MMR-deficiency.²⁹ It has been hypothesized that the observed difference in responsiveness to PD-1/PD-L1 blockade between MMR-deficient and MMR-proficient CRC is related to the higher numbers of somatic mutations in MMR-deficient tumors, due to the reduced ability to repair DNA damage. The increased mutation rate may result in the presence of more mutation-encoded neo-antigens in the tumors, which elicit stronger anti-tumor T cell responses.²⁷ Indeed, MMR-deficient CRC tumors are characterized by denser CD8⁺ T cell infiltration.³⁰ They also have higher expression levels of inhibitory checkpoint molecules, probably to resist immune-mediated tumor elimination.³¹ Together, enhanced immune cell infiltration and upregulation of inhibitory immune checkpoints may render MMR-deficient CRC more sensitive to PD-1/PD-L1 blockade than MMR-proficient CRC.

In LM-CRC the incidence of MMR deficiency is low,³² and it may therefore be expected that LM-CRC poorly respond to immune checkpoint inhibitors. Nevertheless, these tumors contain immune infiltrates, and increased numbers of tumor-infiltrating CD8⁺ T cells are positively associated with overall survival and response to chemotherapy,^{33, 34} indicating that intra-tumoral T cell immunity is an important determinant of LM-CRC progression. In addition, MMR-proficient LM-CRC are immunologically distinct from primary CRC in terms of immune infiltration.³⁵ Moreover, the unique immune environment in the liver³⁶ favors immunological tolerance,³⁶ and one of the mechanisms used by the liver to resist immune responses is the induction of expression of inhibitory receptors on hepatic T cells^{37, 38} and their ligands on hepatocytes and other liver tissue cells.³⁹ Previously we have observed that intra-tumoral CD8⁺ cytotoxic T cells (CTL) and CD4⁺ T helper cells (Th) are functionally compromised in LM-CRC,⁴⁰ and we also demonstrated that the suppression mediated by intra-tumoral regulatory T cells (Treg) in LM-CRC can be alleviated

Figure 1. Comparison of immune infiltrates and inhibitory molecule expression among MMR-proficient liver metastases (LM), peritoneal metastases (PM) and primary CRC. ►

A. The frequencies of CD8⁺ CTL, CD4⁺Foxp3⁻ Th and CD4⁺Foxp3⁺ Treg within CD3⁺ TIL from LM-CRC (LM), primary CRC (P) and PM-CRC (PM). **B.** The frequencies of inhibitory receptor positive cells within CD8⁺ CTL, Th and Treg in LM-CRC, primary CRC and PM-CRC. **C.** The frequencies of B cells, mDC and monocytes (Mono) within CD45⁺ cells from LM-CRC, primary CRC and PM-CRC. **D.** The frequencies of inhibitory ligand positive cells within tumor-infiltrating B cells, mDC and monocytes from LM-CRC, primary CRC and PM-CRC. Values of individual patients are shown, and lines depict medians. Differences were analyzed by unpaired t test or Mann-Whitney test; * p < 0.05, ** p < 0.01, *** p < 0.001.

by blocking the inhibitory receptor CTLA4 and activating the stimulatory receptor GITR.⁴¹ However, the expression and functional roles of inhibitory receptor-ligand pathways in regulating tumor-infiltrating effector T cell responses have not been studied yet in LM-CRC.

Therefore, the aim of this study was to determine whether inhibitory immune checkpoint pathways can be targeted to enhance the functionality of tumor-infiltrating lymphocytes (TIL) in MMR-proficient LM-CRC. We measured the expression of inhibitory receptors and their ligands on leukocytes isolated from paired resected metastatic liver tumors, tumor-free liver tissues (TFL) and blood of patients with LM-CRC, and compared their expression levels with those on leukocytes isolated from peritoneal metastasis of CRC (PM-CRC) and primary CRC. In addition, we studied the effects of antibody blockade of inhibitory pathways on TIL responses of LM-CRC in *ex vivo* functional assays.

RESULTS

Comparison of immune infiltrates and expression of inhibitory molecules among MMR-proficient liver metastases, peritoneal metastases and primary CRC.

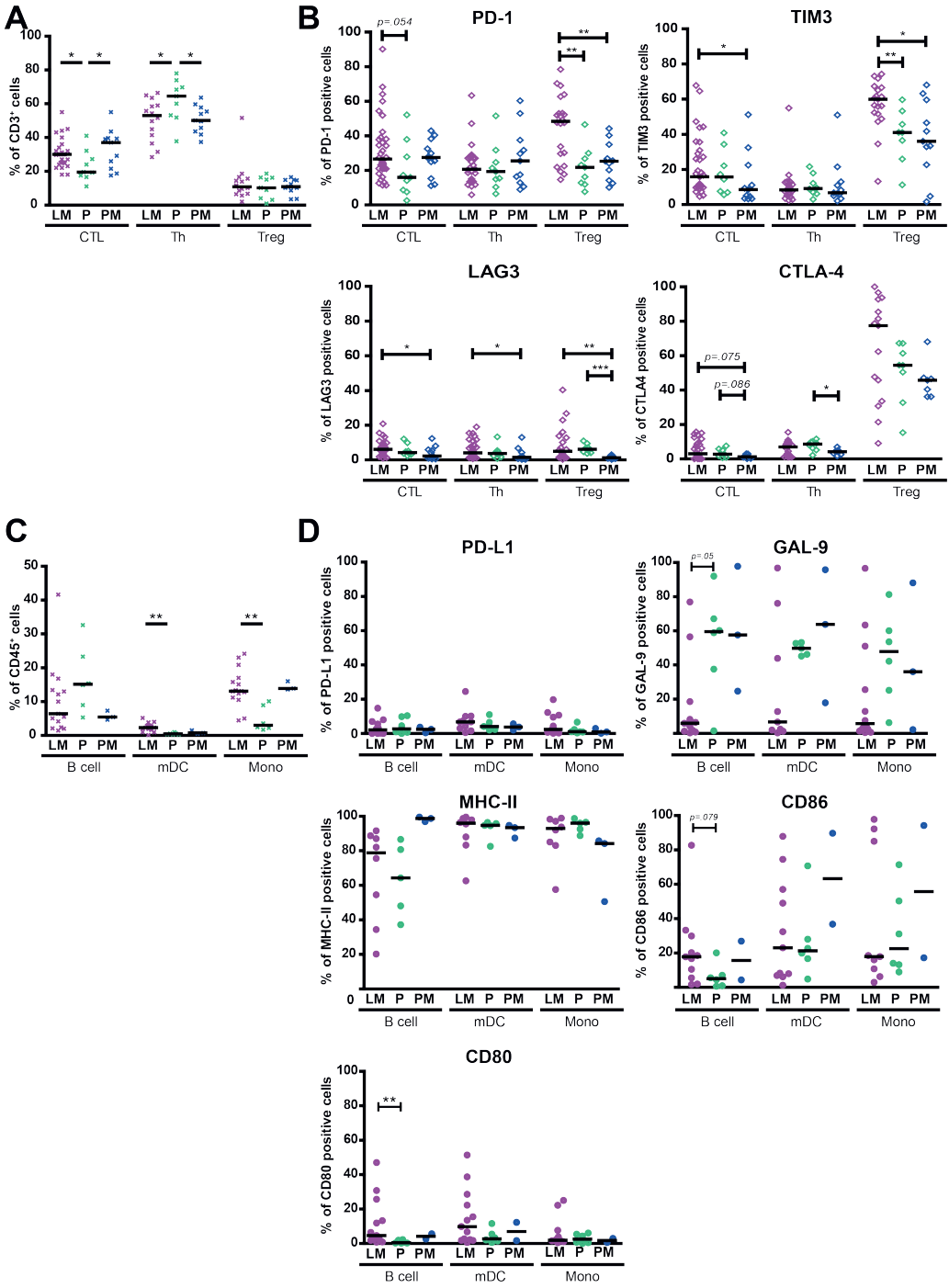
To speculate whether TIL in CRC tumors at different anatomical sites may differ in sensitivity to checkpoint inhibitors, we first compared frequencies of T cell and antigen-presenting cell (APC) subsets,

Table 1. Patient characteristics.

	LM-CRC (n=53)	PM-CRC (n=11)	primary CRC (n=12)
Gender (female/male)	16 / 37	4 / 7	5 / 7
Age (years)**	66.3 ± 3.3	56.9 ± 3.8	63.4 ± 3.4
Stage of disease (TNM)	Stage IV n=53	Stage IV n=11	Stage I n=3, Stage II n=4, Stage III n=4, Stage IV n=1
MMR status (deficient/proficient)	2/51	0/11	3/9

Abbreviations: CRC, colorectal cancer; LM-CRC, liver metastasis of CRC; PM-CRC, peritoneal metastasis of CRC; TNM, tumor-node-metastasis; MMR, mismatch repair.

**Mean ± standard error of the mean.



as well as their expression of inhibitory molecules, between MMR-proficient LM-CRC, primary CRC, and metastases outside the liver. Two in all LM-CRC tumors and three out of twelve primary CRC tumors that we collected were MMR-deficient, whereas all eleven PM-CRC tumors were MMR-proficient (**Table 1** and **Supplementary Table S1**). The data of the five patients with MMR-deficient tumors are shown in **Supplementary Fig. S1**.

We observed several interesting differences among MMR-proficient tumors from different anatomical locations. Firstly, both LM-CRC and PM-CRC contained significantly higher frequencies of CD8⁺ CTL and significantly lower frequencies of CD4⁺Foxp3⁺ Th than primary CRC, while frequencies of Treg were similar in CRC tumors at all three sites (**Fig. 1A**). Secondly, CD8⁺ CTL in LM-CRC displayed a higher frequency of PD1⁺ cells than those in primary CRC, and also contained higher frequencies of TIM3⁺ and LAG3⁺ cells than those in PM-CRC, while CD4⁺ Th in LM-CRC displayed a higher frequency of LAG3⁺ cells than those in PM-CRC (**Fig. 1B**). Thirdly, CD4⁺Foxp3⁺ Treg in LM-CRC contained higher frequencies of PD-1⁺ and TIM3⁺ cells than those in primary CRC and PM-CRC, and also displayed a higher frequency of LAG3⁺ cells than those in PM-CRC (**Fig. 1B**). Finally, LM-CRC contained significantly higher frequencies

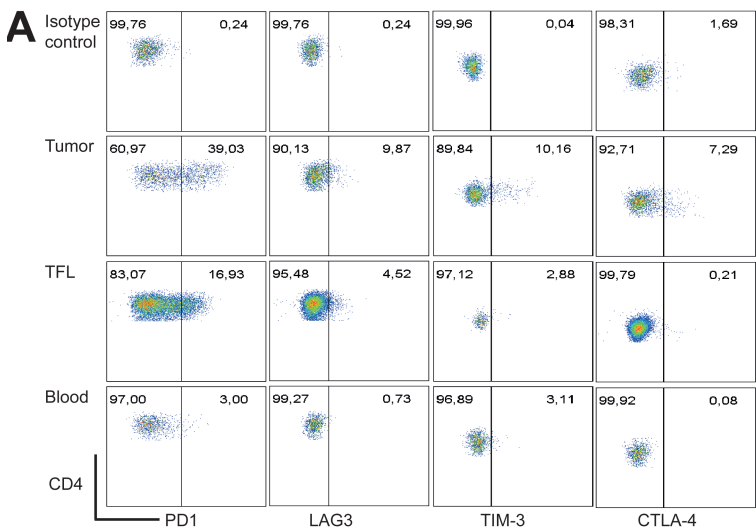
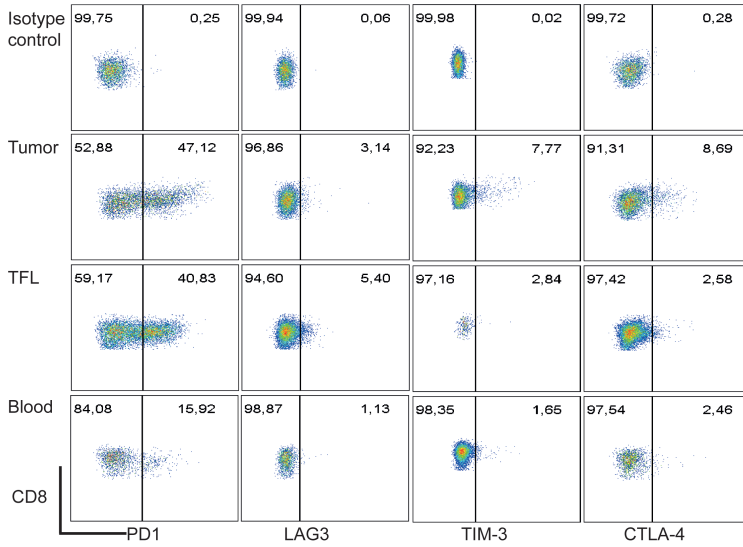


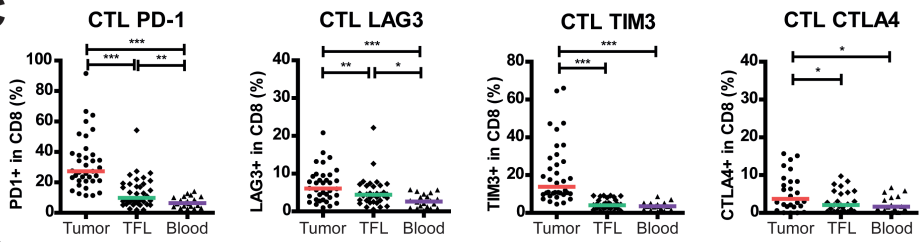
Figure 2. Expression of inhibitory receptors on CD8⁺ CTL, CD4⁺ Th and CD4⁺ Treg in the tumor, TFL and blood of MMR-proficient LM-CRC.

PBMC and leukocytes isolated from LM-CRC tumors and TFL were stained with antibodies against PD-1, LAG3, TIM3 and CTLA4. **A-B**. Representative dot plots of inhibitory receptor expression on **(A)** CD3⁺CD8⁺ CTL and **(B)** CD3⁺CD4⁺Foxp3⁺ Th in the tumor, TFL and blood; the gates were made according to appropriate isotype controls. **C-E**. The frequencies of inhibitory receptor positive cells within **(C)** CD8⁺ CTL, **(D)** CD4⁺Foxp3⁺ Th and **(E)** CD4⁺Foxp3⁺ Treg in the tumor, TFL and blood. Values of individual patients are shown, and lines depict medians. Differences were analyzed by paired t test or Wilcoxon matched pairs test; * p < 0.05, ** p < 0.01, *** p < 0.001.

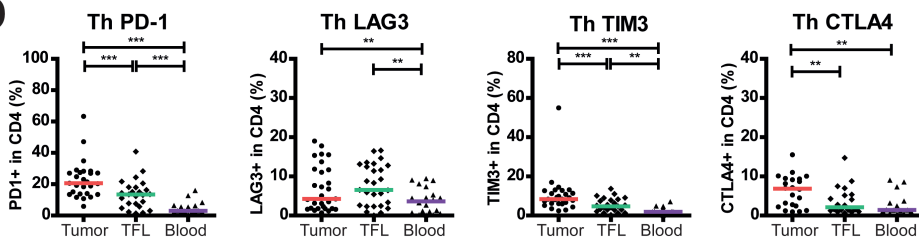
B



C



D



E

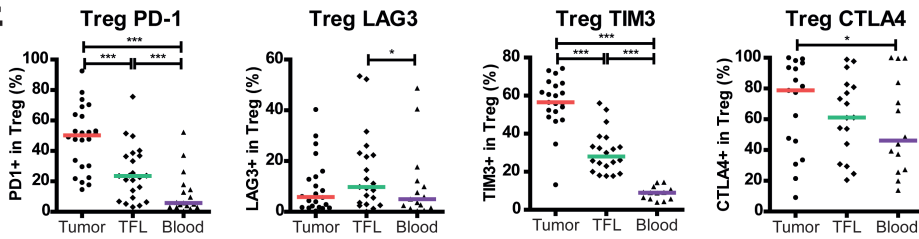


Figure 2. Expression of inhibitory receptors on CD8⁺ CTL, CD4⁺ Th and CD4⁺ Treg in the tumor, TFL and blood of MMR-proficient LM-CRC. (continued)

of myeloid dendritic cells (mDC) and monocytes than primary CRC (**Fig. 1C**), which not only can present tumor antigens to T cells but also express the inhibitory ligands PD-L1 (for PD-1), galectin 9 (for TIM3), MHC class II molecules (for LAG3), CD86 and CD80 (for CTLA4) (**Fig. 1D**). Hierarchical clustering analysis showed that the immunological data of most LM-CRC patients clustered together as did the data of most primary CRC patients (**Supplementary Fig. S2**). Together, these data indicate that the CD8⁺ CTL:Treg ratio, which is critical for immunological tumor control in primary as well as metastasized CRC,⁴² is more favorable in CRC metastases compared to primary CRC. In addition, the increased expression of PD-1 on TIL suggests that TIL of LM-CRC may be more sensitive to blockade of the PD-1/PD-L1 pathway than TIL of primary CRC.

Elevated expression of inhibitory receptors on CD8⁺ cytotoxic T cells, CD4⁺ T helper cells and regulatory T cells in MMR-proficient LM-CRC tumors.

We isolated leukocytes from surgically resected metastatic liver tumors, TFL and blood of LM-CRC patients, and compared the expression levels of five inhibitory receptors (PD-1, TIM3, LAG3, CTLA4 and BTLA) on CD8⁺ CTL, CD4⁺Foxp3⁻ Th and CD4⁺Foxp3⁺ Treg. When compared to TFL and blood, significantly higher proportions of CD8⁺ CTL, Th and Treg in TIL expressed PD-1 and TIM-3. In addition, TIL contained higher frequencies of CTLA4⁺ CTL and CTLA4⁺ Th, while LAG3 was overexpressed on CD8⁺ CTL in TIL when compared to TFL and blood (**Fig. 2**). Interestingly, the highest expression of CTLA4, which is functionally involved in the suppressive capacity of Treg,⁴³ and also of PD-1 and TIM3 was found on tumor-infiltrating Treg. In contrast, frequencies of BTLA⁺ cells in intra-tumoral T cells were low, and they did not differ significantly from those in TFL and blood (**Supplementary Fig. S3**). Therefore, we focused on the other four receptors in the rest of this study. To investigate whether the expression of inhibitory receptors on circulating T cells had a relation with the expression on intra-tumoral T cells, we performed correlation analysis, as illustrated in **Supplementary Fig. S4**. There were significant positive correlations between the frequencies of PD-1⁺ CTL and PD-1⁺ Treg in the tumor and those in the blood, between the frequency of LAG3⁺ Th in the tumor and that in the blood, and between the frequencies of CTLA4⁺ Th and CTLA4⁺ Treg in the tumor and those in the blood. These results indicate that the expression of inhibitory receptors on circulating T cells partly reflects their expression on intra-tumoral T cells.

Figure 3. Intra-tumoral antigen-presenting cells of MMR-proficient LM-CRC express inhibitory ligands. ►

Expression of inhibitory ligands PD-L1, galectin 9 (GAL-9), MHC-II, CD86 and CD80 was measured by flow cytometry. **A.** The frequencies of CD19⁺ B cells, BDCA1⁺CD19⁻ mDC and CD14⁺ monocytes (Mono) within CD45⁺ cells derived from tumors, TFL and blood. Values of individual patients are presented, lines depict medians. **B.** Representative histograms of inhibitory ligand stainings and isotype controls on tumor-infiltrating mDC, monocytes and B cells. **C.** The frequencies of inhibitory ligand positive cells within tumor-infiltrating B cells, mDC and monocytes in individual patients are presented; lines depict medians. **D.** The median fluorescence intensities (MFI) of inhibitory ligands on B cells, mDC and monocytes derived from tumors, TFL and blood of LM-CRC patients. Values of individual patients are shown, and lines depict medians. Differences were analyzed by paired t test or Wilcoxon matched pairs test; * p < 0.05, ** p < 0.01, *** p < 0.001.

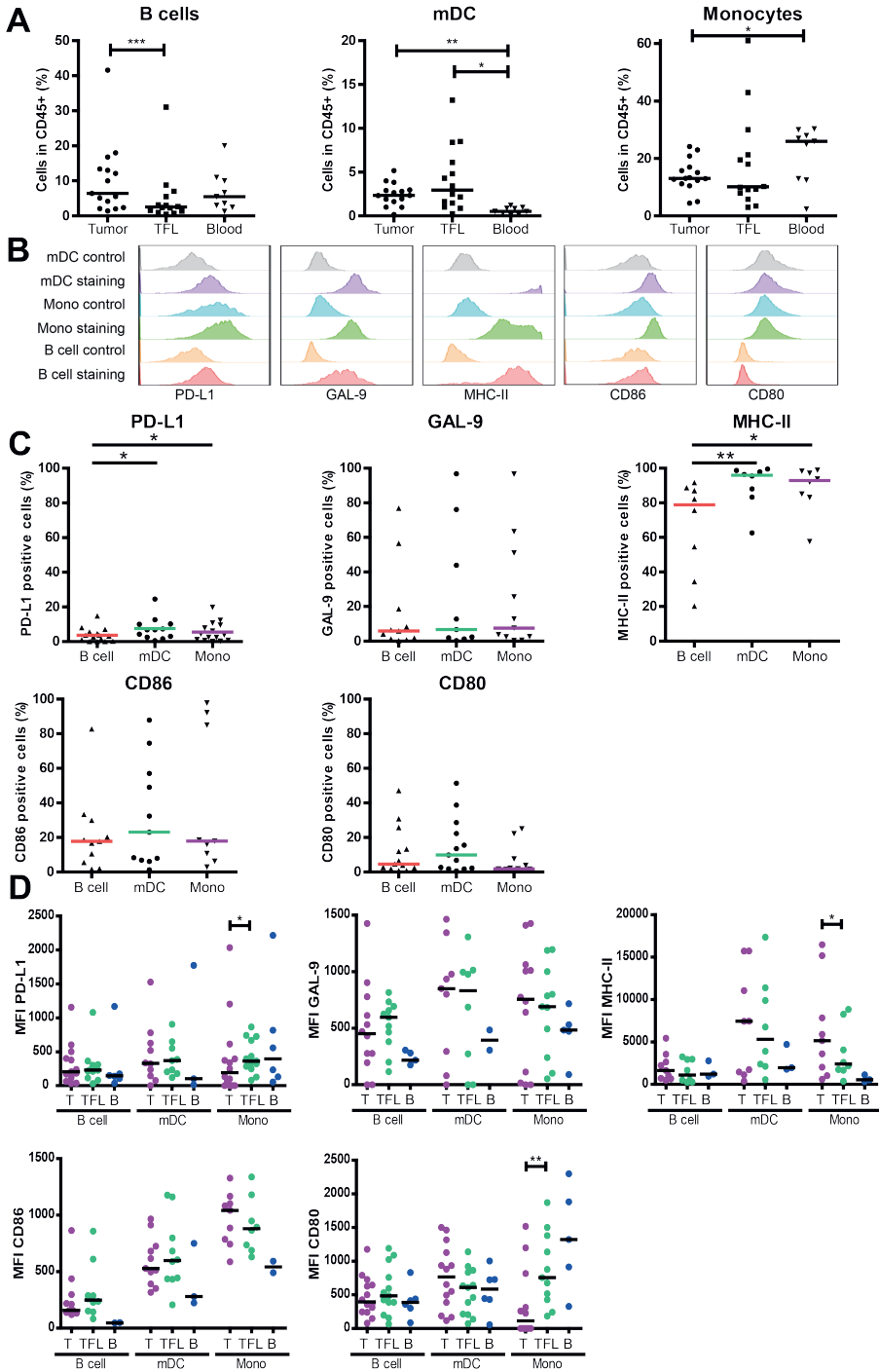


Figure 4. Tumor-infiltrating T cells expressing inhibitory receptors show increased expression of activation markers. ►

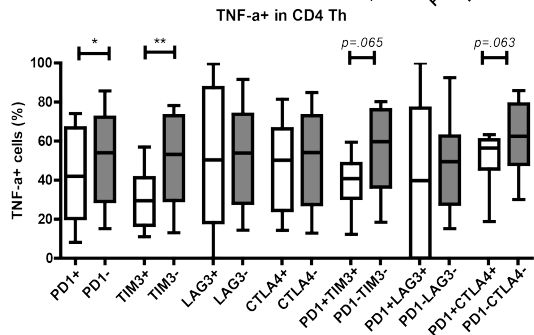
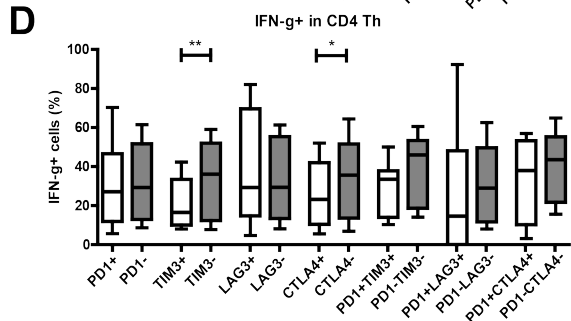
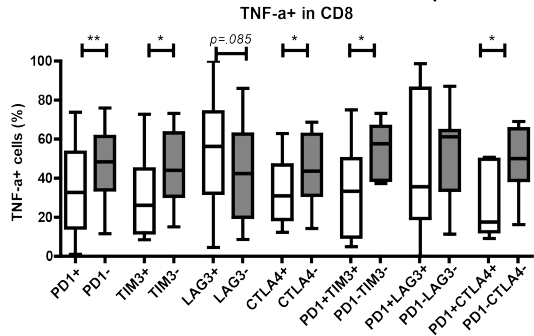
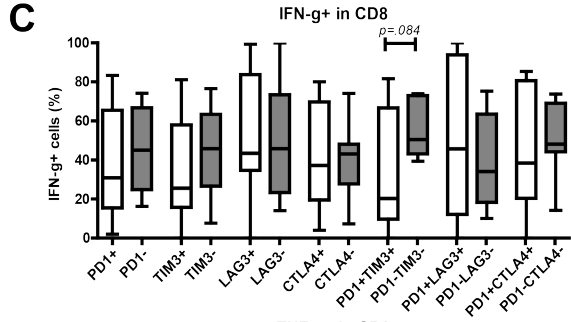
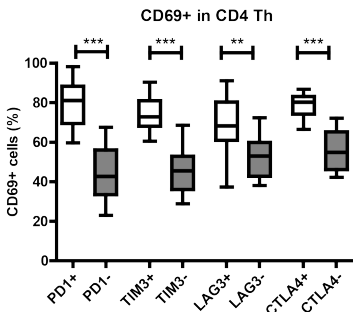
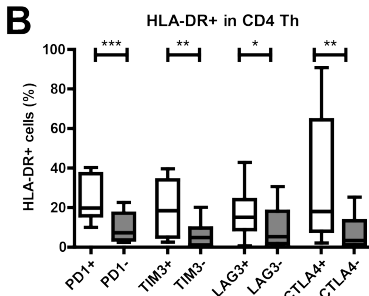
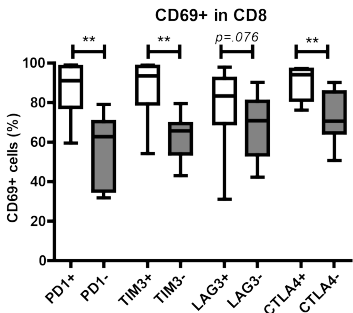
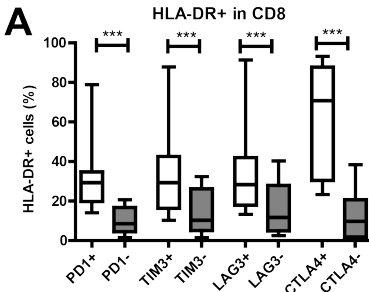
TIL from MMR-proficient LM-CRC were stained *ex vivo* with antibodies against surface activation markers HLA-DR and CD69. **A-B.** The frequencies of HLA-DR⁺ or CD69⁺ cells in **(A)** CD8⁺ CTL and **(B)** CD4⁺ Th that do or do not express PD-1, TIM3, LAG3, or CTLA4 are presented (n=9-11). Lines show medians, whiskers depict minimum to maximum. Differences were analyzed by paired t test or Wilcoxon matched pairs test. **C-D.** TIL from MMR-proficient LM-CRC were stimulated with PMA and ionomycin at 37°C for five hours, in the presence of protein transport inhibitor brefeldin for the last four hours, followed by intracellular cytokine staining. The frequencies of cytokine-producing cells in **(C)** CD8⁺ CTL and **(D)** CD4⁺ Th that do or do not express inhibitory receptors are presented (n=7-12). Lines show medians, whiskers depict Min to Max, boxes indicate the 25th to 75th percentiles. Differences were analyzed by paired t test or Wilcoxon matched pairs test; * p < 0.05, ** p < 0.01, *** p < 0.001.

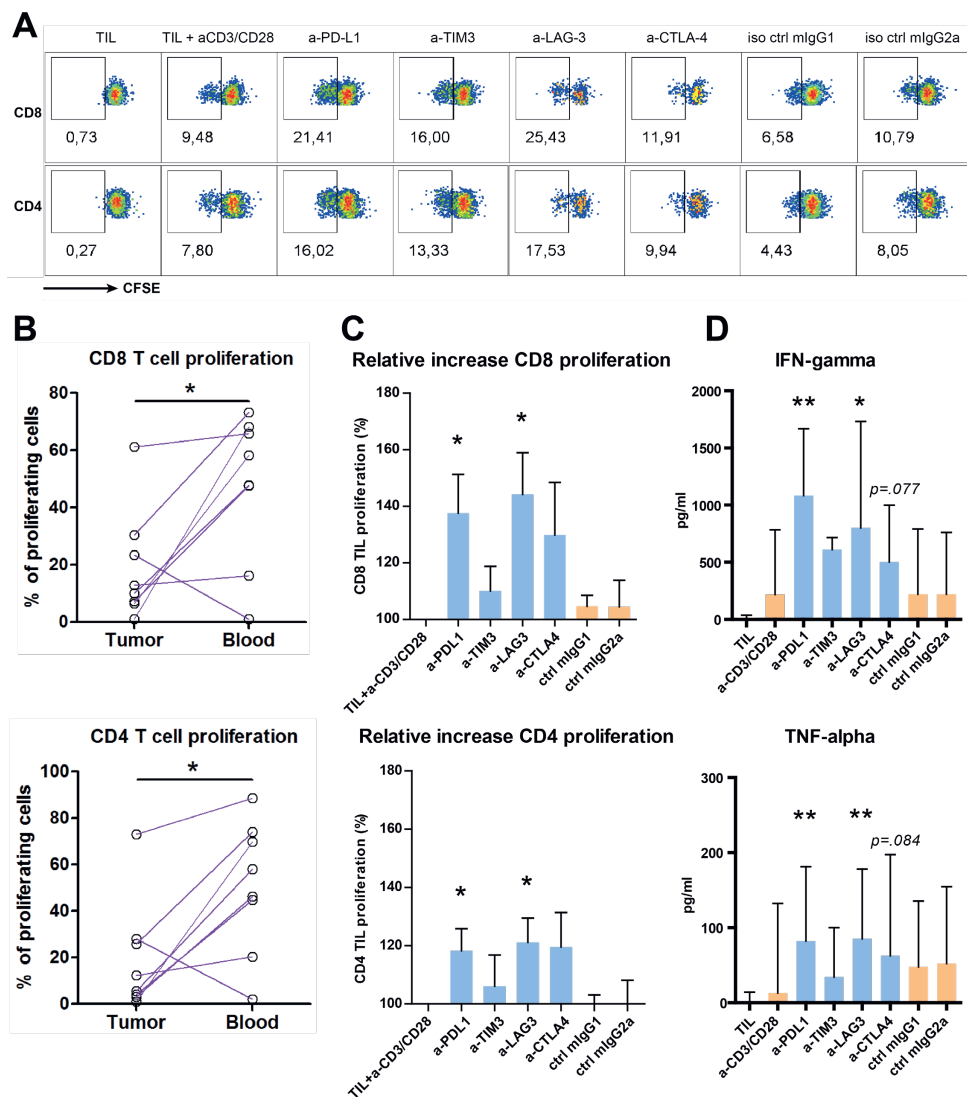
Intra-tumoral antigen-presenting cells express inhibitory ligands.

To study the expression of inhibitory ligands PD-L1, galectin 9, MHC-II molecules, CD86 and CD80 on APC in LM-CRC tissues, we measured these molecules by flow cytometry. Three major APC subsets BDCA-1⁺CD19⁻ mDC, CD14⁺ monocytes and CD19⁺ B cells were found in all tumors. The frequency of B cells was higher in tumors than in TFL, and the frequency of mDC was higher in tumors and TFL than in the blood, whereas the frequency of monocytes was lower in tumors than in the blood (**Fig. 3A**). The three different tumor-infiltrating APC populations expressed the five ligands at different levels and considerable variations between individual patients were observed (**Fig. 3B, C**). Intra-tumoral mDC and monocytes contained higher proportions of PD-L1⁺ and MHC-II⁺ cells than intra-tumoral B cells. The median fluorescence intensities of five ligands in APC subsets in the tumor, TFL and blood are presented in **Fig. 3D**, showing that the expression of inhibitory ligands is generally not increased on tumor-infiltrating APC compared to APC in TFL. Together, the abovementioned data suggest that inhibitory interactions between T cells and APC in MMR-proficient LM-CRC are possible.

Intra-tumoral T cells expressing inhibitory receptors show increased levels of activation markers.

Considering that increased expression of inhibitory receptors on T cells can be induced by recent activation, or by chronic stimulation that may lead to T cell dysfunctionality, we examined the *ex vivo* activation status and *in vitro* effector cytokine production of effector T cells derived from MMR-proficient LM-CRC. First we compared the expression of activation markers HLA-DR and CD69 on intra-tumoral T cells that do or do not express inhibitory receptors. Interestingly, PD-1⁺, TIM3⁺, LAG3⁺ or CTLA4⁺ CTL and Th showed a more activated status than PD-1⁻, TIM3⁻, LAG3⁻ or CTLA4⁻ CTL and Th, respectively (**Fig. 4A, B**). Subsequently, we assessed effector cytokine production of tumor-derived T cells after short-term PMA and ionomycin stimulation. Despite the activated status, the frequencies of inhibitory receptor positive CTL and Th cells that produced IFN- γ and TNF- α were reduced or similar to those in the respective receptor negative T cells (**Fig. 4C, D**). Interestingly, LAG3⁺ CTL and Th cells did not show reduction in cytokine production. Because among all studied inhibitory receptors, tumor-infiltrating CTL and Th showed the highest expression of PD-1 (**Fig. 2C, D**), we analyzed co-expression of PD-1 and the other three receptors. Co-expression of PD-1 and either TIM3, LAG3 or CTLA4 was found, especially in





CD8⁺ CTL, but expression of TIM3, LAG3 or CTLA4 without PD-1 was also observed (**Supplementary Fig. S5**). Similar to single receptor positive CTL and Th, double receptor positive CTL and Th showed reduced or comparable frequencies of IFN- γ and TNF- α producing cells to double receptor negative cells, while LAG3⁺PD-1⁺ CTL and Th did not show significant reduction in cytokine production (**Fig. 4C, D**). These data demonstrate that in general intra-tumoral T cells that express inhibitory receptors do not produce more effector cytokines, despite the activated status.

◀ **Figure 5. Antibody blockade of LAG3 or PD-L1 boosts *ex vivo* proliferation and cytokine production of intra-tumoral T cells from MMR-proficient LM-CRC in response to polyclonal stimuli.**

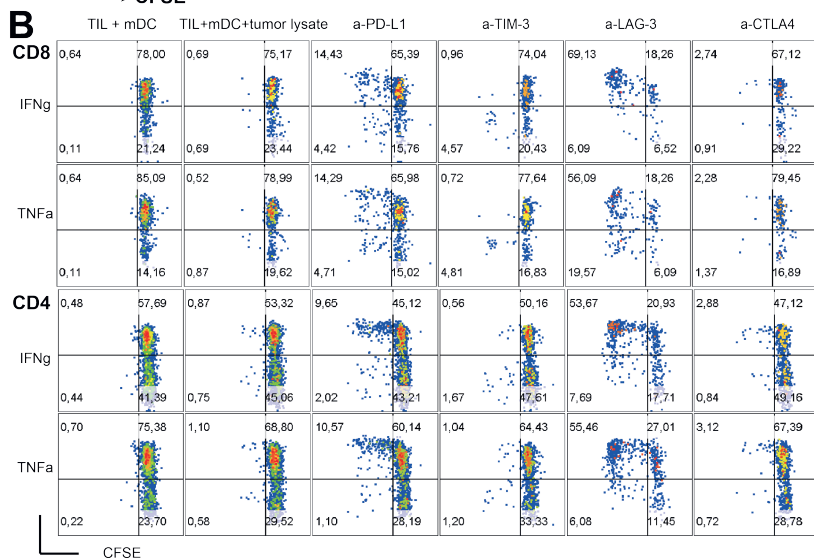
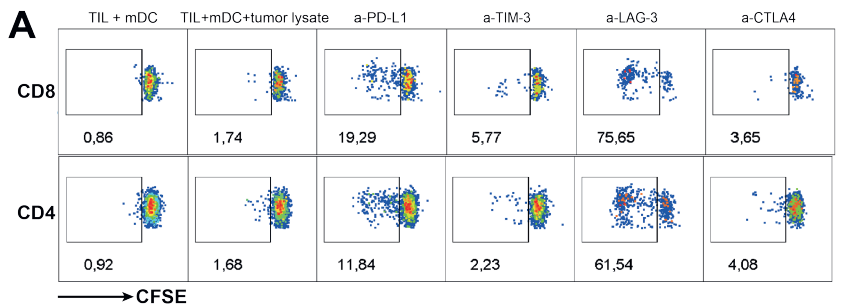
CFSE-labeled TIL from LM-CRC patients were stimulated with CD3/CD28 beads for four days, in the presence or absence of 10 $\mu\text{g}/\text{ml}$ antagonistic antibodies. **A.** Representative dot plots of CD3⁺CD8⁺ and CD3⁺CD4⁺ TIL proliferation in response to CD3/CD28 beads (a-CD3/CD28) in the presence or absence of antagonistic antibodies (a-) or isotype controls (iso ctrl). Dotplots indicated by "TIL" show proliferative responses in the absence of CD3/CD28 beads. In all other conditions, CD3/CD28 beads were added. **B.** The percentages of proliferating cells (CFSE-low) within CD8⁺ and CD4⁺ T cells derived from the tumor or blood in response to CD3/CD28 beads without addition of any antagonistic antibody. Values of individual patients are presented. **C.** Effects of antibody blockade of inhibitory interactions on CD8⁺ and CD4⁺ TIL proliferation (n=7-9). Because the proliferative responses differed between patients, the results are reported as relative proliferation in the presence of antibodies compared to baseline proliferation, which was calculated by dividing the percentages of proliferating (CFSE-low) T cells in the presence of antagonistic antibody or isotype control antibody by the percentages in the control condition with only CD3/CD28 beads. Values are depicted as means with standard error of the mean. **D.** IFN- γ and TNF- α accumulation in culture supernatants was quantified at day four by enzyme-linked immunosorbent assay. Values are depicted as medians with interquartile range (n=10-11). Differences were analyzed by paired t test or Wilcoxon matched pairs test; * p < 0.05, ** p < 0.01.

Antibody blockade of LAG3 or PD-L1 boosts *ex vivo* proliferation and effector cytokine production of T cells derived from MMR-proficient LM-CRC.

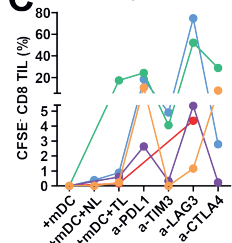
Because PD-1, TIM3, LAG3 and CTLA4 are upregulated on T cells in MMR-proficient LM-CRC tumors, we tested whether blockade of the PD-1/PD-L1, TIM3/galectin 9, LAG3/MHC-II or CTLA4/CD80/CD86 pathways could enhance the effector functions of tumor-derived T cells. We stimulated CFSE-labeled total tumor-infiltrating mononuclear leukocytes with CD3/CD28 beads, in the presence or absence of antagonistic antibodies against human PD-L1, TIM3, LAG3, CTLA4 or isotype controls (mIgG1 or mIgG2a). After four days of culture, T cell proliferation was measured by flow cytometry (**Fig. 5A**), and effector cytokine secretion in the culture supernatants was quantified by enzyme-linked immunosorbent assay. **Fig. 5B** illustrates that the baseline proliferation of CD8⁺ and CD4⁺ T cells derived from tumors was significantly lower than that of T cells from the blood of the same patients, indicating the proliferative function of intra-tumoral T cells is impaired compared to circulating T cells of patients with MMR-proficient LM-CRC. Interestingly, treatment with anti-LAG3 antibody or anti-PD-L1 antibody significantly increased the proliferation of both CD8⁺ and CD4⁺ TIL compared with the control condition without antagonistic antibody (**Fig. 5C**). These two antibodies also significantly increased IFN- γ and TNF- α secretion (**Fig. 5D**).

Antibody blockade of LAG3 or PD-L1 boosts *ex vivo* responses of T cells derived from MMR-proficient LM-CRC to autologous tumor antigens.

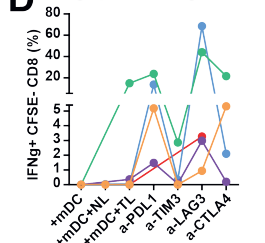
To investigate whether blockade of the aforementioned inhibitory pathways can enhance tumor-specific anti-tumor T cell responses, we stimulated CFSE-labeled total tumor-infiltrating mononuclear leukocytes with autologous blood-derived mDC preloaded with autologous tumor lysates, in the presence or absence of antagonistic antibodies, and measured CD8⁺ and CD4⁺ T cell proliferation after six days.



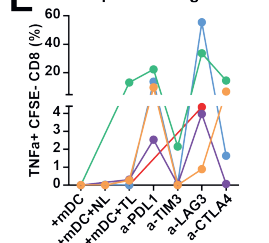
C CD8 TIL proliferation



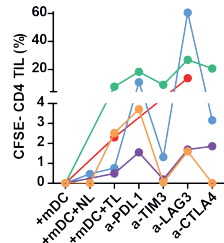
D IFNg+ proliferating CD8 TIL



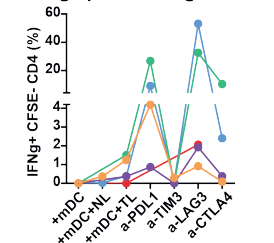
E TNFa+ proliferating CD8 TIL



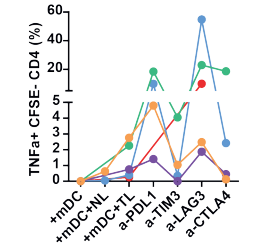
F CD4 TIL proliferation



G IFNg+ proliferating CD4 TIL



H TNFa+ proliferating CD4 TIL



◀ **Figure 6. Antibody blockade of LAG3 or PD-L1 boosts *ex vivo* responses of intra-tumoral T cells from MMR-proficient LM-CRC to autologous tumor antigens.**

Blood mDC loaded with autologous tumor lysates were used to stimulate CFSE-labeled TIL, in the presence or absence of 10 µg/mL antagonistic antibodies. After six days T cell proliferation and intracellular cytokine production were analyzed after re-stimulation with PMA and ionomycin. **A-B.** Representative dot plots of T cell proliferation (**A**), IFN-γ and TNF-α expression (**B**) in CD3⁺CD8⁺ and CD3⁺CD4⁺ TIL, in response to autologous mDC pre-loaded with tumor lysates (TIL+mDC+tumor lysate), in the presence or absence of antagonistic antibodies. TIL responses to mDC that were not pre-loaded with tumor lysates (TIL+mDC) served as controls to determine non-antigen-specific TIL proliferation and cytokine production. **C-E.** Collective data of five patients tested. Each line and each color represent one patient. The results are reported as net tumor-specific responses, calculated by subtracting the percentages of proliferating (CFSE-low) T cells (**C**) or IFN-γ⁺ (**D**) or TNF-α⁺ (**E**) proliferating T cells in the control condition (mDC without tissue lysates) from the percentages in the conditions with tumor lysates (TL) in the absence or presence of antagonistic antibody. In two experiments an additional control was included, in which TIL were stimulated with blood mDC pre-loaded with normal liver lysates (NL), which did not lead to increased TIL responses.

Increased TIL proliferation against mDC loaded with tumor lysates compared with mDC without tissue lysates was observed in all five tested patients, while loading of mDC with normal liver lysates did not increase or minimally increased TIL proliferative responses (**Fig. 6A, C**). Addition of anti-PD-L1 antibody enhanced proliferative responses of TIL in all four tested patients, while treatment with anti-LAG3 antibody increased both CD8⁺ and CD4⁺ TIL proliferation in four out of five patients. In three out of four patients anti-LAG3 antibody boosted CD8⁺ and/or CD4⁺ TIL responses to higher levels than anti-PD-L1 antibody (**Fig. 6A, C**). After five hours of restimulation, intracellular expression of IFN-γ and TNF-α in proliferating T cells was analyzed, and was found to be enhanced by both anti-LAG3 and anti-PD-L1 antibodies in most patients (**Fig. 6B, D, E**). Like in CD3/CD28 stimulations, anti-TIM3 and anti-CTLA4 antibodies boosted TIL responses less strongly and also in less patients.

Higher LAG3 expression on intra-tumoral CD8⁺ T cells is associated with longer progression-free survival of patients with MMR-proficient LM-CRC.

In a subset of patients, we could analyze associations between the frequencies of inhibitory receptor positive TIL and patient progression-free survival after the LM-CRC resection. In survival analysis higher expression of LAG3 on CD8⁺ TIL, CD4⁺ Th and Treg was associated with longer time to recurrence (**Fig. 7**), whereas higher expression of PD-1 or TIM3 on CD8⁺ TIL was associated with shorter time to recurrence (data not shown). In multivariable analysis only LAG3 expression on CD8⁺ TIL was demonstrated to be an independent predictor of progression-free survival (**Table 2**), which supports its functional relevance to anti-cancer immunity in TIL of LM-CRC. We hypothesize that LAG3⁺CD8⁺ TIL may be highly activated T cells (**Fig. 4A**) stimulated by tumor antigens, but subsequently inhibited by increased and continuous expression of LAG3 and interaction with its ligands on APC and tumor cells, yet with preserved effector functions (**Fig. 4C**), which may control tumor growth. Because the sample size is small, these results need conformation in an independent study. In one fourth of the patients we only have data of LAG3 expression on CD8⁺ TIL but not on CD4⁺ Th or Treg, so we did not include the latter T cell subsets in the

multivariable analysis. The death events were too few to analyze overall survival of LM-CRC patients.

DISCUSSION

Checkpoint inhibitors have recently emerged as attractive treatments for several types of solid cancers. However, PD-1 and PD-L1 blocking antibodies were proven unsuccessful in CRC, with the exception of MMR-deficient CRC.^{23-25, 27, 28} The first aim of this study was to investigate whether the composition of the immune infiltrates and the intra-tumoral expression levels of inhibitory molecules in CRC metastases in the liver environment differ from those in primary CRC tumors and metastases outside the liver, which would suggest potential differences in sensitivity to checkpoint inhibitors among CRC tumors at different anatomical locations. The second objective was to determine whether targeting of inhibitory checkpoint pathways by antagonistic antibodies can enhance the functionality and anti-tumor responses of tumor-infiltrating T cells in LM-CRC. Because the incidence of MMR deficiency in LM-CRC is low, we focused on MMR-proficient tumors.

This study is the first to investigate the expression levels of inhibitory receptors on TIL in LM-CRC. Similar to what we reported in hepatocellular carcinoma,⁴⁴ intra-tumoral CD8⁺ CTL and CD4⁺ Th in MMR-proficient LM-CRC displayed increased expression of PD-1, TIM3, CTLA4 and/or LAG3 compared to their counterparts in TFL and blood. In addition, we found selectively enhanced expression of PD-1 and TIM3 on intra-tumoral Treg (**Fig. 2C-E**). The elevated frequencies of inhibitory receptor positive cells in TIL together with the expression of their ligands on tumor-infiltrating APC (**Fig. 3B-D**) suggest that these inhibitory checkpoint pathways may be involved in intra-tumoral suppression of T cells in MMR-proficient LM-CRC.

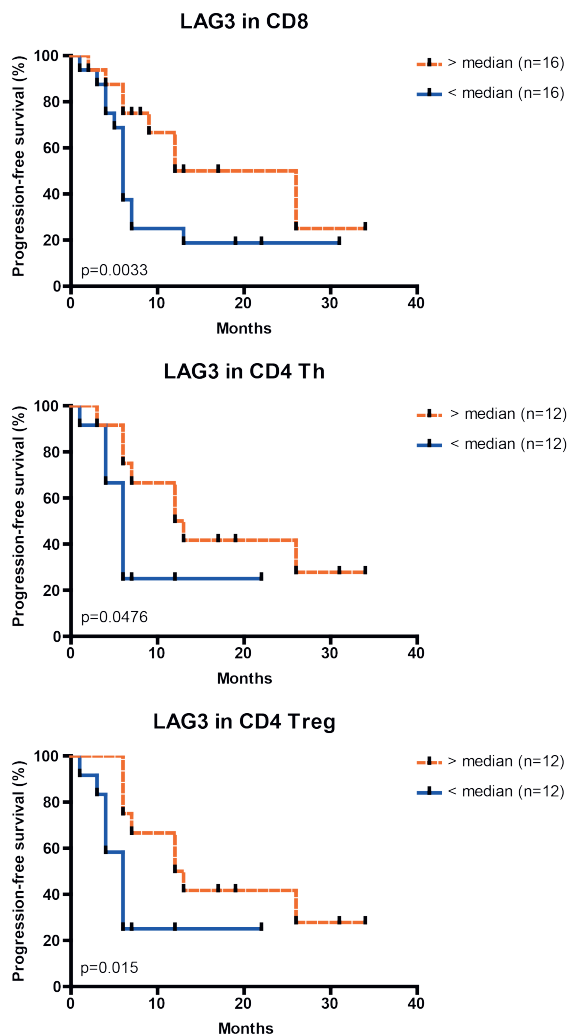
Interestingly, we observed higher expression of PD-1 and/or TIM3 on CD8⁺ CTL and Treg in LM-CRC than in primary CRC, while expression of LAG3, TIM3 and/or PD-1 on CD8⁺ CTL, Th and Treg was higher in LM-CRC than in PM-CRC (**Fig. 1B**). We hypothesize that these differences are due to the unique tolerogenic properties of the liver environment, which induces expression of inhibitory receptors on hepatic T cells both in diseased and healthy conditions.^{37, 38} Furthermore, we found increased proportions of CD8⁺ CTL in LM-CRC and PM-CRC compared with primary CRC (**Fig. 1A**). The observed differences between

Table 2. Multivariable Cox proportional Hazard regression analysis of progression-free survival of patients with MMR-proficient LM-CRC.

Variables	P value	HR	95% CI for HR	
			Lower	Upper
PD-1 on CD8 ⁺ TIL	.160	2.418	.706	8.283
TIM3 on CD8 ⁺ TIL	.774	1.183	.375	3.732
LAG3 on CD8 ⁺ TIL	.032	.351	.135	.912

Abbreviations: TIL, tumor-infiltrating lymphocytes; HR, hazard ratio; CI, confidence interval.

The hazard ratio is interpreted as the chance of recurrence occurring in the "> median" group to the chance of recurrence occurring in the "< median" group.



◀ **Figure 7. Kaplan-Meier curves of progression-free survival (time to recurrence) in relation to LAG3 expression on intra-tumoral T cells in MMR-proficient LM-CRC.**

The cutoff values to divide the patients into two groups are the median percentages of LAG3⁺ cells in tumor-infiltrating CD8⁺ CTL, CD4⁺Foxp3⁺ Th or CD4⁺Foxp3⁺ Treg cells.

Statistical analysis was performed by the Gehan-Breslow-Wilcoxon test, and differences were considered significant when $p < 0.05$.

MMR-proficient LM-CRC and MMR-proficient primary CRC are to some extent reminiscent of those found between MMR-deficient primary CRC and MMR-proficient primary CRC by Llosa *et al.*³¹ They demonstrated that MMR-deficient primary CRC displayed higher infiltration with CD8⁺ CTL as well as upregulated expression of PD-1, PD-L1, CTLA4 and LAG3 compared to MMR-proficient primary CRC, and suggested that these differences contributed to the enhanced clinical

responsiveness to anti-PD-1 therapy of microsatellite instable CRC compared with microsatellite stable CRC.³¹ In addition, we found that LM-CRC contained increased frequencies of professional APC subsets (mDC and monocytes) (**Fig. 1C**), which may result in improved presentation of tumor antigens to intra-tumoral T cells as well as more PD-L1 and MHC-II expression in LM-CRC compared with primary CRC, because in LM-CRC mDC and monocytes expressed more PD-L1 and MHC-II than B cells (**Fig. 3C**). Hierarchical clustering analysis showed that the immune phenotypical data of most LM-CRC tumors clustered together as did the data of most primary CRC tumors (**Supplementary Fig. S2**). These data confirm those of Halama *et al.*, who demonstrated similar heterogeneity in composition of immune infiltrates between paired primary CRC tumors and liver metastases derived from the same patients.³⁵ We extracted and statistically analyzed their paired data of primary CRC and LM-CRC from 16 patients

and found a higher CD8⁺ cell density in LM-CRC than in primary CRC (**Supplementary Fig. S6**).

Moreover, discrepancies in somatic mutations, copy number alterations, genetic and epigenetic molecular alterations between primary CRC tumors and matched liver metastases were revealed in up to a half of the cases, which may lead to higher mutational load and thereby more neo-epitopes in LM-CRC.⁴⁵⁻⁴⁸ Together, these findings indicate major differences between liver metastases and primary CRC as well as peritoneal metastases, including differences in immune cell infiltration and inhibitory molecule expression, which may be at least partly induced by the liver environment. We therefore suggest that TIL of MMR-proficient LM-CRC may be more sensitive to PD-1/PD-L1 blockade and other checkpoint inhibitors than TIL of MMR-proficient primary CRC and CRC metastases at other anatomical locations. Nevertheless, to precisely compare the effects of checkpoint inhibitors on TIL of primary CRC and LM-CRC, experiments with TIL from paired tissues might be needed but were unfortunately not available in the current study.

To determine whether TIL expressing inhibitory receptors represent T cells that are recently activated upon recognition of tumor antigens, or are dysfunctional due to chronic antigenic stimulation, we studied their *ex vivo* activation status and *in vitro* effector cytokine production. Similar to what we reported in hepatocellular carcinoma,⁴⁴ intra-tumoral CD4⁺ Th and CD8⁺ CTL expressing any of the four inhibitory receptors showed a more activated status but produced reduced or similar levels of effector cytokines than their counterparts not expressing the corresponding inhibitory receptor (**Fig. 4**). However, in our *ex vivo* cultures, tumor cells that may express inhibitory ligands are lacking, so the TIL might be less functional *in vivo* and need checkpoint inhibitors. Nevertheless, proliferative responses of tumor-derived T cells to CD3/CD28 stimulation were lower than those of circulating T cells (**Fig. 5B**). Consistent with what others reported on IFN- γ production by CD8⁺ TIL in primary CRC patients,^{49, 50} our results demonstrate a certain degree of dysfunctionality of intra-tumoral CD4⁺ Th and CD8⁺ CTL in MMR-proficient LM-CRC, which may be at least partly due to inhibitory checkpoint interactions between T cells and APC subsets in the TIL cultures, but not complete dysfunctionality.

This study is also the first to investigate the effects of antibody blockade of four inhibitory checkpoint pathways on responses of TIL isolated from MMR-proficient LM-CRC. In both polyclonal T cell activation and tumor-specific TIL stimulation assays, increased proliferation of TIL and increased production of effector cytokines were observed upon the addition of anti-LAG3 antibody or anti-PD-L1 antibody (**Fig. 5 and Fig. 6**). In some patients *ex vivo* anti-tumor responses of TIL were more robustly enhanced by anti-LAG3 antibody than by anti-PD-L1 antibody (**Fig. 6**), suggesting that LAG3 might be the most promising target for immunotherapy of LM-CRC among all four checkpoint pathways tested in this study. However, these data need confirmation using TIL from a larger number of patients. The superiority of LAG3 blockade compared to PD-L1 blockade was more seen in tumor antigen-specific stimulation than in polyclonal stimulation. We hypothesize that the small proportion of LAG3⁺ TIL is strongly enriched with tumor antigen-reactive T cells, which are known to constitute only a small proportion of all tumor-infiltrating T cells. In addition, we propose that PD-1 is expressed on a larger fraction of TIL which

contains more non-tumor antigen-specific T cells. Although TIM3 blockade was reported to reduce T cell apoptosis and inhibit tumor growth in a mouse CT26 colon tumor model,⁵¹ little effect was observed in our experiments using TIL derived from human LM-CRC. This result also contrasts to our recent observation that *ex vivo* responses of TIL isolated from hepatocellular carcinomas can be invigorated by TIM3 blockade.⁴⁴ This difference may relate to the lower expression of galectin 9 on APC subsets in LM-CRC compared to hepatocellular carcinomas.

Because we were interested in the net effects of checkpoint inhibitors on TIL responses in a context that reflected the LM-CRC tumor microenvironment as much as possible, we used total tumor-infiltrating mononuclear leukocytes in our functional assays, which contained both T cells expressing inhibitory receptors and APC expressing inhibitory ligands. As a consequence, tumor-infiltrating Treg,^{40, 41} type 1 regulatory T cells⁵² and probably other types of immune suppressor cells were also present in these assays. Therefore, the reported functional effects of checkpoint inhibitors on effector T cells in these assays may be partly indirect, mediated by effects of these antibodies on suppressor cells. The effects of checkpoint inhibitor on effector T cells in our assays might even be counteracted by its effects on suppressor cells. We found that half of Treg in LM-CRC tumors expressed PD-1, and blocking PD-1/PD-L1 interaction was shown to enhance the suppressive function of Treg isolated from liver tissues of patients with chronic hepatitis C infection.⁵³

Interestingly, higher expression of LAG3 on CD8⁺ TIL was associated with longer time to recurrence of patients with LM-CRC. We hypothesize that LAG3⁺CD8⁺ TIL are cells which have recently been activated (**Fig. 4A**) by recognition of antigens in the tumor, and upregulate LAG3 expression in response to activation but still have functional capacity to exert effector functions and delay tumor growth (**Fig. 4C**). LAG3 expression is upregulated on T cells after activation and differentiation,^{54, 55} and intra-tumoral T cells that recognize tumor antigens are characterized by expression of LAG3 and other inhibitory receptors.⁵⁶ Although chronic tumor antigen stimulation in the tumor microenvironment can induce T cell exhaustion with simultaneous induction of high expression of multiple inhibitory receptors, this does not mean that all CD8⁺ TIL which express one or more inhibitory receptors at any level are functionally exhausted. Indeed, a recent mouse study showed that tumor antigen-specific TIL which expressed LAG3 or PD-1 produced IFN- γ *in situ* and had cytolytic potential.⁵⁷ Likewise, in the current study we observed that LAG3⁺CD8⁺ TIL in LM-CRC were not functionally impaired (**Fig. 4C**). Nevertheless, they could be functionally invigorated upon antibody blockade of LAG3 (**Fig. 5 and Fig. 6**), indicating that interaction of LAG3 with its ligands serves as an extrinsic mechanism in the tumor microenvironment which inhibits their functionality.

Our study has several limitations: (1) Due to the finite numbers of isolated TIL, the tumor-specific stimulation assay could only be performed in a limited number of LM-CRC patients (**Supplementary Table S1**), neither could all the conditions be tested in every functional assay, nor could the relation between the expression of inhibitory molecules on TIL and the effects of checkpoint inhibitors on TIL responses be well analyzed. (2) We could not study paired LM-CRC, primary CRC and PM-CRC tumors

from the same patients because primary and metastatic CRC tumors were resected at different time points and in different hospitals. (3) MMR-deficient tumors could not be studied well, because we received fresh tissues from only a few MMR-deficient tumors during our study.

In conclusion, increased frequencies of CD8⁺ CTL, mDC and monocytes as well as increased inhibitory receptor expression on intra-tumoral T cells in MMR-proficient LM-CRC suggest that TIL of MMR-proficient LM-CRC may be more sensitive to immune checkpoint inhibitors than TIL of MMR-proficient primary CRC. Blockade of LAG3 and PD-L1 can both enhance *ex vivo* functions of tumor-infiltrating T cells from MMR-proficient LM-CRC. Therefore, these two inhibitory pathways may be potential immunotherapeutic targets for the most prevalent metastatic liver cancer, despite the lack of MMR deficiency. Clinical studies focusing on responses of LM-CRC to anti-LAG3 and combination with anti-PD-L1 or anti-PD-1 antibodies^{12, 58} are required to conclude whether this prediction based on our preclinical study is correct.

PATIENTS AND METHODS

Patients and specimens

Fifty-three patients who were eligible for surgical resection of LM-CRC were enrolled in the study from November 2013 to March 2017. Another twelve patients who received surgical resection of primary CRC and another eleven patients whose PM-CRC were surgically resected before hyperthermic intraperitoneal chemotherapy were enrolled in the study from February 2016 to December 2016. Fresh tissue samples from hepatic tumors, tumor-free liver tissues as distant as possible from the tumor (minimum 1cm distance), colorectal tumors and peritoneal tumors were obtained. Peripheral blood from LM-CRC patients was also collected on the day of resection. None of the patients received chemotherapy or immunosuppressive therapy at least three months before surgery. The clinical characteristics of the patients are summarized in **Table 1**. The study was approved by the local ethics committee, and signed informed consent from all patients was obtained before tissue and blood donation.

Cell preparation

Peripheral blood mononuclear cells (PBMC) were isolated by Ficoll density gradient centrifugation. Single cell suspensions from tumors and tumor-free liver were obtained by tissue digestion. Briefly, fresh tissues were first cut into small pieces and then digested with 0.125 mg/mL collagenase IV (Sigma-Aldrich, St. Louis, MO) and 0.2 mg/mL DNase I (Roche, Indianapolis, IN) in Hanks' Balanced Salt solution with Ca²⁺ and Mg²⁺ (Sigma, Zwijndrecht, The Netherlands) for 30 minutes at 37 °C with interrupted gently swirling. Cell suspensions were filtered through 100 µm pore cell strainers (BD Biosciences, Erembodegem, Belgium) and mononuclear leukocytes were obtained by Ficoll density gradient centrifugation. Viability was determined by trypan blue exclusion.

Flow cytometric analysis

Fresh peripheral blood mononuclear cells (PBMC) and leukocytes isolated from tissues were analyzed for expression of surface and intracellular markers using specific antibodies (**Supplementary Table S2**). Cell surface staining with fluorochrome-conjugated antibodies was performed in the dark at 4°C for 30 minutes, then cells were washed and resuspended in phosphate buffered saline with 0.2 mM EDTA and 0.5% human serum. For Foxp3 and CTLA4 staining, cells were fixed and permeabilized using the Foxp3 staining buffer set (eBioscience, Vienna, Austria). For intracellular cytokine staining, cells were stimulated with 40 ng/mL PMA (Sigma, Zwijndrecht, The Netherlands) and 1 µg/mL ionomycin (Sigma) at 37°C for five hours in the presence of 5 µg/mL brefeldin (Sigma) for the last four hours, followed by staining of IFN-γ and TNF-α upon fixation and permeabilization using the Foxp3 staining buffer set. Dead cells were excluded by using a LIVE/DEAD fixable dead cell stain kit with aqua fluorescent reactive dye (Invitrogen, Paisley, UK). Cells were measured using a FACS Canto II flow cytometer (BD Biosciences, San Diego, USA) and analyzed using FlowJo software (version 10.0, LLC). Appropriate isotype control antibodies were used for gating purposes (**Supplementary Table S2**).

Ex vivo polyclonal T cell activation assay

All LM-CRC cell cultures were performed in complete medium RPMI 1640 (Lonza, Breda, The Netherlands) supplemented with 10% human AB serum (Invitrogen), 2mM L-glutamine (Invitrogen), 50 mM HEPES Buffer (Lonza), 1% penicillin-streptomycin (Life Technologies), 5mM Sodium Pyruvate (Gibco) and 1% minimum essential medium non-essential amino acids, at 37°C. TIL and PBMC from LM-CRC were labeled with 0.1 µM carboxyfluorescein diacetate succinimidyl ester (CFSE, Invitrogen); afterwards 10⁵ TIL or PBMC were cultured in 200 µl complete medium in each well of a 96-well round-bottom culture plate and stimulated with anti-human CD3/CD28 dynabeads (Gibco-Life Technologies AS, Norway) at a cell : bead ratio of 10:1, in the presence or absence of 10 µg/ml antagonistic monoclonal antibodies against human PD-L1 (clone 5H1, kindly provided by Dr. Haidong Dong, Mayo Clinic College of Medicine⁵⁹), TIM3 (clone F38-2E2, Biolegend, San Diego, USA^{60,61}), LAG3 (clone 17B4, AdipoGen, Liestal, Switzerland⁶²) or CTLA4 (clone BNI3, Beckman Coulter, Marseille, France⁶³), or isotype-matched control antibodies (mIgG1 and mIgG2a, Biolegend, London, UK). In preliminary experiments a cell : bead ratio of 10:1 was established to provide sub-optimal stimulation of T cell proliferation. After four days, culture supernatant was collected and frozen at -20°C until secretion of IFN-γ and TNF-α was quantified by enzyme-linked immunosorbent assay (ELISA, Ready-SET-Go!, eBioscience). CFSE-labeled cells were harvested and stained with CD8, CD4 and CD3 antibodies. Dead cells were excluded by using the LIVE/DEAD fixable dead cell stain kit with aqua fluorescent reactive dye, and T cell proliferation was determined based on CFSE dilution by flow cytometric analysis.

Ex vivo tumor-specific T cell stimulation assay

Tumor lysates and normal liver lysates were generated from a small piece of freshly resected metastatic liver tumor or TFL by five cycles of freezing and thawing in phosphate buffered saline, followed by filtration (0.2 µm syringe filter), as previously described.^{40,41} Myeloid dendritic cells (mDC) were isolated

from patient autologous PBMC by depletion of CD19⁺ B cells followed by positive selection for BDCA-1 (BDCA-1 DC isolation kit, Miltenyi Biotec). mDC were cultured overnight with or without 20 µg/mL autologous tumor lysates or normal liver lysates, in the presence of 10 ng/mL granulocyte-macrophage colony-stimulating factor (Miltenyi Biotec) and 0.5 µg/mL polyinosinic : polycytidylic acid (InvivoGen, San Diego, CA). Simultaneously TIL isolated from LM-CRC were kept at 4°C in complete medium overnight. Thereafter TIL were labeled with 0.1 µM carboxyfluorescein diacetate succinimidyl ester (CFSE, Invitrogen), and 10⁵ TIL were co-cultured with autologous mDC preloaded with or without tumor lysates or normal liver lysates at an mDC : TIL ratio of 1:5, in the presence or absence of 10 µg/ml antagonistic monoclonal antibodies against human PD-L1 (clone 5H1, kindly provided by Dr. Haidong Dong, Mayo Clinic College of Medicine⁵⁹), TIM3 (clone F38-2E2, Biolegend, San Diego, USA⁴⁴), LAG3 (clone 17B4, AdipoGen, Liestal, Switzerland⁴⁴) or CTLA4 (clone BNI3, Beckman Coulter, Marseille, France⁶³), in 200 µl complete medium in each well of a 96-well round-bottom culture plate. After six days, cells were restimulated with PMA (40 ng/mL) and ionomycin (1 µg/mL) for five hours in the presence of 5 µg/mL brefeldin for the last four hours. Cells were then stained with CD8, CD4 and CD3 antibodies, followed by intracellular staining of IFN-γ and TNF-α upon fixation and permeabilization according to the manufacturer's instructions (eBioscience A&B fixation/permeabilization kit). Dead cells were excluded by using the LIVE/DEAD fixable dead cell stain kit with aqua fluorescent reactive dye, and T cell proliferation was determined based on CFSE dilution by flow cytometric analysis.

Determination of mismatch repair status by immunohistochemistry

Immunostainings were performed on formalin-fixed paraffin-embedded whole tissue sections (4 µm thick) using the Benchmark Ultra autoimmunostainer (Ventana Medical Systems Inc, Roche Group, Tucson, USA) according to the manufacturer's protocols and instructions. Briefly, deparaffinization was followed by heat-induced epitope retrieval in Ultra CC1 pre-diluted buffer for 48-60 minutes at 100°C. Primary antibodies anti-MLH1 (Novocastra; Leica Microsystems B.V., Amsterdam, The Netherlands; clone ES05; dilution 1:75), anti-PMS2 (Cell Marque, Rocklin, USA; clone EPR3947, ready to use), anti-MSH2 (Cell Marque, clone G219-1129; ready to use) and anti-MSH6 (Dako, Glostrup, Denmark; clone EP49; dilution 1:75) were applied and followed by incubation (from 40 minutes to 1 hour and 32 minutes). Upon antibody incubation Ventana standard signal amplification was performed, followed by ultraWash counter-staining with one drop of Hematoxylin (for 20 minutes) and one drop of bluing reagent (for 4 minutes). Then slides were removed from the stainer, washed in water with a drop of dishwashing detergent and mounted. These immunohistochemical stainings detected the presence or absence of the protein products of the MMR genes MLH1, PMS2, MSH2 and MSH6. The pattern of their loss provides information about which gene is not functioning properly. IHC staining was evaluated under a light microscope as follows: nuclear expression of all MMR proteins indicates an MMR-proficient tumor status, loss of nuclear expression of any of the proteins indicates an MMR-deficient tumor status.

Statistical analysis

The distributions of all continuous data set were analyzed for normality by the Shapiro-Wilk normality test. Differences between paired groups of data were analyzed by either paired t test or Wilcoxon matched pairs test according to their distribution. Differences between different groups of patients were analyzed by either unpaired t test or Mann-Whitney test according to their distributions. Correlation was analyzed by either Pearson or Spearman correlation test according to their distributions. These statistical analyses were performed using GraphPad Prism 5 (GraphPad Software). Hierarchical clustering was analyzed by one minus Pearson correlation using GENE-E (Broad Institute). Progression-free survival (time to recurrence) was calculated from the date of LM-CRC surgery to the date of event (LM-CRC recurrence), or the date of last follow-up. Patients lost to follow-up were censored as of the last day of follow-up. Survival curves were estimated by the Kaplan-Meier method. The Breslow test was used to assess differences between survival curves of different groups. For multivariable analysis, the Cox proportional Hazard regression analysis was used. These statistical analyses were performed using SPSS Statistics 21 (IBM). P values less than 0.05 were considered statistically significant (* $p < 0.05$; ** $p < 0.01$; *** $p < 0.001$).

Acknowledgements

We acknowledge Sonja Buschow from department of Gastroenterology and Hepatology for assisting with hierarchical clustering analysis and Nicole Elerer from department of Biostatistics for assisting with survival and multivariable analyses.

REFERENCES

1. Torre LA, Bray F, Siegel RL, Ferlay J, Lortet-Tieulent J, Jemal A. Global cancer statistics, 2012. *CA Cancer J Clin* 2015; 65:87-108.
2. Jalili-Nik M, Soltani A, Moussavi S, Ghayour-Mobarhan M, Ferns GA, Hassanian SM, Avan A. Current status and future prospective of Curcumin as a potential therapeutic agent in the treatment of colorectal cancer. *J Cell Physiol* 2017.
3. Kallini JR, Gabr A, Abouchaleh N, Ali R, Riaz A, Lewandowski RJ, Salem R. New Developments in Interventional Oncology: Liver Metastases From Colorectal Cancer. *Cancer J* 2016; 22:373-80.
4. Zarour LR, Anand S, Billingsley KG, Bisson WH, Cercek A, Clarke MF, Coussens LM, Gast CE, Geltzeiler CB, Hansen L, et al. Colorectal Cancer Liver Metastasis: Evolving Paradigms and Future Directions. *Cell Mol Gastroenterol Hepatol* 2017; 3:163-73.
5. Kemeny N. The management of resectable and unresectable liver metastases from colorectal cancer. *Curr Opin Oncol* 2010; 22:364-73.
6. Fonseca GM, Herman P, Faraj SF, Kruger JAP, Coelho FF, Jeismann VB, Ceconello I, Alves VAF, Pawlik TM, de Mello ES. Pathological factors and prognosis of resected liver metastases of colorectal carcinoma: implications and proposal for a pathological reporting protocol. *Histopathology* 2018; 72:377-90.
7. Engstrand J, Nilsson H, Stromberg C, Jonas E, Freedman J. Colorectal cancer liver metastases - a population-based study on incidence, management and survival. *BMC Cancer* 2018; 18:78.
8. Bartlett EK, Simmons KD, Wachtel H, Roses RE, Fraker DL, Kelz RR, Karakousis GC. The rise in metastasectomy across cancer types over the past decade. *Cancer* 2015; 121:747-57.
9. Tomlinson JS, Jarnagin WR, DeMatteo RP, Fong Y, Kornprat P, Gonen M, Kemeny N, Brennan MF, Blumgart LH, D'Angelica M. Actual 10-year survival after resection of colorectal liver metastases defines cure. *J Clin Oncol* 2007; 25:4575-80.
10. Nordlinger B, Sorbye H, Glimelius B, Poston GJ, Schlag PM, Rougier P, Bechstein WO, Primrose JN, Walpole ET, Finch-Jones M, et al. Perioperative FOLFOX4 chemotherapy and surgery versus surgery alone for resectable liver metastases from colorectal cancer (EORTC 40983): long-term results of a randomised, controlled, phase 3 trial. *Lancet Oncol* 2013; 14:1208-15.
11. Van Cutsem E, Kohne CH, Hitre E, Zaluski J, Chang Chien CR, Makhson A, D'Haens G, Pinter T, Lim R, Bodoky G, et al. Cetuximab and chemotherapy as initial treatment for metastatic colorectal cancer. *N Engl J Med* 2009; 360:1408-17.
12. Ascierto PA, McArthur GA. Checkpoint inhibitors in melanoma and early phase development in solid tumors: what's the future? *J Transl Med* 2017; 15:173.
13. Granier C, De Guillebon E, Blanc C, Roussel H, Badoual C, Colin E, Saldmann A, Gey A, Oudard S, Tartour E. Mechanisms of action and rationale for the use of checkpoint inhibitors in cancer. *ESMO Open* 2017; 2:e000213.
14. Rotte A, Jin JY, Lemaire V. Mechanistic overview of immune checkpoints to support the rational design of their combinations in cancer immunotherapy. *Ann Oncol* 2018; 29:71-83.
15. Anderson AC, Joller N, Kuchroo VK. Lag-3, Tim-3, and TIGIT: Co-inhibitory Receptors with Specialized Functions in Immune Regulation. *Immunity* 2016; 44:989-1004.
16. Buchbinder EI, Desai A. CTLA-4 and PD-1 Pathways: Similarities, Differences, and Implications of Their Inhibition. *Am J Clin Oncol* 2016; 39:98-106.
17. Schachter J, Ribas A, Long GV, Arance A, Grob JJ, Mortier L, Daud A, Carlino MS, McNeil C, Lotem M, et al. Pembrolizumab versus ipilimumab for advanced melanoma: final overall survival results of a multicentre, randomised, open-label phase 3 study (KEYNOTE-006). *Lancet* 2017; 390:1853-62.

18. Kang YK, Boku N, Satoh T, Ryu MH, Chao Y, Kato K, Chung HC, Chen JS, Muro K, Kang WK, et al. Nivolumab in patients with advanced gastric or gastro-oesophageal junction cancer refractory to, or intolerant of, at least two previous chemotherapy regimens (ONO-4538-12, ATTRACTION-2): a randomised, double-blind, placebo-controlled, phase 3 trial. *Lancet* 2017; 390:2461-71.
19. Rittmeyer A, Barlesi F, Waterkamp D, Park K, Ciardiello F, von Pawel J, Gadgeel SM, Hida T, Kowalski DM, Dols MC, et al. Atezolizumab versus docetaxel in patients with previously treated non-small-cell lung cancer (OAK): a phase 3, open-label, multicentre randomised controlled trial. *Lancet* 2017; 389:255-65.
20. Bellmunt J, de Wit R, Vaughn DJ, Fradet Y, Lee JL, Fong L, Vogelzang NJ, Climent MA, Petrylak DP, Choueiri TK, et al. Pembrolizumab as Second-Line Therapy for Advanced Urothelial Carcinoma. *N Engl J Med* 2017; 376:1015-26.
21. Larkin J, Chiarion-Sileni V, Gonzalez R, Grob JJ, Cowey CL, Lao CD, Schadendorf D, Dummer R, Smylie M, Rutkowski P, et al. Combined Nivolumab and Ipilimumab or Monotherapy in Untreated Melanoma. *N Engl J Med* 2015; 373:23-34.
22. El-Khoueiry AB, Sangro B, Yau T, Crocenzi TS, Kudo M, Hsu C, Kim TY, Choo SP, Trojan J, Welling THR, et al. Nivolumab in patients with advanced hepatocellular carcinoma (CheckMate 040): an open-label, non-comparative, phase 1/2 dose escalation and expansion trial. *Lancet* 2017; 389:2492-502.
23. Topalian SL, Hodi FS, Brahmer JR, Gettinger SN, Smith DC, McDermott DF, Powderly JD, Carvajal RD, Sosman JA, Atkins MB, et al. Safety, activity, and immune correlates of anti-PD-1 antibody in cancer. *N Engl J Med* 2012; 366:2443-54.
24. Brahmer JR, Tykodi SS, Chow LQ, Hwu WJ, Topalian SL, Hwu P, Drake CG, Camacho LH, Kauh J, Odunsi K, et al. Safety and activity of anti-PD-L1 antibody in patients with advanced cancer. *N Engl J Med* 2012; 366:2455-65.
25. Brahmer JR, Drake CG, Wollner I, Powderly JD, Picus J, Sharfman WH, Stankevich E, Pons A, Salay TM, McMiller TL, et al. Phase I study of single-agent anti-programmed death-1 (MDX-1106) in refractory solid tumors: safety, clinical activity, pharmacodynamics, and immunologic correlates. *J Clin Oncol* 2010; 28:3167-75.
26. O'Neil BH, Wallmark JM, Lorente D, Elez E, Raimbourg J, Gomez-Roca C, Ejadi S, Piha-Paul SA, Stein MN, Abdul Razak AR, et al. Safety and antitumor activity of the anti-PD-1 antibody pembrolizumab in patients with advanced colorectal carcinoma. *PLoS One* 2017; 12:e0189848.
27. Le DT, Uram JN, Wang H, Bartlett BR, Kemberling H, Eyring AD, Skora AD, Luber BS, Azad NS, Laheru D, et al. PD-1 Blockade in Tumors with Mismatch-Repair Deficiency. *N Engl J Med* 2015; 372:2509-20.
28. Le DT, Durham JN, Smith KN, Wang H, Bartlett BR, Aulakh LK, Lu S, Kemberling H, Wilt C, Luber BS, et al. Mismatch repair deficiency predicts response of solid tumors to PD-1 blockade. *Science* 2017; 357:409-13.
29. Grady WM, Carethers JM. Genomic and epigenetic instability in colorectal cancer pathogenesis. *Gastroenterology* 2008; 135:1079-99.
30. Mlecnik B, Bindea G, Angell HK, Maby P, Angelova M, Tougeron D, Church SE, Lafontaine L, Fischer M, Fredriksen T, et al. Integrative Analyses of Colorectal Cancer Show Immunoscore Is a Stronger Predictor of Patient Survival Than Microsatellite Instability. *Immunity* 2016; 44:698-711.
31. Llosa NJ, Cruise M, Tam A, Wicks EC, Hechenbleikner EM, Taube JM, Blosser RL, Fan H, Wang H, Luber BS, et al. The vigorous immune microenvironment of microsatellite instable colon cancer is balanced by multiple counter-inhibitory checkpoints. *Cancer Discov* 2015; 5:43-51.
32. Alvarado-Bachmann R, Smith A, Gundara JS, Kuo SC, Gill AJ, Samra JS, Hugh TJ. The incidence of mismatch repair gene defects in colorectal liver metastases. *Mol Med Rep* 2014; 10:1003-6.

33. Katz SC, Pillarisetty V, Bamboat ZM, Shia J, Hedvat C, Gonen M, Jarnagin W, Fong Y, Blumgart L, D'Angelica M, et al. T cell infiltrate predicts long-term survival following resection of colorectal cancer liver metastases. *Ann Surg Oncol* 2009; 16:2524-30.
34. Halama N, Michel S, Kloor M, Zoernig I, Benner A, Spille A, Pommerencke T, von Knebel DM, Folprecht G, Lubert B, et al. Localization and density of immune cells in the invasive margin of human colorectal cancer liver metastases are prognostic for response to chemotherapy. *Cancer Res* 2011; 71:5670-7.
35. Halama N, Spille A, Lerchl T, Brand K, Herpel E, Welte S, Keim S, Lahrmann B, Klupp F, Kahlert C, et al. Hepatic metastases of colorectal cancer are rather homogeneous but differ from primary lesions in terms of immune cell infiltration. *Oncoimmunology* 2013; 2:e24116.
36. Crispe IN. Immune tolerance in liver disease. *Hepatology* 2014; 60:2109-17.
37. Kroy DC, Ciuffreda D, Cooperrider JH, Tomlinson M, Hauck GD, Aneja J, Berger C, Wolski D, Carrington M, Wherry EJ, et al. Liver environment and HCV replication affect human T-cell phenotype and expression of inhibitory receptors. *Gastroenterology* 2014; 146:550-61.
38. Shi XL, Mancham S, Hansen BE, de Knecht RJ, de Jonge J, van der Laan LJ, Rivadeneira F, Metselaar HJ, Kwekkeboom J. Counter-regulation of rejection activity against human liver grafts by donor PD-L1 and recipient PD-1 interaction. *J Hepatol* 2016; 64:1274-82.
39. Kassel R, Cruise MW, Iezzoni JC, Taylor NA, Pruett TL, Hahn YS. Chronically inflamed livers up-regulate expression of inhibitory B7 family members. *Hepatology* 2009; 50:1625-37.
40. Pedroza-Gonzalez A, Verhoef C, Ijzermans JN, Peppelenbosch MP, Kwekkeboom J, Verheij J, Janssen HL, Sprengers D. Activated tumor-infiltrating CD4+ regulatory T cells restrain antitumor immunity in patients with primary or metastatic liver cancer. *Hepatology* 2013; 57:183-94.
41. Pedroza-Gonzalez A, Zhou G, Singh SP, Boor PP, Pan Q, Grunhagen D, de Jonge J, Tran TK, Verhoef C, JN IJ, et al. GITR engagement in combination with CTLA-4 blockade completely abrogates immunosuppression mediated by human liver tumor-derived regulatory T cells ex vivo. *Oncoimmunology* 2015; 4:e1051297.
42. Katz SC, Bamboat ZM, Maker AV, Shia J, Pillarisetty VG, Yopp AC, Hedvat CV, Gonen M, Jarnagin WR, Fong Y, et al. Regulatory T cell infiltration predicts outcome following resection of colorectal cancer liver metastases. *Ann Surg Oncol* 2013; 20:946-55.
43. Zheng Y, Manzotti CN, Burke F, Dussably L, Qureshi O, Walker LS, Sansom DM. Acquisition of suppressive function by activated human CD4+ CD25- T cells is associated with the expression of CTLA-4 not FoxP3. *J Immunol* 2008; 181:1683-91.
44. Zhou G, Sprengers D, Boor PPC, Doukas M, Schutz H, Mancham S, Pedroza-Gonzalez A, Polak WG, de Jonge J, Gaspersz M, et al. Antibodies Against Immune Checkpoint Molecules Restore Functions of Tumor-infiltrating T cells in Hepatocellular Carcinomas. *Gastroenterology* 2017.
45. Lee SY, Haq F, Kim D, Jun C, Jo HJ, Ahn SM, Lee WS. Comparative genomic analysis of primary and synchronous metastatic colorectal cancers. *PLoS One* 2014; 9:e90459.
46. Munoz-Bellvis L, Fontanillo C, Gonzalez-Gonzalez M, Garcia E, Iglesias M, Esteban C, Gutierrez ML, Abad MM, Bengoechea O, De Las Rivas J, et al. Unique genetic profile of sporadic colorectal cancer liver metastasis versus primary tumors as defined by high-density single-nucleotide polymorphism arrays. *Mod Pathol* 2012; 25:590-601.
47. Kawamata H, Yamashita K, Kojo K, Ushiku H, Ooki A, Watanabe M. Discrepancies between the K-ras mutational status of primary colorectal cancers and corresponding liver metastases are found in codon 13. *Genomics* 2015; 106:71-5.

48. Miranda E, Bianchi P, Destro A, Morengi E, Malesci A, Santoro A, Laghi L, Roncalli M. Genetic and epigenetic alterations in primary colorectal cancers and related lymph node and liver metastases. *Cancer* 2013; 119:266-76.
49. Wu X, Zhang H, Xing Q, Cui J, Li J, Li Y, Tan Y, Wang S. PD-1(+) CD8(+) T cells are exhausted in tumours and functional in draining lymph nodes of colorectal cancer patients. *Br J Cancer* 2014; 111:1391-9.
50. Xu B, Yuan L, Gao Q, Yuan P, Zhao P, Yuan H, Fan H, Li T, Qin P, Han L, et al. Circulating and tumor-infiltrating Tim-3 in patients with colorectal cancer. *Oncotarget* 2015; 6:20592-603.
51. Kang CW, Dutta A, Chang LY, Mahalingam J, Lin YC, Chiang JM, Hsu CY, Huang CT, Su WT, Chu YY, et al. Apoptosis of tumor infiltrating effector TIM-3+CD8+ T cells in colon cancer. *Sci Rep* 2015; 5:15659.
52. Pedroza-Gonzalez A, Zhou G, Vargas-Mendez E, Boor PP, Mancham S, Verhoef C, Polak WG, Grunhagen D, Pan Q, Janssen H, et al. Tumor-infiltrating plasmacytoid dendritic cells promote immunosuppression by Tr1 cells in human liver tumors. *Oncoimmunology* 2015; 4:e1008355.
53. Franceschini D, Paroli M, Francavilla V, Videtta M, Morrone S, Labbadia G, Cerino A, Mondelli MU, Barnaba V. PD-L1 negatively regulates CD4+CD25+Foxp3+ Tregs by limiting STAT-5 phosphorylation in patients chronically infected with HCV. *J Clin Invest* 2009; 119:551-64.
54. Baitsch L, Legat A, Barba L, Fuertes Marraco SA, Rivals JP, Baumgaertner P, Christiansen-Jucht C, Bouzourene H, Rimoldi D, Pircher H, et al. Extended co-expression of inhibitory receptors by human CD8 T-cells depending on differentiation, antigen-specificity and anatomical localization. *PLoS One* 2012; 7:e30852.
55. Legat A, Speiser DE, Pircher H, Zehn D, Fuertes Marraco SA. Inhibitory Receptor Expression Depends More Dominantly on Differentiation and Activation than "Exhaustion" of Human CD8 T Cells. *Front Immunol* 2013; 4:455.
56. Gros A, Robbins PF, Yao X, Li YF, Turcotte S, Tran E, Wunderlich JR, Mixon A, Farid S, Dudley ME, et al. PD-1 identifies the patient-specific CD8(+) tumor-reactive repertoire infiltrating human tumors. *J Clin Invest* 2014; 124:2246-59.
57. Williams JB, Horton BL, Zheng Y, Duan Y, Powell JD, Gajewski TF. The EGR2 targets LAG-3 and 4-1BB describe and regulate dysfunctional antigen-specific CD8+ T cells in the tumor microenvironment. *J Exp Med* 2017; 214:381-400.
58. Paolo Antonio A, Ignacio M, Shailender B, Petri B, Rachel ES, Evan JL, Margaret KC, Thomas G, Carlos AG-R, Hodi FS, et al. Initial efficacy of anti-lymphocyte activation gene-3 (anti-LAG-3; BMS-986016) in combination with nivolumab (nivo) in pts with melanoma (MEL) previously treated with anti-PD-1/PD-L1 therapy. *Journal of Clinical Oncology* 2017; 35:9520-.
59. Dong H, Strome SE, Salomao DR, Tamura H, Hirano F, Flies DB, Roche PC, Lu J, Zhu G, Tamada K, et al. Tumor-associated B7-H1 promotes T-cell apoptosis: a potential mechanism of immune evasion. *Nat Med* 2002; 8:793-800.
60. da Silva IP, Gallois A, Jimenez-Baranda S, Khan S, Anderson AC, Kuchroo VK, Osman I, Bhardwaj N. Reversal of NK-cell exhaustion in advanced melanoma by Tim-3 blockade. *Cancer Immunol Res* 2014; 2:410-22.
61. Fourcade J, Sun Z, Benallaoua M, Guillaume P, Luescher IF, Sander C, Kirkwood JM, Kuchroo V, Zarour HM. Upregulation of Tim-3 and PD-1 expression is associated with tumor antigen-specific CD8+ T cell dysfunction in melanoma patients. *J Exp Med* 2010; 207:2175-86.
62. Matsuzaki J, Gnjjatic S, Mhawech-Fauceglia P, Beck A, Miller A, Tsuji T, Eppolito C, Qian F, Lele S, Shrikant P, et al. Tumor-infiltrating NY-ESO-1-specific CD8+ T cells are negatively regulated by LAG-3 and PD-1 in human ovarian cancer. *Proc Natl Acad Sci U S A* 2010; 107:7875-80.

63. Boor PP, Metselaar HJ, Jonge S, Mancham S, van der Laan LJ, Kwekkeboom J. Human plasmacytoid dendritic cells induce CD8(+) LAG-3(+) Foxp3(+) CTLA-4(+) regulatory T cells that suppress allo-reactive memory T cells. *Eur J Immunol* 2011; 41:1663-74.

Supplementary Table S1. Numbers of patient samples used in each type of experiments in the study.

Tumor type and number of samples	MMR status and number of samples	T cell or APC subsets	Inhibitory receptors	Inhibitory ligands	Activation or cytokine	Polyclonal T cell activation assay	Tumor-specific T cell stimulation assay
		Figure 1	Figure 1, Figure 2	Figure 1, Figure 3	Figure 4	Figure 5	Figure 6
53 LM-CRC	1 deficient	■					
	1 deficient	■	■				
	1 proficient						■
	1 proficient				■	■	
	1 proficient	■	■			■	
	1 proficient	■	■	■		■	
	1 proficient	■	■	■	■	■	■
	1 proficient	■	■		■	■	■
	2 proficient	■	■				■
	2 proficient	■	■				■
	4 proficient					■	
	5 proficient	■	■			■	
	6 proficient				■		
	11 proficient	■	■				
	15 proficient					■	
11 PM-CRC	2 proficient	■	■	■			
	9 proficient	■	■				
12 pCRC	1 deficient	■	■	■			
	2 deficient	■	■				
	3 proficient						
	6 proficient				■		

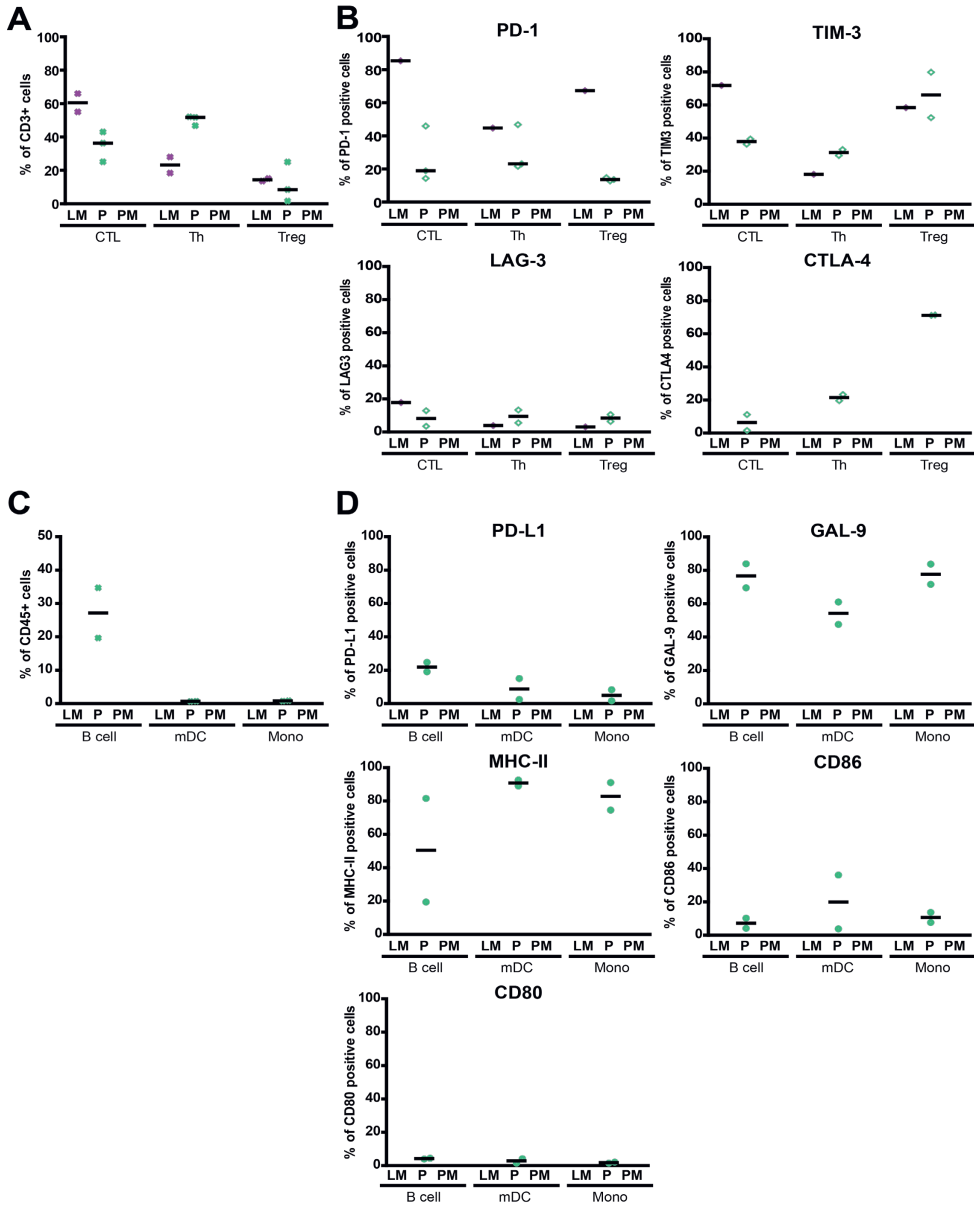
Abbreviations: CRC, colorectal cancer; LM-CRC, liver metastasis of CRC; pCRC, primary CRC; PM-CRC, peritoneal metastasis of CRC; MMR, mismatch repair.

Supplementary Table S2. Multivariable Cox proportional Hazard regression analysis of progression-free survival of patients with MMR-proficient LM-CRC.

Variables	P value	HR	95% CI for HR	
			Lower	Upper
PD-1 on CD8 ⁺ TIL	.160	2.418	.706	8.283
TIM3 on CD8 ⁺ TIL	.774	1.183	.375	3.732
LAG3 on CD8 ⁺ TIL	.032	.351	.135	.912

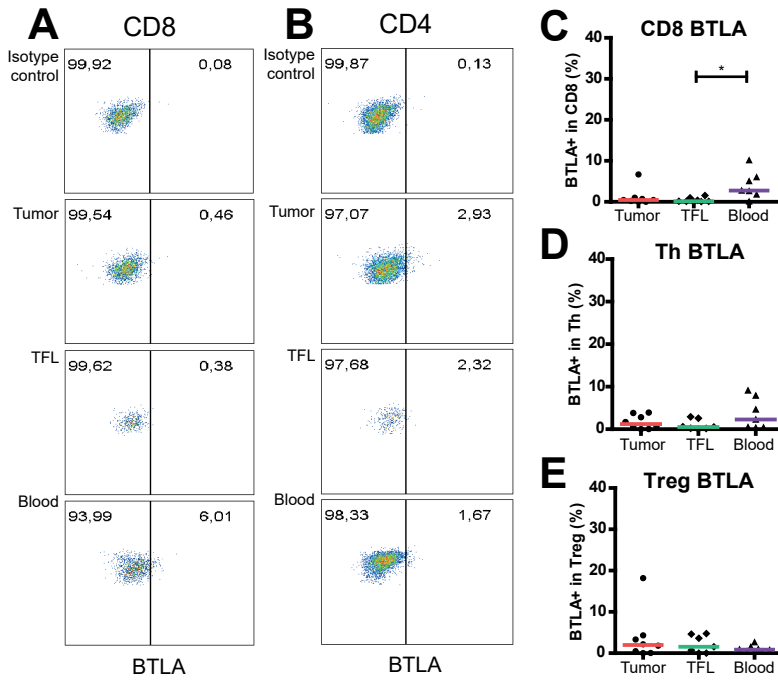
Abbreviations: TIL, tumor-infiltrating lymphocytes; HR, hazard ratio; CI, confidence interval.

The hazard ratio is interpreted as the chance of recurrence occurring in the "> median" group to the chance of recurrence occurring in the "< median" group.



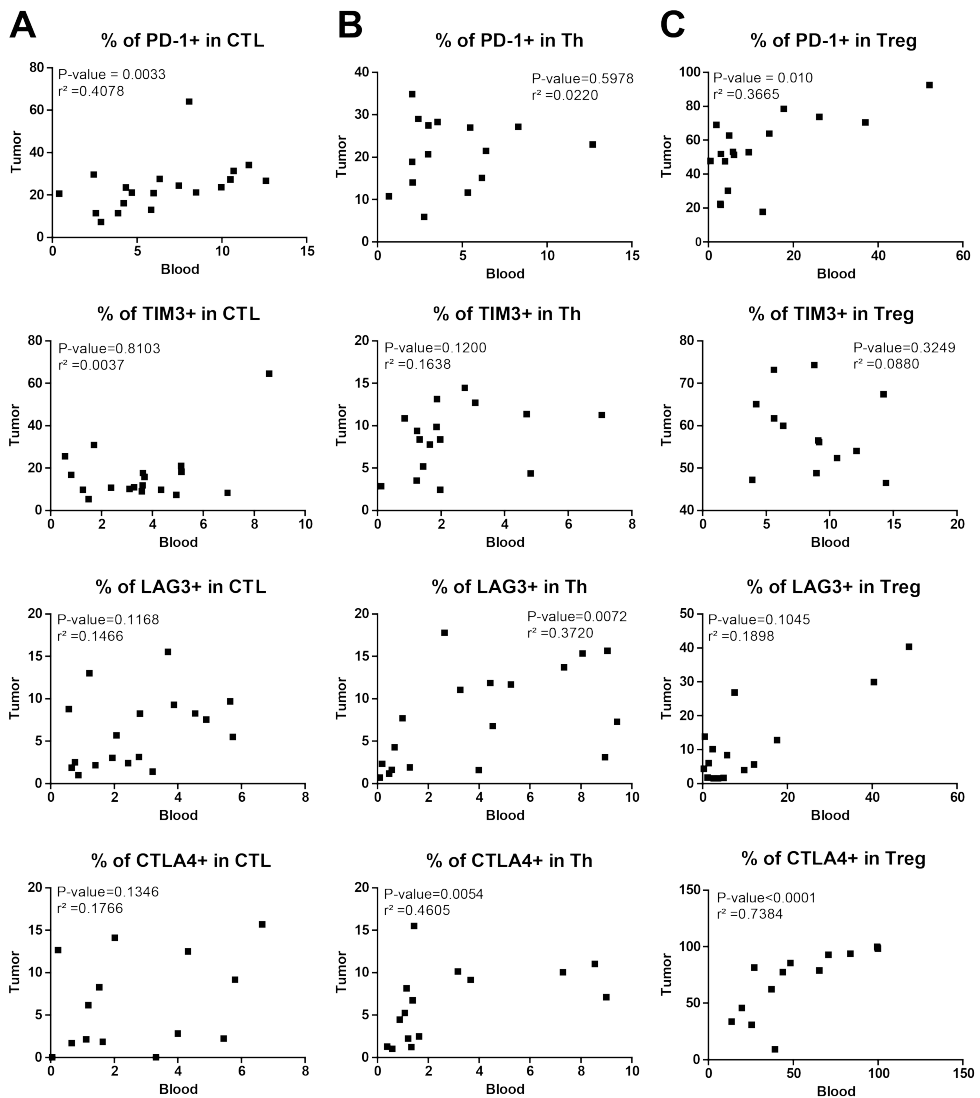
Supplementary Figure S1. Immune infiltrates and inhibitory molecule expression in MMR-deficient liver metastases (LM) and primary CRC.

A. The frequencies of CD8⁺ CTL, CD4⁺Foxp3⁺ Th and CD4⁺Foxp3⁺ Treg within CD3⁺ TIL from LM-CRC and primary CRC. **B.** The frequencies of inhibitory receptor positive cells within CD8⁺ CTL, Th and Treg in LM-CRC and primary CRC. **C.** The frequencies of B cells, mDC and monocytes (Mono) within CD45⁺ cells from primary CRC. **D.** The frequencies of inhibitory ligand positive cells within tumor-infiltrating B cells, mDC and monocytes from primary CRC. Values of individual patients are shown, and lines depict medians.



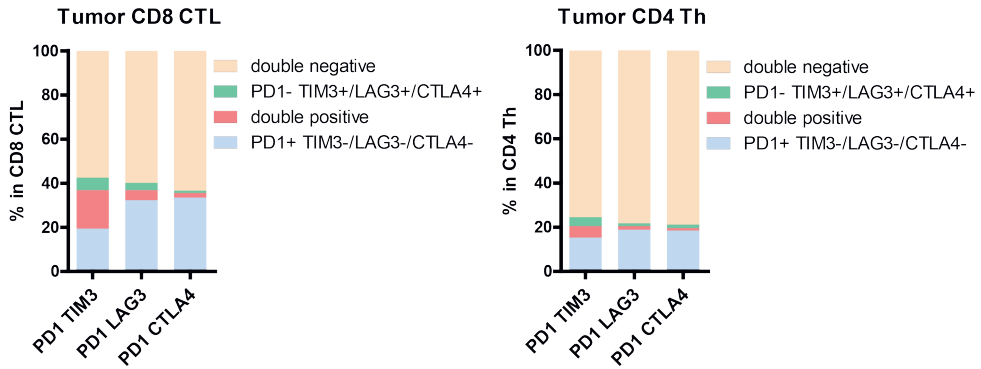
Supplementary Figure S3. Expression of BTLA on CD8⁺ CTL, CD4⁺ Th and CD4⁺ Treg in the tumor, TFL and blood of MMR-proficient LM-CRC.

A-B. Representative dot plots of BTLA expression on CD3⁺CD8⁺ CTL and CD3⁺CD4⁺Foxp3⁻ Th in the tumor, TFL and blood; the gates were made according to appropriate isotype controls. **C-E.** The frequencies of BTLA positive cells within CD8⁺ CTL, CD4⁺ Foxp3⁻ Th and CD4⁺ Foxp3⁺ Treg in the tumor, TFL and blood. Values of individual patients are shown, and lines depict medians. Differences were analyzed by paired t test or Wilcoxon matched pairs test; * $p < 0.05$.



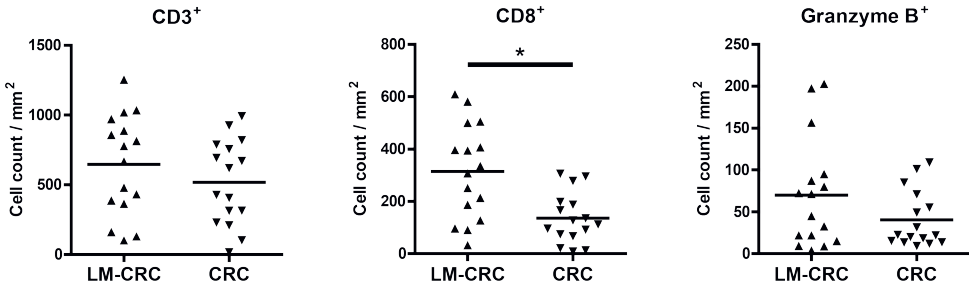
Supplementary Figure S4. Correlation of inhibitory receptor expression on T cells between the tumor and the blood of patients with mismatch repair-proficient LM-CRC.

Spearman correlation analysis demonstrates (A) positive correlation of the frequencies of PD-1⁺ cells in CD8⁺ CTL and CD4⁺ Treg between tumors and blood, (B) positive correlations of the frequencies of LAG3⁺ cells in CD4⁺ Th between tumors and blood, and (C) positive correlations of the frequencies of CTLA4⁺ cells in CD4⁺ Th and CD4⁺ Treg between tumors and blood. Correlations were analyzed by Spearman correlation test.



Supplementary Figure S5. Co-expression of inhibitory receptors on tumor-derived T cells in MMR-proficient LM-CRC.

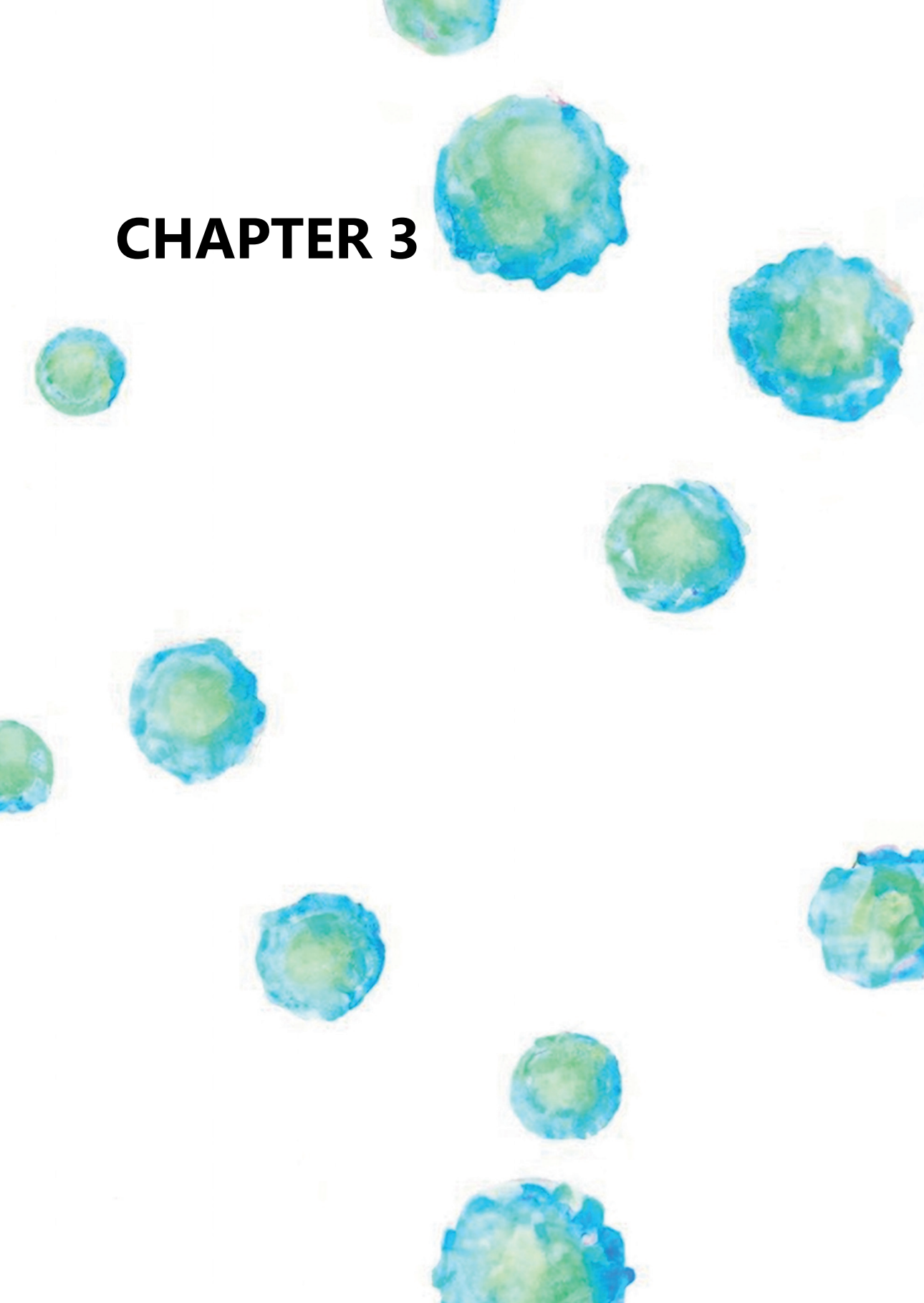
The mean frequencies of co-expression of PD-1 with TIM3, LAG3 or CTLA4 in CD8⁺ CTL (n=20) and CD4⁺ Th (n=10).



Supplementary Figure S6. T cell densities in primary CRC tumors and liver metastases.

CD3⁺, CD8⁺ and granzyme B⁺ cell densities in paired primary CRC and LM-CRC of 16 patients. The data were reanalyzed after being extracted from Halama *et al.* Table 1.³⁵ Values of individual patients are shown, and lines depict means. Differences were analyzed by paired t test or Wilcoxon matched pairs test; * p < 0.05.

CHAPTER 3



A BISPECIFIC ANTIBODY TARGETING CD137 AND PD-L1 BOOSTS IN VITRO RESPONSES OF T CELLS DERIVED FROM GASTRO- INTESTINAL CARCINOMAS

A bispecific antibody targeting CD137 and PD-L1 boosts in vitro responses of T cells derived from gastro-intestinal carcinomas

L. Noordam, P. Tacken, D. Sprengers, M.J. Bruno, C. Geuijen, J. Kwekkeboom

Manuscript in preparation

Introduction

Costimulatory molecules, such as CD137 (4-1BB), on T cells are under investigation for their use in cancer immunotherapy. Despite promising results in animal tumor models, clinical trials with CD137 agonists have not yet been successful due to both dependency on FcγR-mediated clustering and lethal hepatotoxicity. Merus NV has developed an Fc-silenced Biclonic CD137xPD-L1 antibody, whose stimulatory activity is dependent on PD-L1-mediated CD137 clustering and should thus be contained to the PD-L1 expressing tumor microenvironment. The aim of this pilot study was to determine the effect of the CD137xPD-L1 Biclonic antibody on *ex vivo* responses of human tumor-infiltrating T cells.

Patients & Methods

Lymphocytes isolated from hepatocellular carcinoma (HCC; n=5) and colorectal carcinoma (CRC; n=13) tumors and paired tumor-free tissues and blood were analyzed for CD137, PD1 and PD-L1 expression. Additionally, TIL proliferation and cyto- and chemokine production were assessed after *in vitro* stimulation with the CD137xPD-L1 Biclonic, its parent mAb or its clinical counterparts.

Results

CD137 and PD1 are both enriched in TIL, compared to TF tissues and blood with the highest expression on activated T-helper cells and activated regulatory T cells. PD-L1 is mainly expressed on CD3⁺ cells and present on low frequencies of T cells. Treatment with the CD137xPD-L1 Biclonic or the clinical CD137 agonist urelumab led to increased proliferation of HCC-derived CD8 TIL and to enhanced cytokine and chemokine production by TIL isolated from liver metastasis of CRC and HCC, whereas the Fc-silenced parent CD137 mAb did not.

Conclusion

This Biclonic CD137xPD-L1 has the capacity to activate tumor-derived CD8 T cells and the CD137-arm has no agonistic effect by itself, suggesting PD-L1 is necessary for its efficacy, which potentially limits systemic toxicities.

INTRODUCTION

Immune checkpoint blockade has added a new dimension to cancer treatment, and has improved the prospect of some previously deemed terminal cancer patients remarkably.¹ In metastatic melanoma patients, combination of PD1 and CTLA4 blockade has shown impressive efficacy.^{2,3} However, response rates are dependent on tumor type, and only a minority of patients with gastrointestinal solid tumors showed sustained responses upon PD1 or CTLA4 pathway blockade.⁴⁻⁷ While the focus of past clinical trials has been on checkpoint inhibitors (CPI), pre-clinical research has shown that agonistic targeting of co-stimulatory receptors, particularly tumor necrosis factor receptor (TNFR) family members, also has the ability to boost anti-tumor responses and could be a valuable addition to existing CPIs.

CD137 (also known as 4-1BB and TNFR superfamily member 9 [TNFRSF9]), a member of the TNFR family, is expressed on cytotoxic CD8 T cells and regulatory T cells (Treg) upon T cell receptor (TCR) activation.⁸ Upon agonistic targeting or binding of CD137 ligand, CD137-induced signaling stimulates cytokine production, upregulates survival genes and prevents activation-induced cell death in T cells.⁹ In several animal models, agonistic targeting of CD137 induced strong antitumor immune responses and led to tumor regression.¹⁰⁻¹² Additionally, CD137 signaling can reverse established anergy in CD8 T cells, as agonistic CD137 targeting in an OVA antigen-induced T cell anergy mouse model, restored CD8 T cell proliferation and cytokine production.¹³ However, the first clinical trials in patients were less successful. Urelumab, an agonistic human IgG4 monoclonal antibody (mAb) targeting the extracellular domain of CD137, led to moderate-to-severe hepatotoxicity in 10% of patients, and lethal hepatotoxicity in 2 patients, and ongoing clinical trials were withdrawn or terminated: NCT00351325, NCT00461110 and NCT00803374.¹⁴ Only in a very low dose of 0.1 mg/kg urelumab did not show toxicity, but this limited clinical efficacy.¹⁵ Utomilumab, a human anti-CD137 IgG2 agonistic mAb blocking interaction with CD137 ligand, had a favorable safety profile, but inferior clinical potential.^{15, 16}

Merus NV has developed a proprietary single light chain mAb discovery platform which allows efficient generation and manufacturing of fully human bispecific IgG mAb. Using this platform large diverse mAb panels have been generated, amongst others directed against the CPI target PD-L1 and the co-stimulatory target CD137. Furthermore, Merus NV generated a human biclonal C137xPD-L1 antibody (Biclomics™). In mouse models, combinations of mAbs targeting CD137 and PD1 showed synergistic anti-tumor activity.^{17, 18} By combining agonistic targeting of CD137 and antagonistic targeting of PD-L1 in one biclonal antibody (CD137xPD-L1), the agonistic function of the CD137 antigen-binding fragment (Fab) can be limited to environments in which PD-L1 is present, and thereby hepatotoxicity may be prevented. In addition the biclonal antibody can act as a bridge between PD-L1 expressing tumor and/or antigen presenting cells (APC) and CD137 expressing activated T cells.

The aim of this pilot study was to investigate whether the Biclomics™ CD137xPD-L1 can stimulate *ex vivo* responses of human tumor-infiltrating T cells. Its capacity to reactivate T cells isolated from primary and liver-metastases of colorectal carcinoma (CRC) and hepatocellular carcinoma (HCC) was evaluated and compared to the capacities of its parental mAb and their clinical counterparts, urelumab and atezolizumab (anti-PD-L1).

PATIENTS AND METHODS

Patients

In this preliminary study 18 patients eligible for surgical resection of their tumor were enrolled between December 2016 and September 2017. Patients included were diagnosed with hepatocellular carcinoma (HCC; n=5) or colorectal carcinoma (CRC) of which either the primary tumor (n=6) or liver metastasis (LM; n=7) were resected. Clinicopathological characteristics are shown in **Table 1**. Paired fresh tissue samples from tumor and tumor-free surrounding tissue (≥ 2 cm from tumor margin) were collected and consecutively the tumor-infiltrating leukocytes (TIL) as well as intrahepatic or intracolonic leukocytes were isolated. Peri-operatively, blood was collected and peripheral blood mononuclear cells (PBMC) were isolated. In addition blood of HCC-patients was collected prior to surgery for expansion of B cells. None of the patients received chemotherapy or immunosuppressive treatment within at least three months before surgery. The study was approved by the local ethics committee, and the patients were informed and signed consent before blood donation.

Cell preparation

PBMCs were isolated by Ficoll density gradient centrifugation. Single cell suspensions from tumor and surrounding hepatic and colonic tissues were obtained by tissue digestion as described previously.¹⁹ Briefly, fresh tissues were cut into small pieces. Tumor-free colon tissues were first incubated in the presence of Ethylenediaminetetraacetic acid (EDTA), 10% Fetal Calf Serum (FCS, Sigma-Aldrich, St. Louis, MA), 1mM EDTA (Sigma-Aldrich), 10 mM HEPES (Sigma-Aldrich) in Phosphate-buffered saline [PBS, Lonza, Breda, the Netherlands] four times for 15 minutes on a magnetic stirrer at 37°C, and after each incubation the supernatant was discarded. Then, the tumor-free colon, as well as the primary CRC tissue were digested in the presence of 0.2 mg/mL DNase I (Roche, Indianapolis, IN) and 200 U/mL collagenase VIII (Sigma-Aldrich) in HBSS with Ca²⁺ and Mg²⁺ (Sigma-Aldrich) on a magnetic stirrer for 30 minutes at 37°C. Tumor-free liver and HCC tissues were digested with 0.2 mg/mL DNase I (Roche) and 0.5 mg/mL collagenase IV (Sigma-Aldrich) in HBSS with Ca²⁺ and Mg²⁺ on a magnetic stirrer for 30 minutes at 37°C. The obtained cell suspensions were filtered through 100 μ m pore cell strainers (BD Biosciences, Erembodegem, Belgium) and mononuclear leukocytes were obtained by Ficoll density gradient centrifugation. Viability and cell numbers were determined by trypan blue exclusion.

Ex Vivo Polyclonal T-Cell Activation Assay

Purified tumor-infiltrating leukocytes (TIL) derived from primary CRC and LM-CRC patients were labeled with 0.1 μ M carboxyfluorescein diacetate succinimidyl ester (CFSE; Invitrogen, Paisley, UK) and cultured in RPMI 1640 (Gibco) supplemented with 10% human AB serum (Sigma-Aldrich), 2mM L-glutamine (Invitrogen), 50 mM HEPES (Sigma-Aldrich), 1% penicillin-streptomycin (Life-Technologies), 5mM Sodium Pyruvate (Gibco) and 1% minimum essential medium non-essential amino acids (MEM NEAA, Gibco) in 96-well round bottom plates (1-2x10⁵ cells per well) in the presence of CD3/CD28 activation Dynabeads (Gibco-Life Technologies AS, Norway; cell:bead-ratio 20-200:1) and in the presence or absence of 10 μ g/mL of hlgG1 or hlgG4 mAb or Biclomics (described in **Supplementary Table 1**) in duplicate at 37°C.

After 4 days supernatant was collected for Luminex assay analysis and cells were harvested and CFSE-dilution in T cells was analyzed by flowcytometry. Experiments in which baseline proliferation of T cells (in the condition with negative control antibody PG2708 against the irrelevant respiratory syncytial virus (RSV) G (RSV-G) protein) exceeded 50%, were excluded from further analysis since such strong baseline proliferation induced by TCR and CD28 signaling does not allow for quantification of further increase by targeting of other co-signaling receptors using this read-out method (**Supplementary Table 2**).

Preparation of mRNA-electroporated B cells

PBMCs of HCC-patients were isolated by Ficoll density gradient centrifugation 1-2 months prior to surgery for expansion of B cells, as previously described.²⁰ Briefly, autologous B cell blasts were generated from PBMCs cultured in Iscove's modified Dulbecco's medium (IMDM; Lonza, Breda, the Netherlands), supplemented with 10% human AB serum (Sigma-Aldrich), 1% penicillin-streptomycin, 1% insulin-transferrin-selenium solution (Gibco-Invitrogen, Breda, The Netherlands), 40 IU/mL rhIL-4 (Strathmann Bioscience, Hamburg, Germany), and 1 mg/mL soluble human trimeric CD40 ligand (sCD40L; kindly provided by the National Institutes of Health [NIH; Bethesda, MD, USA]). During the first week of culture, 1 ng/mL cyclosporine A (Novartis, Basel, Switzerland) was added to prevent T-cell expansion and after 7 days the residual CD3⁺ cells were depleted by magnetic cell sorting using CD3 microbeads (Miltenyi Biotec, Bergisch Gladbach, Germany). Purity status was checked by flowcytometry using a FACS Canto II flowcytometer (BD Biosciences) after staining with antibodies as indicated in **Supplementary Table 3** and 7-Aminoactinomycin D (7AAD; Invitrogen). The cultures consisted of >98% B cells and <1% T cells. The cells were then frozen and stored at -150°C until further use.

B-cell blasts were thawed and 5x10⁶ B cell blasts were electroporated with 20 µg of messenger RNA (mRNA) encoding full-length tumor antigens (Glypican-3 [GPC3] or melanoma-associated antigen C2 [MAGEC2]) or the negative control antigen (enhanced green fluorescent protein [eGFP]), as previously described.²⁰

Ex Vivo Messenger RNA-encoded Full-length Tumor Antigen-specific T-cell Stimulation Assay

Purified TIL derived from HCC patients were labeled with 0.1 µM carboxyfluorescein diacetate succinimidyl ester (CFSE; Invitrogen, Paisley, UK) and cultured in RPMI 1640 (Gibco) supplemented with 10% human AB serum (Sigma-Aldrich), 2mM L-glutamine (Invitrogen), 50 mM HEPES (Sigma-Aldrich), 1% penicillin-streptomycin (Life-Technologies), 5mM Sodium Pyruvate (Gibco) and 1% MEM NEAA (GIBCO) in 96-well round bottom plates (10⁵ cells per well) in the presence of 10⁵ mRNA-electroporated B cells (TIL:B cell-ratio 1:1) and in the presence or absence of 10 µg/mL of hIgG1 or hIgG4 mAb or Bionics (specified in **Supplementary Table 1**) in duplicate at 37°C. After 6 days supernatant was collected for Luminex assay analysis and cells were harvested and CFSE-dilution in T cells was analyzed by flowcytometry. Only experiments in which a specific response to either one or both tumor antigen, defined as T-cell proliferation ≥ 1.25 compared to the condition with eGFP B cells) was observed, were included (**Supplementary Table 2**).

Flowcytometric Analysis

Fresh PBMC as well as mononuclear leukocytes isolated from tissues were directly analyzed for expression of both surface and intracellular markers and after T cell expansion assays for surface markers, using antibodies detailed in **Supplementary Table 3**. In short, cells were stained with LIVE/Dead Fixable Aqua Dead Cell Stain Kit (Invitrogen, Paisley, UK) in PBS, followed by antibody labeling for surface antigens in FACS-buffer (1%FCS, 0.5 mM EDTA, 0.05% NaN₃ [Sigma-Aldrich] in PBS). For phenotypic analyses, cells were subsequently fixed by the FoxP3 staining buffer kit (eBioscience, Vienna, Austria) and stained for intracellular antigens. Measurements were performed on FACSCanto II or FACSAria SORP II (BD Biosciences). Analyses were done using FlowJo 10.4. Non-viable cells were excluded from analysis.

Luminex assay

Luminex 28-plex assay was performed at the Multiplex facility at UMC-Utrecht on the HCC and LM-CRC samples, and only on samples indicated in green in **Supplementary Table 2**. HCC156, LM-CRC218, LM-CRC220 and LM-CRC231 were not included. LM-CRC219 supernatants were analyzed by Luminex, but this patient was excluded from the proliferation data analysis since background proliferation was too high.

Statistical Analysis

All statistical analyses were performed using Graphpad (Version 8.2.1 for Windows, San Diego, CA) and R Statistical software (Version 3.6.1 for Windows, Foundation for Statistical Computing, Vienna, Austria). Statistical tests are specified for every experiment.

RESULTS

CD137 and PD1 are enriched in tumor-infiltrating T-cells

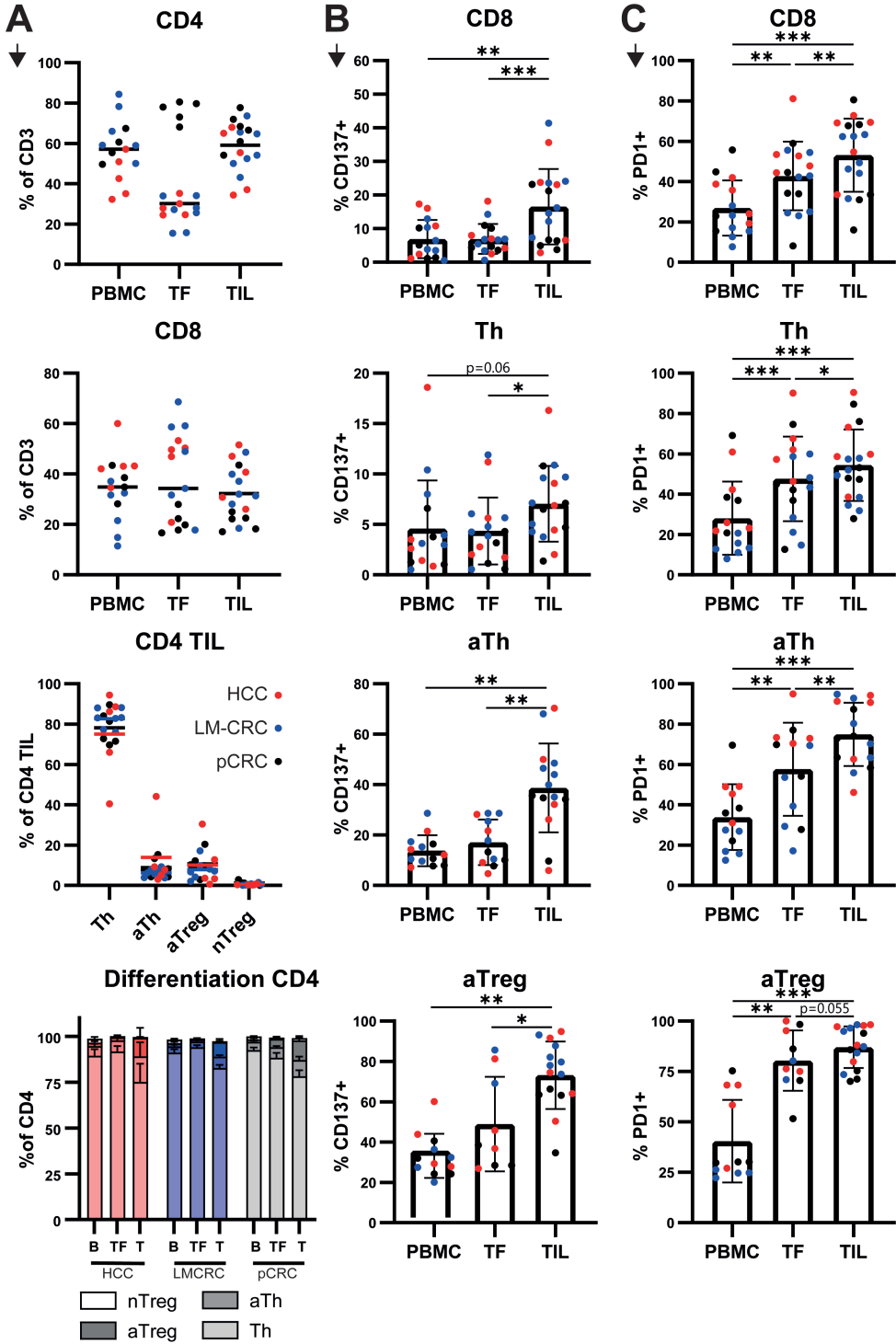
First, we determined which T cells expressed CD137, PD1 and PD-L1 by phenotypical analysis of PBMCs, and mononuclear cells isolated from resected tumor and surrounding tumor-free (TF) tissues. In all patients CD8 and CD4 T cells were present in all tissue compartments, although at highly variable levels (**Figure 1A**). CD4 T cells were subdivided into helper T (Th, FoxP3⁻) cells, activated Th (aTh, CD45RA⁻FoxP3^{lo}) cells, naïve regulatory T cells (nTreg, CD45RA⁺FoxP3^{lo}) and activated regulatory T cells (aTreg, CD45RA⁺FoxP3^{hi}), respectively, based on their FoxP3 and CD45RA expression.²¹ As expected, the majority of CD4 T cells in tumors comprised of Th cells, whereas nTregs were barely present and aTh and aTreg both accounted for approximately 10% of CD4 T cells (**Figure 1A**). Compared to PBMC and TF, aTregs and aTh were enriched in the tumor tissues (**Figure 1A**). Next, CD137, PD1 and PD-L1 expression on these T cell subsets were evaluated. Tumor-derived CD8 T cells, Th, aTh and aTregs all displayed higher CD137 (**Figure 1B**) and PD1 (**Figure 1C**) expression compared to their counterparts in TF and PBMC. Although PD-L1 expression was higher on tumor-derived aTreg and CD8 T cells than on these T cell subsets in TF and blood, its expression on tumor-infiltrating T cells was limited (**Figure 1D**). While Th TIL showed low frequencies of CD137-positive cells, CD8 and aTh TIL contained significantly higher numbers, and aTregs the highest numbers (**Figure 1E**). aTregs also had the highest frequencies of PD1- and PD-L1-positive

cells (**Figure 1E**). As PD-L1 is a ligand and is known to be expressed on monocytes and macrophages (CD14⁺ cells), amongst others, we also assessed PD-L1 expression on this cell type. In PBMC PD-L1 was scarcely expressed on circulating monocytes, and even though monocytes/macrophages in TF and tumor showed significantly higher frequencies of PD-L1 positive cells, the frequencies were still low and comparable to those found in tumor-derived T cells (**Figure 1F**). However, in the total TIL fraction, there is a substantial percentage of CD3⁺ cells expressing PD-L1 in LM-CRC and HCC, but not in pCRC (**Figure 1F**).

Taken together, CD3⁺ TILs derived from HCC and (LM-)CRC tumor tissues expressed increased levels of the co-stimulatory molecule CD137 and the co-inhibitory receptor PD1 compared to blood- or TF-derived T cells with highest expression on aTh and aTreg, while PD-L1 expression on tumor-infiltrating T cells is limited. However, in LM-CRC and HCC PD-L1 is expressed on a significant percentage of CD3⁺ TIL.

Biclonic CD137xPD-L1 mAb enhances proliferation of tumor-derived T cells

Next, we assessed the effects of the CD137xPD-L1 Biclonic on T cell proliferation of TILs isolated from (LM-)CRC and HCC tissues. CFSE-labeled TILs freshly isolated from (LM-)CRC were cultured in the presence of CD3/CD28 activation beads to provide initial TCR and CD28 signaling and either CD137xPD-L1 Biclonic, the parental CD137 or PD-L1 mAb or their clinical counterparts, urelumab and atezolizumab, or irrelevant anti-RSV-G mAb. After 4 days *in vitro* culture, T cell proliferation was determined by CFSE-dilution, measured by flowcytometry (**Supplementary Figure 1A**). CFSE-labeled primary TILs isolated from HCC were co-cultured with autologous B-cell blasts electroporated with mRNA that encodes the tumor-associated antigens (TAA) glypican-3 (GPC3) and/or melanoma-associated antigen (MAGE)-C2, and either CD137xPD-L1 Biclonic, the parental mAb, their clinical counterparts or irrelevant anti-RSV-G mAb, to study tumor-specific responses (**Supplementary Figure 1B**). Upon stimulation of both pCRC and LM-CRC TIL, we failed to see an effect of the parental CD137 antibody (**Figure 2A and 2B**). Interestingly, whereas CD8 TIL of LM-CRC seemed to show an increase in proliferation upon treatment with the CD137xPD-L1 Biclonic ($p=0.06$), proliferation in pCRC was not changed, even though the parental PD-L1 ($p=0.13$) antibody did seem to have an effect in pCRC, but not in LM-CRC (**Figure 2A and 2B**). The CD137xPD-L1 Biclonic had a remarkable effect on the TIL-response of one LM-CRC patient (LM-CRC 217) in particular, with a 3.4-fold increase in CD4⁺ TIL proliferation and a 7.6-fold increase in CD8 TIL proliferation, compared to the condition treated with CD3/CDC28 beads and the RSV-G-specific negative control Ab. HCC TIL stimulated with TAA-electroporated B cells showed increased proliferation compared to TIL stimulated with eGFP-electroporated B cells, indicating the presence of TAA-specific T cells (**Figure 2C and 2F**). Comparable to CRC TIL, also in HCC TIL stimulated with TAA-electroporated B cells no effect was observed of the CD137 parental Ab. In CD4 TIL we observed a trend of increased proliferation of TIL treated with CD137xPD-L1 Biclonic ($p=0.13$) and the PD-L1 parental Ab ($p=0.2$). The Biclonic mAb significantly increased proliferation in CD8 TIL compared to the RSV-G-specific negative control mAb, while both parent mAb did not (**Figure 2D**). So, the CD137xPD-L1 Biclonic could enhance both LM-CRC and HCC CD8 TIL proliferation, and its effect on CD8 TIL seemed to be synergistic compared to both parental mAb.



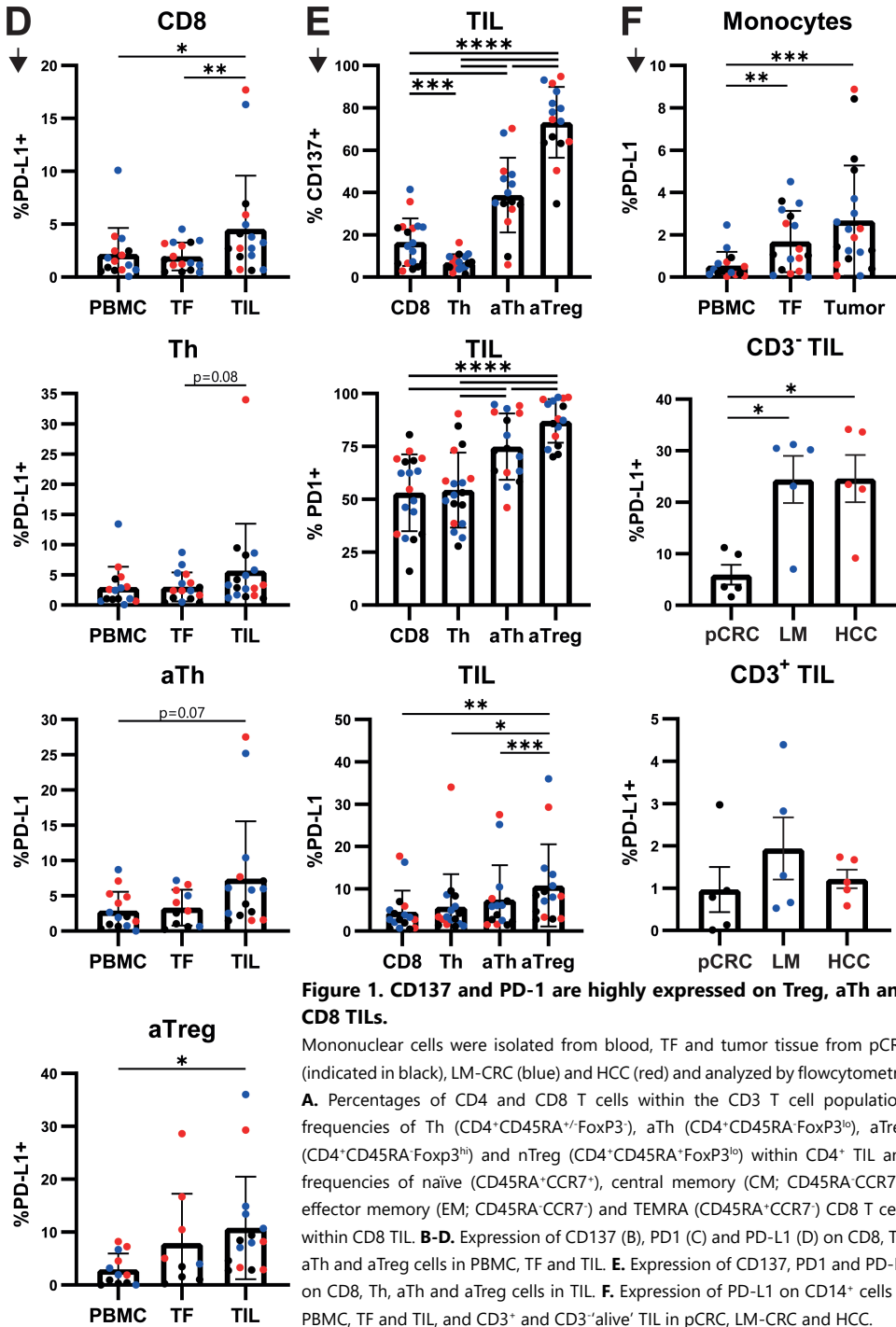


Figure 1. CD137 and PD-1 are highly expressed on Treg, aTh and CD8 TILs.

Mononuclear cells were isolated from blood, TF and tumor tissue from pCRC (indicated in black), LM-CRC (blue) and HCC (red) and analyzed by flowcytometry. **A.** Percentages of CD4 and CD8 T cells within the CD3 T cell population; frequencies of Th (CD4⁺CD45RA⁺FoxP3⁻), aTh (CD4⁺CD45RA⁺FoxP3^{lo}), aTreg (CD4⁺CD45RA⁺FoxP3^{hi}) and nTreg (CD4⁺CD45RA⁺FoxP3^{lo}) within CD4⁺ TIL and frequencies of naive (CD45RA⁺CCR7⁻), central memory (CM; CD45RA⁺CCR7⁺), effector memory (EM; CD45RA⁺CCR7⁻) and TEMRA (CD45RA⁺CCR7⁺) CD8 T cells within CD8 TIL. **B-D.** Expression of CD137 (B), PD1 (C) and PD-L1 (D) on CD8, Th, aTh and aTreg cells in PBMC, TF and TIL. **E.** Expression of CD137, PD1 and PD-L1 on CD8, Th, aTh and aTreg cells in TIL. **F.** Expression of PD-L1 on CD14⁺ cells in PBMC, TF and TIL, and CD3⁺ and CD3⁺ 'alive' TIL in pCRC, LM-CRC and HCC. Wilcoxon test. * p≤0.05, ** p≤0.01, *** p≤0.001

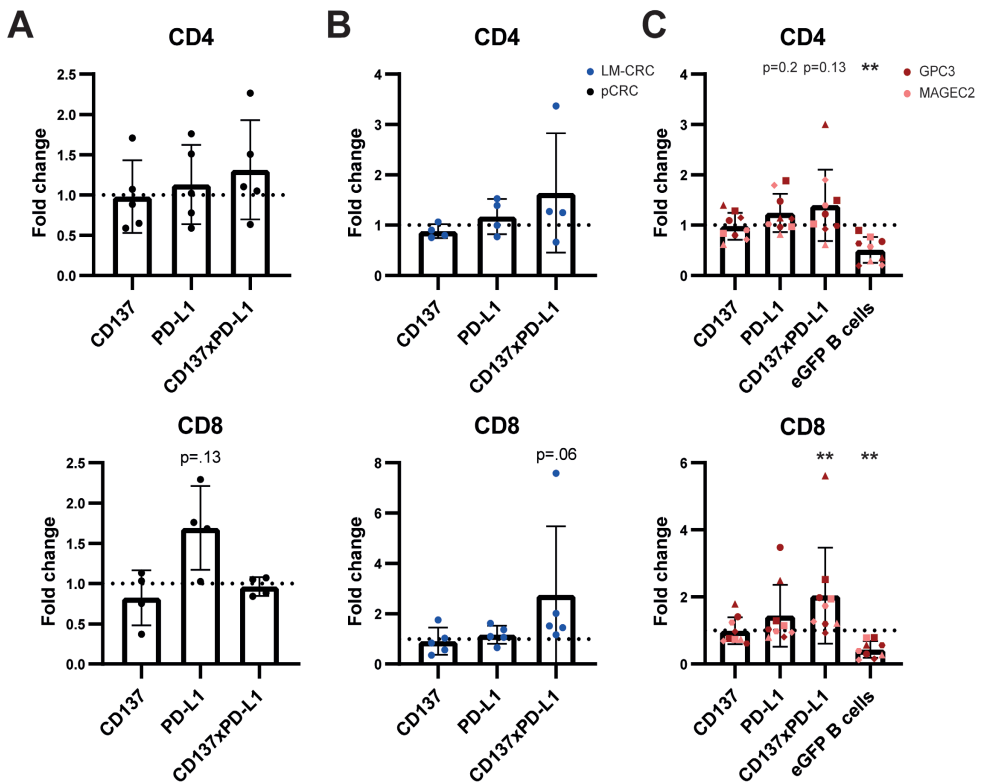


Figure 2. CD137xPD-L1 Biclonic enhances proliferation of LM-CRC and HCC TIL.

TILs were isolated from tumor tissues from (LM)-CRC and HCC patients, labeled with CFSE and cultured in vitro in the presence of CD3/CD28 activation beads ([LM]-CRC) or TAA-electroporated B cells (HCC) and Ab for 4 ([LM]-CRC) or 6 days (HCC). **A/B/D/E.** CFSE-dilution of pCRC (**A, D**) and LM-CRC (**B, E**) TIL upon stimulation with CD3/CD28 activation beads and indicated Ab was measured by flowcytometry and normalized to the percentages CFSE^{low} cells in the condition with the RSV-G (neg control) mAb (indicated by the dotted line). Relative changes in percentages of CFSE^{low} cells in the conditions with the parental CD137 or PD-L1 parent mAb or the Biclonic CD137xPD-L1 mAb (**A, B**), or clinical counterparts urelumab or atezolizumab or Biclonic CD137xPD-L1 (**D, E**) are depicted (n=5 for both pCRC and LM-CRC). **C/F.** CFSE-dilution of HCC TIL upon stimulation with B-cell blasts transfected with GPC-3, MAGEC-2, or eGFP (irrelevant negative control antigen) and indicated Ab was measured by flowcytometry and normalized to the proliferation responses to GPC-3 or MAGEC-2 in the condition with RSV-G (neg control) mAb (indicated by the dotted line). Relative changes in percentages of CFSE^{low} cells in response to GPC-3 or MAGEC-2 in the presence of the parental CD137 or PD-L1 mAb or the Biclonic CD137xPD-L1 mAb (**D**) or the clinical counterparts urelumab and atezolizumab or the Biclonic CD137xPD-L1 mAb compared to responses in the presence of RSV-G mAb are shown (n=5). Wilcoxon tests. Each condition was compared to the RSV-G (neg co) mAb. * p≤0.05, ** p≤0.01.

In contrast to the parental mAb, the clinical CD137 mAb urelumab tended to increase CD8 TIL proliferation derived from LM-CRC (p=0.06) and significantly increased proliferation of HCC-derived CD8 TIL (p=0.03), but not from pCRC (**Figure 2D, 2E and 2F**). However, 2 out of 4 pCRC CD8 TILs treated

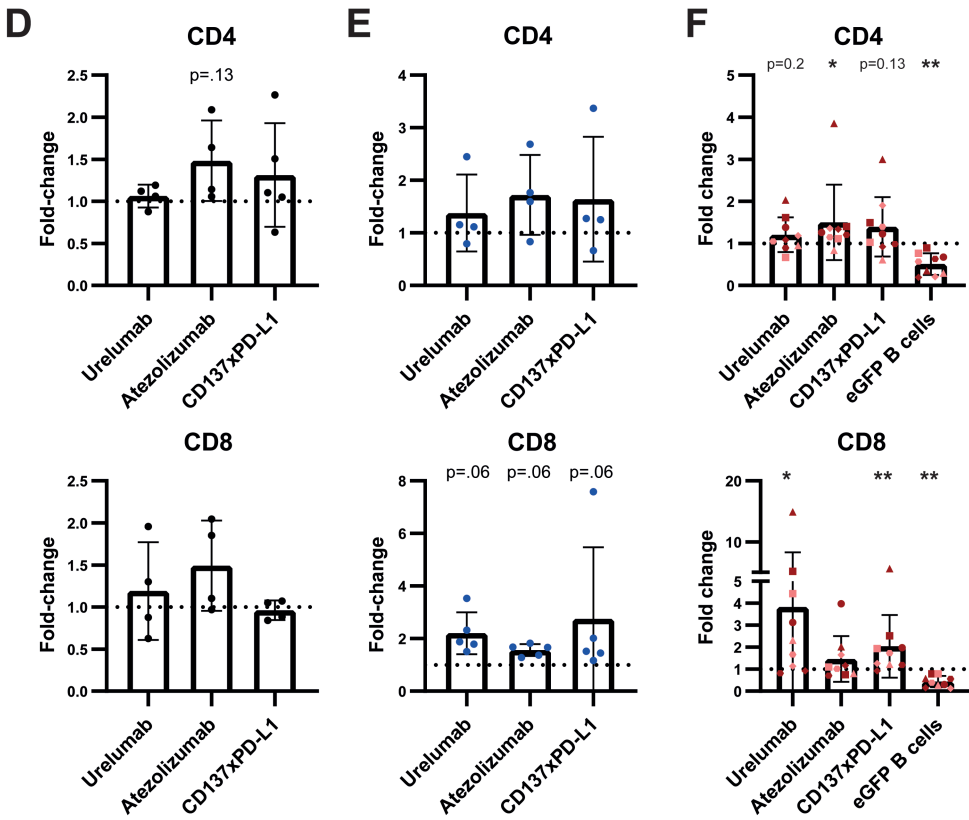


Figure 2. CD137xPD-L1 Biclonic enhances proliferation of LM-CRC and HCC TIL. (continued)

with urelumab seemed to have increased proliferation, even though these TILs did not show increased proliferation when treated with CD137xPDL1 (**Figure 2D**). Whereas urelumab only increased CD8 TIL proliferation, atezolizumab, the clinical anti-PD-L1 mAb, tended to increase both CD4 pCRC TIL ($p=0.13$) and CD8 LM-CRC TIL ($p=0.06$) proliferation and significantly increased HCC-derived CD4 TIL ($p=0.02$) proliferation.

Taken together, the CD137xPD-L1 Biclonic enhanced both (LM-)CRC and HCC CD8 TIL proliferation, whereas the parental CD137 mAb did not.

The CD137xPD-L1 Biclonic stimulates cytokine and chemokine production by TIL

In animal models it has been shown agonistic targeting of CD137 stimulates production of several cytokines, including IFN γ , and IL-2.^{12, 22-24} To test the impact of the Biclonic CD137xPDL1 stimulation on the cytokine and chemokine production profile of human tumor-derived TILs, we analyzed the culture supernatants of LM-CRC and HCC derived TIL by Luminex multiplex assay.

As we used different T cell stimuli for LM-CRC and HCC TIL cultures, cytokine and chemokine production were separately analyzed. In LM-CRC TIL secretion of several pro-inflammatory cytokines such as TNF α , the Th2 cytokines IL-4, IL-5 and IL-13, and chemokine IP10 (also known as CXCL10) were upregulated in all patient-TILs treated with CD137xPD-L1, but not in the presence of the parent mAb CD137 (**Figure 3A and 3D**). However, secretion of Th17 family cytokines, IL-6 and IL-17, and the effector cytokines IFN γ , IL-2, IL-21, TNF β and GM-CSF was only increased in two and three out of the four LM-CRC patients, respectively. Interestingly, the TILs of the LM-CRC patient that showed the highest increase in proliferation upon CD137xPD-L1 treatment (LM-CRC 217), also showed the most prominent increase in secretion of almost all cytokines measured upon CD137xPD-L1 treatment (**Figure 3A**). Urelumab did not lead to consistent changes in the cytokine and chemokine secretion profile.

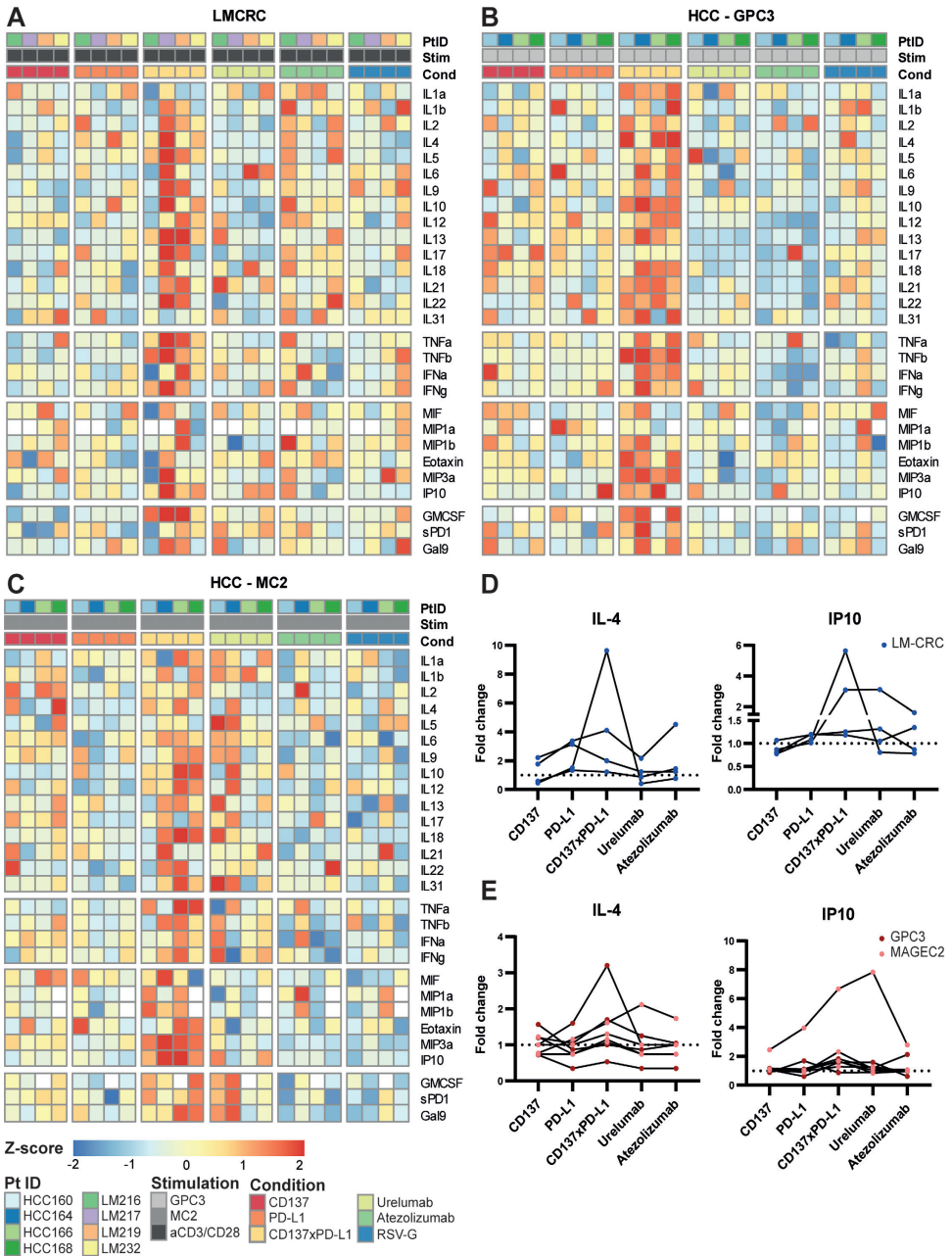
Similarly, *in vitro* CD137xPD-L1 treatment of HCC TILs stimulated with TAAs, led to increased cytokine and chemokine secretion in all HCC patients, while treatment with the parent CD137 mAb did not (**Figure 3B, 3C and 3E**). Generally, TILs treated with CD137xPD-L1 secreted more Th1/CD8-associated effector cytokines, such as IL-2, TNF α , TNF β , GM-CSF and IFN γ , Th2 family cytokines, such as IL-4, the immune-regulatory cytokine IL-10, and the chemokines MIP3a (CCL20) and IP10 (CXCL10). Also cytokines produced by the innate immune system, IL1a and IL-18, were increased. Interestingly, the TAA used to stimulate the TIL also seemed to exert different effects on the cytokine production profile. In the TILs stimulated with GPC3 electroporated B cells, the most prominent effect on cytokine and chemokine production was seen in the CD137xPD-L1-treated conditions, whereas in TIL stimulated with MAGEC2 electroporated B cells, cytokine production was increased in both the CD137xPD-L1 and urelumab treated conditions, but chemokines seemed to specifically be increased in the CD137xPD-L1 treated conditions.

Thus, the CD137xPD-L1 Biclonic altered the immunological profile of most TILs by boosting CD8-, Th1- and Th2-related cytokines, and pro-inflammatory chemokine production, while the parent CD137 mAb did not.

Figure 3. CD137xPD-L1 Biclonic enhances cytokine and chemokine production.

TILs were isolated from tumor tissue from LM-CRC and HCC and cultured *in vitro* in the presence of CD3/CD28 activation beads (LM-CRC; n=4) or TAA-electroporated B cells (HCC; n=4) and the indicated Ab for 4 ([LM]-CRC) or 6 days (HCC), after which supernatant was harvested and analyzed by luminex assay. **A**. Heatmap indicating change in cytokines and chemokines in LMCRC TIL treated with parental CD137 or PD-L1 mAb, clinical counterparts urelumab or atezolizumab, RSV-G (neg control) or the biclonic CD137xPD-L1 mAb. **B/C**. Heatmap indicating change in cytokines and chemokines in HCC TIL stimulated with GPC3 (**B**) or MC2 (**C**)-electroporated B cells and parental CD137 or PD-L1 mAb, clinical counterparts urelumab or atezolizumab, RSV-G (neg control) or the biclonic CD137xPD-L1 mAb. **D/E**. IL-4 and IP10 (CXCL10) secretion upon treatment with the various antibodies in LM-CRC (**D**) and HCC (**E**). IL-4 and IP10 secretion are depicted as relative to the RSV-G negative control Ab (indicated by the dotted line).

Heatmaps were created with the 'pheatmap' package in R, data was Z-score normalized for each patient. Color bar indicates the Z-score.



DISCUSSION

In this pilot study, we investigated whether the CD137xPD-L1 Biclonic could enhance *ex vivo* human TIL-responses. Several (pre-)clinical studies have shown the potential of CD137 targeting to maintain long-term functionality of T cells, T cell survival and memory formation and thereby T cell mediated tumor eradication.¹⁴⁻¹⁶ However, CD137 agonistic mAb have not yet advanced in phase III clinical trials. Urelumab is limited by hepatotoxicity and utomilumab has shown limited clinical efficacy. It has been hypothesized that the lack of efficacy of utomilumab, a human IgG2 mAb, is due to its low FcγR-binding affinity, since FcγR-mediated CD137 crosslinking is required for weak CD137 agonists to induce sufficient CD137 signaling.^{25,26} The dependency on crosslinking is a hallmark of the human TNFR family, in which three receptor units bind to a single homotrimeric ligand. Generally two or more of these ligand-receptor complexes need to cluster on the cell membrane to induce sufficient receptor signaling.²⁷ In contrast, strong agonistic CD137 mAb, such as urelumab, can co-stimulate T cells in absence of FcγRs. The observed hepatotoxicity in patients treated with urelumab may have been caused by the interaction of this mAb with FcγRIIB expressed by liver sinusoidal endothelial cells, macrophages and dendritic cells, which led to superactivation of hepatic T cells^{25, 26}, which also express CD137 as shown in the present study.

Here, we have used Fc-silenced antibodies to abrogate such interactions. The CD137xPD-L1 Biclonic is designed to promote target-mediated clustering of CD137. In theory, in the absence of PD-L1, minimal clustering should occur and therefore immune activation via CD137 will be limited. However, in the presence of PD-L1, crosslinking will induce CD137 activated signaling. As previously shown by Merus NV, this Biclonic induces CD137 signaling only in presence of PD-L1.²⁸ This was confirmed in our experiments, in which the Fc-silenced parental CD137 mAb had no effect on both TIL proliferation and cytokine and chemokine production, whereas urelumab was able to increase both. In contrast, the CD137xPD-L1 Biclonic, also Fc-silenced, was able to increase TIL proliferation and both cytokine and chemokine production. As CD137 clustering and signal induction by this Biclonic is dependent on PD-L1, which is overexpressed in the tumor micro-environment, toxicities outside of the tumor micro-environment should be limited. This may allow increased dosing, which in turn would lead to increased accumulation of the Biclonic in the tumor.²⁹ Additionally, the CD137xPD-L1 Biclonic may function as a bridge between PD-L1 expressing tumor cells or intra-tumoral APCs and CD137 expressing T cells, which could lead to increased tumoricidal effects or antigen-presentation to T cells, respectively.

PD-L1 expression on both HCC and CRC tumor cells is limited,^{4, 30-32} and therefore PD-L1 on tumor cells possibly hardly plays a role. Alternatively, the Biclonic may bind to immune cells expressing PD-L1. We found expression, although limited, of PD-L1 on T cells and CD14⁺ cells in tumors but more substantial expression on CD3⁺ TIL. The lack of these PD-L1 expressing cells in pCRC, may explain the lack of effect of the CD137xPD-L1 Biclonic in pCRC TIL *in vitro*. However, with the current experimental set-up, we could not further characterize these PD-L1 expressing cells. Alternative to this trans-activation hypothesis, PD-L1 on T cells themselves may lead to cis-activation. However, which mechanism activates CD8 TIL by

CD137xPD-L1 *in vitro*, is currently unknown and further research should elucidate this. Additionally, it is not known which subsets of T cells are directly targeted by the CD137xPD-L1 Biclonic. It might have a direct effect on CD8 TIL, as CD137 is expressed on tumor-specific activated CD8 TIL in HCC and we observed the largest effect on proliferation in CD8 TIL.³³ Alternatively, the Biclonic may target aTregs, as CD137 expression in HCC and (LM-) CRC TILs is highest on aTregs. However, the effects of targeting CD137 on Tregs are poorly understood. It has been shown that CD137 ligation on Tregs inhibits their suppressive function and reprograms them into TNFa-producing effector cells,³⁴⁻³⁶ whereas another study showed that agonistic CD137 targeting promotes the expansion of Tregs.³⁷ Finally, also aTh may be targeted, as they have considerable CD137 expression. Future research should give more insight into which T cell subsets are directly targeted by this Biclonic.

Apart from containing CD137 activation within the tumor microenvironment, blockade of PD-L1 by the Biclonic may also be able to stimulate TIL. PD1 was highly expressed on all T cell subsets in HCC and CRC tumors, and we observed trends that suggested that the parent anti-PD-L1 mAb can exert stimulatory effects on TIL proliferation and cytokine production. Binding of PD-1 to PD-L1 or programmed death ligand 2 (PD-L2) leads to diminished T cell proliferation, cytokine production, cytolytic activity and survival of T cells.^{38, 39} PD-L1 is constitutively expressed on professional APCs,⁴⁰ and is upregulated on tumor cells of various cancer types in response to cytokines produced by infiltrating immune cells, such as IFNg and TNFa.^{41, 42} We observed that T cells in the tumor micro-environment also expressed PD-L1, and it has been shown PD-L1 can be upregulated on T cells upon activation,⁴³ however, its functions in T cells are controversial. One study showed that binding of PD-L1 on T cells to CD80 (its second ligand) inhibits T cell activation *in vitro*.⁴³ However, in a graft-versus-host disease (GvHD) mouse model, expression of PD-L1 on donor T cells improved the T cells' survival and worsened GvHD.⁴⁴ Therefore the functional relevance of PD-L1 signaling in T cells is not known yet.

Considering this was a pilot study, we have shown proof-of-concept of this CD137xPD-L1 Biclonic being able to stimulate human TIL proliferation and cytokine and chemokine production, whereas the parent CD137 mAb was not. Otherwise this study is severely limited; numbers of independent experiments were limited, and we have not compared the effectivity of the Biclonic to the combination of the single parent CD137 and anti-PD-L1 mAb. As already mentioned, future studies should focus on elucidating the mechanism of action and clinical trials should prove the safety and efficacy in human cancer patients. Nevertheless, we have provided the first evidence that this CD137xPD-L1 Biclonic has the capacity to activate tumor-derived CD8 T cells, and this treatment may be especially effective in patients with preexisting or induced T-cell inflamed tumors. Additionally, we have shown that the CD137-arm of the Biclonic does not stimulate T cells without the PD-L1-arm, thereby confirming previous observations by Merus NV,²⁸ and thus systemic toxicities are expected to be limited. Whether the Biclonic can be safely used in patients and has clinical anti-tumor efficacy should be investigated in a clinical trial.

REFERENCES

1. Ott PA, Hodi FS, Robert C. CTLA-4 and PD-1/PD-L1 blockade: new immunotherapeutic modalities with durable clinical benefit in melanoma patients. *Clin Cancer Res* 2013; 19:5300-9.
2. Schummer P, Schilling B, Gesierich A. Long-Term Outcomes in BRAF-Mutated Melanoma Treated with Combined Targeted Therapy or Immune Checkpoint Blockade: Are We Approaching a True Cure? *Am J Clin Dermatol* 2020.
3. Larkin J, Chiarion-Sileni V, Gonzalez R, Grob JJ, Rutkowski P, Lao CD, Cowey CL, Schadendorf D, Wagstaff J, Dummer R, et al. Five-Year Survival with Combined Nivolumab and Ipilimumab in Advanced Melanoma. *N Engl J Med* 2019; 381:1535-46.
4. El-Khoueiry AB, Sangro B, Yau T, Crocenzi TS, Kudo M, Hsu C, Kim TY, Choo SP, Trojan J, Welling THR, et al. Nivolumab in patients with advanced hepatocellular carcinoma (CheckMate 040): an open-label, non-comparative, phase 1/2 dose escalation and expansion trial. *Lancet* 2017; 389:2492-502.
5. Overman MJ, McDermott R, Leach JL, Lonardi S, Lenz HJ, Morse MA, Desai J, Hill A, Axelson M, Moss RA, et al. Nivolumab in patients with metastatic DNA mismatch repair-deficient or microsatellite instability-high colorectal cancer (CheckMate 142): an open-label, multicentre, phase 2 study. *Lancet Oncol* 2017; 18:1182-91.
6. Sangro B, Gomez-Martin C, de la Mata M, Inarrairaegui M, Garralda E, Barrera P, Riezu-Boj JI, Larrea E, Alfaro C, Sarobe P, et al. A clinical trial of CTLA-4 blockade with tremelimumab in patients with hepatocellular carcinoma and chronic hepatitis C. *J Hepatol* 2013; 59:81-8.
7. Chung KY, Gore I, Fong L, Venook A, Beck SB, Dorazio P, Criscitiello PJ, Healey DI, Huang B, Gomez-Navarro J, et al. Phase II study of the anti-cytotoxic T-lymphocyte-associated antigen 4 monoclonal antibody, tremelimumab, in patients with refractory metastatic colorectal cancer. *J Clin Oncol* 2010; 28:3485-90.
8. Schoenbrunn A, Frensch M, Kohler S, Keye J, Dooms H, Moewes B, Dong J, Loddenkemper C, Sieper J, Wu P, et al. A converse 4-1BB and CD40 ligand expression pattern delineates activated regulatory T cells (Treg) and conventional T cells enabling direct isolation of alloantigen-reactive natural Foxp3+ Treg. *J Immunol* 2012; 189:5985-94.
9. Vinay DS, Kwon BS. Immunotherapy of cancer with 4-1BB. *Mol Cancer Ther* 2012; 11:1062-70.
10. Gaultier V, Judor JP, Le Guen V, Cany J, Ferry N, Conchon S. Agonistic anti-CD137 antibody treatment leads to antitumor response in mice with liver cancer. *Int J Cancer* 2014; 135:2857-67.
11. Narazaki H, Zhu Y, Luo L, Zhu G, Chen L. CD137 agonist antibody prevents cancer recurrence: contribution of CD137 on both hematopoietic and nonhematopoietic cells. *Blood* 2010; 115:1941-8.
12. Houot R, Goldstein MJ, Kohrt HE, Myklebust JH, Alizadeh AA, Lin JT, Irish JM, Torchia JA, Kolstad A, Chen L, et al. Therapeutic effect of CD137 immunomodulation in lymphoma and its enhancement by Treg depletion. *Blood* 2009; 114:3431-8.
13. Wilcox RA, Tamada K, Flies DB, Zhu G, Chapoval AI, Blazar BR, Kast WM, Chen L. Ligation of CD137 receptor prevents and reverses established anergy of CD8+ cytolytic T lymphocytes in vivo. *Blood* 2004; 103:177-84.
14. Segal NH, Logan TF, Hodi FS, McDermott D, Melero I, Hamid O, Schmidt H, Robert C, Chiarion-Sileni V, Ascierto PA, et al. Results from an Integrated Safety Analysis of Urelumab, an Agonist Anti-CD137 Monoclonal Antibody. *Clin Cancer Res* 2017; 23:1929-36.
15. Chester C, Sanmamed MF, Wang J, Melero I. Immunotherapy targeting 4-1BB: mechanistic rationale, clinical results, and future strategies. *Blood* 2018; 131:49-57.

16. Tolcher AW, Sznol M, Hu-Lieskovan S, Papadopoulos KP, Patnaik A, Rasco DW, Di Gravio D, Huang B, Gambhire D, Chen Y, et al. Phase Ib Study of Utomilumab (PF-05082566), a 4-1BB/CD137 Agonist, in Combination with Pembrolizumab (MK-3475) in Patients with Advanced Solid Tumors. *Clin Cancer Res* 2017; 23:5349-57.
17. Wei H, Zhao L, Li W, Fan K, Qian W, Hou S, Wang H, Dai M, Hellstrom I, Hellstrom KE, et al. Combinatorial PD-1 blockade and CD137 activation has therapeutic efficacy in murine cancer models and synergizes with cisplatin. *PLoS One* 2013; 8:e84927.
18. Chen S, Lee LF, Fisher TS, Jessen B, Elliott M, Evering W, Logronio K, Tu GH, Tsaparikos K, Li X, et al. Combination of 4-1BB agonist and PD-1 antagonist promotes antitumor effector/memory CD8 T cells in a poorly immunogenic tumor model. *Cancer Immunol Res* 2015; 3:149-60.
19. Pedroza-Gonzalez A, Verhoef C, Ijzermans JN, Peppelenbosch MP, Kwekkeboom J, Verheij J, Janssen HL, Sprengers D. Activated tumor-infiltrating CD4+ regulatory T cells restrain antitumor immunity in patients with primary or metastatic liver cancer. *Hepatology* 2013; 57:183-94.
20. Zhou G, Sprengers D, Boor PPC, Doukas M, Schutz H, Mancham S, Pedroza-Gonzalez A, Polak WG, de Jonge J, Gaspersz M, et al. Antibodies Against Immune Checkpoint Molecules Restore Functions of Tumor-Infiltrating T Cells in Hepatocellular Carcinomas. *Gastroenterology* 2017; 153:1107-19 e10.
21. Miyara M, Yoshioka Y, Kitoh A, Shima T, Wing K, Niwa A, Parizot C, Taffin C, Heike T, Valeyre D, et al. Functional delineation and differentiation dynamics of human CD4+ T cells expressing the FoxP3 transcription factor. *Immunity* 2009; 30:899-911.
22. Morales-Kastresana A, Catalan E, Hervas-Stubbs S, Palazon A, Azpilikueta A, Bolanos E, Anel A, Pardo J, Melero I. Essential complicity of perforin-granzyme and FAS-L mechanisms to achieve tumor rejection following treatment with anti-CD137 mAb. *J Immunother Cancer* 2013; 1:3.
23. Chacon JA, Wu RC, Sukhumalchandra P, Molldrem JJ, Sarnaik A, Pilon-Thomas S, Weber J, Hwu P, Radvanyi L. Co-stimulation through 4-1BB/CD137 improves the expansion and function of CD8(+) melanoma tumor-infiltrating lymphocytes for adoptive T-cell therapy. *PLoS One* 2013; 8:e60031.
24. Curran MA, Kim M, Montalvo W, Al-Shamkhani A, Allison JP. Combination CTLA-4 blockade and 4-1BB activation enhances tumor rejection by increasing T-cell infiltration, proliferation, and cytokine production. *PLoS One* 2011; 6:e19499.
25. Claus C, Ferrara C, Xu W, Sam J, Lang S, Uhlenbrock F, Albrecht R, Herter S, Schlenker R, Husser T, et al. Tumor-targeted 4-1BB agonists for combination with T cell bispecific antibodies as off-the-shelf therapy. *Sci Transl Med* 2019; 11.
26. Qi X, Li F, Wu Y, Cheng C, Han P, Wang J, Yang X. Optimization of 4-1BB antibody for cancer immunotherapy by balancing agonistic strength with FcγR affinity. *Nat Commun* 2019; 10:2141.
27. Wajant H. Principles of antibody-mediated TNF receptor activation. *Cell Death Differ* 2015; 22:1727-41.
28. Mayes P, Tacken P, Wang S, Loo P-Fv, Condamine T, Maaden Hvd, Rovers E, Engels S, Franssen F, Kulkarni A, et al. Abstract 539: A bispecific Fc-silenced IgG1 antibody (MCLA-145) requires PD-L1 binding to activate CD137. *Cancer Research* 2019; 79:539-.
29. Thurber GM, Dane Wittrup K. A mechanistic compartmental model for total antibody uptake in tumors. *J Theor Biol* 2012; 314:57-68.
30. Zhu AX, Finn RS, Edeline J, Cattani S, Ogasawara S, Palmer D, Verslype C, Zagonel V, Fartoux L, Vogel A, et al. Pembrolizumab in patients with advanced hepatocellular carcinoma previously treated with sorafenib (KEYNOTE-224): a non-randomised, open-label phase 2 trial. *Lancet Oncol* 2018; 19:940-52.

31. D'Alterio C, Nasti G, Polimeno M, Ottaiano A, Conson M, Circelli L, Botti G, Scognamiglio G, Santagata S, De Divitiis C, et al. CXCR4-CXCL12-CXCR7, TLR2-TLR4, and PD-1/PD-L1 in colorectal cancer liver metastases from neoadjuvant-treated patients. *Oncoimmunology* 2016; 5:e1254313.
32. Inaguma S, Lasota J, Felisiak-Golabek A, Kowalik A, Wang Z, Zieba S, Kalisz J, Ikeda H, Miettinen M. Histopathological and genotypic characterization of metastatic colorectal carcinoma with PD-L1 (CD274)-expression: Possible roles of tumour micro environmental factors for CD274 expression. *J Pathol Clin Res* 2017; 3:268-78.
33. Kim HD, Park S, Jeong S, Lee YJ, Lee H, Kim CG, Kim KH, Hong SM, Lee JY, Kim S, et al. 4-1BB Delineates Distinct Activation Status of Exhausted Tumor-Infiltrating CD8(+) T Cells in Hepatocellular Carcinoma. *Hepatology* 2020; 71:955-71.
34. Valzasina B, Guiducci C, Dislich H, Killeen N, Weinberg AD, Colombo MP. Triggering of OX40 (CD134) on CD4(+)CD25+ T cells blocks their inhibitory activity: a novel regulatory role for OX40 and its comparison with GITR. *Blood* 2005; 105:2845-51.
35. Smith SE, Hoelzinger DB, Dominguez AL, Van Snick J, Lustgarten J. Signals through 4-1BB inhibit T regulatory cells by blocking IL-9 production enhancing antitumor responses. *Cancer Immunol Immunother* 2011; 60:1775-87.
36. Akhmetzyanova I, Zelinskyy G, Littwitz-Salomon E, Malyshkina A, Dietze KK, Streeck H, Brandau S, Dittmer U. CD137 Agonist Therapy Can Reprogram Regulatory T Cells into Cytotoxic CD4+ T Cells with Antitumor Activity. *J Immunol* 2016; 196:484-92.
37. Zhang P, Gao F, Wang Q, Wang X, Zhu F, Ma C, Sun W, Zhang L. Agonistic anti-4-1BB antibody promotes the expansion of natural regulatory T cells while maintaining Foxp3 expression. *Scand J Immunol* 2007; 66:435-40.
38. Keir ME, Butte MJ, Freeman GJ, Sharpe AH. PD-1 and its ligands in tolerance and immunity. *Annu Rev Immunol* 2008; 26:677-704.
39. Pardoll DM. The blockade of immune checkpoints in cancer immunotherapy. *Nat Rev Cancer* 2012; 12:252-64.
40. Francisco LM, Sage PT, Sharpe AH. The PD-1 pathway in tolerance and autoimmunity. *Immunol Rev* 2010; 236:219-42.
41. Ohaegbulam KC, Assal A, Lazar-Molnar E, Yao Y, Zang X. Human cancer immunotherapy with antibodies to the PD-1 and PD-L1 pathway. *Trends Mol Med* 2015; 21:24-33.
42. Kan-o K, Matsumoto K, Asai-Tajiri Y, Fukuyama S, Hamano S, Seki N, Nakanishi Y, Inoue H. PI3K-delta mediates double-stranded RNA-induced upregulation of B7-H1 in BEAS-2B airway epithelial cells. *Biochem Biophys Res Commun* 2013; 435:195-201.
43. Butte MJ, Keir ME, Phamduy TB, Sharpe AH, Freeman GJ. Programmed death-1 ligand 1 interacts specifically with the B7-1 costimulatory molecule to inhibit T cell responses. *Immunity* 2007; 27:111-22.
44. Saha A, O'Connor RS, Thangavelu G, Lovitch SB, Dandamudi DB, Wilson CB, Vincent BG, Tkachev V, Pawlicki JM, Furlan SN, et al. Programmed death ligand-1 expression on donor T cells drives graft-versus-host disease lethality. *J Clin Invest* 2016; 126:2642-60.

Supplementary Table S1. Culture conditions.

CRC			HCC		
#	Stimulus	Antibody	#	Stimulus	Antibody
1	aCD3/CD28	CD137xPD-L1	1	TAA-B cells	CD137xPD-L1
2	aCD3/CD28	CD137	2	TAA-B cells	CD137
3	aCD3/CD28	PD-L1	3	TAA-B cells	PD-L1
4	aCD3/CD28	Neg co (RSV-G)	4	TAA-B cells	Neg co (RSV-G)
5	aCD3/CD28	Urelumab	5	TAA-B cells	Urelumab
6	aCD3/CD28	Atezolizumab	6	TAA-B cells	Atezolizumab
7	aCD3/CD28	-	7	TAA-B cells	-
8	-	-	8	eGFP- B cells	-
			9	-	-

Supplementary Table S2. Overview included patients.

pCRC	Phenotype	Proliferation	Cyto- & chemokine
PCRC-29			
PCRC-31			
PCRC-44		CD4	
PCRC-45			
PCRC-46			
PCRC-51			
LM-CRC	Phenotype	Proliferation	Cyto- & chemokine
LMCRC-216		CD8	
LMCRC-217			
LMCRC-218			
LMCRC-219			
LMCRC-220			
LMCRC-231			
LMCRC-232			
HCC	Phenotype	Proliferation	Cyto- & chemokine
HCC-156			
HCC-160			
HCC-164			
HCC-166			
HCC-168			

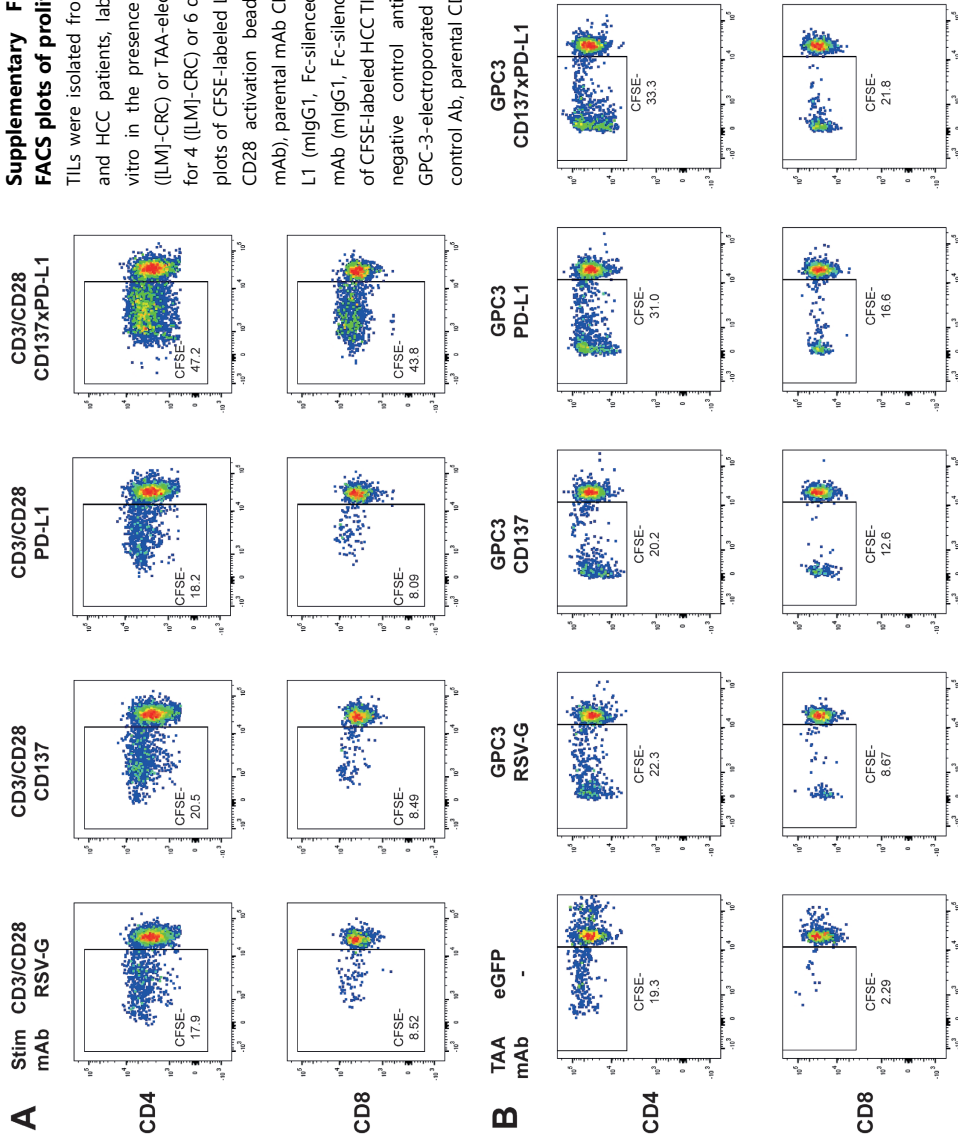
Green: included (if a T cell population is mentioned in a green box, it means that only that specific T cell subset has been included in the results); Black: excluded

Supplementary Table S3. Antibody list for flowcytometric analysis and TIL cultures.

Specificity	Fluorochrome	Clone	Company
CCR7	FITC	150503	R&D Systems
CD3	APC-R700	UCHT1	BD
CD3	eF506	UCHT1	eBioscience
CD3	PE-Cy7	UCHT1	eBioscience
CD4	eVolve605	SK3	eBioscience
CD4	eF450	OKT4	eBioscience
CD45RA	PE-CF594	HI100	BD
CD8	APC-Cy7	OKT8	eBioscience
CD14	eVolve605	61D3	eBioscience
CD19	PE	HIB19	eBioscience
CD38	eF450	HIT2	eBioscience
CD80	FITC	MAB104	Beckman Coulter
CD86	APC	IT2.2	Biolegend
CD137	APC	4B4-1	BD
CD137	BV421	4B4-1	BD
CD274 (PD-L1)	APC-R700	MIH1	BD
CD274 (PD-L1)	PerCP-Cy5.5	MIH1	eBioscience
CD279 (PD1)	PE-Cy7	J105	eBioscience
FoxP3	APC	236A/E7	eBioscience
HLA-DR	APC-Cy7	LN3	eBioscience
mlgG1	APC	MOPC-21	Biolegend
mlgG1	APC-R700	X40	BD
mlgG1	BV421	X40	BD
mlgG1	PE-Cy7	MOPC-21	Biolegend
mlgG1	PerCP-Cy5.5	X40	BD
Specificity	Format	Clone	Company
CD137xPD-L1	hulgG1, Fc-silenced	PB17311p01	Merus
CD137	hulgG1, Fc-silenced	PG6797p02	Merus
PD-L1	hulgG1, Fc-silenced	PG7702p01	Merus
RSV-G	hulgG1, Fc-silenced	PG2708p217	Merus
CD137	hulgG4	Urelumab	Merus
PD-L1	hulgG1	PG6269p01/Atezolizumab	Merus

Supplementary Figure S1. Representative FACS plots of proliferation assay.

TILs were isolated from tumor tissues from (LM)-CRC and HCC patients, labeled with CFSE and cultured in vitro in the presence of CD3/CD28 activation beads ((LM)-CRC) or TAA-electroporated B cells (HCC) and Ab for 4 ((LM)-CRC) or 6 days (HCC). **A.** Representative dot plots of CFSE-labeled LM-CRC TIL stimulated with CD3/CD28 activation beads and RSV-G (negative control mAb), parental mAb CD137 (mlgG1, Fc-silenced) or PD-L1 (mlgG1, Fc-silenced) or the Bionic CD137xPD-L1 mAb (mlgG1, Fc-silenced). **B.** Representative dot plots of CFSE-labeled HCC TIL stimulated with eGFP (irrelevant negative control antigen)-electroporated B cells or GPC-3-electroporated B cells plus the RSV-G negative control Ab, parental CD137 (mlgG1, Fc-silenced) or PD-L1 (mlgG1, Fc-silenced) mAbs or the Bionic CD137xPD-L1 (mlgG1, Fc-silenced).



The background of the page is a watercolor illustration featuring several circular, cell-like shapes. These shapes are rendered in various shades of pink, magenta, and purple, with some darker, more saturated areas in the center of each circle, suggesting a nucleus or a specific organelle. The overall effect is soft and artistic, typical of watercolor painting.

CHAPTER 4

EXPRESSION OF CANCER TESTIS ANTIGENS IN TUMOR-ADJACENT NORMAL LIVER IS ASSOCIATED WITH POST-RESECTION RECURRENCE OF HEPATOCELLULAR CARCINOMA

Expression of Cancer Testis Antigens in tumor-adjacent normal liver is associated with post-resection recurrence of hepatocellular carcinoma

L. Noordam, Z. Ge, H. Ozturk, M. Doukas, S. Mancham, P.C.C. Boor, L. Campos Carrascosa, G. Zhou, T.P.P. van den Bosch, Q. Pan, J.N.M. IJzermans, M.J. Bruno, D. Sprengers, J. Kwekkeboom
Cancers. May 2021, Vol. 13, No. 10: :2499.

This chapter has been published in Cancers.

High recurrence rates after resection of hepatocellular carcinoma (HCC) with curative intent impair clinical outcomes of HCC. Cancer/testis antigens (CTAs) are suitable targets for cancer immunotherapy if selectively expressed in tumor cells. The aims were to identify CTAs that are frequently and selectively expressed in HCC-tumors, and to investigate whether CTAs could serve as biomarker for occult metastasis. Tumor and paired tumor-free liver (TFL) tissues of HCC-patients, and healthy tissues were assessed for mRNA expression of 49 CTAs by RT-qPCR and protein expression of 5 CTAs by immunohistochemistry. Twelve CTA-mRNAs were expressed in $\geq 10\%$ of HCC-tumors and not in healthy tissues except testis. In tumors, mRNA and protein of ≥ 1 CTA was expressed in 78% and 71% of HCC-patients, respectively. In TFL, CTA mRNA and protein was found in 45% and 30% of HCC-patients, respectively. Interestingly, CTA-expression in TFL was an independent negative prognostic factor for post-resection HCC-recurrence and survival. We established a panel of 12 testis-restricted CTAs expressed in tumors of most HCC-patients. The increased risk of HCC-recurrence in patients with CTA expression in TFL, suggests that CTA-expressing (pre-)malignant cells may be a source of HCC-recurrence and reflects the relevance of targeting these to prevent HCC-recurrence.

INTRODUCTION

Liver cancer is the fourth leading cause of cancer related death, with hepatocellular carcinoma (HCC) being the most common subtype.¹ HCC is often diagnosed at advanced stage and these patients can only be offered palliative therapies.^{2,3} However, with the help of intensive monitoring, at-risk-patients can be diagnosed at an early stage and can therefore be treated with curative intent; either by surgical resection or radiofrequency ablation. However, recurrence rates are high and currently no therapies are available to prevent recurrence. Patients experiencing early recurrence likely have occult multifocality at the time of resection, whereas late recurrences are more likely to represent de novo tumors.⁴⁻⁶ Several clinicopathological factors, such as tumor size and vascular invasion, have been used to predict clinical outcome after surgery, but none have consequences for the management of HCC after surgical treatment.⁷ It remains of great importance to identify occult metastasis at the time of resection to allow identification of patients at risk for recurrence, ideally by targetable tumor markers. Once occult micro-metastasis or de novo (pre-)malignant lesions can be characterized, therapeutic approaches targeting these markers may be developed to prevent tumor recurrence.

Cancer testis antigens (CTAs) are expressed in immune-privileged germ cells and are expressed in cancer cells of various histological subtypes.⁸ Based on their expression profile in adult healthy tissues, they are classified into testis-restricted, testis/brain-restricted and testis-selective CTAs with the last group having additional expression in somatic tissues.⁹ Since testis-restricted CTAs lack expression in healthy adult tissues, and have the potential to induce antitumor immune responses, they are considered ideal targets for cancer immunotherapy.^{8,10} Moreover, as testis-restricted CTAs are not expressed in healthy, tumor-free, tissues, sensitive techniques detecting these CTAs can potentially be used to recognize occult metastasis in surrounding macro- and microscopically tumor-free tissue.

The aims of this study were: 1) To establish a panel of CTAs that are frequently and selectively expressed in tumors of HCC patients; 2) To determine whether these CTAs are expressed in adjacent macroscopically tumor-free liver tissues of HCC-patients and whether they are an indication of occult metastasis, e.g. by being associated with early recurrence and/or worse HCC-specific survival.

PATIENTS, MATERIALS & METHODS

This study followed the REMARK (Reporting Recommendations for Tumor Marker Prognostic Studies) guidelines.¹¹

HCC Patients and tissues

Ethical approval for this study was granted by the Ethics Committee at Erasmus MC, Rotterdam, the Netherlands, waiving the requirement for informed consent. For the discovery and validation cohorts 100 and 89, respectively, archived surgically-resected fresh frozen HCC-tumor and paired tumor-free liver (TFL) tissue samples (obtained at a distance of > 2 cm from the tumors) were collected after surgery or retrieved from the archives of the Department of Pathology, Erasmus Medical Center Rotterdam. For protein expression analysis 76 formalin-fixed paraffin-embedded (FFPE) paired HCC-tumor and TFL tissues were retrieved from the Dutch nationwide pathology archives (PALGA) respectively.

The HCC-patients included in the discovery cohort underwent hepatic resection (n=97 and n=73 for fresh frozen and FFPE samples respectively) or liver transplantation (n=3 for both fresh frozen and FFPE samples) for HCC in our center between February 1995 and September 2017, and diagnosis of HCC was confirmed by pathological examination. The patients included in the validation cohort underwent hepatic resection (n=89) for HCC in our center between December 2008 and August 2019, and diagnosis of HCC was confirmed by pathological examination.

Medical records were reviewed for clinicopathological variables (listed in **Supplementary Table S1**) and date of first recurrence, HCC-specific death and last follow-up. Date of recurrence was defined as the first date a patient was diagnosed with a LI-RADS5 lesion during radiological follow-up.¹² Local recurrence was defined as intra-hepatic tumor recurrence, all other tumor localizations were classified distant recurrence. Patients that had no recurrence during follow-up or that underwent liver transplantation were censored. HCC-specific death was defined as death due to HCC. Patients that died due to other causes (e.g. postoperative complications, trauma or other malignancies), did not die during follow-up or underwent liver transplantation were censored. Time to event was calculated from the day of surgery.

All patients were retrospectively included. Further details of these and other included tissues can be found in the supplementary materials and methods.

Selection of CTAs

A literature search to identify CTAs reported to be expressed in HCC was conducted in PubMed on October 4th, 2018. A summary of this search is provided in **Figure 1A** and the query in the Supplementary data. Papers written in English that described CTA expression in HCC patients and/or HCC cell lines were included. In addition, the CTA database (<http://www.cta.lncc.br/>) was consulted to find additional CTAs expressed in HCC and one relevant paper was added.¹³

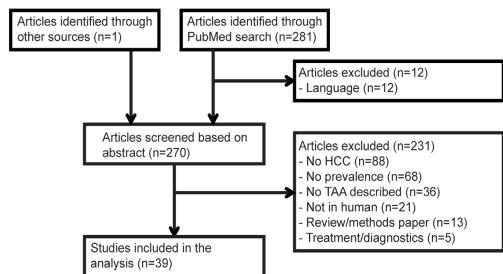
Quantitative real-time PCR

RNA was isolated from the frozen tissues and RT-qPCR was performed. The sequences, T_m-values and product lengths of the used primers are provided in **Supplementary Table S2**, and detailed methods can be found in the supplementary data file.

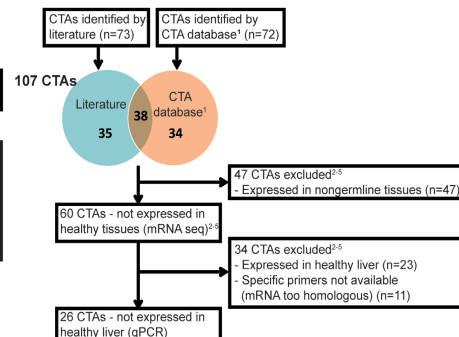
Immunohistochemistry

Protein expression was determined by immunohistochemistry (IHC) on tissue microarrays (TMA), that contained three 1 mm cores of each tumor and TFL tissue, as described in the supplementary data file. The stained TMAs were scored blindly by two researchers, based on the intensity of the staining (none, low, intermediate, strong) and the percentage of positive tumor cells or hepatocytes (<10%, 10-50%, 50-90%, >90%). If less than 5 positive cells per core were observed, the core was scored as 0, and cores smaller than 50% of the original surface were excluded. The final scores were the average scores of the three cores.

A Literature search



B TAA selection



C Expression in healthy liver

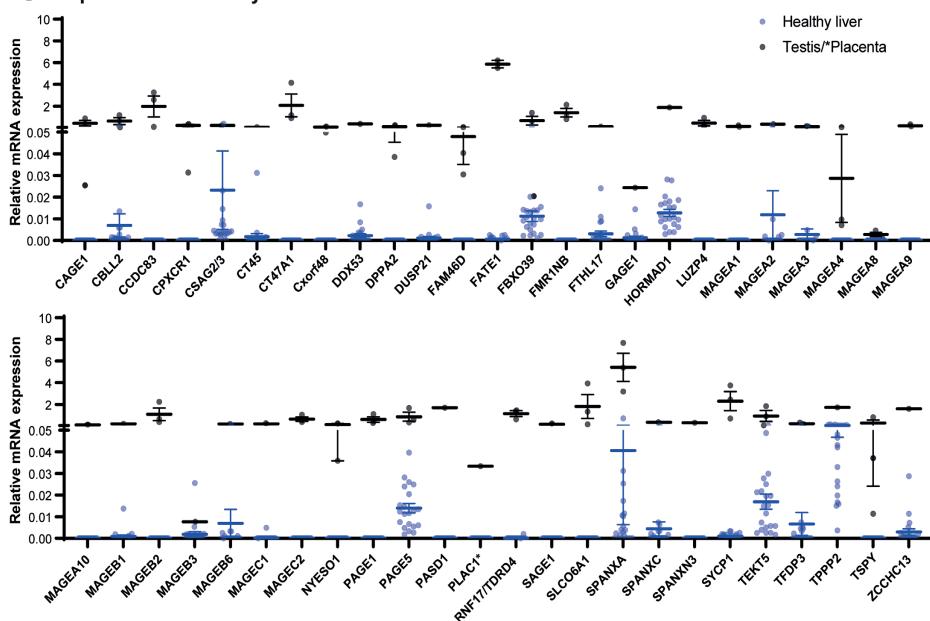


Figure 1. Selection of CTAs.

A/B. Study Flow Diagram. **C.** Relative mRNA expression of selected CTAs in healthy donor livers (n=21) in blue and in the respective positive control tissues in black. Control tissues were: placenta (for PLAC1; n=1) or testis (all other CTAs; n=1-3). ¹<http://www.cta.lncc.br/>, ²Hofmann, et al. ³FANTOM consortium, ⁴HPA consortium, ⁵GTex consortium. ^{9,14,15}

Statistical analysis

All statistical analyses were performed using Graphpad (Version 8.2.1 for Windows, San Diego, CA) and R Statistical software (Version 3.6.1 for Windows, Foundation for Statistical Computing, Vienna, Austria). The correlation analysis was performed in RStudio with the 'corplot' package, using Pearson's correlation coefficient. For creating heatmaps, RStudio was used with the 'gplots' and 'pheatmap' packages. Survival analysis was performed by the Kaplan-Meier method and the Cox proportional hazards model, using the 'survminer' and 'survival' packages. Used statistical tests are indicated in the figures. P-values < 0.05 were considered significant.

RESULTS

Selection of 26 CTAs after literature study and exclusion of those expressed in healthy liver

To determine which CTAs are frequently expressed in HCC tumor tissue, a literature study was conducted. Using a query to identify publications on CTAs expressed in HCC tissue, 281 publication records were obtained through the PubMed search and one relevant paper¹³ was added. After removal of non-English publications, 270 publications were screened on title and abstract, of which 231 papers were excluded. Full texts were screened of the remaining 39 studies, which all met the inclusion criteria (**Figure 1A**). In these 39 studies, expression of 73 different CTAs in HCC was reported; mRNA expression of 51, protein expression of 1, and both mRNA and protein expression of 21 CTAs (**Supplementary Table S3**). In

	mRNA-+ HCC (%) ¹	mean in mRNA-+ HCC (range) ²	RE HCC (compared to testis) ³	mRNA-+ TFL (%) ⁴	mean in mRNA-+ TFL (range) ⁵	RE TFL (compared to testis) ⁶	mRNA-+ cirrhotic tissue ⁷
CAGE1	14.4	0.082 (0.003-0.711)	0.188	2.0	0.009 (0.003-0.015)	0.020	0
CT47A1	26.8	1.311 (0.001-20.565)	0.632	6.1	0.255 (0.01-0.769)	0.123	0
MAGEA1	58.6	0.403 (0.003-1.926)	4.170	13.0	0.055 (0.005-0.188)	0.567	0
MAGEA9	14.1	0.41 (0.001-4.953)	2.848	1.0	0.035 (0.035-0.035)	0.243	0
MAGEA10	12.4	0.123 (0.002-0.518)	1.080	4.1	0.028 (0.004-0.088)	0.249	0
MAGEB2	24.2	0.395 (0.002-2.4)	0.761	6.0	0.053 (0.018-0.127)	0.102	0
MAGEC1	47.5	0.109 (0.001-0.841)	0.407	32.0	0.047 (0.002-0.466)	0.174	28.6
MAGEC2	55.6	0.692 (0.001-9.305)	1.542	19.0	0.041 (0.003-0.28)	0.091	25.7
NYESO1	10.1	0.13 (0.007-1.04)	0.525	1.0	0.018 (0.018-0.018)	0.071	0
PAGE1	18.2	0.37 (0.002-2.225)	1.001	5.0	0.059 (0.009-0.179)	0.159	2.9
SLCO6A1	25.8	0.095 (0.002-0.411)	0.053	4.1	0.011 (0.004-0.017)	0.006	2.9
TSPY*	21.0	0.827 (0.004-7.401)	34.135	4.8	0.218 (0.001-0.641)	9.012	4.2

Table 1. mRNA expression of CTAs in tumor and TFL of HCC-patients.

¹Percentage of hepatocellular carcinomas (HCC) expressing mRNA of the CTA – meaning a Ct-value <35 and relative expression > 0.001 (n=100); ²Mean relative expression (relative to the geometric mean of the 3 household genes- GUSB, HPRT1, PMM1) level in HCCs expressing the CTA and range; ³Mean relative expression of the CTA in HCC expressing the CTA, relative to the relative mean expression in 3 testis tissues; ⁴Percentage of paired tumor-free liver (TFL) tissues expressing mRNA of the CTA (n=100); ⁵Mean relative expression level in TFLs expressing the CTA and range; ⁶Mean relative expression of the CTA in TFL expressing the CTA, relative to the relative mean expression in 3 testis tissues; ⁷Percentage of non-cancerous/non-dysplastic cirrhotic liver tissues expressing the CTA (n=35); *% in male.

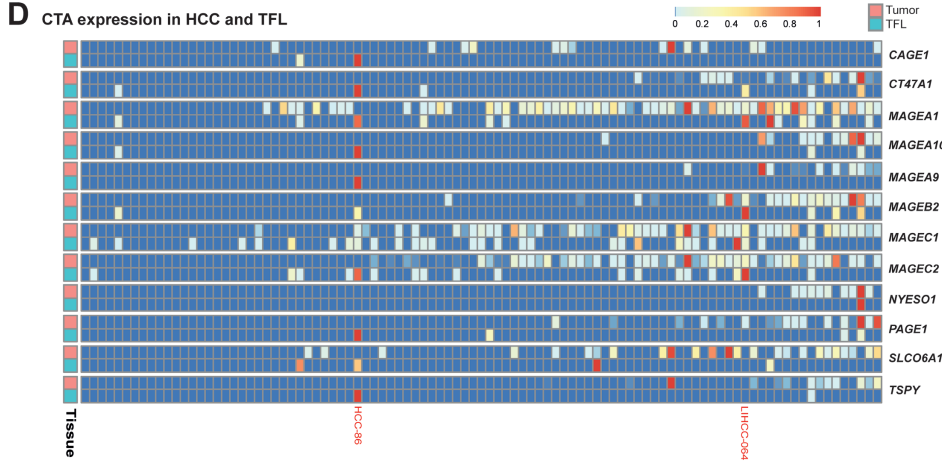
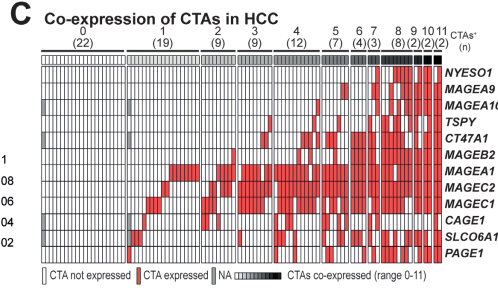
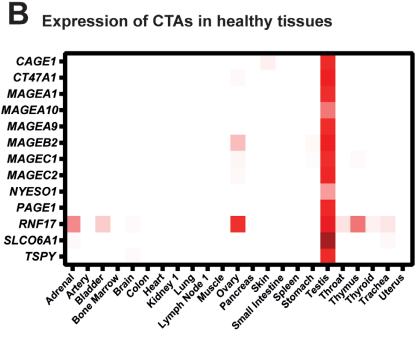
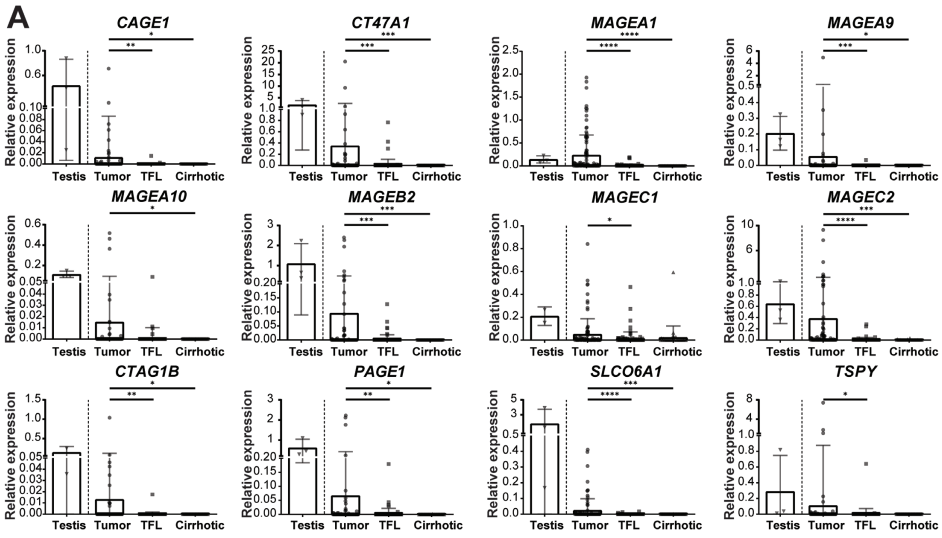
addition, the CTA database (<http://www.cta.lncc.br/>) was consulted, which resulted in identification of 34 different CTAs expressed in HCC; 27 by mRNA, 4 by protein and 3 by protein and mRNA expression. Furthermore, 38 CTAs identified by the CTA database had already been identified in the literature search (**Figure 1B**). Consecutively, to exclude expression of these 107 CTAs in healthy tissues, studies using next-generation sequencing to quantify mRNA expression levels in samples obtained from a large array of healthy tissues and organs, provided by the FANTOM consortium,^{14, 15} Human Protein Atlas (HPA) consortium¹⁵ and genome-based tissue expression (GTEx) consortium,¹⁶ summarized on www.proteinatlas.org, and the genome-wide analysis of CTA mRNA expression by Hofmann *et al.*⁹ were consulted, which led to the exclusion of 47 CTAs expressed in non-germline tissues (**Figure 1B**).

To verify the absence of expression in healthy adult non-germline tissues, the expression of the remaining 60 CTAs was first determined in 21 healthy livers by RT-qPCR. For 11 CTAs it was not feasible to design specific primers, due to high sequence homology with other genes, and these were excluded. Of the 49 CTAs tested, 23 were expressed in healthy livers, with prevalence rates varying from 14 – 100%, and therefore also excluded from further analysis. Twenty-four CTAs showed undetectable mRNA expression levels in healthy livers. Two CTAs (*MAGEC1* and *RING finger protein 17 [RNF17]*) were each found to be expressed in 1 out of 21 tested healthy livers (with very low relative expression levels of 0.005 and 0.002 respectively), and therefore not excluded (**Figure 1C** and **Supplementary Table S4**). These 26 CTAs were selected for further study.

A panel of 12 CTAs is expressed in more than 10% of HCC tumors and not in healthy tissues

The mRNA expression of these 26 CTAs was determined in 100 paired HCC tumors and TFL and in 35 non-malignant cirrhotic liver tissues. Thirteen CTAs were expressed in tumors of >10% of HCC patients at variable expression levels (**Table 1**, **Figure 2A** and **Supplementary Table S5**) and selected for further study. To verify the absence of these 13 CTAs in healthy adult non-germline tissues, and to confirm they are targetable tumor markers, mRNA expression was determined in 23 types of healthy adult tissues other than liver (**Figure 2B**). Most tissues did not express any CTA, except for ovary which expressed five CTAs. Four CTAs were expressed at very low relative expression levels in ovary (*MAGEB2* 0.002, *cancer/testis antigen family 47 member A1 [CT47A1]* 0.002, *MAGEC1* 0.003 and *MAGEC2* 0.002). However, *RNF17* had a higher relative expression level (0.097) and was also expressed in other tissues (thyroid, adrenal gland, bladder, brain, throat, trachea, ovary and thymus), and was therefore excluded from further analysis.

Among the 12 remaining CTAs (**Table 1**) were 6 members of the MAGE gene family (*MAGEA1*, *MAGEA9*, *MAGEA10*, *MAGEB2*, *MAGEC1* and *MAGEC2*). *MAGEA1*, *MAGEC1* and *MAGEC2* were most frequently expressed, with expression rates between 48% and 59% of the tumors. Other CTAs that were expressed in more than 10% of tumors are *cancer antigen 1 (CAGE1)*; 14%), *CT47A1* (27%), *cancer/testis antigen 1B (CTAG1B)*; 10%), *PAGE family member 1 (PAGE1)*; 18%), *solute carrier organic anion transporter family member 6A1 (SLCO6A1)*; 26%) and *testis-specific Y-encoded protein 1 (TSPY1)*; in 21% of male HCC patients and 0% of female HCC patients, as expected from a gene located on the Y-chromosome).¹⁷



◀ **Figure 2. Panel of 12 CTAs expressed in >10% of HCC tumors, but not in healthy tissues.**

mRNA expression of 12 CTAs in 100 paired HCC and TFL tissues, 35 cirrhotic tissues and 22 different adult healthy tissues, as determined by RT-qPCR. **A.** mRNA expression of the 12 CTAs that are expressed in more than 10% of HCCs and not in healthy tissues. Dots show individual patient tissues, bars show the mean relative expression level, and error bars show the standard deviation. Wilcoxon signed-rank test, * $p < 0.05$, ** $p < 0.01$, *** $p < 0.001$. **B.** Heatmap indicating relative mRNA expression levels of all CTAs that are expressed in >10% of HCCs, in healthy adult tissues. **C.** Heatmap indicating co-expression of CTA mRNA in tumor tissue **D.** Heatmap of mRNA expression of the 12 CTAs expressed in $\geq 10\%$ of HCC tumors (rows), in HCC tumors and TFL for every patient (columns). Patients were ordered by number of CTAs expressed in each individual tumor. The $-\Delta Ct$ values were used and for normalization this data was scaled between 0 and 1 for each CTA in each tissue $[\frac{x - \min(x)}{\max(x) - \min(x)}]$. Colors correspond to the value between 0 and 1 and patients LIHCC-064 and HCC-86 are highlighted in red. Heatmap was made in R, using the pheatmap package.

Thus, based on mRNA expression data, we identified a panel of 12 CTAs prevalently expressed in tumors of HCC-patients, but not in healthy adult tissues except testis. Seventy-eight percent of tumors expressed at least one of these 12 CTAs, 59% expressed at least 2 CTAs, 50% expressed at least 3 CTAs, and 40% expressed 4 or more CTAs (**Figure 2C** and **Supplementary Figure S1**).

CTAs are expressed in tumor-free liver tissues of HCC patients

To investigate whether CTA expression in TFL could be an indication of occult metastasis, the expression of these CTAs was also determined in TFL. Despite the TFL being located at least 2 cm away from the tumor and being classified as tumor-free by a pathologist, all 12 CTAs were expressed in these tumor-free liver tissues of HCC patients, although at significantly lower levels (**Table 1**, **Figure 2A** and **Supplementary Table S5**). Forty-five percent of patients expressed at least one CTA in TFL (**Supplementary Figure S1**). The CTAs most frequently expressed in TFL were *MAGEA1* (13% of patients), *MAGEC1* (32%) and *MAGEC2* (19%). The latter two were also found to be expressed in approximately 25% of cirrhotic liver tissues of HCC-patients without liver cancer, suggesting that their expression may be activated during early (pre-) malignant transformations in the liver. Interestingly, when a particular CTA was detected in TFL, it was often also present in the tumor (**Figure 2D**); 85% of patients that expressed any CTA in TFL, also had CTA expression in tumor. For example, LIHCC-064 expressed 7 CTAs in their tumor, of which 5 were also expressed in TFL, suggesting that CTA-expressing cells in TFL were derived from the primary tumor.

CTAs are expressed on protein level in HCC tumors and TFL

Consecutively, we examined protein expression of these CTAs in tumor and TFL tissues of 78 HCC-patients of which FFPE blocks were available (patient characteristics are shown in **Supplementary Table S6**). Protein expression of *MAGEA1*, *MAGEA10*, *MAGEC1*, *MAGEC2* and *NYESO1* in HCC tumors has previously been reported by our group.¹⁸ For *CAGE1* no suitable IHC antibodies (Ab) are available. The *MAGEB2* IHC Ab showed reliable staining in testis tissue, however, we could not detect any positive cells in HCC and TFL tissues. *TSPY1* and *SCLO6A1* Abs demonstrated an unspecific staining pattern and a punctate staining that did not allow for quantification of positive cells, respectively, and were therefore discarded (**Supplementary Figure S2**).¹⁷

Figure 3. Proteins CT47A1, PAGE1, MAGEA9, MAGEC2 and MAGEA1 are expressed in HCC tumors and TFL. ►

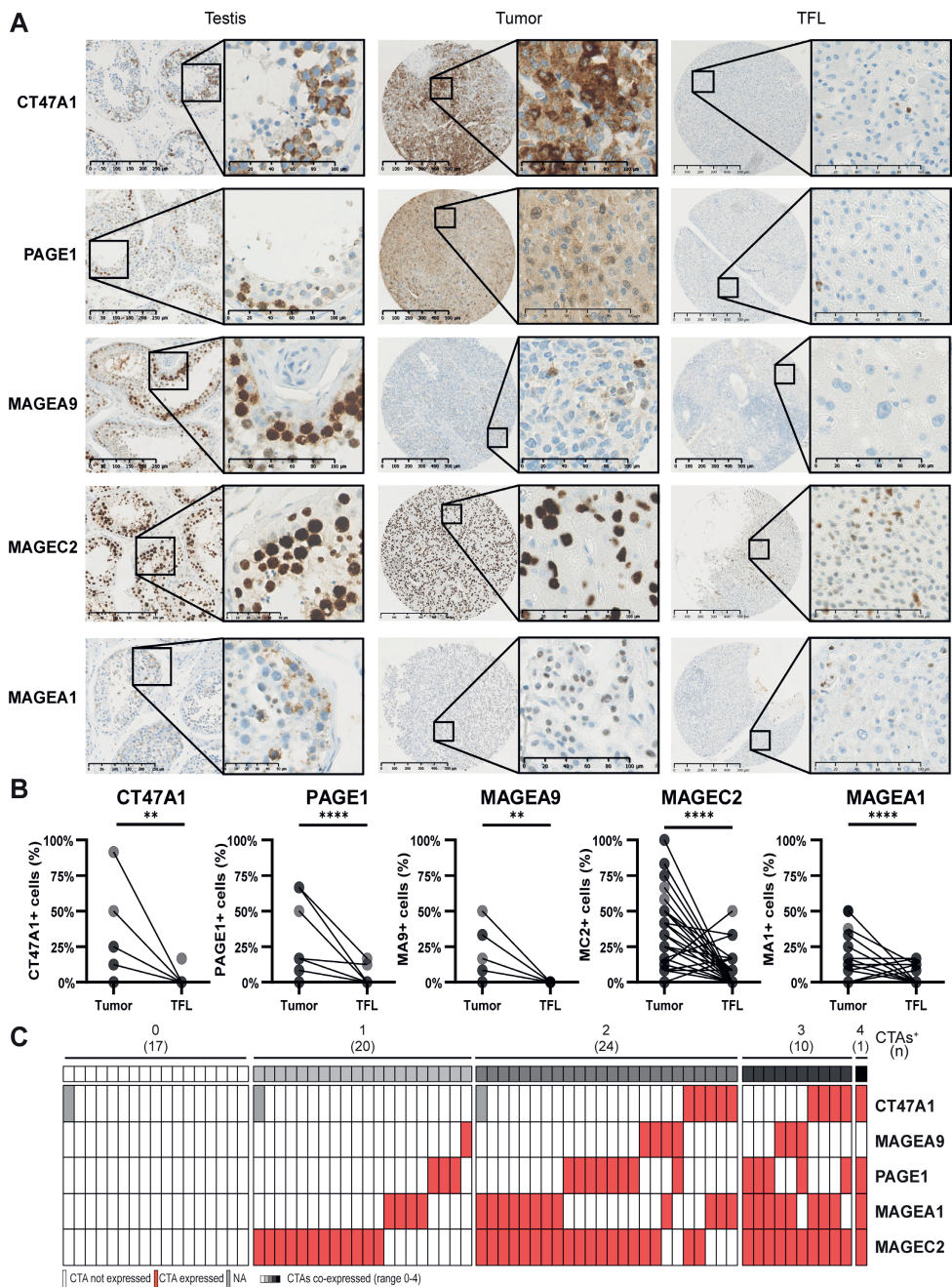
TMA of tumor and TFL tissues were immunohistochemically stained to study the protein expression of aforementioned CTAs. **A.** Representative examples of immunohistochemical stains in testis, a positive HCC tumor tissue and TFL tissue. **B.** Scores of percentages of tumor cells or hepatocytes expressing CT47A1, PAGE1, MAGEA9, MAGEC2 and MAGEA1 in tumors and paired TFL (n=78). Average scores of three tissue cores are shown. Wilcoxon signed-rank test, **p<0.01, ****p<0.0001. **C.** Heatmap indicating co-expression of CTA-proteins in tumor tissue. TMA slides were scanned by a Nanozoomer (Hamamatsu), and analyzed by NDP.view2 software (Hamamatsu).

CT47A1, PAGE1, MAGEA9, MAGEC2 and MAGEA1 were detected at protein level in tumor tissues (CT47A1 in 14%, PAGE1 in 23%, MAGEA9 in 11%, MAGEC2 in 59% and MAGEA1 in 34% of tumors; **Figure 3, Supplementary Figure S3**). These CTAs were expressed by tumor cells, similar to MAGEA10, MAGEC1 and CTAG1B proteins as demonstrated in our previous study.¹⁸ Seventy-one percent of HCC tumor tissues expressed at least one of these CTAs on protein level (**Figure 3C**). In the majority of patients, only part of the tumor cells expressed these CTAs. Proportions of tumor cells which expressed these CTAs were variable between different patients (**Figure 3B**), similar to expression intensity (**Supplementary Figure S3**). MAGEA9 was not expressed in any TFL tissue, while we observed expression of CT47A1, PAGE1, MAGEC2 and MAGEA1 in single scattered hepatocytes in 1%, 3%, 17% and 9% of TFL tissues respectively (**Figure 3B** and **Supplementary Figure S3**). Thirty percent of patients expressed at least one CTA protein in their TFL tissue. Most CTA protein expression was focal, as illustrated by the observation that in most patients only part of the tumor cores included in the TMA showed protein expression (**Supplementary Figure S4**).

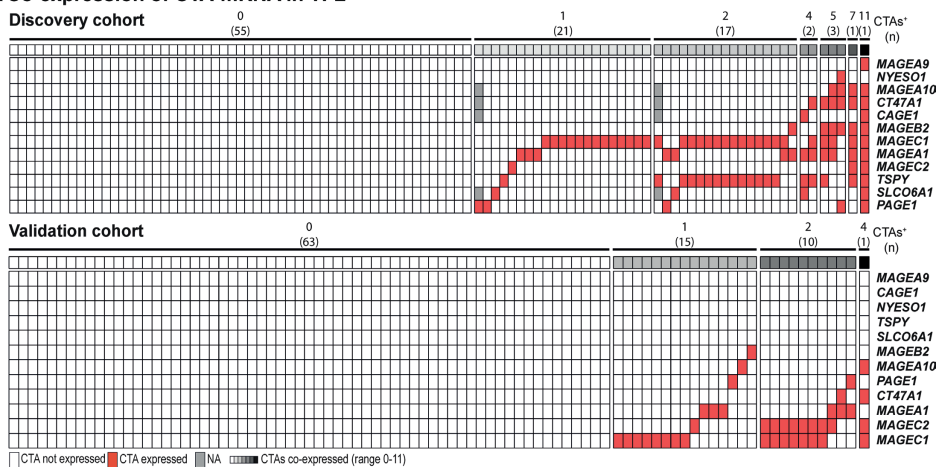
In conclusion, the CTAs that were studied for protein expression, also showed protein expression in tumors and, except MAGEA9, also in TFL.

CTA expression in TFL is correlated with early HCC recurrence and HCC-specific survival after surgical resection

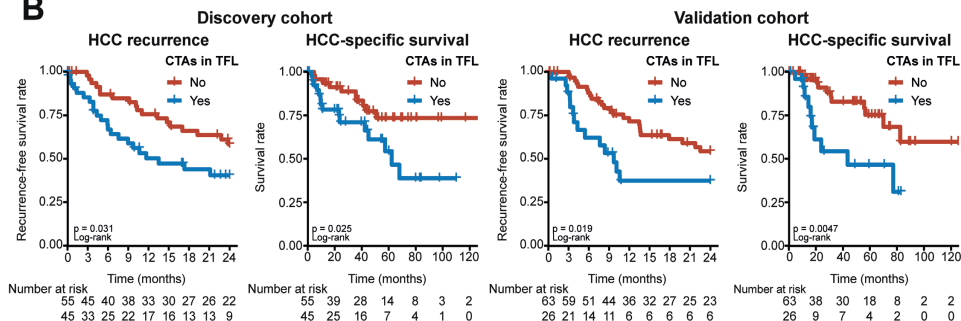
To determine whether CTA expression in TFL could be an indication occult micrometastasis, we analyzed its association with early HCC recurrence, defined as HCC recurrence within 2 years, and HCC-specific survival. Expression of CTA mRNA in TFL (**Figure 4A**) was negatively associated with both early HCC recurrence and HCC-specific patient survival after surgical resection (**Figure 4B** and **Supplementary Figure S5**). Early recurrence was observed in 64% of patients with CTA expression in TFL versus 40% in those without. Two-year HCC-specific survival rates were 71% and 89% in patients with and without CTA expression in TFL, respectively. These results were confirmed in a validation cohort, consisting of 89 HCC patients. In this cohort 29% of HCC patients expressed 1 or more CTAs in TFL, with a maximum of 4 CTAs. Early recurrence was observed in 54% of patients with CTA expression in TFL versus 38% in those without. Two-year HCC-specific survival rates were 69% and 94% in patients with and without CTA expression in TFL, respectively. Interestingly, when we discriminated between local intra-hepatic and distant cancer recurrence, patients with CTA-expression in TFL showed more and faster intra-hepatic



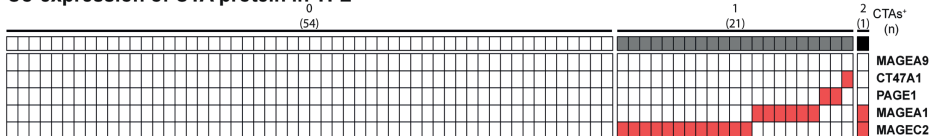
A Co-expression of CTA-mRNA in TFL



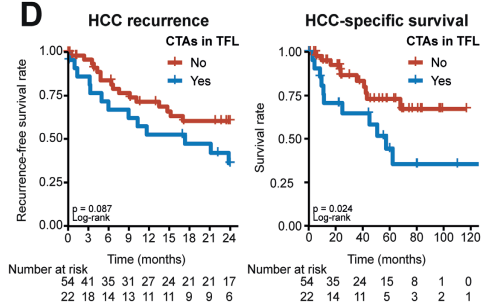
B



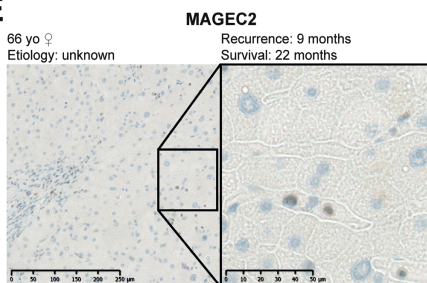
C Co-expression of CTA protein in TFL



D



E



◀ **Figure 4. Both mRNA and protein expression of CTAs in TFL are associated with HCC recurrence and HCC-specific survival.**

A. Heatmap indicating co-expression of CTA mRNA in tumor-free liver tissue in the discovery and validation cohort. **B.** Early HCC recurrence and HCC-specific survival in HCC patients by CTA mRNA expression in TFL in the discovery and validation cohort. Plus-signs indicate censored data. Cox-Mantel log-rank test. **C.** Heatmap indicating co-expression of CTA protein in tumor-free liver tissue. **D.** Early HCC recurrence and HCC-specific survival in HCC patients by CTA protein expression in TFL. Plus-signs indicate censored data. Cox-Mantel log-rank test. **E.** Representative example of IHC staining of MAGEC2 protein expression in TFL, and accompanying patient data. TMA slides were scanned by a Nanozoomer (Hamamatsu), and analyzed by NDP.view2 software (Hamamatsu).

cancer recurrence in both cohorts. In contrast, there was no difference in distant cancer recurrence between patients with or without CTA-expression in TFL in the discovery cohort, while in the validation cohort the difference in distant cancer recurrence between patients with and without CTA-expression in TFL was small and borderline significant ($p=0.046$) (**Supplementary Figure S6**). The robust association with intra-hepatic recurrence in both cohorts supports the hypothesis that CTA-expression in TFL may reflect the presence of histologically non-distinguishable intra-hepatic micro-metastases.

Patients with and without CTA-expression in TFL did not differ in any clinical or histological characteristic, including type of surgery, tumor differentiation grade, and vascular invasion (**Supplementary Table S1**; p -values > 0.05 , not shown). In multivariate analysis, mRNA expression in TFL was an independent prognostic factor for early HCC recurrence (hazard ratio [HR] 2.3 and 2.1, for the discovery and validation cohort respectively) and HCC-specific survival (HR 2.3 and 3.6, respectively) in both cohorts, as is shown in **Table 2**. CTA protein expression in TFL (**Figure 4C**) was associated with poor postsurgical outcome as well (**Figure 4D**). In multivariate analysis CTA protein expression in TFL was also an independent prognostic factor for HCC recurrence (HR 2.5) and HCC-specific survival (HR 3.8; **Supplementary Table S7**). An example of CTA protein expression in TFL is shown in **Figure 4E**, the MAGEC2 expressing cells were scattered across the TFL. All TFL tissues with CTA expression were reassessed by a medical pathologist to verify the absence of histologically detectable HCC metastasis. Except for extensive vascular invasion in one patient, which also expressed PAGE1 in TFL (**Supplementary Figure S7**), no histological indications for the presence of malignant cells in TFL were present. Notably, both survival analysis and cox-regression analysis of CTA expression in tumor tissues did not show associations with postsurgical outcome (**Supplementary Table S8** and **Supplementary Figure S8**), and neither did CTA protein expression (data not shown).

In conclusion, we found that CTA expression in TFL is an independent negative prognostic factor of both HCC recurrence and HCC-specific survival, and we validated these findings in a validation cohort. This may indicate that occult CTA-expressing (pre-)malignant cells are present in the remaining liver tissue after tumor resection and that these cells could be responsible for HCC recurrence, especially for intra-hepatic recurrence, after surgery.

DISCUSSION

We established a novel panel of 12 CTAs, each expressed in at least 10% of HCC tumors and not in healthy tissues except immune-privileged testis. Based on mRNA analysis, approximately 80% of HCC-patients expressed one or more of these antigens in their tumor tissues, whereas protein expression of five of these CTAs was detected in approximately 70% of HCC tumors. In addition, we found that 45% of HCC-patients included in the discovery cohort expressed one or more of the 12 CTAs of our panel in their histologically tumor-free liver tissue, which was associated with early HCC recurrence and worse patient survival after curative surgery. These associations were confirmed in a validation cohort, in which 29% of HCC patients expressed one or more CTAs in TFL.

High recurrence rates after surgery with curative intent worsens the survival of HCC patients. Aufhauser, et al.¹⁹ hypothesized that early recurrence, defined as recurrence within 2 years after tumor resection, is due to occult metastasis rather than de novo tumor formation, but failed to find biomarkers identifying occult metastasis at the time of resection. Therefore, we aimed to find biomarkers detecting occult multifocality at the time of resection, in order for these patients to be selected for adjuvant treatment. We hypothesized that biomarkers identifying occult multifocality should be abundantly and relatively frequently expressed in tumor tissues, to allow for high sensitivity, and should be completely absent in healthy tissues, to allow for high specificity.

CTA expression in tumors of HCC-patients has been studied before, however, as demonstrated by the results of our literature study (**Supplementary Table S3**), most studies investigated only a few CTAs, determined either RNA or protein expression but not both, did not exclude CTAs expressed in healthy tissues, and most notably, did not look at or acknowledge CTA expression in tumor-free liver (**Figure 1B and C, Supplementary Table S5**). Thus, to assure we would determine the CTAs most likely to serve as markers for occult multifocality in TFL, we repeated CTA expression analysis in tumor tissues and confirmed absence of the selected CTAs in healthy tissues. As far as we are aware, the present study is the most comprehensive investigation of CTA-expression in tumor and paired TFL tissues of HCC-patients performed. Another recent report used the GEPIA database to analyze CTA expression in tumors of HCC patients, but did not investigate CTA expression in non-cancerous liver tissues of HCC patients.²⁰ An additional benefit of excluding CTAs expressed in healthy tissues would be their suitability for therapeutic targeting, as targeting proteins exclusively expressed in the tumor will not lead to therapy-induced auto-immunity in potential future clinical applications.⁸

As the expression of CTAs in tumor-free (liver) tissues of patients with HCC or other cancer types has barely been investigated before, their association with cancer recurrence or patient survival has also not been investigated in HCC, nor any other types of cancer. Therefore it was unknown if CTAs could serve as biomarkers for occult multifocality. The 2-year recurrence rate in the study of Aufhauser, et al¹⁹ of 46% is comparable to the observed rate of 50% and 43% in the discovery and validation cohorts of this study, respectively, and therefore we expect the cohorts to be comparable. Unexpectedly, we observed mRNA expression of one or more of the 12 CTAs of our panel in histologically tumor-free liver tissues

Discovery cohort								
Variable	Early recurrence (<2 yr)				HCC-specific survival			
	Univariate analysis		Multivariate analysis		Univariate analysis		Multivariate analysis	
	HR (95% CI)	p-value	HR (95% CI)	p-value	HR (95% CI)	p-value	HR (95% CI)	p-value
≥1 CTA in TFL	2.3 (1.3-4.0)	0.0034	2.5 (1.47-4.5)	0.003	2.4 (1.1-5.4)	0.03	2.3 (1.0-5.3)	0.044
≥2 CTAs in TFL	2.1 (1.2-3.7)	0.013			1.7 (0.7-3.9)	0.22		
≥3 CTAs in TFL	4.2 (1.9-9.4)	0.00053			5.1 (1.9-14)	0.0015		
Number of CTAs in TFL (numeric)	1.3 (1.2-1.5)	2.0E-05			1.3 (1.1-1.5)	0.0011		
>1 tumor	1.2 (0.7-2.0)	0.56			1.1 (0.5-2.4)	0.83		
>2 tumors	2.6 (1.3-4.9)	0.0042	2.4 (1.2-4.7)	0.02	1.8 (0.7-4.9)	0.22		
Cirrhosis	1.6 (0.9-2.8)	0.12			1.5 (0.7-3.4)	0.33		
Chronic viral hepatitis	2.3 (1.3-4.0)	0.0031	2.7 (1.5-5.0)	0.001	3.3 (1.5-7.2)	0.0032	4.63 (2.0-10.8)	0.0004
Vascular invasion	1.3 (0.7-2.3)	0.41			2.2 (0.96-4.9)	0.063		
Tumor > 5 cm	1.3 (0.7-2.3)	0.37			2.3 (0.9-5.7)	0.081		
AFP > 200 ug/l	1.9 (1.0-3.4)	0.034			2.7 (1.2-6)	0.013		
AFP > 400 ug/l	2.4 (1.3-4.5)	0.0051	3.0 (1.5-5.8)	0.001	3.3 (1.5-7.3)	0.0038	4.0 (1.7-9.4)	0.002

Validation cohort								
Variable	Early recurrence (<2 yr)				HCC-specific survival			
	Univariate analysis		Multivariate analysis		Univariate analysis		Multivariate analysis	
	HR (95% CI)	p-value	HR (95% CI)	p-value	HR (95% CI)	p-value	HR (95% CI)	p-value
≥1 CTA in TFL	2.2 (1.1-4.2)	0.022	2.1 (1.1-4.1)	0.03	3.3 (1.4-7.7)	0.0074	3.6 (1.5-8.8)	0.004
≥2 CTAs in TFL	1.5 (0.58-3.8)	0.41			2.3 (0.83-6.3)	0.11		
≥3 CTAs in TFL	1.1e-07 (0-Inf)	1			3.9e-08 (0-Inf)	1		
Number of CTAs in TFL (numeric)	1.2 (0.89-1.7)	0.21			1.4 (0.95-2)	0.095		
>1 tumor	2.1 (1-4.2)	0.043	2.2 (1.1-4.5)	0.03	0.9 (0.27-3.1)	0.87		
>2 tumors	1.7 (0.67-4.4)	0.26			0.96 (0.22-4.1)	0.96		
Cirrhosis	0.77 (0.39-1.5)	0.45			2.3 (0.97-5.5)	0.059	2.6 (1.1-6.3)	0.03
Chronic viral hepatitis	0.91 (0.42-2)	0.82			0.98 (0.36-2.7)	0.97		
Vascular invasion	2.1 (0.98-4.4)	0.055			1.5 (0.59-3.9)	0.38		
Tumor > 5 cm	2.5 (1.2-5)	0.011	2.6 (1.3-5.3)	0.007	1.5 (0.61-3.6)	0.38		
AFP > 200 ug/l	1.6 (0.8-3.3)	0.18			0.83 (0.28-2.5)	0.74		
AFP > 400 ug/l	1.3 (0.61-2.9)	0.46			0.65 (0.19-2.2)	0.5		

Table 2. CTA mRNA-expression in TFL is an independent prognostic factor of HCC recurrence and HCC-specific survival.

Univariate and multivariate analyses of factors associated with recurrence and survival according to the cox proportional hazard model. Abbreviations: AFP, alphafoetoprotein; 95% CI, 95% confidence interval; CTA, cancer testis antigen; HR, hazard ratio; TFL, tumor-free liver.

in a substantial percentage of patients; 45% of tumor-free tissues included in the discovery cohort and in 29% of tumor-free tissues in the validation cohort. Protein expression of one or more of 4 of these CTAs was detected in non-cancerous liver tissues of 40% of patients of the discovery cohort. The 2-year recurrence rates in our cohorts were significantly higher in patients with CTA mRNA-expression in TFL compared to patients without CTA-expression in TFL; 64% vs 40% in the discovery cohort and 54% vs 38% in the validation cohort. Interestingly, in both cohorts CTA expression in TFL was associated with local intra-hepatic recurrence, but in the discovery cohort not with distant cancer recurrence. Moreover, CTA mRNA expression profiles in TFL were generally similar to those in the corresponding tumors, and our preliminary immunohistochemical data show that CTA-expressing cells in TFL were either single cells or small foci. Based on these observations, we hypothesize that CTA-expressing cells in TFL of patients with early intra-hepatic HCC recurrence indeed represent occult intra-hepatic micro-metastases, and are less likely to represent de novo tumors. This hypothesis is supported by a study performed in colorectal cancer patients with liver metastasis.²¹ In TFL, they detected low frequencies of somatic mutations that were also observed in matched tumor samples, despite normal histological appearance. Since these mutations were not found in the matched blood samples, it was hypothesized that tumor DNA or tumor cells diffused or migrated into the surrounding normal tissue.²¹ However, the authors did not correlate this to either cancer recurrence or survival. Similarly, a previous study detected MAGE-antigen expression in lung tissues of former smokers at risk for NSCLC development,²² but also did not show any data regarding actual NSCLC development.

Determining lymph node involvement is a widely accepted method for staging a wide variety of cancers. The lymph node metastases themselves are not the cause of death in most patients, however, lymph node involvement is correlated with the spread to vital organs.²³ Therefore it is correlated with reduced patient survival and an important prognostic factor.^{24, 25} Likewise, we showed that CTA expression in tumor-free tissue is correlated with recurrence of HCC after curative surgery, independent of conventional prognostic factors. We hypothesize that these CTAs in TFL are expressed by micro-metastases, leading to tumor recurrence and eventually HCC-related death. Detection of occult metastasis in tumor-free tissue, by detection of CTA expression or other methods such as mutation analysis, could be used as a new concept to identify patients at risk for developing (local) metastasis. Moreover, these CTAs could serve as targets to prevent and/or treat these (micro-)metastases.

One way to target these CTAs is by vaccination. Most therapeutic cancer vaccination studies targeting CTAs have been performed in advanced cancer patients with high tumor load in which an immunosuppressive tumor microenvironment has been established, and showed modest clinical results.²⁶ Based on our data showing the presence of scattered single CTA-expressing cells and small foci of CTA-expressing cells in TFL of 29-45% of resected HCC-patients, therapeutic vaccination with CTAs after tumor resection might be a promising approach to prevent HCC recurrence in such patients. Compared to vaccination in advanced cancer, we expect that the low tumor load remaining after resection of detectable tumors may enhance the probability of effective immunological eradication of CTA-expressing (pre-)malignant

cells. A prerequisite for therapeutically targeting antigens by vaccination, is that the antigens are immunogenic. Most of the CTAs included in our panel have previously been proven immunogenic in cancer patients.²⁷ More specifically in HCC patients, we and other research groups have demonstrated the presence of MAGEA1-, MAGEA10-, MAGEC2- and NY-ESO-1-specific T-cells, both in blood and in tumors.²⁸⁻³² In addition, NY-ESO-1 and TSPY-specific IgG have been detected in HCC-patients,^{33, 34} while CT47A1-, PAGE1- and SLCO6A1-specific antibodies were recently detected in NSCLC patients.³⁵

Several CTAs of our panel, such as the MAGE-family members, *CTAG1B*, *TSPY1* and *CAGE1*, are functionally involved in tumorigenesis and cancer progression by modulating gene expression, regulating mitosis and tumorigenic signaling.^{8, 10, 36-38} More specifically, MAGE-A9 and TSPY have been shown to be involved in HCC tumor cell proliferation.^{36, 38} Their role in cancer progression is further supported by data showing that CTA expression is more prevalent in advanced tumors.^{39, 40} Importantly, the involvement of these CTAs in cancer progression may prevent antigen loss upon therapeutic targeting.³⁷

We acknowledge several limitations of this study. First, since the etiologies of HCC differ geographically, this CTA-panel might not be applicable to non-Western HCC-populations. Secondly, future research is required to investigate whether CTA-expressing cells in TFL are really (pre-)malignant cells that can give rise to cancer recurrence. Moreover, as not all HCC tumors expressed the selected CTAs, occult micro-metastasis of the tumors not expressing CTAs may be missed. Finally, for the concept – detection and treatment of occult multifocality by detection of therapeutically targetable CTAs in supposedly tumor-free tissues – to become widely applicable, it should be validated in other cancer types.

CONCLUSIONS

We established a panel of 12 testis-restricted CTAs that are expressed in tumors of almost 80% of HCC patients. In addition, we demonstrated expression of these CTAs in tumor-free liver tissues of 45% and 29% of HCC-patients in two different cohorts. The negative association between expression of these CTAs in TFL and HCC-recurrence and patient survival, independent of clinical and histological tumor characteristics, combined with immunohistochemistry data showing scattered CTA-expressing cells in TFL, suggests that CTA-expressing (pre-)malignant cells remain present in the liver after tumor resection, and are indicative for the potential relevance of therapeutic targeting of these antigens. To prevent tumor recurrence, HCC patients with CTA expression in TFL could be selected for adjuvant therapy, either by therapeutic targeting of these CTAs, other (immuno-) therapeutic strategies, or a combination of both.

Acknowledgments

RNA from testicular tissues was kindly provided to us by Prof. L.H.J. Looijenga and FFPE blocks of testis tissues by Dr. R. Hersmus (Department of Pathology, Erasmus MC). RNA from healthy bone marrow was provided to us by Dr. E. Braakman (Department of Hematology, Erasmus MC), and healthy donor kidney by Prof. Carla Baan (Department of Internal Medicine, both from Erasmus MC). Anti-MAGEA9 mAb was kindly provided by Prof. Y. Fradet, Laboratoire d'Uro-Oncoïe Expérimentale, Université Laval, Québec, Canada. We would like to thank Prof. dr. Kees Melief (ISA Pharmaceuticals, Leiden) for carefully reviewing our manuscript and dr. Nicole S. Erler (Department of Epidemiology and Biostatistics, Erasmus MC) for statistical advice.

REFERENCES

1. Bray F, Ferlay J, Soerjomataram I, Siegel RL, Torre LA, Jemal A. Global cancer statistics 2018: GLOBOCAN estimates of incidence and mortality worldwide for 36 cancers in 185 countries. *CA Cancer J Clin*. 2018.
2. Llovet JM, Ricci S, Mazzaferro V, Hilgard P, Gane E, Blanc JF, de Oliveira AC, Santoro A, Raoul JL, Forner A, et al. Sorafenib in advanced hepatocellular carcinoma. *N Engl J Med*. 2008;359(4):378-90.
3. Bruix J, Qin S, Merle P, Granito A, Huang YH, Bodoky G, Pracht M, Yokosuka O, Rosmorduc O, Breder V, et al. Regorafenib for patients with hepatocellular carcinoma who progressed on sorafenib treatment (RESORCE): a randomised, double-blind, placebo-controlled, phase 3 trial. *Lancet*. 2017;389(10064):56-66.
4. Ulahannan SV, Duffy AG, McNeel TS, Kish JK, Dickie LA, Rahma OE, McGlynn KA, Greten TF, Altekruze SF. Earlier presentation and application of curative treatments in hepatocellular carcinoma. *Hepatology*. 2014;60(5):1637-44.
5. Poon RT. Differentiating early and late recurrences after resection of HCC in cirrhotic patients: implications on surveillance, prevention, and treatment strategies. *Ann Surg Oncol*. 2009;16(4):792-4.
6. Finkelstein SD, Marsh W, Demetris AJ, Swalsky PA, Sasatomi E, Bonham A, Subotin M, Dvorchik I. Microdissection-based allelotyping discriminates de novo tumor from intrahepatic spread in hepatocellular carcinoma. *Hepatology*. 2003;37(4):871-9.
7. Hoshida Y, Villanueva A, Kobayashi M, Peix J, Chiang DY, Camargo A, Gupta S, Moore J, Wrobel MJ, Lerner J, et al. Gene expression in fixed tissues and outcome in hepatocellular carcinoma. *N Engl J Med*. 2008;359(19):1995-2004.
8. Gjerstorff MF, Andersen MH, Ditzel HJ. Oncogenic cancer/testis antigens: prime candidates for immunotherapy. *Oncotarget*. 2015;6(18):15772-87.
9. Hofmann O, Caballero OL, Stevenson BJ, Chen YT, Cohen T, Chua R, Maher CA, Panji S, Schaefer U, Kruger A, et al. Genome-wide analysis of cancer/testis gene expression. *Proc Natl Acad Sci U S A*. 2008;105(51):20422-7.
10. Whitehurst AW. Cause and consequence of cancer/testis antigen activation in cancer. *Annu Rev Pharmacol Toxicol*. 2014;54:251-72.
11. Altman DG, McShane LM, Sauerbrei W, Taube SE. Reporting Recommendations for Tumor Marker Prognostic Studies (REMARK): explanation and elaboration. *PLoS Med*. 2012;9(5):e1001216.
12. Tang A, Bashir MR, Corwin MT, Cruite I, Dietrich CF, Do RKG, Ehman EC, Fowler KJ, Hussain HK, Jha RC, et al. Evidence Supporting LI-RADS Major Features for CT- and MR Imaging-based Diagnosis of Hepatocellular Carcinoma: A Systematic Review. *Radiology*. 2018;286(1):29-48.
13. Charoentong P, Finotello F, Angelova M, Mayer C, Efremova M, Rieder D, Hackl H, Trajanoski Z. Pan-cancer Immunogenomic Analyses Reveal Genotype-Immunophenotype Relationships and Predictors of Response to Checkpoint Blockade. *Cell Rep*. 2017;18(1):248-62.
14. Yu NY, Hallstrom BM, Fagerberg L, Ponten F, Kawaji H, Carninci P, Forrest AR, Fantom C, Hayashizaki Y, Uhlen M, et al. Complementing tissue characterization by integrating transcriptome profiling from the Human Protein Atlas and from the FANTOM5 consortium. *Nucleic Acids Res*. 2015;43(14):6787-98.
15. Keen JC, Moore HM. The Genotype-Tissue Expression (GTEx) Project: Linking Clinical Data with Molecular Analysis to Advance Personalized Medicine. *J Pers Med*. 2015;5(1):22-9.
16. Lizio M, Abugessaisa I, Noguchi S, Kondo A, Hasegawa A, Hon CC, de Hoon M, Severin J, Oki S, Hayashizaki Y, et al. Update of the FANTOM web resource: expansion to provide additional transcriptome atlases. *Nucleic Acids Res*. 2019;47(D1):D752-D8.
17. Schnieders F, Dork T, Arnemann J, Vogel T, Werner M, Schmidtke J. Testis-specific protein, Y-encoded (TSPY) expression in testicular tissues. *Hum Mol Genet*. 1996;5(11):1801-7.

18. Sideras K, Bots SJ, Biermann K, Sprengers D, Polak WG, JN IJ, de Man RA, Pan Q, Sleijfer S, Bruno MJ, et al. Tumour antigen expression in hepatocellular carcinoma in a low-endemic western area. *Br J Cancer*. 2015;112(12):1911-20.
19. Aufhauser DD, Jr., Sadot E, Murken DR, Eddinger K, Hoteit M, Abt PL, Goldberg DS, DeMatteo RP, Levine MH. Incidence of Occult Intrahepatic Metastasis in Hepatocellular Carcinoma Treated With Transplantation Corresponds to Early Recurrence Rates After Partial Hepatectomy. *Ann Surg*. 2018;267(5):922-8.
20. Zhang YP, Bao ZW, Wu JB, Chen YH, Chen JR, Xie HY, Zhou L, Wu J, Zheng SS. Cancer-Testis Gene Expression in Hepatocellular Carcinoma: Identification of Prognostic Markers and Potential Targets for Immunotherapy. *Technol Cancer Res Treat*. 2020;19:1533033820944274.
21. Beije N, Helmijr JC, Weerts MJA, Beaufort CM, Wiggin M, Marziali A, Verhoef C, Sleijfer S, Jansen M, Martens JWM. Somatic mutation detection using various targeted detection assays in paired samples of circulating tumor DNA, primary tumor and metastases from patients undergoing resection of colorectal liver metastases. *Mol Oncol*. 2016;10(10):1575-84.
22. Jang SJ, Soria JC, Wang L, Hassan KA, Morice RC, Walsh GL, Hong WK, Mao L. Activation of melanoma antigen tumor antigens occurs early in lung carcinogenesis. *Cancer Res*. 2001;61(21):7959-63.
23. Wong SY, Hynes RO. Lymphatic or hematogenous dissemination: how does a metastatic tumor cell decide? *Cell Cycle*. 2006;5(8):812-7.
24. Jones D, Pereira ER, Padera TP. Growth and Immune Evasion of Lymph Node Metastasis. *Front Oncol*. 2018;8:36.
25. Nathanson SD. Insights into the mechanisms of lymph node metastasis. *Cancer*. 2003;98(2):413-23.
26. Hollingsworth RE, Jansen K. Turning the corner on therapeutic cancer vaccines. *NPJ Vaccines*. 2019;4:7.
27. Andersen RS, Thruue CA, Junker N, Lyngaa R, Donia M, Ellebaek E, Svane IM, Schumacher TN, Thor Straten P, Hadrup SR. Dissection of T-cell antigen specificity in human melanoma. *Cancer Res*. 2012;72(7):1642-50.
28. Flecken T, Schmidt N, Hild S, Gostick E, Drognitz O, Zeiser R, Schemmer P, Bruns H, Eiermann T, Price DA, et al. Immunodominance and functional alterations of tumor-associated antigen-specific CD8+ T-cell responses in hepatocellular carcinoma. *Hepatology*. 2014;59(4):1415-26.
29. Bricard G, Bouzourene H, Martinet O, Rimoldi D, Halkic N, Gillet M, Chaubert P, Macdonald HR, Romero P, Cerottini JC, et al. Naturally acquired MAGE-A10- and SSX-2-specific CD8+ T cell responses in patients with hepatocellular carcinoma. *J Immunol*. 2005;174(3):1709-16.
30. Zhou G, Sprengers D, Boor PPC, Doukas M, Schutz H, Mancham S, Pedroza-Gonzalez A, Polak WG, de Jonge J, Gaspersz M, et al. Antibodies Against Immune Checkpoint Molecules Restore Functions of Tumor-Infiltrating T Cells in Hepatocellular Carcinomas. *Gastroenterology*. 2017;153(4):1107-19 e10.
31. Shang XY, Chen HS, Zhang HG, Pang XW, Qiao H, Peng JR, Qin LL, Fei R, Mei MH, Leng XS, et al. The spontaneous CD8+ T-cell response to HLA-A2-restricted NY-ESO-1b peptide in hepatocellular carcinoma patients. *Clin Cancer Res*. 2004;10(20):6946-55.
32. Inada Y, Mizukoshi E, Seike T, Tamai T, Iida N, Kitahara M, Yamashita T, Arai K, Terashima T, Fushimi K, et al. Characteristics of Immune Response to Tumor-Associated Antigens and Immune Cell Profile in Patients With Hepatocellular Carcinoma. *Hepatology*. 2019;69(2):653-65.
33. Yin YH, Li YY, Qiao H, Wang HC, Yang XA, Zhang HG, Pang XW, Zhang Y, Chen WF. TSPY is a cancer testis antigen expressed in human hepatocellular carcinoma. *Br J Cancer*. 2005;93(4):458-63.
34. Korangy F, Ormandy LA, Bleck JS, Klempnauer J, Wilkens L, Manns MP, Gretten TF. Spontaneous tumor-specific humoral and cellular immune responses to NY-ESO-1 in hepatocellular carcinoma. *Clin Cancer Res*. 2004;10(13):4332-41.

35. Djureinovic D, Dodig-Crnkovic T, Hellstrom C, Holgersson G, Bergqvist M, Mattsson JSM, Ponten F, Stahle E, Schwenk JM, Micke P. Detection of autoantibodies against cancer-testis antigens in non-small cell lung cancer. *Lung Cancer*. 2018;125:157-63.
36. Deng Q, Li KY, Chen H, Dai JH, Zhai YY, Wang Q, Li N, Wang YP, Han ZG. RNA interference against cancer/testis genes identifies dual specificity phosphatase 21 as a potential therapeutic target in human hepatocellular carcinoma. *Hepatology*. 2014;59(2):518-30.
37. Maxfield KE, Taus PJ, Corcoran K, Wooten J, Macion J, Zhou Y, Borromeo M, Kollipara RK, Yan J, Xie Y, et al. Comprehensive functional characterization of cancer-testis antigens defines obligate participation in multiple hallmarks of cancer. *Nat Commun*. 2015;6:8840.
38. Tu W, Yang B, Leng X, Pei X, Xu J, Liu M, Dong Q, Tao D, Lu Y, Liu Y, et al. Testis-specific protein, Y-linked 1 activates PI3K/AKT and RAS signaling pathways through suppressing IGFBP3 expression during tumor progression. *Cancer Sci*. 2019;110(5):1573-86.
39. Velazquez EF, Jungbluth AA, Yancovitz M, Gnjatic S, Adams S, O'Neill D, Zavilevich K, Albukh T, Christos P, Mazumdar M, et al. Expression of the cancer/testis antigen NY-ESO-1 in primary and metastatic malignant melanoma (MM)--correlation with prognostic factors. *Cancer Immun*. 2007;7:11.
40. Barrow C, Browning J, MacGregor D, Davis ID, Sturrock S, Jungbluth AA, Cebon J. Tumor antigen expression in melanoma varies according to antigen and stage. *Clin Cancer Res*. 2006;12(3 Pt 1):764-71.

SUPPLEMENTARY DATA

Materials & Methods

Liver and healthy tissue samples

Cirrhotic and healthy (liver) tissues

Freshly frozen healthy liver tissues (n=21) were obtained during liver transplantation from donor liver grafts at the end of cold ischemic storage. Archived freshly frozen tissue samples of non-cancerous cirrhotic livers (n=35) were retrieved from the tissue bank of the Department of Pathology, Erasmus Medical Center Rotterdam. The non-cancerous cirrhotic liver tissues had been retrieved from patients who underwent liver transplantation for liver cirrhosis in our center between May 2007 and June 2017. The etiology of the cirrhosis was determined by information from medical records, laboratory tests and pathological examination of the explanted livers. Cirrhotic livers with malignancies, diagnosed by pathological examination, were excluded.

RNA isolated from fresh frozen healthy adrenal gland (R1234004-50), artery (HR-810), brain (R1234035-50), colon (R1234090-50), heart (R1234122-50), lung (R1234152-50), muscle (R1234171-50), ovary (HR-406), pancreas (R1234188-50), skin (R1234218-50), small intestine (R1234226-50), stomach (HR-302), testis (R1234260-50), throat (R1234263-10), thymus (HR-702), thyroid (R1234265-50), trachea (R1234160-50), urinary bladder (R1234010-50) and uterus (R1234274-50) tissues were purchased from AMS Biotechnology Ltd, Abingdon, UK. Bone marrow derived from a healthy donor (Department of Hematology, Erasmus MC), healthy kidney tissue obtained from a donor kidney (Department of Internal Medicine, Erasmus MC) and RNA of healthy testis tissues (Department of Pathology, Erasmus MC) were kindly provided. Lymph node and spleen tissues were collected from samples retrieved during liver transplantation in our center in September 2019.

Quantitative real-time PCR

RNA was isolated using the NucleoSpin® RNA isolation kit of Macherey-Nagel (Dueren, Germany) according to manufacturer's instructions. RNA quality was assessed with NanoDrop 2000 (Thermo Scientific), using 260/230 ratios. Samples with a ratio <2.0 were excluded and if possible RNA was re-isolated. RNA (4 ug) was reverse-transcribed into cDNA using PrimeScript™ RT master Mix (Perfect Real Time, Takara, cat# RR036A), according to the manufacturer's instructions. RT-qPCR was performed using SYBR™ Green PCR Master Mix (ThermoFisher) in a StepOnePlus™ Real-Time PCR System (Applied Biosystems), using 12.5 ng cDNA per reaction, with the following conditions: 50°C for 2 minutes, 95°C for 2 minutes, then 38 cycles of 95°C for 15 seconds, 58-62°C for 15 seconds (according to the T_m of the primers), 72°C for 1 minute, and then finally for the Melt Curve stage 95°C for 15 seconds, 60°C for 1 minute and a 0.7°C step-wise increase until 95°C was reached. All Ct-values over 35 were considered negative. The level of target gene expression relative to the geometric mean of three control genes (HPRT1, GUSB, PMM1)¹ was calculated by 2^{-ΔΔT} method, after which a cut-off of 0.001 was used to define expression. All amplifications were performed in at least two technical repeats. Means of technical

replicates were used for analysis. Primers were designed with Primer Blast (NCBI), efficiency was determined by dilution of cDNA and product length was determined by gel electrophoresis.

Immunohistochemistry

The FFPE blocks of the HCC and TFL tissues were examined by a pathologist (MD) to mark tumor and tumor-free liver tissues. A TMA Grand Master (2.5; 3D Histech) was used to create tissue microarrays (TMA). Three tissue cores of 1 mm were taken of each tissue and placed in a recipient formalin block. Immunohistochemistry (IHC) was performed using an automated, validated and accredited staining system (Ventana Benchmark ULTRA, Ventana Medical Systems, Tucson, AZ, USA) using the optiview universal DAB detection Kit (cat.760-700, Ventana Medical Systems). In brief, following deparaffinization and heat-induced antigen retrieval tissue sections were incubated with each of the primary antibodies according to their optimized incubation time and concentration (**Supplementary Table S9**). The antibodies were titrated using testis as a positive control tissue and placenta and spleen as negative control tissues. Incubation was followed by hematoxylin II counter stain for 12 minutes and then a blue colouring reagent for 8 minutes according to the manufacturer's instructions (Ventana Medical Systems, Tucson, AZ, USA). The stained TMAs were then scanned using a Nanozoomer (Hamamatsu), and analyzed using NDP.view2 software (Hamamatsu).

Search query:

```
((("cancer testis antigen"[All Fields] OR (((("cancer"[All Fields] OR "neoplas*"[All Fields]) AND ("testis"[All Fields] OR "testes"[All Fields]) AND ("Antigens, Neoplasm"[Majr] OR "antigen*"[All Fields] OR "Ags"[All Fields] OR "ag"[All Fields] OR "gene"[All Fields] OR "genes"[All Fields] OR "antigen*"[All Fields]))) AND ((("Carcinoma, Hepatocellular"[Majr]) OR "Fibrolamellar hepatocellular carcinoma" [Supplementary Concept] OR "liver cell carcinoma"[All Fields] OR "liver cancer"[All Fields] OR "hepatocellular carcinoma cell line"[All Fields] OR ("liver"[All Fields] OR "hepat*"[All Fields]) AND ("carcinoma*"[All Fields] OR "ca"[All Fields] OR "cas"[All Fields] OR "cancer*"[All Fields]) OR "hepatocarcinom*"[All Fields]) AND "Humans"[Mesh])
```

Pubmed search 04-10-2018

Supplementary Table S1. Patient characteristics of HCC-patients in the discovery and validation cohort based on CTA expression in TFL.

Characteristic	Discovery cohort		Validation cohort	
	CTA in TFL- (n=55)	CTA in TFL+ (n=45)	CTA in TFL - (n=63)	CTA in TFL+ (n=26)
Age at surgery (years)				
Mean \pm SD	60.0 \pm 14.3	59.8 \pm 15.0	65.9 \pm 10.7	60.4 \pm 11.0
Median (range)	63 (11-82)	64 (16-80)	67 (34-85)	61 (36-76)
Sex – no. (%)				
Male	36 (65.5)	27 (60)	49 (77.8)	15 (57.7)
Female	19 (34.5)	18 (40)	14 (22.2)	11 (42.3)
Race – no. (%)				
White	47 (85.5)	36 (80)	52 (82.5)	20 (76.9)
African	3 (5.5)	5 (11.1)	4 (6.3)	-
Asian	4 (7.3)	4 (8.9)	5 (7.9)	5 (19.2)
Not reported	1 (1.8)	-	2 (3.2)	1 (3.8)
Etiology – no. (%)				
No known liver disease	14 (25.5)	19 (42.2)	19 (30.2)	7 (26.9)
Alcohol	16 (29.1)	5 (11.1)	11 (17.5)	8 (30.8)
Hepatitis B	8 (14.5)	4 (8.9)	10 (15.9)	3 (11.5)
NASH	5 (9.1)	3 (6.7)	12 (19.0)	4 (15.4)
Hepatitis C + Alcohol	3 (5.5)	5 (11.1)	-	-
Hepatitis B + Alc/HepC/HepD/NASH	2 (3.6)	4 (8.9)	1 (1.6)	1 (3.8)
Hepatitis C	4 (7.3)	2 (4.4)	5 (7.9)	1 (3.8)
Fibrolamellar HCC	2 (3.6)	2 (4.4)	-	-
Hemochromatosis (+ NASH/Alcohol)	1 (1.8)	1 (2.2)	3 (4.8)	1 (3.8)
Autoimmune hepatitis	-	-	-	-
Primary sclerosing cholangitis	-	-	-	1 (3.8)
Other	-	-	2 (3.2)	-
Hepatitis status – no. (%)				
Hepatitis B or C positive	17 (30.9)	15 (33.3)	16 (25.4)	5 (19.2)
Chronic Hepatitis B	10 (18.2)	8 (17.8)	11 (17.5)	4 (15.4)
Chronic Hepatitis C	8 (14.5)	7 (15.6)	5 (7.9)	2 (7.7)
Cirrhosis – no. (%)				
Yes	22 (40)	12 (26.7)	24 (38.1)	10 (38.5)
No	33 (60)	33 (73.3)	39 (61.9)	16 (61.5)
Surgery – no. (%)				
(Extended) Hemi-hepatectomy	30 (54.5)	26 (57.8)	28 (44.4)	14 (53.8)
Partial resection (\geq 2 segments)	12 (21.8)	8 (17.8)	24 (38.1)	6 (23.1)
Partial resection (1 segment)	11 (20.0)	10 (22.2)	11 (24.4)	6 (23.1)
LTx	2 (3.6)	1 (2.2)	-	-

Supplementary Table S1. (continued)

Characteristic	Discovery cohort		Validation cohort	
	CTA in TFL- (n=55)	CTA in TFL+ (n=45)	CTA in TFL- (n=63)	CTA in TFL+ (n=26)
Tumor differentiation – no. (%)				
Good	8 (14.5)	4 (8.9)	8 (12.7)	3 (11.5)
Moderate	30 (54.5)	22 (48.9)	36 (57.1)	15 (57.7)
Poor	9 (16.4)	9 (20)	14 (22.2)	5 (19.2)
Unknown	8 (14.5)	10 (22.2)	5 (7.9)	3 (11.5)
Vascular invasion – no. (%)				
Yes	23 (41.8)	26 (57.8)	41 (65.1)	18 (69.2)
No	27 (49.1)	15 (33.3)	22 (34.9)	6 (23.1)
Unknown	5 (9.1)	4 (8.9)	-	2 (7.7)
BCLC stage – no. (%)				
0	1 (1.8)	-	4 (6.3)	-
A	36 (65.5)	30 (66.7)	47 (74.6)	22 (84.6)
B	18	15 (33.3)	12 (19.0)	4 (15.4)
Number of lesions – no. (%)				
1	30 (54.5)	26 (57.8)	49 (77.8)	22 (84.6)
>1	25 (45.5)	19 (42.2)	14 (22.2)	4 (15.4)
Median (range)	1 (1-11)	1 (1-10)	1 (1-11)	1 (1-11)
Size of largest lesion (cm)				
Mean ± SD	6.2 ± 4.3	9.1 ± 6.9	7.0 ± 4.7	8.0 ± 4.7
Median (range)	5.2 (1.3-24)	7.5 (1-34)	5.7 (0.8-21.0)	7.15 (1.7-16.5)
AFP level before resection (ug/l)				
Mean ± SD	711 ± 2384	113360 ± 519877	1850 ± 6673	784 ± 1641
Median (range)	7 (1-10709)	12 (1-3118700)	9 (1-45803)	47 (1-4973)

Supplementary Table S2. Primer sequences and annealing temperatures (T_m) used for RT-qPCR.

Primer	T _m	Forward Primer	Reverse Primer	Product Length
CAGE1	60	TCATCCGAAGTCCATGACCA	GACTTCTCTGGAGTGGTTG	118
CBLL2	62	TTCCACCAGAACAGCACACC	AACGGTTTCCCACTGGATGG	146
CCDC83	60	AGGAGGGCAGGCCTTTTAATC	TCCATTGTGCTGGTTAGCTATGA	148
CPXCR1	60	CAGCCAGTCATACTATCCTC	CTACAGTCATTAGGAGGCTC	118
CSAG2/3	58	GGAGTGGGCCAACACTATCC	GGCTGTCCGAAGAGAGACTG	123
CT45	62	ATGCACATCACTCCCAGGTG	TTGTTTCTTGCTGGAGGAGA	147
CT47A1	60	ACCTAGACGCAGCAGAGGT	AACTTGAACACTGTCACATACATCC	141
CTAG1A/B	60	GGCTTCAGGGCTGAATGGA	TGTTGCCGGACACAGTGAAC	191
Cxorf48	60	CTGGCAACGTGCCTCTAAAAG	AAGATGGCGAGGCACAACAT	110
DDX53	60	GTTGGTGTGGCTATTGGTTAC	CGCTTTGGCCTTGTCTTCAT	144
DPPA2	62	CAATCTCCTCCATCCAGGGT	ACCAGTGTCAAATCACACTTTCC	118
DUSP21	62	TTGTCAATGCCTCGGTGGAA	CGAGTCACGAGCATCGGTAA	86
FAM46D	60	AGCCTTAACGGATGAAGGAAAA	AAACTCCAGCTAGTGAACCTCC	92
FATE1	62	ATGGAGCTTGGATCTCGGTC	CTCAGCATTCTGGGCTTTGG	155
FBXO39	60	TGATAGATCTCCTGCCACCT	CTCGTCGAGTACTCATGGTT	83
FMR1NB	60	TCCTGCTTTCGTGTGCTAC	TCAGCAAAGCTTCCAATGCG	147
FTHL17	60	ATCAACAGCCACATCAGCT	CATTTTGTCTGTCGACAGGC	132
GAGE1	60	ACCTGAGTCATCTTAAAACATGTGA	AGTAAACATGAAGCAGAGTGCC	80
GPC3	60	AACCATGTCTATGCCCAAAGGT	CCAGAGCCTCCAATGCACTC	108
GUSB	58	CAGGTGATGGAAGAAGTGG	GTTGCTCACAAGTCCACAG	171
HORMAD1	60	CAACGAATCTAGCATGTTGTC	CACAATCACCATCCTTAAACC	188
HPRT1	58	GCTATAAATCTTTGCTGACCTGCTG	AATTACTTTTATGTCCCTGTTGACTGG	140
LUZP4	60	CTTCGTTTCGGAAGCTAACGC	CTCCGATGGCGATGCTATGA	217
MAGEA1	60	AGAAGCGAGGTTTCCATTCTGA	GGAATCCTGTCTCTGGGTTG	116
MAGEA2	62	CTCCAGCTTCTGACTACCATC	GACTCCAGGTGGGAAACATTC	148
MAGEA3	62	ATCTTCAGCAAAGCTTCCAGT	GGTGGCAAAGATGTACAAGTGG	93
MAGEA4	58	GAGCTTCTGCTGCTGACTCG	TGCTGCTCAGAACCTTGTCTC	85
MAGEA8	60	GGTCGGCTTGAGATCGGCT	CCTCAGCTTGACTGTACTACTG	150
MAGEA9B	60	GCTTGATACCGGTGGAGGAG	GGTTAGCCTGTCCCAGAAC	124
MAGEA10	62	GAGATCGGCTGAAGAGAGCG	ACTCTTGTGAGTCTGCGAC	140
MAGEB1	60	TGAAGTAGTGAGCAGCCAAGA	GCTGGCAGCACCAATAAATGT	172
MAGEB2	58	TCTGACTTCCGCTTTGGAGGC	GCACGGAGCTTACTTCTGACC	135

Supplementary Table S2. (continued)

Primer	Tm	Forward Primer	Reverse Primer	Product Length
MAGEB3	60	CTACCCAAACCTCTTCTCAGCC	AGACCCTGGATCCTCCCTCTA	144
MAGEB6	62	ACCCTTGTCAGCAAGCTAGG	GATCACAACCAGGAGCGACA	99
MAGEC1	62	GGCCATCTTGGGAGTCTGAA	TGGAGCACCTTGAAGACTGG	106
MAGEC2	62	GGAGTCAAGGCTGTGGAT	GGGAGGCATGACGACTTCTT	84
PAGE1	62	GGCTGAAGTTGTAAATATGGGT	CTGAGATGCTCCCTCATCC	177
PAGE5	62	TGATGTCAGGGAGGGGACTC	TGGTTTCAGTCTTCATTGTCTTGG	105
PASD1	62	TGCAGAGGTTGAGCAGTATGG	GGATTACCTCAGGCTCACC	153
PLAC1	60	ACACAGCAAGTTCCTTCTCC	GAGGATTTCTTCTTGCGACG	118
PMM1	58	CGAGTTCCTCGAACTGGAC	CTGTTTTCAGGGCTCCAC	86
RNF17	60	GGACAATGCAGTGGTCCAAG	AGGAGCACCAAGAGAATCGAA	137
SAGE1	58	CCTTAGCTGACTCTGGTGCTC	GACTCGTTTGAAGTGGAGAAGC	150
SLCO6A1	62	TGGCCTTGGGTGTAAGCTATG	ATCCAACAACGTCCTGTGTG	136
SPANXA	62	ATGATGCCGGAGACCCCAAC	GTGGTCATTGAGTTCCTCT	144
SPANXC	60	CGCTACAGGAGGAACGTGAA	ATTCCTCTCTCCATTGG	100
SPANXN3	62	ACCAGAATCATGGAACAGCCAA	TGTTTGGTACCTCTTGCATCTC	106
SYCP1	62	CTATCTGTGGACATCTGCCAA	TTGGTTTTGTTGGTGTCTCAC	80
TEKT5	62	GGTCCATGACAACGTGGAGA	TGCTGAGCATCCCGTTATC	126
TFDP3	60	TTGGAGGTGTGTTCACGACG	CTGAGATCCACCGAGCTTG	113
TPPP2	60	GCAAAGTCAAGGCCAAGAACG	CTGGACTCTTCCCTTTGAAGC	99
TSPY	62	ACAAGATTGCTGAGTCCCTG	TCAACAACGGGAGTCCCT	149
ZCCHC13	62	TGCTACAACGTGGGAGAAGC	TGACGATCACAGTCACGAGC	122

Supplementary Table S3. Results of the literature search and overview of included articles.

Study	Gene(s)	Population	Detection method	Outcome
Wei Y, et al. Int J Oncol. 2018 ²	MAGEA9	HCC patients (n=90; China)	IHC	IHC: 40/90 (44%) MAGEA9+
Jiao Y, et al. PLoS One. 2017 ³	TFDP3	HCC cell line (HepG2) and normal human hepatocyte cell line (L-02) and HCC patients (China)	RT-qPCR and IHC	mRNA and IHC: HepG2 and L02 are both TFDP3+, expression is higher in HepG2. Also protein expression in HCC patients.
Liu, et al. Cancer Lett. 2017 ⁴	CTCF	HCC cell lines (HepG2, SMMC-7721, Huh7, HCCLM3, PLC/PRF/5), normal human hepatocyte cell lines (L-02 and WRL68) and HCC patients (n=25; China)	RT-qPCR and IHC	RT-qPCR: all cell lines positive, expression higher in HCC cell lines than normal human hepatocyte cell lines IHC: 18/25 (72%) CTCF ^{high} and 7/25 (28%) CTCF ^{low}
Xie, et al. Drug target. 2017 ⁵	TTK	Review	n.a.	Liu, Oncotarget 2015: 118/152 (77.63%) of HCC patients mRNA TTK+ – China
Charoentong, et al. Cell Rep. 2017 ⁶	BRDT, CAGE1, CCDC83, CPXCR1, CSAG2, CT45A1, DDX53, DPPA2, FMR1NB, FTHL17, GAGE1, LUZP4, MAGEA1, MAGEA2, MAGEA3, MAGEA4, MAGEA5, MAGEA9, FAM46D, MAGEB1, MAGEB2, MAGEB3, MAGEC1, PAGE1, PASD1, POTE, POTE, POTE, POTED, SLC06A1, SPANXC, SPANXN3, SSX3, SSX5, SSX7, TSPY2, TSPY3, TSSK6, XAGE2, ZNF645,	The Cancer Genome Atlas (TCGA); including 363 HCC patients	RNA sequencing	Aforementioned genes are all correlated with CD4 and/or CD8 T cells in HCC
Kido, et al. J Genet Genomics. 2016 ⁷	TSPY	TCGA and refers to Kido, et al. 2014 IHC: male HCC patients (n=287; TMA purchased from US Biomax) and RT-qPCR: male HCC patients (n=32; China)	TCGA: RNA seq Kido, et al. 2014: RT-qPCR and IHC	This paper researches the TSPY co-expression network (TCN), which is activated in 30% of HCCs (TCGA). Kido, et al. 2014: RT-qPCR: 15/32 (46.9%) TSPY+ IHC: 55/287 (19.2%) TSPY+
Fu, et al. Int J Clin Exp Pathol. 2015 ⁸	ACRBP	HCC cell lines (Bel-7404 ¹ , HepG2 ² , QGY-7703 ³ , QGY-7701 ⁴ , BEL-7402 ⁵ , SMMC-7721 ⁹)	RT-PCR ¹⁻⁶ , IHC ^{1,2} and WB ^{1,2}	RT-PCR: 6/6 cell lines IHC: 2/2 cell lines WB: 2/2 cell lines
Wang, et al. Int J Clin Exp Pathol. 2015 ⁹	MAGEA3, MAGEA4, MAGEC2, NY-ESO-1	HCC cell lines (LO2, HepG2, Hep3B, Huh7, SMMC-7721) and HCC patients (China; n=142)	RT-PCR and IHC	Cell lines: 4/5 cell lines for 4 TAAs. HCC patients: 112/142 (78.9%) MA3+, 48/142 (33.8%) MA4+, 106/142 (74.6%) MC2+, 20/142 (14.1%) NY-ESO-1+. No expression in TFL. IHC: 108/142 (76.1%) MA3+, 44/142 (31.0%) MA4+, 99/142 (69.7%) MC2+, 19/142 (13.4%) NY-ESO-1+
Sideras, et al. Br J Cancer. 2015 ¹⁰	MAGEA1, MAGEA3/4, MAGEA10, MAGEC1, MAGEC2, NY-ESO-1, SSX2, SP17	HCC patients (Netherlands; n=133)	IHC	9.8% MAGEA1+, 3.0% MAGEA3/4+, 7.5% MAGEA10+, 17.3% MAGEC1+, 19.5% MAGEC2+, 3.8% NY-ESO-1+, 0% SSX2+, 87% SP17+. No expression in TFL, except SP17 (88.0%)
Melis, et al. J Transl Med. 2014 ¹¹	NUF2, TTK, MAGEA3, CEP55	HBV+ HCC patients (n=10; Italy)	RT-PCR	Expression of 4 TAAs in 10 patients, both in HCC and TFL, but higher in HCC.
Li, et al. J Transl Med. 2014 ¹²	TSPY	HCC cell lines (HepG2, SMMC7721, Huh7, MHC-C97L, MHCC97H, HC-CLM3) and HCC patients (n= 52;China)	RT-PCR	6/6 cell lines and expression of TSPY in male HCC tissues, but not female HCC tissues

Supplementary Table S3. (continued)

Study	Gene(s)	Population	Detection method	Outcome
Deng, et al. Hepatology. 2014 ¹³	DUSP21, CT45, ZCCHC13, MAGEA9, MAGEB6, PIHD3, PNMA5, MPC1L, IL13RA1	HCC patients (n=24; China?)	RT-PCR	8/24 (33.3%) DUSP21+, 7/24 (29.2%) CT45+, 4/24 (16.7%) ZCCHC13+, 3/24 (12.5%) MAGEA9+, 3/24 (12.5%) MAGEB6+, 4/24 (16.7%) PIHD3+, 6/24 (25%) PNMA5+, 6/24 (25%) MPC1L+, 1/24 (4.2%) IL13RA1+
Xia, et al. Int J Clin Exp Pathol. 2013 ¹⁴	SP17, MAGEC1, NY-ESO-1	HCC patients (n=45; China)	IHC	16/45 (35.6%) MAGEC1+, 7/45 (15.6%) NY-ESO-1+, 36/45 (80%) SP17+
Zhou, et al. Oncol Rep. 2013 ¹⁵	FAM9C	HCC cell lines (SSMC-7721, QGY-7703, BEL-7404, BEL-7405, YJ-8103, Huh7) and HCC patients (n=46; China)	RT-qPCR and IHC	RT-qPCR: 25/46 HCC patients have upregulation of FAM9C in T compared to TFL Cell lines: 2/6 FAM9C+ IHC showed nuclear staining (T>TFL)
Chen, et al. Genet Test Mol Biomarkers. 2013 ¹⁶	CTCF	HCC cell lines (SSMC-7721, BEL-7402, Huh7, HepG2) and HCC patients (n=105; China)	RT-PCR, IHC and WB	Cell lines: 3/4 CTCF+ (RT-PCR and WB) HCC patients: 58/105 (55.2%) CTCF+ (IHC)
Song, et al. Oncol Rep. 2012 ¹⁷	AKAP3, Ctp11	HCC cell lines (SNU-354, SNU-398, SNU-423, SNU-449, HepG2) and HCC patients (n= 10; Korea)	RT-PCR	5/10 (50%) AKAP3+, 1/9 (11.1%) Ctp11+
Li, et al. Bull Cancer. 2012 ¹⁸ – no full text	CABYR-c	HCC patients (n=20; China)	RT-PCR and WB	Both mRNA and protein expression are significantly higher in HCC compared to TFL
Yoon, et al. Tohoku J Exp Med. 2011 ¹⁹	RNF17	HCC patients (n=28; Korea), CCA patients (n=5) and combined HCC-CCA (n=8) – Korea	RT-qPCR	4/28 (14.3%) HCC RNF17+, 1/5 (20%) CCA RNF17+, 2/8 (25%) combined HCC/CCA RNF17+. No expression in TFL.
Tseng, et al. Oncol Rep. 2011 ²⁰	CABYR-a/b, CABYR-c/d, CABYR-e	HCC cell lines (HepG2, Huh7) and HCC patients (n=16; Taiwan)	RT-PCR and WB	Cell lines: 2/2 expressed CABYR-a/b and CABYR-c/d HCC patients: 7/16 (43.8%) CABYR-a/b+, 14/16 (87.5%) CABYR-c/d+, 0/16 (0%) CABYR-e+
Wang, et al. Oncol Rep. 2009 ²¹	NY-ESO-1, CTAG2, SSX1	HCC patients (n=64; China)	RT-PCR	19/64 (29.7%) NY-ESO-1+, 29/64 (45.3%) CTAG2+, 24/64 (37.5%) SSX1+
Riener, et al. Int J Cancer. 2009 ²²	MAGEA4, MAGEC1, MAGEC2, GAGE, NY-ESO-1	HCC patients (n=146; Switzerland), CCA (n=50), GBC (n=32)	IHC	HCC: 0/146 (0%) MAGEA4+, 17/146 (12%) MAGEC1+, 50/146 (34%) MAGEC2+, 16/146 (11%) GAGE+, 3/146 (2%) NY-ESO-1+. No expression in CCA. GBC: 4/32 (13%) MAGEC2+, 1/32 (3%) GAGE+, 1 (3%) NY-ESO-1+, 0/32 MAGEC1/MAGEA4+
Lu, et al. Chin Med J. 2007 ²³	NY-ESO-1, SSX1	HCC patients (n=36; China)	RT-PCR	4/36 (11.1%) NY-ESO-1+, 22/36 (61.1%) SSX1+
Wu, et al. Life Sci. 2006 ²⁴	SSX2, SSX5	HCC patients (n=36; China)	RT-PCR	13/36 (36.1%) SSX2, 17/36 (47.2%) SSX5
Watanabe, et al. Cancer Sci. 2005 ²⁵	IGSF11	HCC cell line (Alexander, Huh7, HepG2, SNU475)	RT-PCR	HCC cell lines: 3/4 IGSF11+
Yin, et al. Br J Cancer. 2005 ²⁶	TSPY	HCC cell lines (hep-hcc-1, hep-hcc-2, hep-hcc-HLE, Hep3B, COS7) and HCC patients (n= 57; China)	RT-PCR	20/57 (35%) TSPY+
Shi, et al. Br J Cancer. 2005 ²⁷	DDX53	HCC patients (n=33; China)	RT-PCR	13/33 (39.4%) DDX53+

Supplementary Table S3. (continued)

Study	Gene(s)	Population	Detection method	Outcome
Peng, et al. Cancer Lett. 2005 ²⁸	MAGEA1, MAGEA3, MAGEA4, MAGEA10, SSX1, SSX2, SSX4, SSX5, NY-ESO-1, MAGEB1, MAGEB2, MAGEC1, MAGEC2, SYCP1	HCC patients (n=73; China)	RT-PCR	51/73 (69.9%) MAGEA1+, 35/73 (47.9%) MAGEA3+, 6/30 (20%) MAGEA4+, 11/30 (36.7%) MAGEA10+, 29/43 (67.4%) SSX1+, 26/73 (35.6%) SSX2+, 21/43 (48.8%) SSX4+, 13/43 (30.2%) SSX5+, 31/73 (42.5%) NY-ESO-1+, 13/25 (52%) MAGEB1+, 15/25 (60%) MAGEB2+, 12/25 (48%) MAGEC1+, 17/25 (68%) MAGEC2+, 10/30 (33.3%) SYCP1+
Sato, et al. Int J Oncol. 2005 ²⁹ – no full text	NY-ESO-1, CTAG2	HCC patients – Japan	RT-PCR and IHC	IHC: 3/10 (30%) NY-ESO-1+ - all 10 samples expressed NY-ESO-1 mRNA 1/6 (16.7%) CTAG2+ - all 6 samples expressed CTAG2 mRNA
Yang, et al. Lab Invest. 2005 ³⁰	FATE	HCC patients (n=35; China)	RT-PCR and IHC	RT-PCR: 10/15 (66%) FATE+ IHC: 7/35 (20%) FATE+
Dong, et al. Biochem Cell Biol. 2004 ³¹ – no full text	FATE	HCC patients (China)	RT-PCR	25% of HCC samples FATE+
Dong, et al. Br J Cancer. 2004 ³²	ZNF165	HCC patients (n=42; China)	RT-PCR	22/42 (52%) ZNF165+
Zhao, et al. World J Gastroenterol. 2004 ³³	MAGEA1, MAGEC2, SSX1, SPANXC	HCC patients (n=105; China)	RT-PCR	79/105 (75.2%) MAGEA1+, 59/105 (56.2%) MAGEC2+, 76/105 (72.4%) SSX1+, 66/105 (62.9%) SPANXC+
Li, et al. Lab Invest. 2003 ³⁴ – no full text	MAGEC2	HCC patients (n=70; China)	IHC	26/70 (37.1%) MAGEC2+
Dong, et al. Br J Cancer. 2003 ³⁵	FATE, TPTE	HCC patients (n=62; China)	RT-PCR	41/62 (66%) FATE1+, 24/62 (39%) TPTE+
Luo, et al. Cancer Immun. 2002 ³⁶	MAGEA1, MAGEA3, MAGEA4, GAGE, NY-ESO-1, SSX1, SSX2, SSX4, SYCP1, LUZP4	HCC patients (n=21; China)	RT-PCR	4/21 (19%) MAGEA1+, 5/21 (24%) MAGEA3+, 1/21 (4.8%) MAGEA4+, 8/21 (38%) GAGE+, 0/21 (0%) NY-ESO-1+, 8/21 (38%) SSX1+, 2/21 (9.5%) SSX2+, 2/21 (9.5%) SSX4+, 6/21 (29%) SYCP1+, 4/21 (19%) LUZP4+
Wang, et al. J Immunol. 2002 ³⁷	MAGEC2, TFDP3	HCC patients (n=20; China)	RT-PCR	14/20 (70%) MAGEC2+, 5/17 (29.4%) TFDP3+
de Wit, et al. Int J Cancer. 2002 ³⁸	DSCR8	HCC cell lines (Hep3B, HepG2, PLC/RPF/5, Huh7)	RT-PCR	1/4 cell lines DSCR8+
Ono, et al. Proc Natl Acad Sci U S A. 2001 ³⁹	ACRBP	HCC patients (n=5; Japan)	RT-PCR	2/5 (40%) ACRBP+
Chen, et al. Cancer Lett. 2001 ⁴⁰	SSX1, SSX2, SSX4, SSX5, SYCP1, NY-ESO-1	HCC patients (n=30; Taiwan)	RT-PCR	24/30 (80%) SSX1+, 14/30 (46.7%) SSX2+, 22/30 (73.3%) SSX4+, 10/30 (33.3%) SSX5+, 2/30 (6.7%) SYCP1+, 11/30 (36.7%) NY-ESO-1+

Supplementary Table S4. Frequency table of healthy liver tissues (n=21) expressing mRNA of the CTAs.

	mRNA ⁺ healthy liver (%)		mRNA ⁺ healthy liver (%)
CAGE1	0.0	MAGEA10	0.0
CBLL2	42.9	MAGEB1	19.0
CCDC83	0.0	MAGEB2	0.0
CPXCR1	0.0	MAGEB3	28.6
CSAG2/3	85.7	MAGEB6	28.6
CT45	14.3	MAGEC1	4.8
CT47A1	0.0	MAGEC2	0.0
Cxorf48	0.0	NYESO1	0.0
DDX53	47.6	PAGE1	0.0
DPPA2	0.0	PAGE5	100.0
DUSP21	23.8	PASD1	0.0
FAM46D	0.0	PLAC1	0.0
FATE1	33.3	RNF17	4.8
FBXO39	100.0	SAGE1	0.0
FMR1NB	0.0	SLCO6A1	0.0
FTHL17	42.9	SPANXA	66.7
GAGE1	23.8	SPANXC	38.1
HORMAD1	100.0	SPANXN3	0.0
LUZP4	0.0	SYCP1	47.6
MAGEA1	0.0	TEKT5	100.0
MAGEA2	23.8	TFDP3	33.3
MAGEA3	14.3	TPPP2	100.0
MAGEA4	0.0	TSPY	0.0
MAGEA8	0.0	ZCCHC13	38.1
MAGEA9	0.0		

Colors correlate to the percentage of positive healthy liver tissues.

Supplementary Table S5. Expression of excluded CTAs in HCC patients and in cirrhotic liver tissues without malignancy.

	mRNA-positive HCC (%) ¹	mean in mRNA+ HCC (range) ²	Relative expression HCC (compared to testis) ³	mRNA-positive TFL (%) ⁴	mean in mRNA+ TFL (range) ⁵	Relative expression TFL (compared to testis) ⁶	mRNA-positive cirrhotic tissue ⁷
CCDC83	0.00			0.00			0
CPXCR1	2.02	0.001 (0.001-0.001)	0.00378	0.00			0
Cxorf48	8.25	0.157 (0.002-0.991)	1.839	2.04	0.012 (0.001-0.023)	0.139	2.9
DPPA2	1.03	0.135 (0.135-0.135)	1.204	0.00			0
FAM46D	5.15	0.003 (0.002-0.004)	0.058	0.00			2.9
FMR1NB	6.19	0.031 (0.002-0.124)	0.022	1.02	0.088 (0.088-0.088)	0.062	0
LUZP4	6.19	0.106 (0.001-0.49)	0.242	1.02	0.279 (0.279-0.279)	0.636	0
MAGEA4	6.19	0.803 (0.001-2.559)	28.036	0.00			0
MAGEA8	3.09	0.014 (0.004-0.022)	5.115	0.00			0
PASD1	2.02	0.017 (0.007-0.026)	0.007	2.00	0.02 (0.019-0.021)	0.009	0
PLAC1	4.12	0.014 (0.001-0.041)	0.146	0.00			0
RNF17	21.65	0.053 (0.001-0.507)	0.04570	13.27	0.023 (0.002-0.134)	0.01964	5.7
SAGE1	4.12	0.086 (0.008-0.15)	0.505	3.06	0.19 (0.006-0.543)	1.117	0
SPANXN3	1.01	0.004 (0.004-0.004)	52.644	3.00	0.002 (0.001-0.003)	27.174	0.0

¹Percentage of hepatocellular carcinomas (HCC) expressing mRNA of the excluded CTAs – meaning a Ct-value <35 and relative expression > 0.001 (n=100); ²Mean relative expression (relative to the geometric mean of the 3 household genes- GUSB, HPRT1, PMM1) level in HCCs expressing the CTA and range; ³Mean relative expression of the CTA in HCC expressing the CTA, relative to the relative mean expression in 3 testis tissues; ⁴Percentage of paired tumor-free liver tissues (TFL) expressing mRNA of the excluded CTAs (n=100); ⁵Mean relative expression level in TFLs expressing the CTA and range; ⁶Mean relative expression of the CTA in TFL expressing the CTA, relative to the relative mean expression in 3 testis tissues; ⁷Percentage of non-cancerous cirrhotic liver tissues expressing the CTA (n=35).

Supplementary Table S6. Patient characteristics of HCC-patients included in protein expression analysis.

Characteristic	HCC patients (n=76)
Age at surgery (years)	
Mean \pm SD	60.4 \pm 14.4
Median (range)	64 (16-82)
Sex – no. (%)	
Male	47 (61.8)
Female	29 (38.2)
Race – no. (%)	
White	64 (84.2)
African	6 (7.9)
Asian	5 (6.6)
Not reported	1 (1.3)
Etiology – no. (%)	
No known liver disease	21 (27.6)
Alcohol	17 (22.4)
Hepatitis B	9 (11.8)
NASH	8 (10.5)
Hepatitis C + Alcohol	6 (7.9)
Hepatitis B + Alc/HepC/HepD/NASH	6 (7.9)
Hepatitis C	5 (6.6)
Fibrolamellar HCC	3 (4.0)
Hemochromatosis + NASH	1 (1.3)
Autoimmune hepatitis	-
Primary sclerosing cholangitis	-
Hepatitis status – no. (%)	
Hepatitis B or C positive	26 (34.2)
Chronic Hepatitis B	15 (19.7)
Chronic Hepatitis C	12 (15.8)
Cirrhosis – no. (%)	
Yes	23 (30.3)
No	53 (69.7)
Tumor differentiation – no. (%)	
Good	8 (10.5)
Moderate	41 (54.0)
Poor	14 (18.4)
Unknown	13 (17.1)

Supplementary Table S6. (continued)

Characteristic	HCC patients (n=76)
Vascular invasion – no. (%)	
Yes	40 (52.6)
No	29 (38.2)
Unknown	7 (9.2)
Number of lesions – no. (%)	
1	40 (52.6)
>1	36 (47.4)
Median (range)	1 (1-11)
Size of largest lesion (cm)	
Mean ± SD	7.4 ± 5.2
Median (range)	6.1 (1-24)
AFP level before resection (ug/l)	
Mean ± SD	64965 ± 401956
Median (range)	9.5 (2-3118700)

Supplementary Table S7. Cox regression analysis of HCC recurrence and HCC-specific survival based on CTA protein expression in TFL.

Variable	Early recurrence				HCC-specific survival			
	Univariate analysis		Multivariate analysis		Univariate analysis		Multivariate analysis	
	HR (95% CI)	p-value	HR (95% CI)	p-value	HR (95% CI)	p-value	HR (95% CI)	p-value
≥1 CTA in TFL	1.9 (0.9-3.9)	0.092	2.5 (1.2-5.2)	0.02	2.6 (1.1-6.1)	0.03	3.8 (1.5-9.6)	0.004
Number of CTAs in TFL (numeric)	1.9 (0.98-3.7)	0.058			2.7 (1.2-6)	0.012		
>2 tumors	4.7 (2-11)	0.00029	3.7 (1.5-8.9)	0.004	2.6 (0.9-7.2)	0.066		
Chronic viral hepatitis	3.4 (1.6-7.1)	0.0011	2.8 (1.3-6.2)	0.01	3.1 (1.3-7.3)	0.01	4.4 (1.8-11.1)	0.001
Vascular invasion	1.6 (0.73-3.7)	0.23			1.3 (0.5-3.1)	0.57		
Tumor > 5 cm	1.1 (0.49-2.3)	0.89			1.7 (0.7-4.5)	0.26		
AFP > 400 ug/l	1.9 (0.84-4.3)	0.12			2.2 (0.9-5.6)	0.083		

Abbreviations: HR, hazard ratio; CI, confidence interval; CTA, cancer-testis antigen; TFL, tumor-free liver; AFP, alphafetoprotein

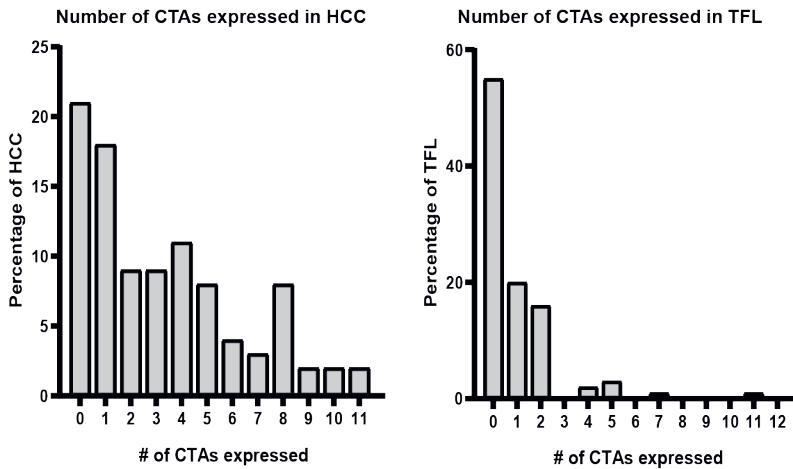
Supplementary Table S8. Cox regression analysis of HCC recurrence and HCC-specific survival based on CTA mRNA expression in HCC tumors.

Variable	HCC recurrence		HCC survival	
	Univariate analysis		Univariate analysis	
	HR (95% CI)	p-value	HR (95% CI)	p-value
≥1 CTA in tumor	1.8 (0.86-3.6)	0.12	1 (0.41-2.6)	0.94
≥2 CTAs in tumor	1.1 (0.65-1.9)	0.67	0.86 (0.39-1.9)	0.7
≥3 CTAs in tumor	1.1 (0.62-1.8)	0.85	0.74 (0.34-1.6)	0.47
Number of CTAs in tumor (numeric)	1 (0.96-1.1)	0.29	1 (0.87-1.1)	1
>1 tumor	1.2 (0.68-2)	0.56	1.1 (0.49-2.4)	0.83
>2 tumors	2.6 (1.3-4.9)	0.0042	1.8 (0.69-4.9)	0.22
Cirrhosis	1.6 (0.89-2.8)	0.12	1.5 (0.66-3.4)	0.33
Chronic viral hepatitis	2.3 (1.3-4)	0.0031	3.3 (1.5-7.2)	0.0032
Vascular invasion	1.3 (0.72-2.3)	0.41	2.2 (0.96-4.9)	0.063
Tumor > 5 cm	1.3 (0.74-2.3)	0.37	2.3 (0.9-5.7)	0.081
AFP > 200 ug/l	1.9 (1-3.4)	0.034	2.7 (1.2-6)	0.013
AFP > 400 ug/l	2.4 (1.3-4.5)	0.0051	3.3 (1.5-7.3)	0.0038

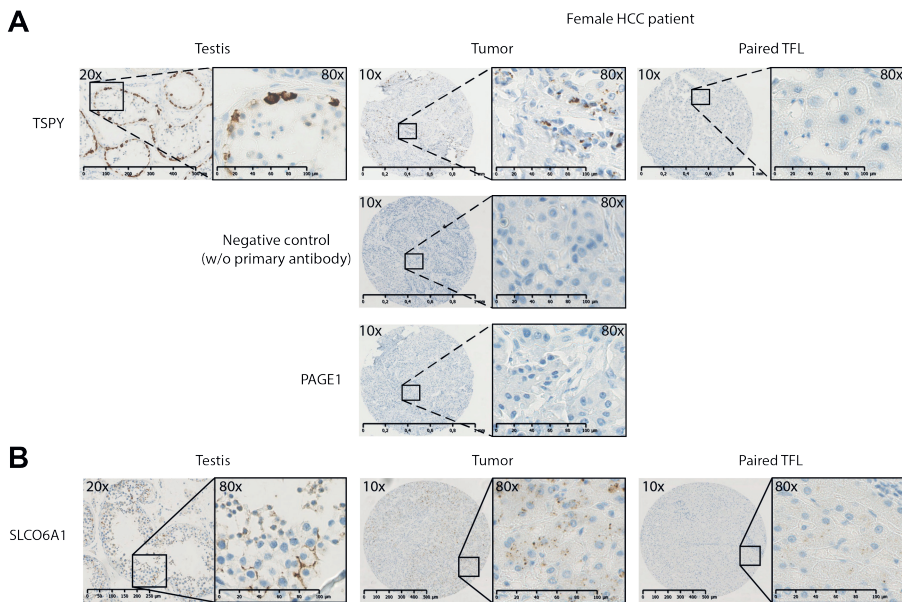
Abbreviations: HR, hazard ratio; CI, confidence interval; CTA, cancer-testis antigen; AFP, alphafetoprotein

Supplementary Table S9. Antibodies used for immunohistochemistry.

Antibody	Host Species	Dilution	Company	Clone	Lot number	Procedure	Ab incubation at 37°C
PAGE1	Rabbit	1:1000	Sigma-Aldrich	Poly-clonal	R04065	Optiview CC1 32'	32 minutes
TSPY	Rabbit	1:200	Sigma-Aldrich	Poly-clonal	R59337	Optiview CC1 32'	32 minutes
MAGEA9	Mouse	1:50	Prof. Y. Fradet, Québec, Canada ⁴¹	14A11	N/A	Optiview CC1 32'	32 minutes
MAGEC2	Rabbit	1:500	Sigma-Aldrich	Poly-clonal	A115364	Optiview CC1 32'	32 minutes
CT47A1	Rabbit	1:8000	Sigma-Aldrich	Poly-clonal	R39285	Optiview CC1 32'	32 minutes
MAGEA1	Mouse	1:50	Santa Cruz	MA454	B0507	Optiview CC1 32'	32 minutes
MAGEB2	Rabbit	1:500	Sigma-Aldrich	Poly-clonal	R109336	Optiview CC1 32'	32 minutes
SLCO6A1	Rabbit	1:200	Sigma-Aldrich	Poly-clonal	R72094	Optiview CC1 32'	32 minutes
MAGEC1	Mouse	1:3200	Santa Cruz	CT7-33	A1807	Optiview CC1 32'	32 minutes

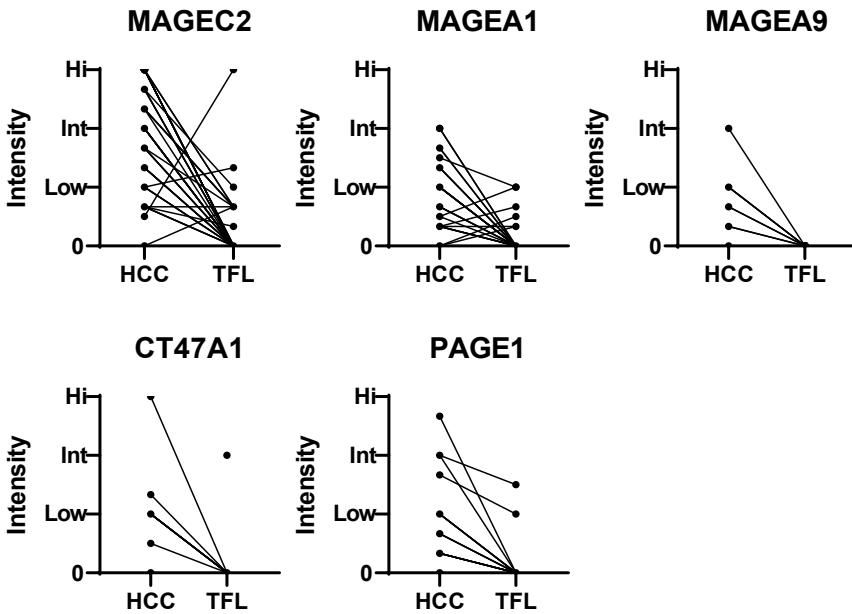


Supplementary Figure S1. Number of CTAs co-expressed in HCC tumors and TFL, based on mRNA expression.



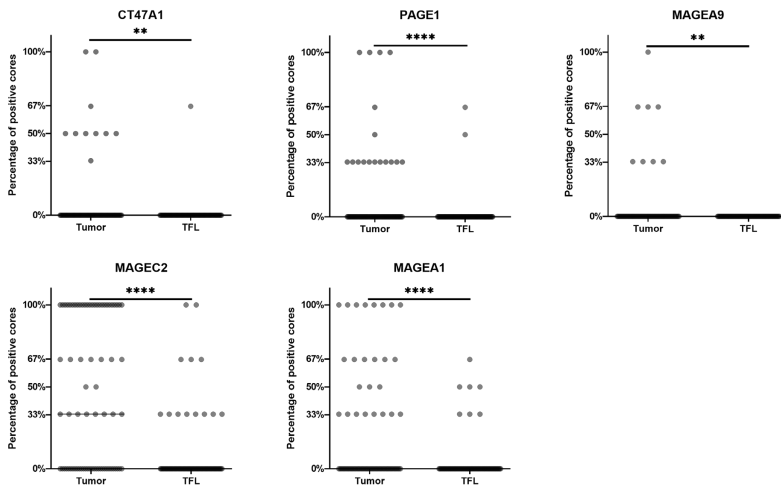
Supplementary Figure S2. TSPY expression in female HCC tumors and SLCO6A1 expression.

A. TSPY protein expression was determined by IHC. TSPY is expressed in spermatogonia of normal testis, as expected.⁴² However, TSPY protein expression was also found in two female HCC patients, of which one example is shown above. The staining is absent in the negative control and in the PAGE1 stained core. TSPY is encoded by the y-chromosome, expression in women is thus biologically impossible. **B.** Representative example of immunohistochemical stains of SLCO6A1 in testis, a positive HCC tumor tissue and the paired TFL tissue.



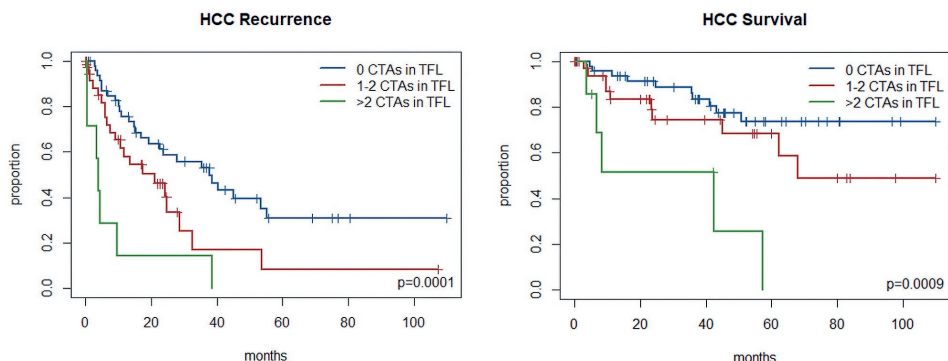
Supplementary Figure S3. Protein expression of CTAs in HCC tumors paired tumor free liver.

TMA of tumor and TFL tissues were immunohistochemically stained to study the protein expression of aforementioned CTAs. The average intensity scores of three different tissue cores is depicted.



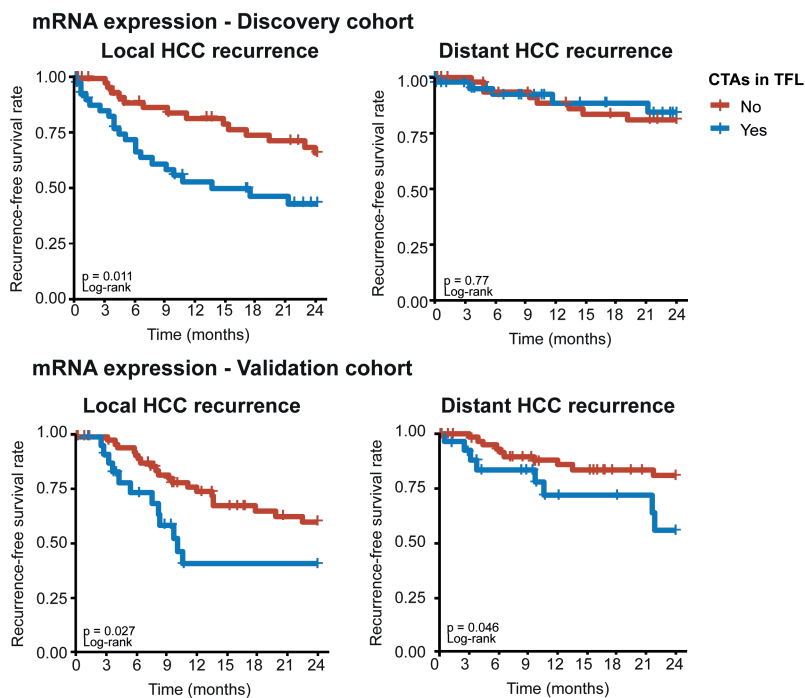
Supplementary Figure S4. Proteins are focally expressed in most tumors.

Protein expression was determined on TMAs, which had 3 cores of each tumor and TFL. The graphs display the percentage of cores containing protein-expressing cells (a score $\geq 1A$). Most tumors and TFL express the proteins focally, illustrated by not all cores being positive. Wilcoxon signed-rank test. ** $P < 0.01$, **** $P < 0.0001$



Supplementary Figure S5. HCC recurrence and HCC-specific survival by number of CTAs expressed in the discovery cohort (based on mRNA expression) in TFL.

Log-rank test.



Supplementary Figure S6. Local and distant HCC recurrence by expression of CTAs in TFL in the discovery and validation cohort.

Log-rank test.

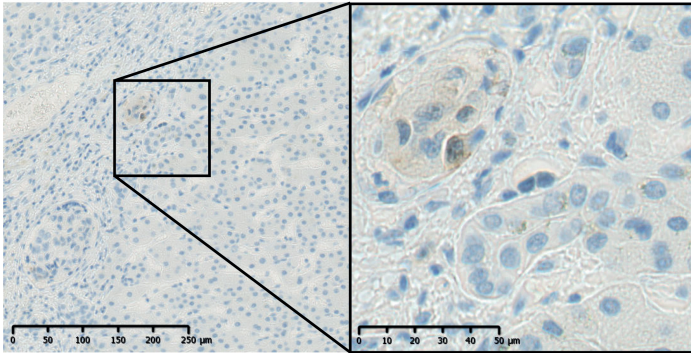
PAGE1

47 yo ♂

Etiology: HBV + HDV

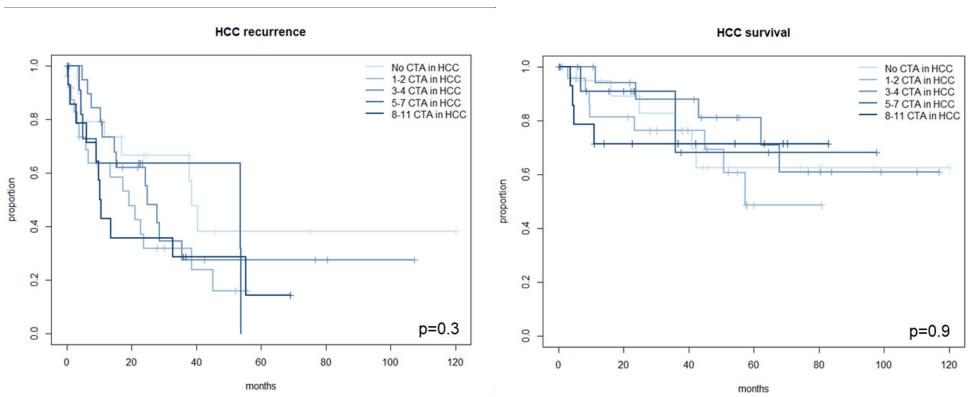
Recurrence: 2 months

Survival: 3 months



Supplementary Figure S7. PAGE1 expressing tumor nodule in TFL.

Example of IHC staining of PAGE1 protein expression in an intravascular tumor nodule in TFL, and accompanying patient data.



Supplementary Figure S8. HCC recurrence and HCC-specific survival by CTA mRNA-expression in tumor tissue in the discovery cohort.

Log-rank test.

REFERENCES

1. Sideras K, Biermann K, Verheij J, Takkenberg BR, Mancham S, Hansen BE, Schutz HM, de Man RA, Sprengers D, Buschow SI, et al. PD-L1, Galectin-9 and CD8(+) tumor-infiltrating lymphocytes are associated with survival in hepatocellular carcinoma. *Oncoimmunology*. 2017;6(2):e1273309.
2. Wei Y, Wang Y, Gong J, Rao L, Wu Z, Nie T, Shi D, Zhang L. High expression of MAGE-A9 contributes to stemness and malignancy of human hepatocellular carcinoma. *Int J Oncol*. 2018;52(1):219-30.
3. Jiao Y, Ding L, Chu M, Wang T, Kang J, Zhao X, Li H, Chen X, Gao Z, Gao L, et al. Effects of cancer-testis antigen, TFDP3, on cell cycle regulation and its mechanism in L-02 and HepG2 cell lines in vitro. *PLoS One*. 2017;12(8):e0182781.
4. Liu Q, Chen K, Liu Z, Huang Y, Zhao R, Wei L, Yu X, He J, Liu J, Qi J, et al. BORIS up-regulates OCT4 via histone methylation to promote cancer stem cell-like properties in human liver cancer cells. *Cancer Lett*. 2017;403:165-74.
5. Xie Y, Wang A, Lin J, Wu L, Zhang H, Yang X, Wan X, Miao R, Sang X, Zhao H. Mps1/TTK: a novel target and biomarker for cancer. *J Drug Target*. 2017;25(2):112-8.
6. Charoentong P, Finotello F, Angelova M, Mayer C, Efremova M, Rieder D, Hackl H, Trajanoski Z. Pan-cancer Immunogenomic Analyses Reveal Genotype-Immunophenotype Relationships and Predictors of Response to Checkpoint Blockade. *Cell Rep*. 2017;18(1):248-62.
7. Kido T, Lau YC. Identification of a TSPY co-expression network associated with DNA hypomethylation and tumor gene expression in somatic cancers. *J Genet Genomics*. 2016;43(10):577-85.
8. Fu J, Luo B, Guo WW, Zhang QM, Shi L, Hu QP, Chen F, Xiao SW, Xie XX. Down-regulation of cancer/testis antigen OY-TES-1 attenuates malignant behaviors of hepatocellular carcinoma cells in vitro. *Int J Clin Exp Pathol*. 2015;8(7):7786-97.
9. Wang M, Li J, Wang L, Chen X, Zhang Z, Yue D, Ping Y, Shi X, Huang L, Zhang T, et al. Combined cancer testis antigens enhanced prediction accuracy for prognosis of patients with hepatocellular carcinoma. *Int J Clin Exp Pathol*. 2015;8(4):3513-28.
10. Sideras K, Bots SJ, Biermann K, Sprengers D, Polak WG, JN IJ, de Man RA, Pan Q, Sleijfer S, Bruno MJ, et al. Tumour antigen expression in hepatocellular carcinoma in a low-endemic western area. *Br J Cancer*. 2015;112(12):1911-20.
11. Melis M, Diaz G, Kleiner DE, Zamboni F, Kabat J, Lai J, Mogavero G, Tice A, Engle RE, Becker S, et al. Viral expression and molecular profiling in liver tissue versus microdissected hepatocytes in hepatitis B virus-associated hepatocellular carcinoma. *J Transl Med*. 2014;12:230.
12. Li S, Mo C, Huang S, Yang S, Lu Y, Peng Q, Wang J, Deng Y, Qin X, Liu Y. Over-expressed Testis-specific Protein Y-encoded 1 as a novel biomarker for male hepatocellular carcinoma. *PLoS One*. 2014;9(2):e89219.
13. Deng Q, Li KY, Chen H, Dai JH, Zhai YY, Wang Q, Li N, Wang YP, Han ZG. RNA interference against cancer/testis genes identifies dual specificity phosphatase 21 as a potential therapeutic target in human hepatocellular carcinoma. *Hepatology*. 2014;59(2):518-30.
14. Xia QY, Liu S, Li FQ, Huang WB, Shi LN, Zhou XJ. Sperm protein 17, MAGE-C1 and NY-ESO-1 in hepatocellular carcinoma: expression frequency and their correlation with clinical parameters. *Int J Clin Exp Pathol*. 2013;6(8):1610-6.
15. Zhou JD, Shen F, Ji JS, Zheng K, Huang M, Wu JC. FAM9C plays an anti-apoptotic role through activation of the PI3K/Akt pathway in human hepatocellular carcinoma. *Oncol Rep*. 2013;30(3):1275-84.
16. Chen K, Huang W, Huang B, Wei Y, Li B, Ge Y, Qin Y. BORIS, brother of the regulator of imprinted sites, is aberrantly expressed in hepatocellular carcinoma. *Genet Test Mol Biomarkers*. 2013;17(2):160-5.

17. Song MH, Choi KU, Shin DH, Lee CH, Lee SY. Identification of the cancer/testis antigens AKAP3 and CTp11 by SEREX in hepatocellular carcinoma. *Oncol Rep.* 2012;28(5):1792-8.
18. Li H, Fang L, Xiao X, Shen L. The expression and effects the CABYR-c transcript of CABYR gene in hepatocellular carcinoma. *Bull Cancer.* 2012;99(3):E26-33.
19. Yoon H, Lee H, Kim HJ, You KT, Park YN, Kim H, Kim H. Tudor domain-containing protein 4 as a potential cancer/testis antigen in liver cancer. *Tohoku J Exp Med.* 2011;224(1):41-6.
20. Tseng YT, Hsia JY, Chen CY, Lin NT, Chong PCS, Yang CY. Expression of sperm fibrous sheath protein CABYR in human cancers and identification of α -enolase as an interacting partner of CABYR-a. *Oncol Rep.* 2011;25(4):1169-75.
21. Wang XY, Chen HS, Luo S, Zhang HH, Fei R, Cai J. Comparisons for detecting NY-ESO-1 mRNA expression levels in hepatocellular carcinoma tissues. *Oncol Rep.* 2009;21(3):713-9.
22. Riener MO, Wild PJ, Soll C, Knuth A, Jin B, Jungbluth A, Hellerbrand C, Clavien PA, Moch H, Jochum W. Frequent expression of the novel cancer testis antigen MAGE-C2/CT-10 in hepatocellular carcinoma. *Int J Cancer.* 2009;124(2):352-7.
23. Lu Y, Wu LQ, Lu ZH, Wang XJ, Yang JY. Expression of SSX-1 and NY-ESO-1 mRNA in tumor tissues and its corresponding peripheral blood expression in patients with hepatocellular carcinoma. *Chin Med J (Engl).* 2007;120(12):1042-6.
24. Wu LQ, Lu Y, Wang XF, Lv ZH, Zhang B, Yang JY. Expression of cancer-testis antigen (CTA) in tumor tissues and peripheral blood of Chinese patients with hepatocellular carcinoma. *Life Sci.* 2006;79(8):744-8.
25. Watanabe T, Suda T, Tsunoda T, Uchida N, Ura K, Kato T, Hasegawa S, Satoh S, Ohgi S, Tahara H, et al. Identification of immunoglobulin superfamily 11 (IGSF11) as a novel target for cancer immunotherapy of gastrointestinal and hepatocellular carcinomas. *Cancer Sci.* 2005;96(8):498-506.
26. Yin YH, Li YY, Qiao H, Wang HC, Yang XA, Zhang HG, Pang XW, Zhang Y, Chen WF. TSPY is a cancer testis antigen expressed in human hepatocellular carcinoma. *Br J Cancer.* 2005;93(4):458-63.
27. Shi YY, Wang HC, Yin YH, Sun WS, Li Y, Zhang CQ, Wang Y, Wang S, Chen WF. Identification and analysis of tumour-associated antigens in hepatocellular carcinoma. *Br J Cancer.* 2005;92(5):929-34.
28. Peng JR, Chen HS, Mou DC, Cao J, Cong X, Qin LL, Wei L, Leng XS, Wang Y, Chen WF. Expression of cancer/testis (CT) antigens in Chinese hepatocellular carcinoma and its correlation with clinical parameters. *Cancer Lett.* 2005;219(2):223-32.
29. Sato S, Noguchi Y, Wada H, Fujita S, Nakamura S, Tanaka R, Nakada T, Hasegawa K, Nakagawa K, Koizumi F, et al. Quantitative real-time RT-PCR analysis of NY-ESO-1 and LAGE-1a mRNA expression in normal tissues and tumors, and correlation of the protein expression with the mRNA copy number. *Int J Oncol.* 2005;26(1):57-63.
30. Yang XA, Dong XY, Qiao H, Wang YD, Peng JR, Li Y, Pang XW, Tian C, Chen WF. Immunohistochemical analysis of the expression of FATE/BJ-HCC-2 antigen in normal and malignant tissues. *Lab Invest.* 2005;85(2):205-13.
31. Dong XY, Li YY, Yang XA, Chen WF. BJ-HCC-20, a potential novel cancer-testis antigen. *Biochem Cell Biol.* 2004;82(5):577-82.
32. Dong XY, Yang XA, Wang YD, Chen WF. Zinc-finger protein ZNF165 is a novel cancer-testis antigen capable of eliciting antibody response in hepatocellular carcinoma patients. *Br J Cancer.* 2004;91(8):1566-70.
33. Zhao L, Mou DC, Leng XS, Peng JR, Wang WX, Huang L, Li S, Zhu JY. Expression of cancer-testis antigens in hepatocellular carcinoma. *World J Gastroenterol.* 2004;10(14):2034-8.
34. Li B, Qian XP, Pang XW, Zou WZ, Wang YP, Wu HY, Chen WF. HCA587 antigen expression in normal tissues and cancers: correlation with tumor differentiation in hepatocellular carcinoma. *Lab Invest.* 2003;83(8):1185-92.

35. Dong XY, Su YR, Qian XP, Yang XA, Pang XW, Wu HY, Chen WF. Identification of two novel CT antigens and their capacity to elicit antibody response in hepatocellular carcinoma patients. *Br J Cancer*. 2003;89(2):291-7.
36. Luo G, Huang S, Xie X, Stockert E, Chen YT, Kubuschok B, Pfreundschuh M. Expression of cancer-testis genes in human hepatocellular carcinomas. *Cancer Immun*. 2002;2:11.
37. Wang Y, Han KJ, Pang XW, Vaughan HA, Qu W, Dong XY, Peng JR, Zhao HT, Rui JA, Leng XS, et al. Large scale identification of human hepatocellular carcinoma-associated antigens by autoantibodies. *J Immunol*. 2002;169(2):1102-9.
38. de Wit NJ, Weidle UH, Ruiter DJ, van Muijen GN. Expression profiling of MMA-1a and splice variant MMA-1b: new cancer/testis antigens identified in human melanoma. *Int J Cancer*. 2002;98(4):547-53.
39. Ono T, Kurashige T, Harada N, Noguchi Y, Saika T, Niikawa N, Aoe M, Nakamura S, Higashi T, Hiraki A, et al. Identification of proacrosin binding protein sp32 precursor as a human cancer/testis antigen. *Proc Natl Acad Sci U S A*. 2001;98(6):3282-7.
40. Chen CH, Chen GJ, Lee HS, Huang GT, Yang PM, Tsai LJ, Chen DS, Sheu JC. Expressions of cancer-testis antigens in human hepatocellular carcinomas. *Cancer Lett*. 2001;164(2):189-95.
41. Bergeron A, Picard V, LaRue H, Harel F, Hovington H, Lacombe L, Fradet Y. High frequency of MAGE-A4 and MAGE-A9 expression in high-risk bladder cancer. *Int J Cancer*. 2009;125(6):1365-71.
42. Schnieders F, Dork T, Arnemann J, Vogel T, Werner M, Schmidtke J. Testis-specific protein, Y-encoded (TSPY) expression in testicular tissues. *Hum Mol Genet*. 1996;5(11):1801-7.

The background of the page is a watercolor illustration featuring several circular, cell-like shapes. Each shape is primarily pink with a darker, purple-blue center, suggesting a nucleus. The shapes are scattered across the white background, with some appearing larger and more detailed than others. The overall style is soft and artistic.

CHAPTER 5

SYSTEMIC T-CELL AND HUMORAL RESPONSES AGAINST CANCER TESTIS ANTIGENS IN HEPATOCELLULAR CARCINOMA PATIENTS

Systemic T-cell and antibody responses against tumor-restricted cancer testis antigens in hepatocellular carcinoma patients

L. Noordam, M.T.A. de Beijer, S. Mancham, I. Vogler, P.P.C. Boor, V. de Ruiter, R. Luijten, J.N.M. IJzermans, U. Sahin, M.J. Bruno, D. Sprengers, S. Buschow* and J. Kwekkeboom*

*These co-authors contributed equally

Oncoimmunology, 2022 Oct 5, Vol. 11, No. 1: 2131096

This chapter has been published in Oncoimmunology.

Hepatocellular carcinoma (HCC) is the fourth leading cause of cancer-related deaths worldwide due to high recurrence rates after curative treatment and being frequently diagnosed at an advanced stage. Immune-checkpoint inhibition (ICPI) has yielded impressive clinical successes in a variety of solid cancers, however results in treatment of HCC have been modest. Vaccination could be a promising treatment to synergize with ICPI and enhance response rates. Cancer testis antigens (CTAs) were recently discovered to be widely expressed in HCC and expression in macroscopically tumor-free tissues correlated with recurrence, implying the presence of micro-satellites. To determine whether CTAs are immunogenic in HCC patients, we analyzed systemic T-cell and humoral responses against seven CTAs in 38 HCC patients using a multitude of techniques; flowcytometry, ELISA and whole antigen and peptide stimulation assays. CTA-specific T-cells were detected in all (25/25) analyzed patients, of which most had a memory phenotype but did not exhibit unequivocal signs of chronic stimulation or recent antigen encounter. Proliferative CD4⁺ and CD8⁺ T-cell responses against these CTAs were found in 14/16 analyzed HCC patients. CTA-peptide stimulation induced granzyme B, IL2 and TNF α in 8/8 analyzed patients, including two MAGEA1 peptides included based on in silico prediction. Finally, IgG responses were observed in 13/32 patients, albeit with low titers. The presence of CD4⁺ and CD8⁺ T-cells and IgG responses shows the immunogenicity of these CTAs in HCC-patients. We hypothesize that vaccines based on these tumor-specific antigens may boost pre-existing CTA-specific immunity and could enhance therapeutic efficacy of ICPI in advanced HCC.

INTRODUCTION

Hepatocellular carcinoma (HCC) is the most common occurring liver cancer and the fourth leading cause of cancer related death worldwide.¹ As a result of an increased prevalence of several risk factors such as obesity and diabetes, the incidence of HCC in Western countries is rising.² Early HCC can be treated with curative intent by either radiofrequency ablation (RFA) or surgical resection. However, up to 70% of these patients experience cancer recurrence, and currently there is no therapy to prevent this.³ In addition, most patients are diagnosed at a late stage and can only be offered palliative treatments such as transarterial chemoembolization (TACE) or multikinase inhibitors, which have limited survival benefits.⁴ Recently, combination therapy of the ICPI atezolizumab (a programmed death-ligand 1 [PD-L1] inhibitor) and bevacizumab (blocking vascular endothelial growth factor [VEGF]) showed modest survival benefit compared to treatment with the multikinase inhibitor sorafenib in advanced HCC.⁵

ICPI therapy is generally most effective in patients with T-cell inflamed “hot” tumors,^{6,7} and recent data indicate this is also true for HCC.⁸ Attempts to transform immunologically “cold” tumors into “hot” tumors to sensitize them to ICPI therapy have yielded promising clinical results by combining ICPI therapy with immunogenic cell death-inducing chemotherapeutics.^{6,7,9} Similarly, recent studies suggest synergistic effects of combining ICPI therapy with therapeutic cancer vaccination to enhance anti-tumor immunity and T-cell infiltration.^{10, 11-14} Such combinatorial studies have not been performed yet in HCC, but therapeutic vaccination with tumor-associated antigen (TAA)-derived peptides can elicit systemic TAA-directed T-cell immunity and tumor T-cell infiltration in both early and advanced HCC patients.¹⁵ ¹⁶ Clinical responses, however, were thus far limited and call for a strategy targeting multiple different strongly immunogenic TAA at the same time. Hence there is a need to discover additional TAA targets for example by mass spectrometry-based HLA-peptidomics.¹⁷⁻¹⁹

Target antigens for cancer vaccines need to be selected carefully to avoid on-target/off-tumor toxicities. A subset of cancer-testis antigens (CTAs) is not expressed in adult healthy tissues, except in immune-privileged germ cells, but can reach high levels in cancer cells due to epigenetic aberrations.²⁰ CTAs have therefore been targeted with therapeutic cancer vaccines. A major advantage of CTAs over neo-antigens is shared expression of specific CTAs in tumors of the same type from different patients, enabling their targeting with off-the-shelf vaccines for groups of patients. However, careful selection of CTAs that are highly prevalent in a specific cancer but absent in healthy tissue (except immune-privileged germ cells) is required for inclusion in a therapeutic cancer vaccine.²⁰ Until recently, clinical results of CTA-based vaccines have been largely disappointing,²¹ but new powerful vaccination strategies in combination with ICPI therapy have lately demonstrated the potential of CTAs as vaccine targets in cancer.^{11,12}

Recently, we identified a panel of 12 tumor-restricted CTAs prevalent in HCC, but absent from healthy tissue.²² This panel of CTAs may therefore hold attractive targets for therapeutic vaccination. Moreover, while absent from healthy liver tissue, we detected low-level expression of one or more of these CTAs in histologically tumor-free liver tissues of 28% and 45% of HCC patients respectively in two independent cohorts undergoing primary tumor resection. In both cohorts, CTA expression in tumor-surrounding

liver tissue was independently associated with cancer recurrence and poor survival after resection.²² These data suggest the presence of CTA-expressing occult micro-metastases or (pre-)malignant cells in tumor-surrounding liver tissue that give rise to new tumors after resection. Therefore, we postulated that our panel of HCC-restricted CTAs may be targets for adjuvant vaccination strategy to prevent cancer recurrence after primary tumor resection or to sensitize advanced HCC patients to ICPI therapy.

An important prerequisite for clinical efficacy of vaccines is antigen immunogenicity in the target patient population. Yet, immunogenicity is largely unknown for our panel of CTAs in HCC patients. To determine whether these CTAs are immunogenic in HCC patients, we analyzed systemic CD4⁺ and CD8⁺ T-cell responses as well as IgG-responses against six CTAs of our panel (melanoma-associated antigen 1 [MAGEA1], melanoma-associated antigen 9 [MAGEA9], melanoma-associated antigen B2 [MAGEB2], melanoma-associated antigen C1 [MAGEC1], melanoma associated antigen C2 [MAGEC2], P antigen family member 1 [PAGE1]) in HCC patients. We also included synovial sarcoma, X breakpoint 2 (SSX2), a thoroughly studied tumor-restricted and immunogenic CTA with known expression in HCC.²³⁻²⁵ Because systemic T-cell responses against TAAs may be transiently enhanced after local tumor ablation in HCC patients,^{26,27} we analyzed these immunological responses before and at several time points after RFA or TACE.

MATERIALS AND METHODS

HCC Patients

Thirty-eight patients diagnosed with HCC and referred for RFA or TACE, were enrolled in the Erasmus Medical Center, Rotterdam, the Netherlands, between January 2016 and May 2019. Diagnosis was based on pathognomonic radiological findings, and all lesions were classified as LI-RADS 5.²⁸ Successfulness of treatment of the lesion was assessed by computed tomography (CT) and alfa feto protein (AFP) level in blood. If necessary treatment was repeated. Multiple patients experienced rapid recurrence after initial treatment, and one retreated patient (ITV-016) was included twice. HCC recurrence was evaluated by CT scan routinely after approximately 6 weeks (range 5-11 weeks), and subsequently every 3 months.

Blood was collected before treatment and after 3 (3-5), 7 (5-11) and 25 (13-47) weeks (median (range)) of treatment. Variation in blood collection time was due to differences in individual treatment plans and out-patient clinic visits. Six patients were excluded from analysis because only blood before treatment was collected (**Supplementary Table S1A**). Medical records were reviewed for clinicopathological variables, dates of first cancer recurrence, HCC-specific death, liver transplantation (LTx; after which follow-up stopped) or last follow-up until April 1st 2020 (**Table 1**). All patients signed informed consent before participation. The study adhered to the Helsinki declaration and was approved by the local medical ethical committee (MEC-2015-563).

PBMC isolation, HBsAg and anti-HBsAg determination and flowcytometric HLA-A*02 typing

Blood was collected in Sodium Heparin tubes (BD), which were centrifuged at 120xg for 20 min to collect plasma. Consecutively, the plasma was centrifuged at 3220xg for 15 min to discard platelets. Plasma

samples were stored at -80°C until use. Quantitative measurements of Hepatitis B surface antigen (HBsAg) and anti-HBsAg were performed in thawed plasma using tests from the DiaSorin LIAISON® XL HEPATITIS A and B LINE by the Department of Virology, Erasmus MC, Rotterdam, the Netherlands. Peripheral blood mononuclear cells (PBMC) were isolated from the plasma-depleted fraction by Ficoll density gradient centrifugation. To select human leukocyte antigen (HLA)-A*02-positive patients for analysis of CTA-specific CD8⁺ T-cells using HLA-A*02:01 dextramers, a sample of PBMC was labeled with a fluorochrome-conjugated anti-HLA-A*02 antibody (**Supplementary Table S2**) and analyzed by flow cytometry (FACS Canto II [BD Biosciences]). Remaining PBMC were cryopreserved in 49% RPMI-1640 medium (Gibco), 0.5% penicillin/streptomycin (Gibco), 0.5% ultraglutamin (Lonza), 40% fetal calf serum (FCS, Sigma) and 10% DMSO (Sigma), and stored in liquid nitrogen until use.

Ex vivo CTA-specific T-cell proliferation assay

Autologous B-cell blasts were generated from 10×10^6 PBMC by culturing with 1 $\mu\text{g}/\text{ml}$ soluble human trimeric CD40ligand (CD40L; kindly provided by National Institutes of Health (NIH), Bethesda, MD, USA), 40 IU/ml recombinant interleukin 4 (rIL4; Strathman) and 1 $\mu\text{g}/\text{ml}$ Cyclosporin A (Novartis) for 3 weeks, as previously described.²⁹ Vitality, purity and maturation status were checked by flow cytometry (FACS Canto II [BD Biosciences]) after antibody staining (see **Supplementary Table S2**) and 7-Aminoactinomycin D (7AAD; Invitrogen), shown in **Supplementary Figure S1**. B-cell blasts were electroporated with 10 μg of messenger RNA (mRNA) encoding MAGEA1, MAGEA9, MAGEB2, MAGEC1₉₃₄₋₁₁₄₂, MAGEC2, PAGE, SSX2, or luciferase, (**Supplementary File**) by electroporation using the square-wave protocol with a single pulse of 800 V and a length of 0.6 ms in a 4 mm cuvette, as previously described.²⁹ After electroporation the B cells were rested for at least two hours at 37°C . Messenger RNAs were synthesized by BioNTech SE by *in vitro* transcription from linearized plasmids in which the full-length (or in case of MAGEC1 amino acids 934-1142, because of its large size and the presence of known immunogenic epitopes in this part³⁰) coding sequences of the respective genes were flanked with an HLA class I signal peptide fragment (sec) at the 5'- and an HLA class I trafficking signal at the 3'-end to facilitate loading in HLA class II.³¹ For comparison, B-cell blasts were electroporated with 10 μg glypican 3 (GPC-3) or enhanced green fluorescent protein (eGFP) encoding mRNAs, purchased from eTheRNA (Belgium), which we used in previous studies.^{29, 32} In these constructs, antigens were fused to the transmembrane and luminal regions of DCLamp for endo-lysosomal targeting. mRNA encoding New York esophageal squamous cell carcinoma-1 (NY-ESO-1) was not available.

HCC patient PBMC were thawed, stained with CellTrace CFSE (Invitrogen), and co-cultured with transfected autologous B-cell blasts at a 1:10 B-cell:PBMC ratio in RPMI1640 supplemented with ultraglutamine (Lonza), 10% normal human AB serum (Sigma), 1% penicillin/streptomycin (Gibco), 10mM Hepes buffer (Lonza), 1mM Sodium Pyruvate (Invitrogen) and 1% MEM Non-Essential Amino Acids Solution 100x (MEM-NEAA, Invitrogen) for 6 days at 37°C in a humidified atmosphere supplemented with 5% CO_2 . Triplicate cultures were set up for each CTA as well as for luciferase, GPC-3, and eGFP. As a positive control, PBMC were stimulated with 25 ng/ml Staphylococcal Endotoxin B (SEB; Sigma). Total numbers

Table 1. Patient Characteristics.

Characteristic	HCC patients (n=32)	Healthy controls (n=15)
Age at surgery (years)		
Mean \pm SD	68.7 \pm 7.0	63.9 \pm 3.8
Median (range)	68.5 (54-81)	64 (56-69)
Sex – no. (%)		
Male	27 (84.4)	13 (86.7)
Female	5 (15.6)	2 (13.3)
Race – no. (%)		
White	30 (93.8)	-
African	1 (3.1)	-
Asian	1 (3.1)	-
Unknown	-	15 (100)
Etiology – no. (%)		
Alcohol	13 (40.6)	NA
NASH	6 (18.8)	NA
No known liver disease	4 (12.5)	NA
Hepatitis B	3 (9.4)	NA
Hepatitis C	3 (9.4)	NA
Hepatitis C + Alcohol	1 (3.1)	NA
Hemochromatosis + NASH	1 (3.1)	NA
Porphyria	1 (3.1)	NA
Hepatitis status – no. (%)		
Chronic Hepatitis B	3 (9.4)	0 (0)
Cleared Hepatitis B	2 (6.3)	0 (0)
Hepatitis C + Cleared Hepatitis B	2 (6.3)	0 (0)
Hepatitis C	2 (6.3)	0 (0)
Cirrhosis – no. (%)		
Yes	31 (96.9)	0 (0)
No	1 (3.1)	15 (100)
Initial treatment – no. (%)		
RFA	25 (78.1)	NA
TACE	5 (15.6)	NA
RFA + TACE	2 (6.3)	NA
BCLC stage – no. (%)		
A	27 (84.4)	NA
B	5 (15.6)	NA
Number of lesions – no. (%)		
1	17 (53.1)	NA
>1	15 (46.9)	NA
Median (range)	1 (1-3)	NA
Size of largest lesion (cm)		
Mean \pm SD	2.8 \pm 1.4	NA
Median (range)	2.3 (1.2-7.0)	NA
AFP level before resection (ug/l)		
Mean \pm SD	763 \pm 3148	NA
Median (range)	7 (1-17276)	NA

of PBMC varied between $1.1\text{--}2.2 \times 10^5$ cells per well, depending on the number of available PBMC. After 6 days cells were harvested, technical triplicate cultures were pooled, and CFSE-dilution in CD4⁺ and CD8⁺ T-cells was analyzed by flow cytometry (FACS Canto II [BD Biosciences]), after surface labeling for 20 min at 4°C with antibodies (anti-CD3 PE-Cy7, anti-CD4 APC-Cy7, anti-CD8 PerCP-Cy5.5, and anti-CD56 PE; see **Supplementary Table S2**), followed by 7AAD (Invitrogen).²⁹ Percentages of proliferated (CFSE-low) CD4⁺ and CD8⁺ T-cells were determined. Antigen-specific T-cell responses were considered positive when percentages of CFSE-low T-cells in cultures with CTA or GPC3 mRNA transfected B-cell blasts were at least 2-fold higher compared to percentages of CFSE-low T-cells in co-cultures of B-cell blasts transfected with luciferase or eGFP mRNA, respectively. Because >50% of T-cells were CFSE-low in all SEB-stimulated PBMC, all cultures could be accepted for analysis. A minimum of 50 (range 50-13845) CFSE⁻ cells, 520 (range 520-32012) CD8⁺ T cells and 3091 (range 3091-107528) CD4⁺ T cells in the CTA-stimulated conditions were acquired.

Flow cytometric PBMC phenotyping

For phenotypic analysis without HLA-A*02:01 dextramer labeling, PBMC were thawed, stained with a CCR7-specific mAb for 1 hour at room temperature (RT), followed by a fixable live/dead stain (eBioscience) for 20 min at 4°C, antibody labelling of other surface antigens for 20 min at 4°C, fixation with the FoxP3 staining buffer kit (eBioscience) for 20 min at 4°C and staining of intracellular antigens for 20 min at 4°C. For phenotypic analysis including peptide-loaded HLA-A*02:01 dextramer labeling, PBMC of HLA-A*02⁺ patients and HLA-A*02⁺ healthy blood bank donors (with written informed consent from the donors provided by Sanquin Blood bank, Amsterdam) were thawed and stained with a CCR7-specific mAb for 1 hr at RT, followed by a fixable live/dead stain (eBioscience) for 20 min at 4°C. Consecutively, before staining with CTA peptide-loaded HLA-A*02:01 dextramers, PBMC were incubated with 50 nM dasatinib (Sigma) for 30 min at 37°C to enhance T-cell receptor expression,³³ followed by incubation with a pool of APC-labeled HLA-A*02:01 dextramers loaded with previously described immunogenic epitopes derived from 7 different CTAs (Immudex. **Supplementary Table S3**), or single CTA peptide-loaded dextramers for 10 min at RT. Cytomegalovirus (CMV)pp65 peptide loaded dextramer was included as a reference. Thereafter, cells were labelled for surface antigens for 20 min at 4°C, permeabilized and fixed with the FoxP3 staining buffer kit (eBioscience) for 20 min at 4°C and stained for intracellular antigens for 20 min at 4°C. As no immunogenic epitope of PAGE1 is known, we could not include a PAGE1 dextramer labeling. For the PE-labeled CMVpp65-peptide loaded HLA-A*02:01 dextramer, pre-incubation with dasatinib was not required and therefore omitted. A threshold of a minimum of 10 events was set.

A detailed list of fluorochrome-conjugated antibodies used for phenotyping is listed in **Supplementary Table S2**. All antibody stains were carried out in presence of 0,2% Fc-block (BD Biosciences). Flow cytometric phenotyping was performed using a FACS Symphony (BD Biosciences), and analysis was performed using FlowJo version 10.4 software (FlowJo).

High resolution HLA-I typing and peptide stimulation

For high-resolution HLA-typing of HCC patients selected for peptide stimulation assays, DNA was isolated from PBMC using the QIAamp DNA Mini kit (Qiagen) according to manufacturer's instructions. High resolution HLA-I typing was performed by the Department of Internal Medicine, Erasmus MC, Rotterdam, the Netherlands using the Illumina GSA beadchip GSA MD v2. HLA types were imputed from the obtained SNP data (after translation of Illumina IDs to Affymetrix IDs) using the Axiom HLA analysis tool (Affymetrix). Next, *in silico* prediction was performed (NetMHCpan3.0) to expand the CTA-peptide pool that could be tested in donors that were negative for HLA-A*02:01 (ITV-006; ITV-007 and ITV-021). Peptides that were predicted to bind (rank ≤ 2.0) at least one HLA-type of a patient were included in peptide stimulation assays (underlined in **Supplementary Table S4**). Cryopreserved PBMC of 8 HCC patients were subsequently thawed and stimulated with CTA and hepatitis B virus (HBV) peptides (Peptide 2.0 Inc) at 37°C in a humidified atmosphere supplemented with 5% CO₂ as described previously.³⁴ Briefly, PBMC (1x10⁶ cells/ml) were stimulated with pools of a maximum of 5 peptides of interest (**Supplementary Table S4**) based on HLA class I types of the patients (**Supplementary Table S5**) at a concentration of 5 µg/ml of each peptide in Iscove's modified Dulbecco's medium (IMDM; Lonza) supplemented with 2% normal human AB serum (Sanquin), 1% ultraglutamine (Lonza), 1% penicillin/streptomycin (Gibco) and 50 IU/ml hIL-2 (Miltenyi). After 14 days, cultured PBMC were re-stimulated for 48 hr at 37°C with 5 µg/ml of each peptide separately or solvent-containing medium as a negative control. Depending on cell availability, 80.000 - 200.000 cultured PBMC were re-stimulated in duplicate. Cytokine production was assessed in pooled duplicate supernatants by the LEGENDplex™ Human CD8/NK Panel (BioLegend) according to the manufacturer's instructions. Plates were read using the MACSQuant Analyzer 10 (Miltenyi) and analyzed using the LEGENDplex™ data analysis software (BioLegend). Peptides for which cytokine concentrations were ≥ 2 fold higher as compared to the corresponding negative control cultures were determined to have evoked a peptide-specific response.

CTA IgG ELISA

Plasma samples of 32 HCC patients and 15 healthy controls (Sanquin blood bank, informed consent supplied) were diluted 1:1 in glycerol (Sigma) for storage at -20°C and used for determination of Immunoglobulin G (IgG) against recombinant full length CTA proteins (**Supplementary Table S6**). Plasma IgG against CTAs was determined by indirect ELISA according to Gnjatic, et al,³⁵ with minor adjustments made in preliminary testing of sera from melanoma patients which contained MAGEA1 or NY-ESO-1 specific IgG, kindly provided by Prof. Dr. S.B. Eichmüller (German Cancer Research Center, Heidelberg, Germany).³⁶ For screening of IgG immune reactivity against CTAs in patient plasma samples, 4 random plasma samples of healthy subjects were included as negative controls in ELISAs for each CTA, and all measurements were performed in duplicate. Maxisorp-plates™ (ThermoFisher) were coated with 1 µg/ml full length recombinant protein or 1 µg/ml bovine serum albumin (BSA, Sigma; negative control protein) in coating buffer (0.2M sodium carbonate, pH 9.5) overnight at 4°C. Plates were then washed eight times with phosphate buffered saline (PBS), and blocked with blocking buffer (5% non-

fat dry milk [Bio-Rad] and 10% fetal calf serum in PBS) for 2 hours at RT. After washing the plates eight times with PBS, they were incubated with plasma samples diluted 1:20 in blocking buffer for 2 hours at RT. Consecutively, plates were washed four times with 0.1% Tween 20 (Sigma) in PBS, four times with PBS, and incubated with a goat anti-human IgG-horseradish peroxidase ([HRP]; 1:6000, BD Biosciences) detection antibody for 1 hour at RT. Plates were washed four times with 0.1% Tween 20 in PBS and four times with PBS, after which TMB substrate (Invitrogen) was added for 15 minutes. The reaction was stopped with 1N H₂SO₃ and absorbance was measured at 450 nm using an Infinite® 200 PRO microplate reader (Tecan).

The delta optical density (Δ OD) of each plasma sample was calculated by subtracting the OD from wells coated with BSA from those coated with the specific CTA. Patient plasma samples were considered positive if the Δ OD value exceeded the mean Δ OD plus ten times the standard deviation of the 4 healthy control plasma samples.³⁵

The positive plasma samples (at the screening dilution of 1:20) were then selected for determination of the CTA-specific IgG titer by testing plasma dilutions of 1:20, 1:40, 1:80, 1:160 and 1:320 using the same protocol.

Statistical analysis

Statistical analyses were performed using Graphpad (Version 8.2.1 for Windows, San Diego, CA) and R Statistical software (Version 3.6.1 for Windows, Foundation for Statistical Computing, Vienna, Austria). Heat maps were created with RStudio and the 'gplots' and 'pheatmap' packages. Used statistical tests are indicated in the figure legends. P-values < 0.05 were considered significant.

RESULTS

Patients and healthy controls

The clinicopathological characteristics of the 32 included HCC patients and 15 age and gender-matched healthy blood bank donors are shown in **Table 1**. The most prevalent etiology of HCC was alcoholic liver disease (n=13, 40.6%), second was non-alcoholic steatohepatitis (NASH; n=6, 18.8%). Most patients were classified as Barcelona clinic liver cancer (BCLC) stage A (n=27, 84.4%), 5 patients were classified as BCLC stage B (15.6%). Most patients were treated with RFA (n=25, 78.1%) and five were treated with TACE (15.6%), whereas two patients underwent both treatments subsequently (6.3%, both of these patients had BCLC stage B disease). During follow-up, 23 patients (71.9%) developed HCC recurrence, 7 (21.9%) died of HCC and 8 (25%) underwent liver transplantation. Treatments, blood collection, tumor recurrence, LTx and HCC-specific death are summarized in **Figure 1**.

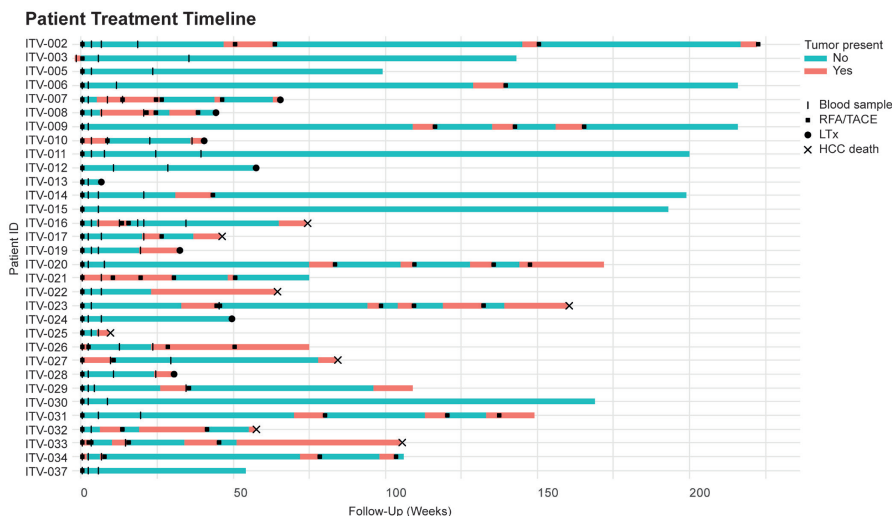


Figure 1. Patient treatment timeline.

Schematic overview of events (blood sample collection, RFA/TACE, LTx, HCC-specific death) in HCC patients included in the study during the follow-up period. The colors indicate the presence or absence of detectable HCC tumor. Patient ITV-016 was retreated with RFA 13 weeks after the first treatment due to rapid recurrence. Of this patient, blood samples were collected before and after the first RFA and before and after the second RFA and were included in the study separately.

HCC patients have enhanced frequencies of circulating CTA-specific CD8⁺ T-cells compared to healthy subjects

It has been described that local ablative therapies can enhance frequencies of circulating tumor-specific T-cells in HCC-patients.^{26, 27, 37} Therefore, to maximize the chance of detecting CTA-specific T-cells in HCC patients, we analyzed PBMC of 26 HCC patients by flow cytometry before treatment and at 3, 7, and 25 weeks after local ablative therapies (**Supplementary Table S1A**). No effect of ablative therapy on any of the major leukocyte (sub)populations was observed (**Figure 2A, 2B and Supplementary Figure S2A, S2B**). Also, the main T-cell subpopulations did not change in response to ablative therapy (**Supplementary Figure S2C**). Next, we determined the frequencies of CTA peptide-specific CD8⁺ T-cells in HLA-A*02:01⁺ patients (n=17, **Supplementary Table S1A**) and compared these with frequencies in 9 healthy HLA-A*02:01⁺ subjects, by staining with a pool of HLA-A*02:01 dextramers loaded with published immunogenic CTA-peptides (MAGEA1₂₇₈₋₂₈₆^r, MAGEA9₂₂₃₋₂₃₁^r, MAGEB2₂₃₁₋₂₄₀^r, MAGEC1₁₀₈₇₋₁₀₉₅^r, MAGEC2₁₉₁₋₂₀₀, NY-ESO-1₁₅₇₋₁₆₅^r and Ssx2₄₁₋₄₉^r; **Supplementary Figure S3A, Supplementary Table S3**). A CMVpp65 dextramer was used as a non-tumor antigen reference. CTA peptide-specific CD8⁺ T-cells in HCC patients ranged between 0.07-1.99%, 0.12-1.45%, 0.09-1.3%, and 0.08-2.4% at t=0, 3, 7 and 25 weeks after treatment, respectively (**Figure 2A**). A maximum of 0.06% of CD8⁺ T-cells recognized these pooled CTA-peptides in healthy controls (**Figure 2C**). Using > 0.06% as a cut-off, these data demonstrate that all 17 HCC patients who were included in this part of the study had enhanced frequencies of circulating CTA

peptide-specific CD8⁺ T-cells compared to healthy subjects. However, there were no marked changes in CTA-specific CD8⁺ T-cell frequencies over time upon local ablative therapies (**Figure 2A**).

Using CD45RA and CCR7 expression, we subsequently analyzed the differentiation status of circulating CD8⁺ T-cells (**Supplementary Figure S4**). In agreement with previous reports³⁸, most CMV-specific CD8⁺ T-cells showed a terminally differentiated phenotype (**Figure 2B**). Most CTA peptide-specific CD8⁺ T-cells also showed a memory phenotype, but contained more effector memory (EM) and central memory (CM) T-cells than CMV-specific CD8⁺ T-cells (**Figure 2B**). To investigate whether CTA-specific CD8⁺ T-cells in HCC patients showed signs of recent activation, we determined their expression of activation marker CD137 and proliferation marker Ki67 (**Figure 2D**). Although we observed tendencies to slightly enhanced expression of CD137 and Ki67 in CTA-specific CD8⁺ T-cells compared to CMV-specific CD8⁺ T-cells and non-CTA recognizing CD8⁺ T-cells, most of these differences did not reach statistical significance (**Figure 2D**).

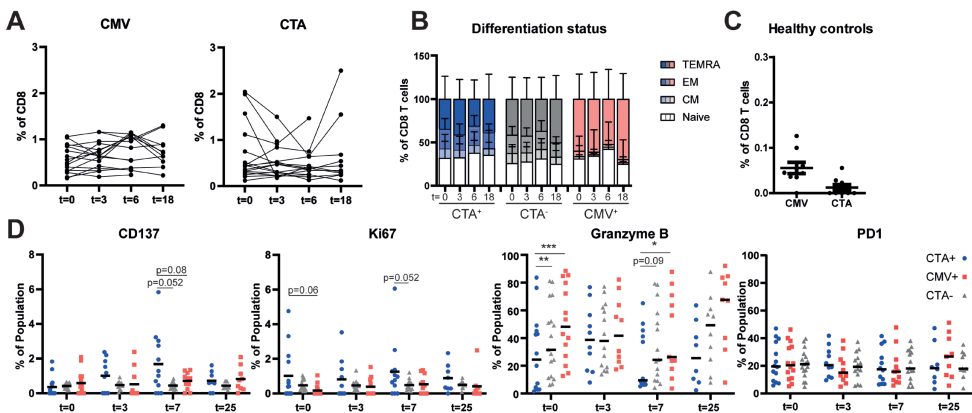


Figure 2. HCC patients show enhanced frequencies of circulating CTA-specific CD8⁺ T-cells compared to healthy subjects.

PBMC from HCC patients before (t=0), and approximately 3, 7, and 25 weeks (see **Figure 1** for the exact time points) after RFA/TACE treatment were phenotyped by flow cytometry (n=26). CTA-specific CD8⁺ T-cells were determined in HLA-A*02:01-positive patients (n=17) using CTA peptide-loaded HLA-A*02:01 dextramers. Patient ITV-016 was included twice, before and after a first RFA and before and after a second RFA treatment. **A.** CTA-specific CD8⁺ T-cells were detected using a pool of 7 CTA peptide-loaded HLA-A*02:01 dextramers (**Supplementary Table S3**). Frequencies of CMVpp65₄₉₅₋₅₀₃-specific CD8⁺ T-cells were measured for comparison. **B.** Differentiation status of CMVpp65₄₉₅₋₅₀₃-dex⁺, CTA-dex⁺ and CTA-dex⁻ CD8⁺ T-cells was determined based on CD45RA and CCR7 expression (Naïve; CD45RA⁺CCR7⁺; central memory [CM]; CD45RA⁺CCR7⁺; effector memory [EM]; CD45RA⁺CCR7⁻; and TEMRA; CD45RA⁺CCR7⁻). **C.** CMV-specific CD8⁺ T-cells were detected in healthy blood bank donors, but only a maximum of 0.06% of CD8⁺ T-cells recognized the pooled CTA-peptides. **D.** Surface expression of activation marker CD137, intracellular expression of proliferation marker Ki67, cytotoxic effector molecule granzyme B and checkpoint inhibitor PD1 were determined in CTA-dex⁺, CMV-dex⁺ and CTA-dex⁻ CD8⁺ T-cells. Wilcoxon signed-rank test, * p<0.05, **p<0.01, ***p<0.001.

Compared to non-CTA recognizing CD8⁺ T-cells, CTA-specific CD8⁺ T-cells showed reduced Granzyme B expression before local tumor ablation (**Figure 2D**). This was not accompanied by further signs of chronic stimulation and exhaustion as expression of the inhibitory receptors PD1, LAG3 and TIM3 was not elevated on CTA-specific CD8⁺ T-cells compared to their CMV-specific or non-CTA recognizing counterparts (**Figure 2D** and **Supplementary Figure 3B**). Moreover, LAG3 expression on CTA-specific CD8⁺ T-cells was reduced compared to CMV-specific CD8⁺ T-cells (**Supplementary Figure S3B**). Finally, we measured the binding of the individual CTA peptide-loaded HLA-A*02:01 dextramers to CD8⁺ T-cells. For this purpose, we pre-selected 5 HCC patients in which >0.5% of CD8⁺ T-cells bound the pool of CTA peptide-loaded HLA-A*02:01 dextramers at a given time point (**Figure S5**). We detected CD8⁺ T-cells specific for each individual CTA in these patients. Frequencies were low, but comparable to those of CD8⁺ T-cells that recognized the established immunogenic NY-ESO-1₁₅₇₋₁₆₆ epitope. However, no consistent effect of local tumor ablation was observed, which is consistent with the pooled CTA-peptide dextramer results.

Taken together, we detected higher frequencies of CTA peptide-specific circulating CD8⁺ T-cells in all 17 HCC patients compared to healthy subjects. Most of these cells had a memory phenotype, suggesting *in vivo* priming, but they did not exhibit unambiguous signs of chronic stimulation (co-inhibitory receptor expression), or recent antigen encounter (CD137 or Ki-67 expression). In addition, neither frequency nor differentiation or activation status of CTA peptide-specific CD8⁺ T-cells was influenced by local tumor ablation.

CD4⁺ and CD8⁺ T-cells of HCC patients show *in vitro* proliferative responses to CTA-specific stimulation

To study whether circulating CTA-specific T-cells in HCC patients are functionally competent, we first quantified *in vitro* proliferative responses of peripheral T-cells from 16 HCC-patients (**Supplementary Tables S1A** and **S1B**) against CTAs. One patient (ITV-016) was included twice in the study, using blood samples collected before and after an initial RFA and a second RFA performed 13 weeks after the first due to rapid cancer recurrence. CFSE-labeled PBMC were stimulated for 6 days with expanded autologous B-cell blasts electroporated with CTA-encoding mRNA or, as a negative control, with luciferase mRNA (see **Supplementary Figure S1** for phenotyping results of generated B-cell blasts). Proliferative CD4⁺ and CD8⁺ T-cell responses were subsequently measured by CFSE-dilution and observed against all of the seven tested CTAs (MAGEA1, MAGEA9, MAGEB2, MAGEC1, MAGEC2, PAGE1 and SSX2). Overall, strong proliferative CD4⁺ and/or CD8⁺ T-cell responses (≥ 4-fold over response to luciferase) against each of the CTAs were observed in at least one patient. All but two HCC patients (ITV-011 and ITV-031) showed a proliferative T-cell response to at least 1 and maximally 6 CTAs (**Figure 3A, B**). MAGEC2-, PAGE1 and SSX2-specific T-cell responses were most frequently observed (in 11/16, 9/16 and 9/16 patients, respectively), while T-cell responses against each of the other 4 CTAs were detected in 7 HCC patients. GPC3, a well-known immunogenic HCC-associated antigen^{16, 39} was included as a reference antigen and induced a maximum fold-change in proliferation of 2.7-fold in CD4⁺ T-cells and 3.9-fold in CD8⁺

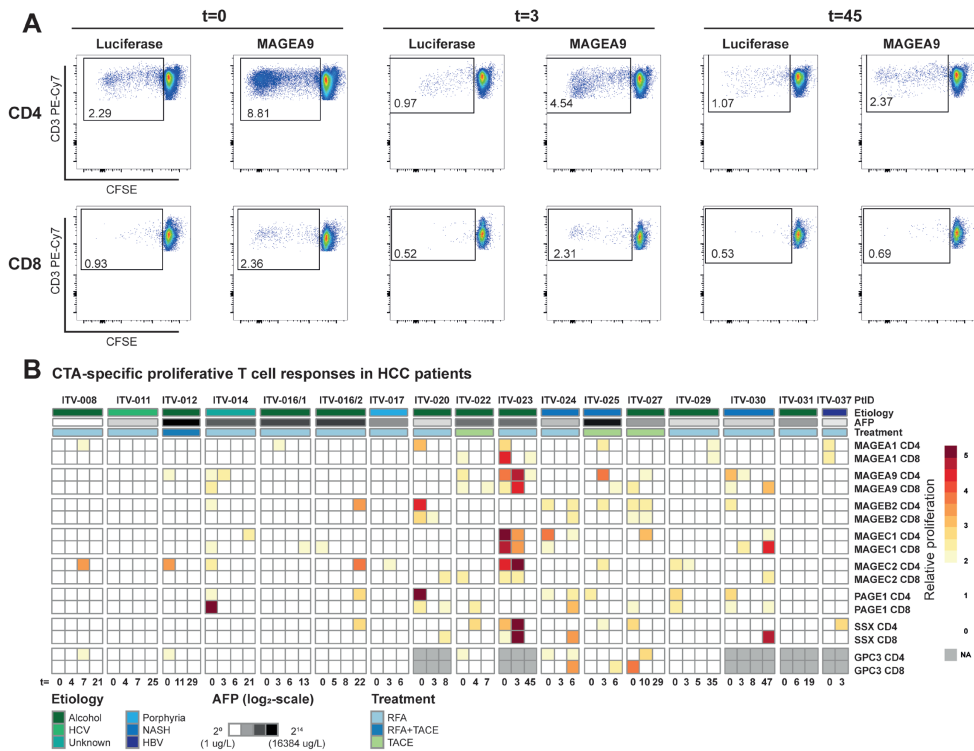
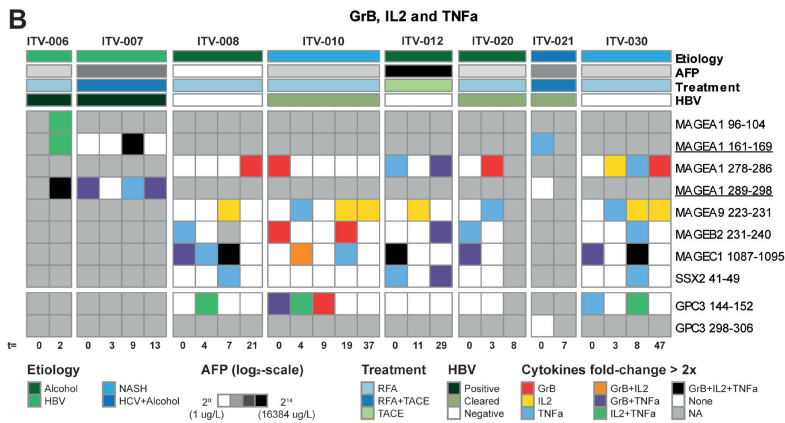
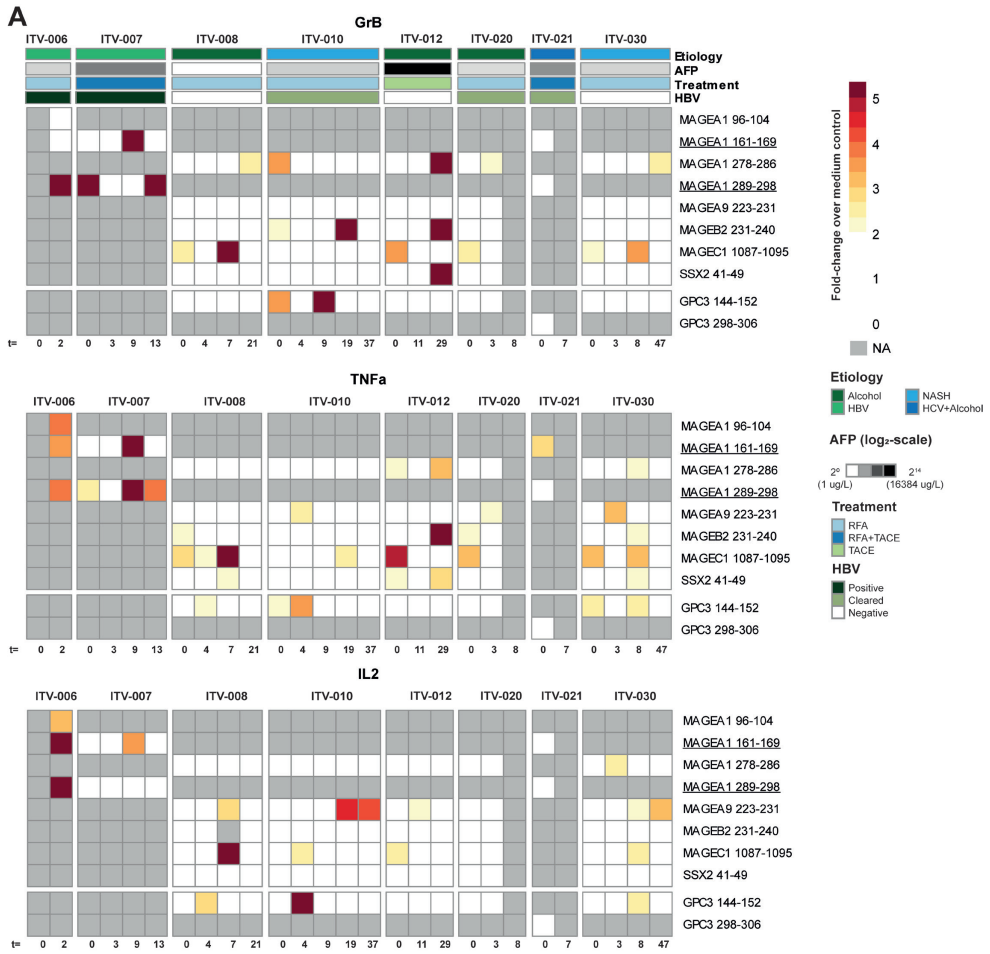


Figure 3. CTA-specific stimulation induces proliferative responses in CD4⁺ and CD8⁺ T-cells of HCC patients.

CTA-specific CD4⁺ and CD8⁺ T-cell proliferation was measured in 16 HCC patients by 6-day stimulation of CFSE-labeled PBMC with CTA mRNA or luciferase mRNA (negative control)-electroporated autologous B-cell blasts. CTA-specific proliferation was then calculated by dividing the percentage proliferated (CFSE-low) T-cells upon CTA-stimulation by the percentage proliferated T-cells upon luciferase-stimulation. **A.** Gating example of proliferation of CD4⁺ and CD8⁺ T-cells collected before (t=0) and t=3 and t=45 weeks after RFA from patient ITV-023 upon 6 days of stimulation with MAGEA9 or luciferase mRNA electroporated B-cell blasts. **B.** Heat map indicates fold-changes in proliferation of peripheral CD4⁺ and CD8⁺ T-cells upon stimulation with individual CTAs compared to stimulation with luciferase (colored legend). CTA-specific T-cell responses were considered positive with a \geq two-fold increase compared to luciferase-stimulated T-cell proliferation was observed. For comparison, proliferative responses against the onco-fetal tumor-associated antigen GPC3 were measured in 11 patients and depicted as fold changes compared to stimulation with eGFP. Patient ITV-016 was included after initial RFA and after a second RFA 13 weeks after the first treatment due to rapid cancer recurrence. Annotation above the heat map indicates the etiology of HCC, AFP levels before treatment, and the treatment (RFA or TACE) which the patients received. Annotation below the heat map indicates the actual weeks after treatment at which blood samples of the individual patients were collected (t=0: before local tumor ablation).



◀ **Figure 4. CTA-specific peptide stimulation induces cytokine and granzyme B production in PBMC of HCC patients.**

Peptide-specific induction of cytokine and granzyme B (GrB) production was measured after re-stimulation of expanded PBMC of 8 HCC patients prior to local ablative treatment (t=0) and at the indicated weeks after intervention. **A.** Heatmaps depicting the fold changes for production of the indicated cytokines and GrB in the peptide stimulated condition compared to the solvent-containing medium condition. Peptides with a ≥ 2 fold change were determined to have evoked a peptide-specific response and are depicted as such (color-coded legend). **B.** Heatmap displaying concomitant production of GrB, IL-2 and/or TNF- α in the combinations indicated by the color-coded legend. Annotation above the heat map indicates the etiology of HCC, AFP levels before treatment, the treatment (RFA or TACE) patients received, and HBV status. Underlined peptides were included in our study based on *in silico* prediction of HLA-binding properties.

T-cells, which is lower than the maximum responses observed against each of the tested CTAs. We did not observe an uniform relation between tumor ablation and proliferative CTA-specific T-cell responses. In addition, we did not find a clear association between CTA-specific proliferative T-cell responses and etiology, AFP levels (**Figure 3B**), or other clinicopathological factors (**Supplementary Figure S6**).

In conclusion, proliferative CD4⁺ T-cell and CD8⁺ T-cell responses were found against one or more of the tested CTAs in 14 out of 16 analyzed HCC patients, but were not enhanced by local ablative therapies.

CTA-peptide-specific stimulation induces pro-inflammatory cytokine and granzyme secretion by PBMC of HCC patients

To investigate whether our selection of CTAs could induce effector responses in T-cells, we tested production of cytokines and cytotoxic molecules secreted upon stimulation of PBMC. For this purpose, we included 8 HCC patients (**Supplementary Tables S1A** and **S1B**) and tested 8 different HLA class I epitopes derived from 5 CTAs (MAGEA1, MAGEA9, MAGEB2, MAGEC1, SSX2). The selected epitopes were matched with the HLA class I types of the included HCC patients (**Supplementary Tables S4-S5**). Five (out of the eight) epitopes had also been included in HLA-A:02:01 dextramer binding analysis of CD8⁺ T-cells (**Supplementary Table S3**). PBMC were pre-stimulated with pools of a maximum of 5 peptides for 14 days and re-stimulated with single peptides for 2 days after which secreted molecules were quantified. Due to limited numbers of PBMC, we could not test each epitope in all patients. Nevertheless, we observed that all CTA-epitopes stimulated production of IL-2, Granzyme B and/or TNF α in one or more patients (**Figure 4A** and **B**). Interestingly, combined production of 2 or 3 of these pro-inflammatory factors against CTA epitopes was identified 13 and 5 times across patients and time points, respectively (**Figure 4B**). Production levels were similar to those invoked by a known immunogenic peptide of GPC3 (**Figure 4**). It is noteworthy that cytokine production was also observed in response to two MAGEA1 peptides (MAGEA1₁₆₁₋₁₆₉ and MAGEA1₂₈₉₋₂₉₈) that are thus far only described as immunogenic in context of HLA-types not expressed in these 8 HCC patients. These peptides were included in our study based on *in silico* prediction of HLA-binding properties (indicated with an asterisk in **Supplementary Table S4** and underlined in **Figure 4**).

Since 5 of the HCC-patients included in the peptide stimulation experiments had a (clinical history of) HBV infection, we additionally investigated functional responses against well-known HBV-derived HLA class I epitopes (**Supplementary Figures S7-9**). A total of 23 HBV-derived epitopes were tested, representing all HBV proteins and several common HLA-types. Production of IL-2, Granzyme B and/or TNF α was observed in response to 21 out of 23 epitopes, with numerous responses both in patients with an ongoing chronic (ITV-006 and ITV-007) or resolved (ITV-010 and ITV-021) HBV infection. The HBV parameters HBsAg and anti-HBsAg did not seem to relate to local ablative intervention, although numbers of patients are too few to draw definitive conclusions (**Supplementary Figure S10**).

HCC patients have IgG-responses against CTAs

To gain further insight into the immunogenic potential of the selected CTAs, we investigated humoral IgG responses by ELISA. We screened 105 plasma samples, obtained from 32 HCC patients, and 15 healthy subjects (negative controls) for IgG antibodies against MAGEA1, MAGEA9, MAGEB2, MAGEC2, PAGE1 and SSX2 recombinant full length CTA proteins. We additionally investigated IgG titers against the established immunogenic tumor antigen NY-ESO-1 (**Supplementary Table S6**) as reference. We could not include MAGEC1 in antibody screening, because neither full-length nor MAGEC1₉₃₄₋₁₁₄₂ protein are commercially available. Compared to healthy subjects, we detected enhanced levels of specific IgG against every CTA in at least one HCC patient (**Figure 5A**). In 13 out of 32 HCC patients we found IgG specific for at least one CTA, and in 11 patients the anti-CTA antibodies were already present before tumor ablation. These pre-existing humoral responses were generally stable over time, with titers ranging between 1:20 and 1:640 (**Figures 5A, B and C**). In comparison, two positive control sera from melanoma patients showed NY-ESO-1-specific IgG titers of 1:1000, and a positive control serum from a melanoma patient showed a MAGEA1-specific IgG titer of 1:200 (**Supplementary Figure S11**). *De novo* induction of CTA-specific IgG after local tumor ablation was observed in 4 patients.

Taken together, IgG responses against all 7 CTAs were observed in our HCC patient cohort. In general, local tumor ablation may induce *de novo* anti-CTA IgG responses or enhance CTA-specific IgG titers, however, numbers are too small to draw any conclusions.

DISCUSSION/CONCLUSION

Recently, we have identified a panel of 12 CTAs prevalent in HCC, but absent from healthy tissue except immune-privileged germ cells. Moreover, we demonstrated that expression of these CTAs in non-tumor liver tissues was associated with early cancer recurrence after primary tumor resection and may indicate presence of occult micro-metastases or pre-malignant transformation of liver tissue. Therefore, we postulated that vaccination strategies targeting these CTAs in early-stage HCC may have clinical utility as adjuvant therapy to prevent cancer recurrence after primary tumor resection.²² In advanced HCC such vaccination approach may synergize with ICPI therapy.

Here, we comprehensively studied the immunogenicity of six of these pre-defined CTAs and of SSX-2 in HCC patients before and after local tumor ablation. We demonstrate systemic IgG responses against one

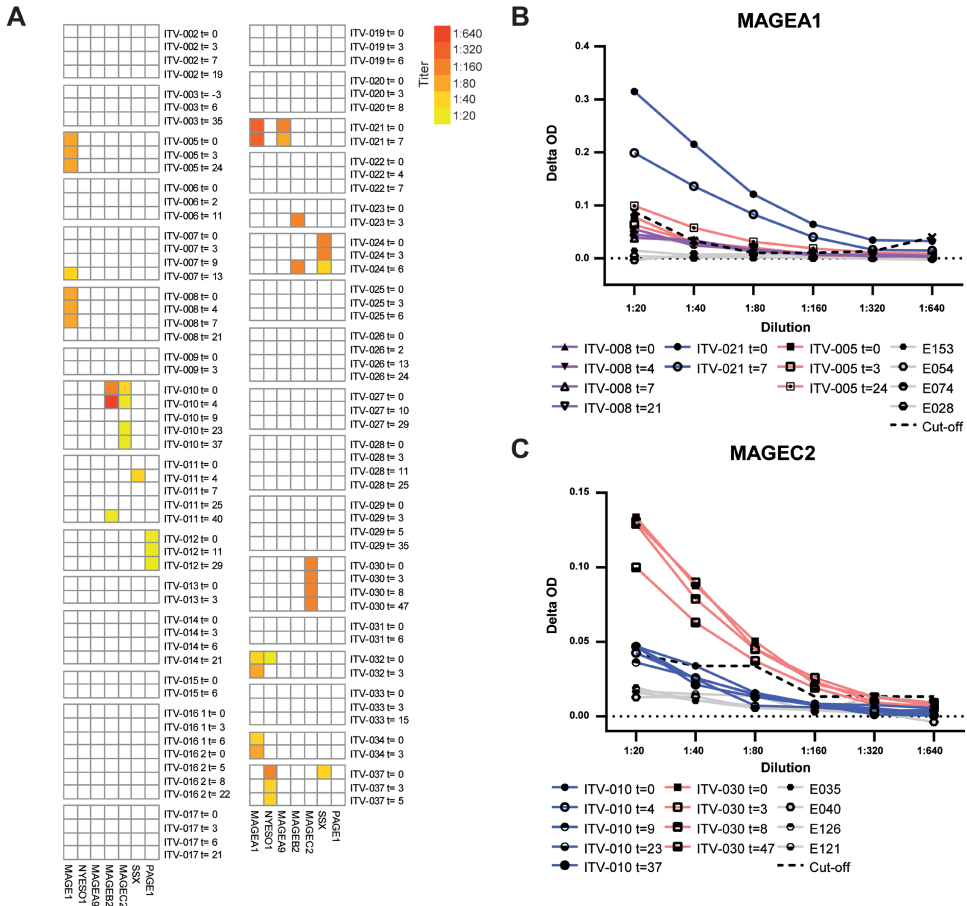


Figure 5. HCC-patients mount CTA-specific IgG responses.

CTA-specific IgG responses were measured in 32 HCC patients by indirect ELISA. ELISA plates were coated with human recombinant full length CTA protein, and after incubation with HCC patients' plasma, CTA-specific IgG was detected by anti-human IgG-HRP. After screening of 1:20 plasma dilutions, the positive samples were titrated. **A**. Heat map displaying the CTA-specific IgG responses in individual before and at different time points (weeks) after local tumor ablation. Columns show IgG titers against the 7 different CTAs. Colors indicate the detected titers (legend). **B, C**. Examples of serial dilutions of plasma samples of 3 HCC-patients in MAGEA1 ELISA (**B**) and of 2 patients in MAGEC2 ELISA (**C**). The delta optical density (Δ OD) of each plasma sample was calculated by subtracting the sample's OD in wells coated with BSA from the OD in wells coated with the specific CTA protein. In each ELISA, plasma samples of 4 healthy individuals (indicated by E numbers) were included as negative controls to determine the cut-off OD-value that was used to determine positivity of patient samples. The dotted line indicates the cut-off for each dilution, which was determined by the average plus 10 times the standard deviation of the OD-values of 4 healthy control samples.

or more CTAs in 40% of HCC patients and establish the presence of CD4⁺ and CD8⁺ T-cells which mount proliferative responses against one or more CTAs in the circulation of most HCC patients. In addition, we found higher frequencies of circulating CTA peptide-specific CD8⁺ T-cells in HCC patients compared to healthy subjects. Moreover, we demonstrate that HLA class I epitopes derived from five of the CTAs induce cytokine and granzyme B production in PBMC, indicating that CTA-specific T-cells, most likely CD8⁺, in HCC patients are functionally competent.

Whereas MAGEA1-, MAGEC1, MAGEC2-, and SSX2-specific CD8⁺ T-cells have been detected in HCC patients in previous studies,^{23, 29, 37, 40-43} the current study is the first to demonstrate MAGEA9, MAGEB2, and PAGE1-specific CD8⁺ T-cell responses in HCC patients. Using CTA peptide-loaded HLA class I multimers, we observed that already prior to ablative therapy more than 50% of CTA-specific CD8⁺ T-cells displayed a phenotype that suggested they were antigen experienced. It should be noted that for these multimer experiments CTA peptides were pooled with a peptide from NY-ESO and hence part of the responses may have been directed against this CTA that was not focus of our study. Staining for single multimers, however, indicated T cells against the other CTA contributed as well. We did not find clear signs of recent activation, chronic activation or exhaustion on CTA peptide-specific CD8⁺ T-cells. The observed proliferative CD8⁺ T-cell responses against the CTAs together with the observed cytokine and granzyme B production upon stimulation of PBMC with HLA class I CTA epitopes, indicate that CTA-specific CD8⁺ T-cells in HCC patients are functionally competent. Although viral epitopes, due to their foreign nature,⁴⁴ are considered to be more immunogenic than CTA epitopes, the strength of cytokine and granzyme B production upon stimulation of PBMC with either HBV or CTA peptides was comparable. Moreover, the maximum proliferative CD8⁺ T-cell responses against all CTAs tested were stronger than those against the well-known immunogenic HCC-associated antigen GPC3.^{16, 39} Together, these data may suggest that tumor-restricted CTAs are sufficiently immunogenic to stimulate functional CD8⁺ T-cell responses in HCC patients. This is in accordance with recent data generated by us and others that show abundant presence of peptides derived from CTA such as MAGEA1, MAGEB2 and MAGEC2 in HLA class I restricted epitopes of HCC tumors.⁴⁵

CD4⁺ T-cells are needed for optimal expansion of CD8⁺ T-cells and for CD8⁺ T-cell memory and are therefore indispensable for adequate and sustained anti-tumor immunity.⁴⁶ Recently also the direct anti-tumor potency of CD4⁺ T-cells was demonstrated, as well as their role in directing a sustained anti-tumor response.⁴⁷ Nevertheless, CD4⁺ T-cell responses against CTAs have been rarely studied in HCC. To our knowledge, we are the first to demonstrate CD4⁺ T-cell responses against MAGEA1-, MAGEA9, MAGEB2, MAGEC1, MAGEC2-, PAGE1, and SSX2 in HCC patients, while confirming the presence of MAGEC2- specific CD4⁺ T-cells in HCC.^{29, 48} Similar to CD8⁺ T-cell responses, the maximum proliferative CD4⁺ T-cell responses against CTAs were stronger than those against GPC3.

In contrast to T-cell immunogenicity, the role of tumor-specific antibodies in anti-tumor immunity is not yet clear and a frequently debated topic. However, antibody presence is at least an additional indication for antigen immunogenicity, and could be a sign of the presence of CD4⁺ T helper cells

recognizing the antigen.⁴⁷ Moreover, tumor-specific antibodies can form immune complexes with TAAs and thereby facilitate cross-presentation by dendritic cells.⁴⁹ Even antibodies against intracellular TAAs may contribute via this mechanism to anti-tumor immunity upon release of the TAA from tumor cells.⁵⁰ Importantly, several studies demonstrated positive associations between humoral responses against TAAs and therapeutic outcome after ICPI therapy or vaccination with TAA-containing cancer vaccines.⁵¹⁻⁵³ We detected IgG responses against every tested CTA in our cohort of 32 HCC patients. However, the prevalence of IgG responses against most individual CTAs was rather low. For instance, serum IgG against the established immunogenic tumor antigen NY-ESO-1 was detected in only 2 patients, but this is in line with its low prevalence in HCC.^{48, 54, 55} The most frequently detected humoral response was directed against MAGEA1 (in 6 patients). Antibodies against these CTAs have been detected in other types of cancers,^{36, 56-60} but in HCC patients humoral responses against these CTAs, excluding anti-NY-ESO-1, have not been previously assessed. The titers of CTA-specific IgGs were comparable to previously reported anti-NY-ESO-1 IgG titers in HCC patients^{48, 54, 55} and IgG titers against other CTAs in patients with other types of cancer.⁵⁸ The presence of both IgG- and T-cell responses provides further evidence for their immunogenicity of studied CTA in HCC patients.

Whereas previous studies have reported transient increases in systemic T-cell responses against TAAs between 2 to 4 weeks after local tumor ablation in HCC patients,^{26, 27, 37} we did not find any increase in CTA-specific T-cell responses at 3 weeks or later time points after RFA and/or TACE. This discrepancy may be caused by several factors. Most importantly, we analyzed T-cell responses against tumor-restricted CTAs, whereas Zerbini et al²⁶ studied T-cell responses against autologous tumor lysate and Mizukoshi et al^{27, 37} quantified T-cell responses against a panel of TAAs which are also expressed, although at lower levels, in healthy tissues.⁶¹⁻⁶⁴ Furthermore, the patient cohorts differ quite significantly, as only a few patients in our cohort had HCC caused by chronic viral hepatitis, whereas this was the major etiology in these previous studies. Finally, whereas TAA-specific T-cells were detected by IFN- γ ELISPOT assays in the previous studies, we used three other techniques. A recent study reported transiently enhanced T-cell responses against MAGEA1, MAGEC1 and a few other tumor-restricted CTAs, at 1 week after microwave ablation in 30% of HCC patients.⁴³ Because the earliest time point at which we analyzed T-cell responses was at 3 weeks after local tumor ablation, we might have missed such early T-cell responses. Changes in circulating T-cell and NK cell subsets after tumor ablation in HCC patients were recently shown to be detectable only at 1 day after RFA,⁶⁵ which explains that we did not observe such effects.

The present study provides a comprehensive overview of systemic adaptive immune responses against tumor-restricted CTAs in HCC published to date. Despite demonstrating CD4⁺, CD8⁺ and IgG responses against a large set of CTAs in HCC patients for the first time, we acknowledge that our study has some limitations. Not all included patients were treatment naïve before inclusion in the study, and therefore it is unclear whether the detected CTA-specific immune responses can be considered spontaneous. Second, due to unavailability of reagents such as *in vitro* transcribed mRNA for several CTAs, we could not study the immunogenicity of 6 additional tumor-restricted CTAs we previously described in HCC. Importantly,

we were able to include the most prevalent CTAs in HCC; MAGEA1 (found in 59% of patients), MAGEC1 (48%), and MAGEC2 (56%)²². Third, due to limitations in numbers of PBMC, we could not apply all three techniques for analysis of T-cell responses in all individual patients. This, combined with the usage of different techniques, makes direct comparison of the different results difficult, yet we observed that overall, some patients displayed broader responses than others. Fourth, due to unavailability of tumor biopsies, we could not analyze whether presence and/or intensity of CTA-specific immune responses in individual patients was related to CTA expression in the tumors and could not correlate CTA expression to outcome after local ablative therapies. Last but not least, to establish the therapeutic potential of each of these TAAs, further (pre-)clinical studies are needed.

In conclusion, the presence of CD4⁺ and CD8⁺ T-cell and IgG responses against seven tumor-restricted CTAs shows the immunogenicity of these CTAs in HCC-patients. Further research should elucidate whether vaccines based on these tumor-specific antigens can boost pre-existing CTA-specific immunity sufficiently to combat small malignant foci remaining after primary tumor resection in early HCC and/ or to enhance therapeutic efficacy of ICPI blockade in advanced HCC.

ACKNOWLEDGEMENTS

We would like to thank Dr. Hanneke van Vuuren (Department of Gastroenterology and Hepatology, Erasmus MC, for providing us with frozen plasma samples of healthy blood bank donors. Finally we would like to thank Prof. Dr. Stefan Eichmüller from the department of GMP & T-cell therapy of the Deutsches Krebsforschungszentrum (DKFZ), Heidelberg, Germany, for providing us with positive control sera for the CTA-specific IgG ELISAs.

REFERENCES

1. Bray F, Ferlay J, Soerjomataram I, et al. Global cancer statistics 2018: GLOBOCAN estimates of incidence and mortality worldwide for 36 cancers in 185 countries. *CA Cancer J Clin*. 2018.
2. Llovet JM, Kelley RK, Villanueva A, et al. Hepatocellular carcinoma. *Nat Rev Dis Primers*. 2021;7(1):6.
3. Brown ZJ, Greten TF, Heinrich B. Adjuvant Treatment of Hepatocellular Carcinoma: Prospect of Immunotherapy. *Hepatology*. 2019;70(4):1437-42.
4. Forner A, Reig M, Bruix J. Hepatocellular carcinoma. *Lancet*. 2018;391(10127):1301-14.
5. Finn RS, Qin S, Ikeda M, et al. Atezolizumab plus Bevacizumab in Unresectable Hepatocellular Carcinoma. *N Engl J Med*. 2020;382(20):1894-905.
6. Trujillo JA, Sweis RF, Bao R, et al. T Cell-Inflamed versus Non-T Cell-Inflamed Tumors: A Conceptual Framework for Cancer Immunotherapy Drug Development and Combination Therapy Selection. *Cancer Immunol Res*. 2018;6(9):990-1000.
7. Galon J, Bruni D. Approaches to treat immune hot, altered and cold tumours with combination immunotherapies. *Nat Rev Drug Discov*. 2019;18(3):197-218.
8. Sangro B, Melero I, Wadhawan S, et al. Association of inflammatory biomarkers with clinical outcomes in nivolumab-treated patients with advanced hepatocellular carcinoma. *J Hepatol*. 2020;73(6):1460-9.
9. Voorwerk L, Slagter M, Horlings HM, et al. Immune induction strategies in metastatic triple-negative breast cancer to enhance the sensitivity to PD-1 blockade: the TONIC trial. *Nat Med*. 2019;25(6):920-8.
10. Massarelli E, William W, Johnson F, et al. Combining Immune Checkpoint Blockade and Tumor-Specific Vaccine for Patients With Incurable Human Papillomavirus 16-Related Cancer: A Phase 2 Clinical Trial. *JAMA Oncol*. 2019;5(1):67-73.
11. Sahin U, Oehm P, Derhovanessian E, et al. An RNA vaccine drives immunity in checkpoint-inhibitor-treated melanoma. *Nature*. 2020;585(7823):107-12.
12. De Keersmaecker B, Claerhout S, Carrasco J, et al. TriMix and tumor antigen mRNA electroporated dendritic cell vaccination plus ipilimumab: link between T-cell activation and clinical responses in advanced melanoma. *J Immunother Cancer*. 2020;8(1).
13. Sahin U, Derhovanessian E, Miller M, et al. Personalized RNA mutanome vaccines mobilize poly-specific therapeutic immunity against cancer. *Nature*. 2017;547(7662):222-6.
14. Ott PA, Hu Z, Keskin DB, et al. An immunogenic personal neoantigen vaccine for patients with melanoma. *Nature*. 2017;547(7662):217-21.
15. Sawada Y, Yoshikawa T, Nobuoka D, et al. Phase I trial of a glypican-3-derived peptide vaccine for advanced hepatocellular carcinoma: immunologic evidence and potential for improving overall survival. *Clin Cancer Res*. 2012;18(13):3686-96.
16. Tsuchiya N, Yoshikawa T, Fujinami N, et al. Immunological efficacy of glypican-3 peptide vaccine in patients with advanced hepatocellular carcinoma. *Oncoimmunology*. 2017;6(10):e1346764.
17. Charneau J, Suzuki T, Shimomura M, et al. Peptide-Based Vaccines for Hepatocellular Carcinoma: A Review of Recent Advances. *J Hepatocell Carcinoma*. 2021;8:1035-54.
18. de Beijer MTA, Bezstarosti K, Luijten R, et al. Immuno-peptidome of hepatocytes isolated from patients with HBV infection and hepatocellular carcinoma. *JHEP Reports*. 2022:100576.
19. Loffler MW, Gori S, Izzo F, et al. Phase I/II Multicenter Trial of a Novel Therapeutic Cancer Vaccine, HepaVac-101, for Hepatocellular Carcinoma. *Clin Cancer Res*. 2022;28(12):2555-66.
20. Hofmann O, Caballero OL, Stevenson BJ, et al. Genome-wide analysis of cancer/testis gene expression. *Proc Natl Acad Sci U S A*. 2008;105(51):20422-7.
21. Saxena M, van der Burg SH, Melief CJM, et al. Therapeutic cancer vaccines. *Nat Rev Cancer*. 2021;21(6):360-78.

22. Noordam L, Ge Z, Ozturk H, et al. Expression of Cancer Testis Antigens in Tumor-Adjacent Normal Liver Is Associated with Post-Resection Recurrence of Hepatocellular Carcinoma. *Cancers (Basel)*. 2021;13(10).
23. Bricard G, Bouzourene H, Martinet O, et al. Naturally acquired MAGE-A10- and SSX-2-specific CD8+ T cell responses in patients with hepatocellular carcinoma. *J Immunol*. 2005;174(3):1709-16.
24. Smith HA, McNeel DG. The SSX family of cancer-testis antigens as target proteins for tumor therapy. *Clin Dev Immunol*. 2010;2010:150591.
25. Wang C, Gu Y, Zhang K, et al. Systematic identification of genes with a cancer-testis expression pattern in 19 cancer types. *Nat Commun*. 2016;7:10499.
26. Zerbini A, Pilli M, Penna A, et al. Radiofrequency thermal ablation of hepatocellular carcinoma liver nodules can activate and enhance tumor-specific T-cell responses. *Cancer Res*. 2006;66(2):1139-46.
27. Mizukoshi E, Yamashita T, Arai K, et al. Enhancement of tumor-associated antigen-specific T cell responses by radiofrequency ablation of hepatocellular carcinoma. *Hepatology*. 2013;57(4):1448-57.
28. Tang A, Bashir MR, Corwin MT, et al. Evidence Supporting LI-RADS Major Features for CT- and MR Imaging-based Diagnosis of Hepatocellular Carcinoma: A Systematic Review. *Radiology*. 2018;286(1):29-48.
29. Zhou G, Sprengers D, Boor PPC, et al. Antibodies Against Immune Checkpoint Molecules Restore Functions of Tumor-Infiltrating T Cells in Hepatocellular Carcinomas. *Gastroenterology*. 2017;153(4):1107-19 e10.
30. Anderson LD, Jr., Cook DR, Yamamoto TN, et al. Identification of MAGE-C1 (CT-7) epitopes for T-cell therapy of multiple myeloma. *Cancer Immunol Immunother*. 2011;60(7):985-97.
31. Kreiter S, Selmi A, Diken M, et al. Increased antigen presentation efficiency by coupling antigens to MHC class I trafficking signals. *J Immunol*. 2008;180(1):309-18.
32. van Beek AA, Zhou G, Doukas M, et al. G1TR ligation enhances functionality of tumor-infiltrating T cells in hepatocellular carcinoma. *Int J Cancer*. 2019;145(4):1111-24.
33. Dolton G, Zervoudi E, Rius C, et al. Optimized Peptide-MHC Multimer Protocols for Detection and Isolation of Autoimmune T-Cells. *Front Immunol*. 2018;9:1378.
34. de Beijer MTA, Jansen D, Dou Y, et al. Discovery and Selection of Hepatitis B Virus-Derived T Cell Epitopes for Global Immunotherapy Based on Viral Indispensability, Conservation, and HLA-Binding Strength. *J Virol*. 2020;94(7).
35. Gnjatic S, Old LJ, Chen YT. Autoantibodies against cancer antigens. *Methods Mol Biol*. 2009;520:11-9.
36. Zornig I, Halama N, Lorenzo Bermejo J, et al. Prognostic significance of spontaneous antibody responses against tumor-associated antigens in malignant melanoma patients. *Int J Cancer*. 2015;136(1):138-51.
37. Mizukoshi E, Nakamoto Y, Arai K, et al. Comparative analysis of various tumor-associated antigen-specific t-cell responses in patients with hepatocellular carcinoma. *Hepatology*. 2011;53(4):1206-16.
38. Solana R, Tarazona R, Aiello AE, et al. CMV and Immunosenescence: from basics to clinics. *Immun Ageing*. 2012;9(1):23.
39. Wu Y, Liu H, Ding H. GPC-3 in hepatocellular carcinoma: current perspectives. *J Hepatocell Carcinoma*. 2016;3:63-7.
40. Flecken T, Schmidt N, Hild S, et al. Immunodominance and functional alterations of tumor-associated antigen-specific CD8+ T-cell responses in hepatocellular carcinoma. *Hepatology*. 2014;59(4):1415-26.
41. Gehring AJ, Ho ZZ, Tan AT, et al. Profile of tumor antigen-specific CD8 T cells in patients with hepatitis B virus-related hepatocellular carcinoma. *Gastroenterology*. 2009;137(2):682-90.
42. Tauber C, Schultheiss M, Luca R, et al. Inefficient induction of circulating TAA-specific CD8+ T-cell responses in hepatocellular carcinoma. *Oncotarget*. 2019;10(50):5194-206.

43. Leuchte K, Staib E, Thelen M, et al. Microwave ablation enhances tumor-specific immune response in patients with hepatocellular carcinoma. *Cancer Immunol Immunother.* 2021;70(4):893-907.
44. Calis JJ, Maybeno M, Greenbaum JA, et al. Properties of MHC class I presented peptides that enhance immunogenicity. *PLoS Comput Biol.* 2013;9(10):e1003266.
45. Dong LQ, Peng LH, Ma LJ, et al. Heterogeneous immunogenomic features and distinct escape mechanisms in multifocal hepatocellular carcinoma. *J Hepatol.* 2020;72(5):896-908.
46. Borst J, Ahrends T, Babala N, et al. CD4(+) T cell help in cancer immunology and immunotherapy. *Nat Rev Immunol.* 2018;18(10):635-47.
47. Tay RE, Richardson EK, Toh HC. Revisiting the role of CD4(+) T cells in cancer immunotherapy-new insights into old paradigms. *Cancer Gene Ther.* 2020.
48. Korangy F, Ormandy LA, Bleck JS, et al. Spontaneous tumor-specific humoral and cellular immune responses to NY-ESO-1 in hepatocellular carcinoma. *Clin Cancer Res.* 2004;10(13):4332-41.
49. Luetkens T, Kobold S, Cao Y, et al. Functional autoantibodies against SSX-2 and NY-ESO-1 in multiple myeloma patients after allogeneic stem cell transplantation. *Cancer Immunol Immunother.* 2014;63(11):1151-62.
50. Noguchi T, Kato T, Wang L, et al. Intracellular tumor-associated antigens represent effective targets for passive immunotherapy. *Cancer Res.* 2012;72(7):1672-82.
51. Yuan J, Adamow M, Ginsberg BA, et al. Integrated NY-ESO-1 antibody and CD8+ T-cell responses correlate with clinical benefit in advanced melanoma patients treated with ipilimumab. *Proc Natl Acad Sci U S A.* 2011;108(40):16723-8.
52. Takayama K, Sugawara S, Saijo Y, et al. Randomized Phase II Study of Docetaxel plus Personalized Peptide Vaccination versus Docetaxel plus Placebo for Patients with Previously Treated Advanced Wild Type EGFR Non-Small-Cell Lung Cancer. *J Immunol Res.* 2016;2016:1745108.
53. Somaiah N, Block MS, Kim JW, et al. First-in-Class, First-in-Human Study Evaluating LV305, a Dendritic-Cell Tropic Lentiviral Vector, in Sarcoma and Other Solid Tumors Expressing NY-ESO-1. *Clin Cancer Res.* 2019;25(19):5808-17.
54. Oshima Y, Shimada H, Yajima S, et al. NY-ESO-1 autoantibody as a tumor-specific biomarker for esophageal cancer: screening in 1969 patients with various cancers. *J Gastroenterol.* 2016;51(1):30-4.
55. Nakamura S, Nouse K, Noguchi Y, et al. Expression and immunogenicity of NY-ESO-1 in hepatocellular carcinoma. *J Gastroenterol Hepatol.* 2006;21(8):1281-5.
56. Michels J, Becker N, Suciú S, et al. Multiplex bead-based measurement of humoral immune responses against tumor-associated antigens in stage II melanoma patients of the EORTC18961 trial. *Oncoimmunology.* 2018;7(6):e1428157.
57. Djureinovic D, Dodig-Crnkovic T, Hellstrom C, et al. Detection of autoantibodies against cancer-testis antigens in non-small cell lung cancer. *Lung Cancer.* 2018;125:157-63.
58. Daudi S, Eng KH, Mhawech-Fauceglia P, et al. Expression and immune responses to MAGE antigens predict survival in epithelial ovarian cancer. *PLoS One.* 2014;9(8):e104099.
59. Stockert E, Jager E, Chen YT, et al. A survey of the humoral immune response of cancer patients to a panel of human tumor antigens. *J Exp Med.* 1998;187(8):1349-54.
60. Mizukami M, Hanagiri T, Baba T, et al. Identification of tumor associated antigens recognized by IgG from tumor-infiltrating B cells of lung cancer: correlation between Ab titer of the patient's sera and the clinical course. *Cancer Sci.* 2005;96(12):882-8.
61. Nakao M, Shichijo S, Imaizumi T, et al. Identification of a gene coding for a new squamous cell carcinoma antigen recognized by the CTL. *J Immunol.* 2000;164(5):2565-74.
62. Kuhlmann WD, Peschke P. Hepatic progenitor cells, stem cells, and AFP expression in models of liver injury. *Int J Exp Pathol.* 2006;87(5):343-59.

63. Chai J, He Y, Cai SY, et al. Elevated hepatic multidrug resistance-associated protein 3/ATP-binding cassette subfamily C 3 expression in human obstructive cholestasis is mediated through tumor necrosis factor alpha and c-Jun NH2-terminal kinase/stress-activated protein kinase-signaling pathway. *Hepatology*. 2012;55(5):1485-94.
64. Leao R, Apolonio JD, Lee D, et al. Mechanisms of human telomerase reverse transcriptase (hTERT) regulation: clinical impacts in cancer. *J Biomed Sci*. 2018;25(1):22.
65. Rochigneux P, Nault JC, Mallet F, et al. Dynamic of systemic immunity and its impact on tumor recurrence after radiofrequency ablation of hepatocellular carcinoma. *Oncoimmunology*. 2019;8(8):1615818.

Supplementary Table S1A. Overview of patients included in each experiment.

Patient	Phenotype		CTA-specific T cell responses		Humoral anti-CTA responses
	General Figure 2	CTA peptide-specific Figure 2	Proliferation Figure 3	Cytokine production Figure 4	Plasma IgG Figure 5
ITV-001					
ITV-002					
ITV-003					
ITV-004					
ITV-005					
ITV-006					
ITV-007					
ITV-008					
ITV-009					
ITV-010					
ITV-011					
ITV-012					
ITV-013					
ITV-014					
ITV-015					
ITV-016-1					
ITV-016-2					
ITV-017					
ITV-018					
ITV-019					
ITV-020					
ITV-021					
ITV-022					
ITV-023					
ITV-024					
ITV-025					
ITV-026					
ITV-027					
ITV-028					
ITV-029					
ITV-030					
ITV-031					
ITV-032					
ITV-033					
ITV-034					
ITV-035					
ITV-036					
ITV-037					
ITV-038					

Green: included. Black: not included. Patient ITV-016 was included twice due to rapid tumor progression and re-RFA treatment.

Supplementary Table S1B.

Overview of CTA-specific responses in patients that have been included in CTA-specific assays. Responses above the assay-specific threshold (methods and figure legends) are indicated in red, response below the assay-specific threshold are indicated in green. Conditions that were not tested are indicated in grey.

ITV-	MAGEA1	MAGEA9	MAGEB2	MAGEC1	MAGEC2	SSX2	NYESO1	PAGE1	GPC3	
002										Proliferation CD4+ (Fig 3B)
										Proliferation CD8+ (Fig 3B)
003										Cytokine production (Fig 4B)
										Plasma IgG (Fig 5A)
005										Proliferation CD4+ (Fig 3B)
										Proliferation CD8+ (Fig 3B)
006										Cytokine production (Fig 4B)
										Plasma IgG (Fig 5A)
007										Proliferation CD4+ (Fig 3B)
										Proliferation CD8+ (Fig 3B)
008										Cytokine production (Fig 4B)
										Plasma IgG (Fig 5A)
009										Proliferation CD4+ (Fig 3B)
										Proliferation CD8+ (Fig 3B)
010										Cytokine production (Fig 4B)
										Plasma IgG (Fig 5A)
011										Proliferation CD4+ (Fig 3B)
										Proliferation CD8+ (Fig 3B)
										Cytokine production (Fig 4B)
										Plasma IgG (Fig 5A)

Supplementary Table S1B. (continued)

ITV-	MAGEA1	MAGEA9	MAGEB2	MAGEC1	MAGEC2	SSX2	NYESO1	PAGE1	GPC3	
012	-	+	-	-	+	-		-	+	Proliferation CD4+ (Fig 3B)
	-	-	-	-	-	-		-	-	Proliferation CD8+ (Fig 3B)
	+	+	+	+		+			-	Cytokine production (Fig 4B)
	-	-	-		-	-		+		Plasma IgG (Fig 5A)
013										Proliferation CD4+ (Fig 3B)
										Proliferation CD8+ (Fig 3B)
										Cytokine production (Fig 4B)
	-	-	-		-	-		-	-	Plasma IgG (Fig 5A)
014	-	+	+	+	+	-		+	-	Proliferation CD4+ (Fig 3B)
	-	+	-	+	-	-		+	-	Proliferation CD8+ (Fig 3B)
										Cytokine production (Fig 4B)
	-	-	-		-	-		-	-	Plasma IgG (Fig 5A)
015										Proliferation CD4+ (Fig 3B)
										Proliferation CD8+ (Fig 3B)
										Cytokine production (Fig 4B)
	-	-	-		-	-		-	-	Plasma IgG (Fig 5A)
016 (1)	+	-	-	-	-	-		-	-	Proliferation CD4+ (Fig 3B)
	-	-	-	+	-	-		-	-	Proliferation CD8+ (Fig 3B)
										Cytokine production (Fig 4B)
	-	-	-		-	-		-	-	Plasma IgG (Fig 5A)
016 (2)	-	-	+	-	+	+		+	-	Proliferation CD4+ (Fig 3B)
	-	-	-	+	-	-		-	-	Proliferation CD8+ (Fig 3B)
										Cytokine production (Fig 4B)
	-	-	-		-	-		-	-	Plasma IgG (Fig 5A)
017	-	-	-	-	+	-		-	-	Proliferation CD4+ (Fig 3B)
	-	-	-	-	-	-		-	-	Proliferation CD8+ (Fig 3B)
										Cytokine production (Fig 4B)
	-	-	-		-	-		-	-	Plasma IgG (Fig 5A)
019										Proliferation CD4+ (Fig 3B)
										Proliferation CD8+ (Fig 3B)
										Cytokine production (Fig 4B)
	-	-	-		-	-		-	-	Plasma IgG (Fig 5A)
020	+	-	+	-	-	-		+		Proliferation CD4+ (Fig 3B)
	-	-	+	-	+	+		+		Proliferation CD8+ (Fig 3B)
	+	+	+	+		-			-	Cytokine production (Fig 4B)
	-	-	-		-	-		-	-	Plasma IgG (Fig 5A)

Supplementary Table S1B. (continued)

ITV-	MAGEA1	MAGEA9	MAGEB2	MAGEC1	MAGEC2	SSX2	NYESO1	PAGE1	GPC3	
021										Proliferation CD4+ (Fig 3B)
										Proliferation CD8+ (Fig 3B)
	+								-	Cytokine production (Fig 4B)
	+	+	-		-	-	-	-	-	Plasma IgG (Fig 5A)
022	-	+	-	-	-	+		-	+	Proliferation CD4+ (Fig 3B)
	+	+	-	-	+	-		+	-	Proliferation CD8+ (Fig 3B)
										Cytokine production (Fig 4B)
	-	-	-		-	-	-	-	-	Plasma IgG (Fig 5A)
023	+	+	-	+	+	+		-		Proliferation CD4+ (Fig 3B)
	+	+	-	+	+	+		-		Proliferation CD8+ (Fig 3B)
										Cytokine production (Fig 4B)
	-	-	+		-	-	-	-	-	Plasma IgG (Fig 5A)
024	-	-	+	+	-	-		+	+	Proliferation CD4+ (Fig 3B)
	-	-	+	+	-	+		+	+	Proliferation CD8+ (Fig 3B)
										Cytokine production (Fig 4B)
	-	-	+		-	+	-	-	-	Plasma IgG (Fig 5A)
025	+	+	+	-	+	+		+	-	Proliferation CD4+ (Fig 3B)
	-	+	-	-	-	-		-	+	Proliferation CD8+ (Fig 3B)
										Cytokine production (Fig 4B)
	-	-	-		-	-	-	-	-	Plasma IgG (Fig 5A)
026										Proliferation CD4+ (Fig 3B)
										Proliferation CD8+ (Fig 3B)
										Cytokine production (Fig 4B)
	-	-	-		-	-	-	-	-	Plasma IgG (Fig 5A)
027	-	+	+	+	-	+		-	+	Proliferation CD4+ (Fig 3B)
	-	+	+	-	-	-		+	+	Proliferation CD8+ (Fig 3B)
										Cytokine production (Fig 4B)
	-	-	-		-	-	-	-	-	Plasma IgG (Fig 5A)
028										Proliferation CD4+ (Fig 3B)
										Proliferation CD8+ (Fig 3B)
										Cytokine production (Fig 4B)
	-	-	-		-	-	-	-	-	Plasma IgG (Fig 5A)
029	+	-	-	-	+	-		+	-	Proliferation CD4+ (Fig 3B)
	+	-	-	-	-	-		+	-	Proliferation CD8+ (Fig 3B)
										Cytokine production (Fig 4B)
	-	-	-		-	-	-	-	-	Plasma IgG (Fig 5A)

Supplementary Table S1B. (continued)

ITV-	MAGEA1	MAGEA9	MAGEB2	MAGEC1	MAGEC2	SSX2	NYESO1	PAGE1	GPC3	
030	-	+	+	+	-	-		+		Proliferation CD4+ (Fig 3B)
	-	+	-	+	+	+		+		Proliferation CD8+ (Fig 3B)
	+	+	+	+		+			+	Cytokine production (Fig 4B)
	-	-	-		+	-	-	-		Plasma IgG (Fig 5A)
031	-	-	-	-	-	-		-		Proliferation CD4+ (Fig 3B)
	-	-	-	-	-	-		-		Proliferation CD8+ (Fig 3B)
										Cytokine production (Fig 4B)
	-	-	-		-	-	-	-		Plasma IgG (Fig 5A)
032										Proliferation CD4+ (Fig 3B)
										Proliferation CD8+ (Fig 3B)
										Cytokine production (Fig 4B)
	+	-	-		-	-	+	-		Plasma IgG (Fig 5A)
033										Proliferation CD4+ (Fig 3B)
										Proliferation CD8+ (Fig 3B)
										Cytokine production (Fig 4B)
	-	-	-		-	-	-	-		Plasma IgG (Fig 5A)
034										Proliferation CD4+ (Fig 3B)
										Proliferation CD8+ (Fig 3B)
										Cytokine production (Fig 4B)
	+	-	-		-	-	-	-		Plasma IgG (Fig 5A)
037	+	-	-	-	-	+		-		Proliferation CD4+ (Fig 3B)
	+	-	-	-	-	-		-		Proliferation CD8+ (Fig 3B)
										Cytokine production (Fig 4B)
	-	-	-		-	+	+	-		Plasma IgG (Fig 5A)

Supplementary Table S2.

Antibodies used for flow cytometric analysis of PBMC, expanded B-cell blasts, and CTA-specific T cell assays

Specificity	Fluorochrome	Clone	Company
CCR7	FITC	150503	R&D Systems
CD137	BV750	4B4-1	Biolegend
CD14	PerCP-Cy5.5	61D3	eBioscience
CD154	APC	TRAP1	BD
CD16	BV650	3G8	Biolegend
CD19	PE	HIB19	eBioscience
CD3	PE-Cy7	UCHT1	eBioscience
CD3	APC-R700	UCHT1	BD
CD38	eFluor450	HIT2	eBioscience
CD4	APC-H7	RPA-T4	BD
CD45RA	BV570	HI100	Biolegend
CD56	PE	TULY56	eBioscience
CD56	PE-Dazzle594	HCD56	Biolegend
CD8	PerCP-Cy5.5	SK1	BD
CD80	FITC	MAB104	Beckman&Coulter
CD86	APC	IT2.2	Biolegend
CTLA4	BV786	BNI3	Biolegend
FoxP3	PE	236A/E7	eBioscience
GrB	BV421	GB11	BD
HLA-A2	AF488	BB7.2	Biorad
HLA-DR	APC-eFluor780	LN3	eBioscience
Ki67	BV711	B56	BD
LAG3	BV650	11C3C65	Biolegend
PD-1	PE-Cy7	J105	eBioscience
TIM3	BV421	F38-2E2	Biolegend
TIM3	BV786	F38-2E2	Biolegend
mIgG1	PE	P3.6.2.8.1	eBioscience
mIgG1	PE-Cy7	MOPC-21	Biolegend
mIgG1	APC	MOPC-21	Biolegend
mIgG1	BV421	X40	BD
mIgG1	PE-CF594	X40	BD
mIgG1	BV650	MOPC-21	Biolegend
mIgG1	BV711	MOPC-21	Biolegend
mIgG1	PE-CF594	MOPC-21	Biolegend
mIgG1	BV750	MOPC-21	Biolegend

Supplementary Table S3.

Peptides in HLA-A*02:01 dextramers with literature references for the selected peptides

Protein	Position	Epitope sequence	Fluorochrome	Literature
CMVpp65	495-503	NLVPMVATV	PE	Gamadia et al 2001 ¹
MAGEA1	278-286	KVLEYVIKV	APC	Ottaviani et al 2005 ²
MAGEA9	223-231	ALSVMGVYV	APC	Oehlrich et al 2005 ³
MAGEB2	231-240	GVYDGEEHSV	APC	Barnea et al 2002 ⁴
MAGEC1	1087-1095	FLAMLKNTV	APC	Tyler et al 2014 ⁵
MAGEC2	191-200	LLFGLALIEV	APC	Zhou et al 2017 ⁶
NYESO1	157-165	SLLMWITQV	APC	Chen et al 2000 ⁷
SSX2	41-49	KASEKIFYV	APC	Smith et al 2011 ⁸

Supplementary Table S4.

Peptides used for peptide stimulation assays. Immunogenic peptides were selected from the referred literature

Protein	Position	Sequence	Literature	IEDB entry	A*01	A*02	A*03	A*11	A*23	A*26	A*68	B*15	B*35	B*53	C*04	C*07
GPC3	144-152	FVGEFFTDV	Sawada, et al. ⁹ , Tsuchiya, et al. ¹⁰	735828	x											
GPC3	298-306	EYLSLEEL	Sawada, et al. ⁹ , Tsuchiya, et al. ¹⁰	735825				x*								
MAGEA1	96-104	SLFRAVITK	Chaux, et al. ¹¹	59101			x									
MAGEA1	161-169	EADPTGHYS	Celis, et al. ¹²	11010					x*							
MAGEA1	278-286	KVLEYIKV	Ottaviani, et al. ²	34095	x							x*		x*		
MAGEA1	289-298	RVREFFPSL	Luiten, et al. ¹³	179897												
MAGEA9	223-231	ALSVIMGYV	Oehlich, et al. ³	1075179	x											x*
MAGEA10	254-262	GLYDGMHL	Huang, et al. ¹⁴	189401	x											
MAGEB2	231-240	GYDGEHSH	Bamea, et al. ⁴	23214	x											
MAGEC1	1087-1095	FLMLKNTV	Tyler, et al. ⁵	N.A.	x											
SSX2	41-49	KASEKIFV	Smith, et al. ⁶	451342	x											
HBcAg	18-27	FLPSDFPSV	Bertoni, et al. ¹⁵	16833	x					x						
HBcAg	88-96	YVNVNMGK	Tan, et al. ¹⁶	76370				x								
HBcAg	139-148	ILSTLPETV	Lee, et al. ¹⁷	27365	x											
HBcAg	141-151	STLPETVRR	Depla, et al. ¹⁸	61745				x		x						
HBsAg	183-191	FLTRILTI	Depla, et al. ¹⁸	16755	x											
HBsAg	199-207	WTSLNFLGG	Desmond, et al. ¹⁹	N.A.				x								
HBsAg	313-321	IPIPSWAF	Bertoni, et al. ¹⁵	27878												
HBsAg	324-332	YLWEWASVR	Desmond, et al. ¹⁹	226809				x					x			
HBsAg	335-343	WLSLVPFV	Depla, et al. ¹⁸	72794						x						x
HBsAg	348-357	GLSPTVWLSV	van der Burg, et al. ²⁰	21139	x											
HBV Pol	47-55	NVISPWTHK	Depla, et al. ¹⁸	46480				x								
HBV Pol	149-159	HTLWKAGILYK	Bertoni, et al. ¹⁵	24943				x								
HBV Pol	354-363	TPARVTGGVF	Bertoni, et al. ¹⁵	65509												x
HBV Pol	377-386	LVVDFSQFSR	Depla, et al. ¹⁸	40624												
HBV Pol	442-450	GLSRVVARL	Depla, et al. ¹⁸	21145				x								

Protein	Position	Sequence	Literature	IEDB entry	A*01	A*02	A*03	A*11	A*23	A*26	A*68	B*15	B*35	B*53	C*04	C*07
HBV Pol	489-497	KLHLYSHPI	Gehring, et al. ²¹	31898		x										
HBV Pol	538-545	YMDDVVLG	Depla, et al. ¹⁶	N.A.							x					
HBV Pol	562-570	FLLSLGIHL	Depla, et al. ¹⁶	16751		x										
HBV Pol	612-620	PVNRPIDWK	Bertoni, et al. ¹⁵	49923			x	x								
HBV Pol	654-663	QAFTFSPTYK	Bertoni, et al. ¹⁵	50253			x	x								
HBxAg	52-60	HLSLRGLPV	Ding, et al. ²²	24302		x										
HBxAg	115-123	CLFKDWEEEL	Ding, et al. ²²	6556		x										
HBxAg	135-143	GGCRHKLVLC	Desmond, et al. ¹⁹	N.A.				x								

*Based on *in silico* prediction of HLA-binding properties (NetMHCpan3.0; rank \leq 2.0)

Supplementary table S5.

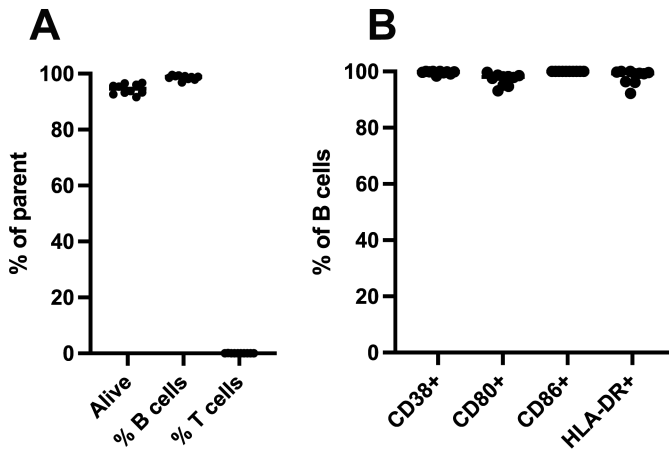
HLA-I types of HCC patients used for peptide stimulation assays

Patient	HLA-A		HLA-B		HLA-C	
ITV-006	68:02	03:01	35:01	53:01	04:01	04:01
ITV-007	26:01	11:01	39:01	15:02	07:02	08:01
ITV-008	02:01	03:01	07:02	44:02	05:01	07:02
ITV-010	02:01	01:01	44:02	08:01	07:04	07:01
ITV-012	02:01	02:01	57:01	40:02	02:02	06:02
ITV-020	02:01	11:01	55:01	07:02	07:02	03:03
ITV-021	23:01	26:01	08:01	15:03	02:10	03:04
ITV-030	02:01	32:01	44:02	56:01	01:02	05:01

Supplementary Table S6.

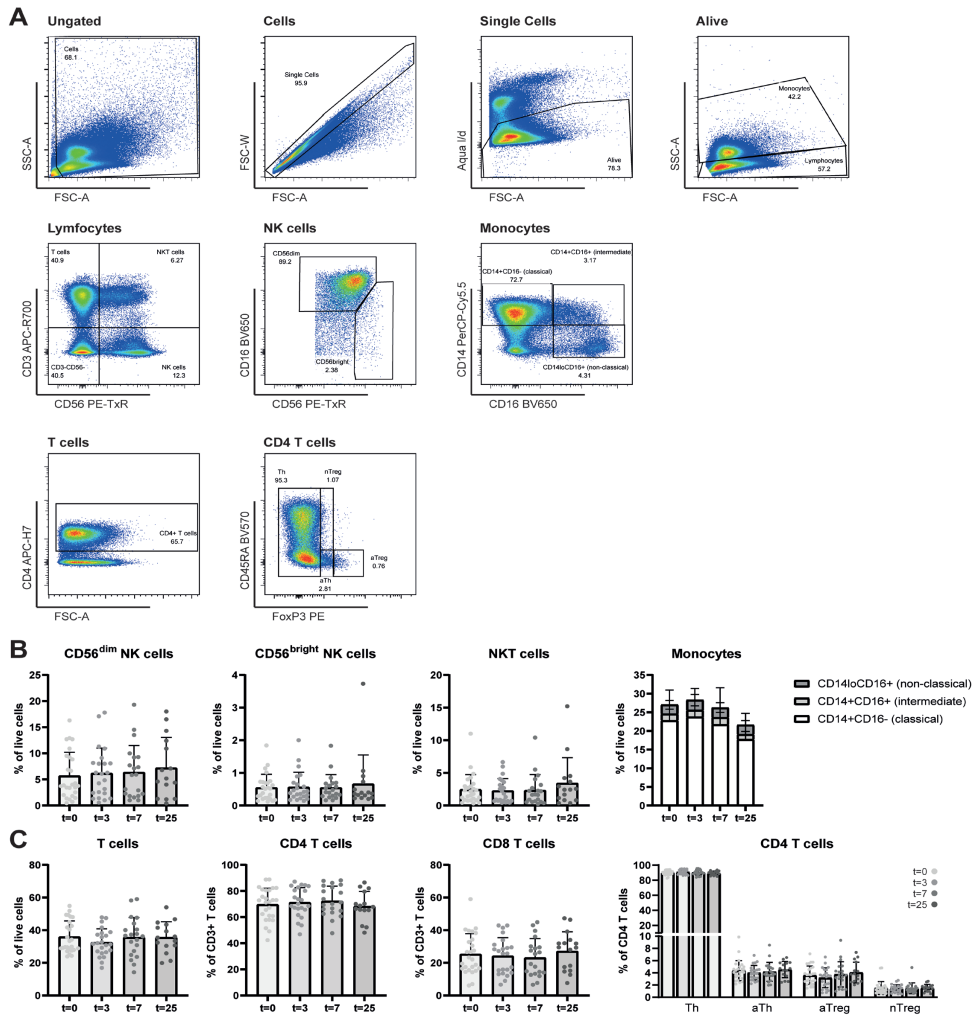
Recombinant full length CTA proteins used for ELISA.

CTA	Host	Company
MAGEA1	Wheat germ	Abnova
MAGEA9	Wheat germ	Abnova
MAGEB2	Wheat germ	Abnova
MAGEC2	Sf9	OriGene
NYESO1	HEK293T	OriGene
PAGE1	Wheat germ	Abnova
SSX2	HEK293T	OriGene



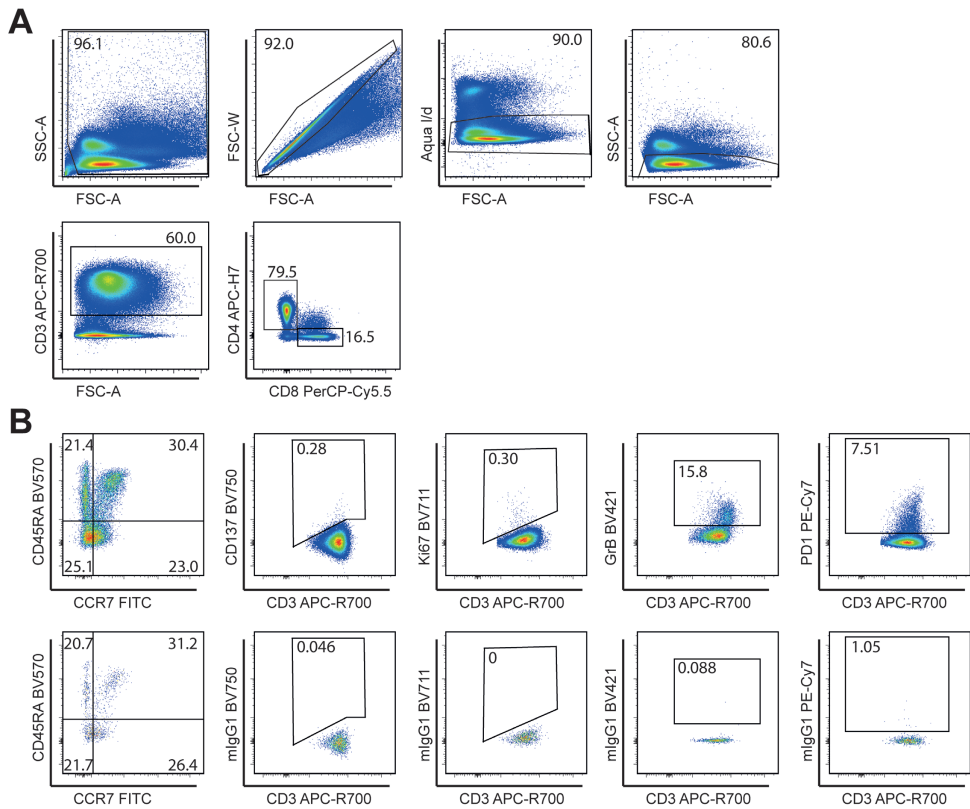
Supplementary Figure S1. Characteristics of expanded B cell blasts.

Expanded autologous B cell blasts were used as antigen-presenting cells in CTA-specific T-cell proliferation assays, n=16. **A.** Percentages of viable cells (percentage 7AAD⁻ of total measured cells) and percentages of CD19⁺ B cells and CD3⁺ T cells within expanded viable cells. **B.** Percentages of CD19⁺ B cells expressing CD38, CD80, CD86 or HLA-DR.



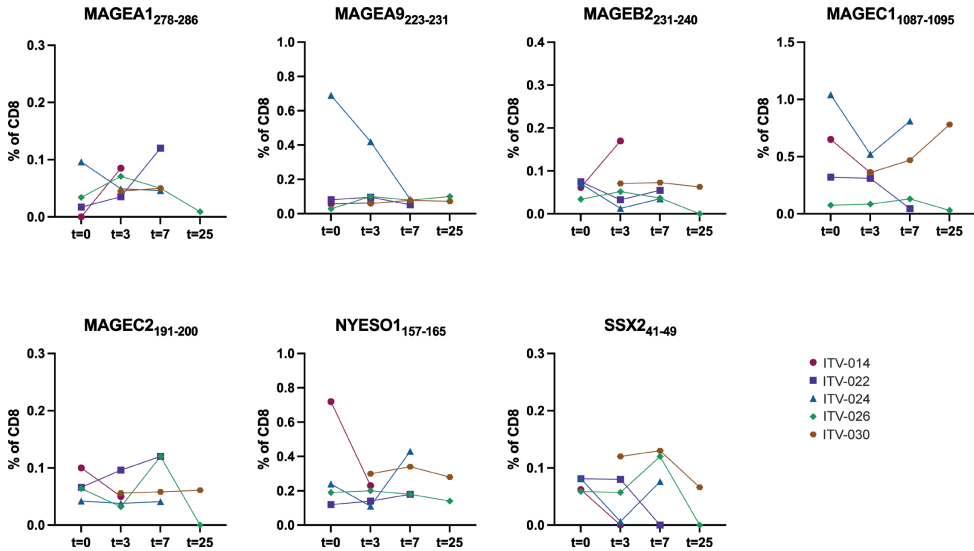
Supplementary Figure S3. Detection of peptide-loaded HLA-A*02:01 dextramer-binding CD8⁺ T cells.

A. Flow cytometric dot plots showing binding of a CMV-pp65 peptide-loaded HLA-A*02:01 dextramer (upper row) or a pool of HLA-A*02:01 dexamers loaded with 7 CTA-peptides (lower row) to CD4⁺ T cells and CD8⁺ T cells of HLA-A*02:01⁺ patient ITV-024. We were unable to collect blood 18 weeks after tumor ablation of this patient. To calculate specific binding to CD8⁺ T cells, percentages of dextramer-positive CD4⁺ T cells were subtracted from percentages of dextramer-positive CD8⁺ T cells. **B.** Percentages of CTA-dextramer binding (indicated in blue), CMV-dextramer binding (red) and CTA-dextramer non-binding cells (grey) expressing LAG3 or TIM3 before treatment and at various time points after local ablative therapy. Wilcoxon signed-rank test, * p<0.05, **p<0.01, ***p<0.001.



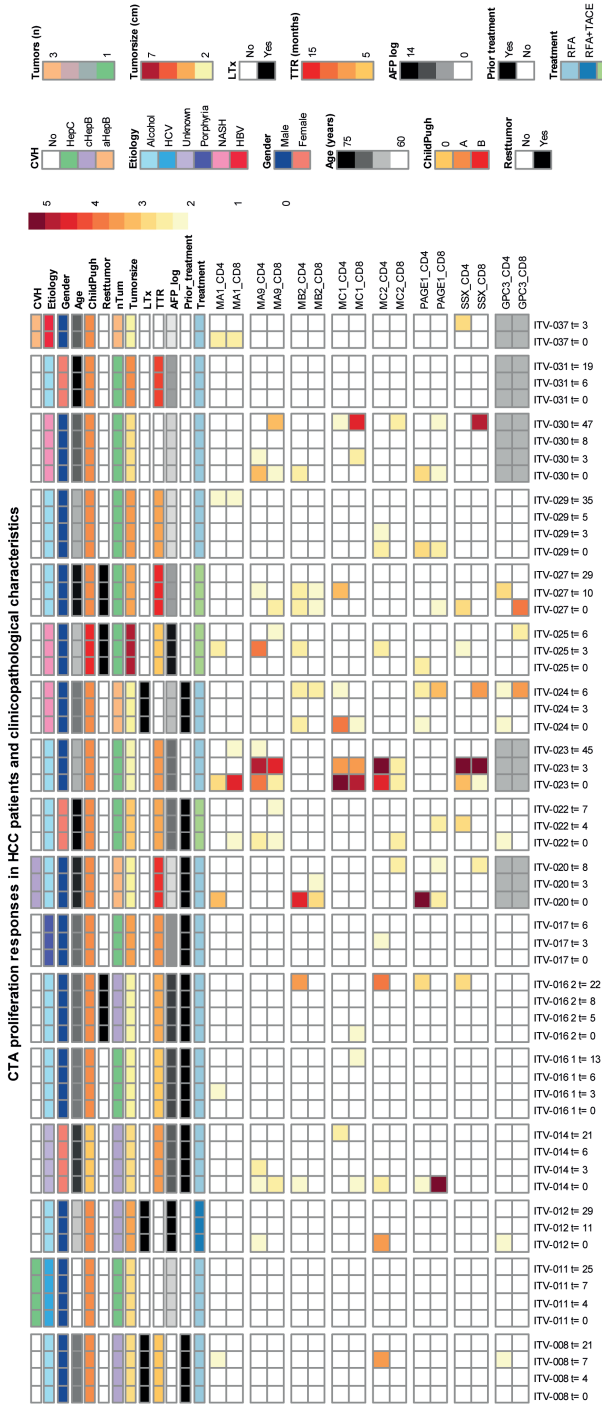
Supplementary Figure S4. Gating strategy of differentiation status and expression of various markers on CD8⁺ T cells.

A. Cell debris was excluded by gating on FSC-A and SSC-A, and single cells were selected based on FSC-W and FSC-A. The non-viable cells were excluded by use of Aqua I/d dye, and lymphocytes were selected by gating on FSC-A and SSC-A. T cells were selected based on CD3 expression, and CD4⁺ and CD8⁺ T cells were selected based on CD4 and CD8 expression. **B.** Within CD8⁺ T cells, naïve (CD45RA⁺CCR7⁺), central memory (CM; CD45RA⁺CCR7⁺), effector memory (EM; CD45RA⁺CCR7⁺) and EM that re-express CD45RA (TEMRA; CD45RA⁺CCR7⁺) were discriminated, as shown in the most left panels. In addition, expression of surface CD137 (4-1BB), intracellular Ki67, intracellular granzyme B and surface Programmed Cell Death Protein 1 (PD1; CD279) in CD8⁺ T cells was analyzed, as shown in the upper panels from left to right. The bottom panels show the isotype-matched antibody control stains.



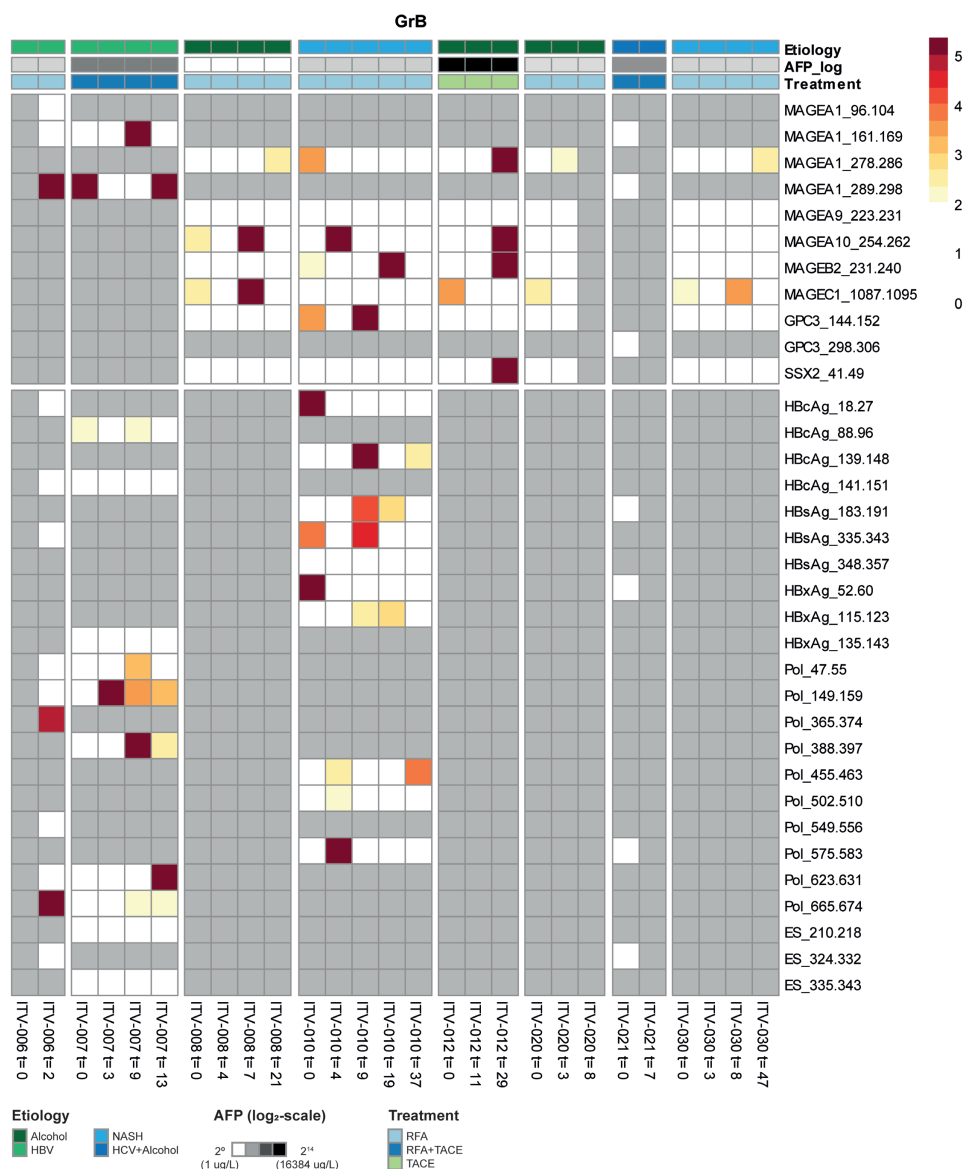
Supplementary Figure S5. Circulating CTA-specific CD8+ T cells.

PBMC from HCC patients before (t=0), and approximately 3, 7, and 25 weeks (see **Figure 1** for the exact time points) after RFA/TACE treatment were phenotyped by flow cytometry. Binding of individual CTA peptide-loaded HLA-A*02:01 dextramers to CD8⁺ T-cells was measured in 5 patients that had >0.5% CTA-dex-pool⁺ CD8⁺ T-cells at any time point (due to lack of samples not every time point was included in the analysis).



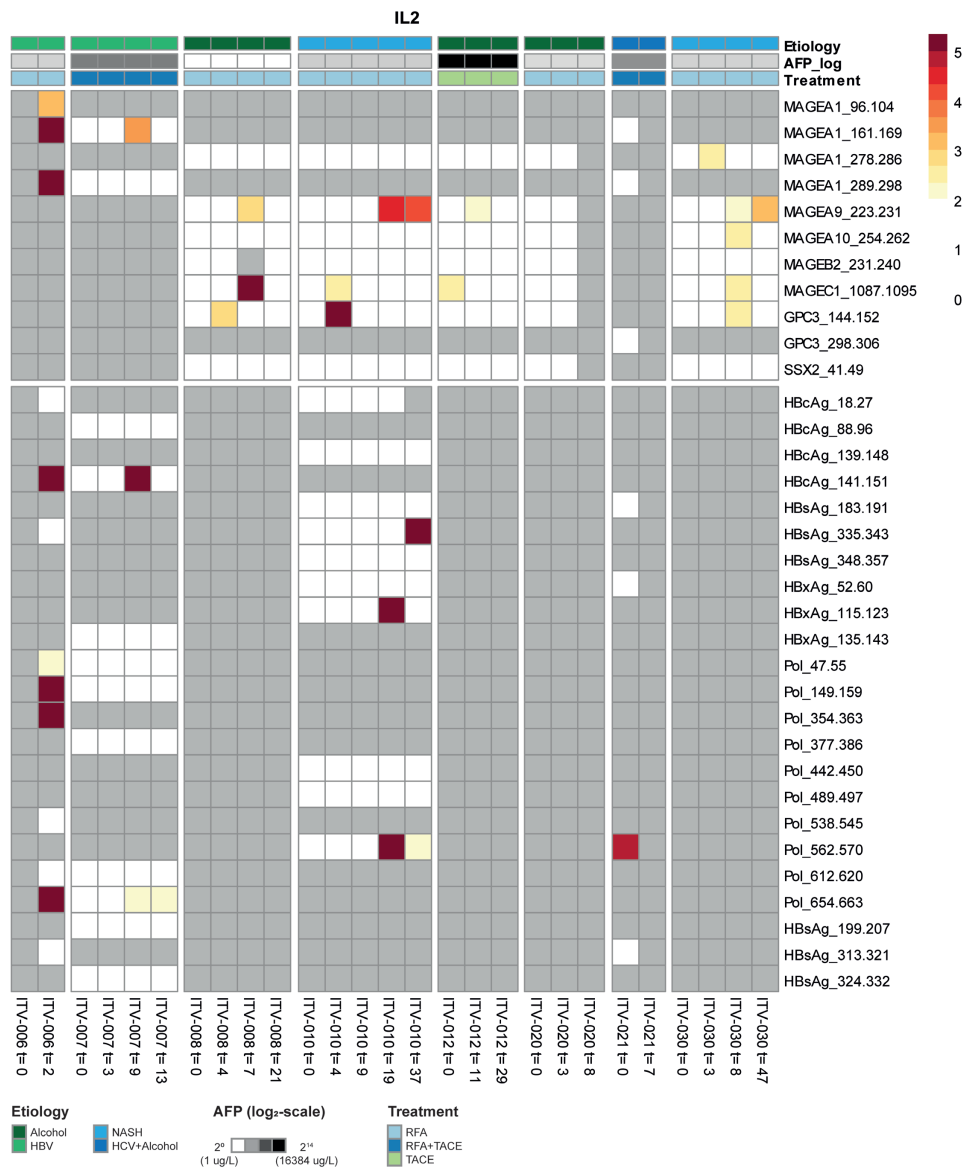
Supplementary Figure S6. CTA-specific stimulation induces proliferative responses in CD4⁺ and CD8⁺ T cells of HCC patients, stratified by clinicopathological parameters.

CTA-specific CD4⁺ and CD8⁺ T cell proliferation (as shown in **Figure 3**) with further specification of clinicopathological parameters. Annotation above the heat map indicates: CVH (chronic viral hepatitis) status; Hepatitis B status is subdivided into cleared (cHepB) and active (aHepB) infection; etiology; gender; age in years; Child Pugh score; presence of remaining tumor after ablation; the number of tumors; the size of the tumor (in case of multiple tumors, this indicates the size of the biggest tumor); liver transplantation post RFA; TTR (time to recurrence) in months; AFP levels; prior treatment; and the current treatment.



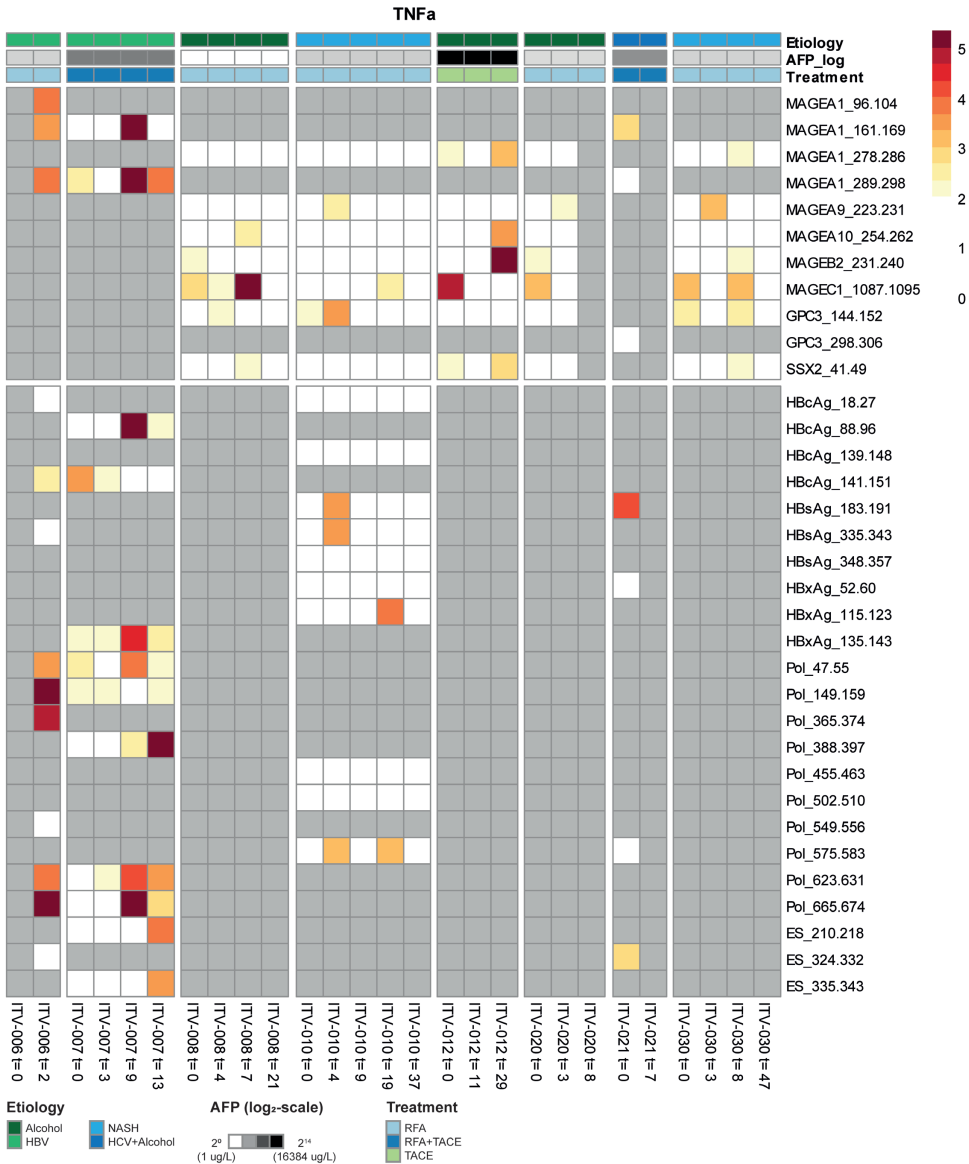
Supplementary Figure S7. CTA and HBV-specific peptide stimulation induces granzyme B production in PBMC of HCC patients.

Peptide-specific induction of granzyme B production was measured after re-stimulation of expanded PBMCs of 8 HCC patients prior to local ablative treatment (t=0) and at the indicated weeks after intervention. Heatmaps depict the fold changes for production of granzyme B in the peptide stimulated condition compared to the solvent-containing medium condition. Peptides with a ≥ 2 fold change were determined to have evoked a peptide-specific response and are depicted as such (color-coded legend). Annotation above the heat map indicates the etiology of HCC, AFP levels before treatment and the treatment (RFA or TACE) that patients received.



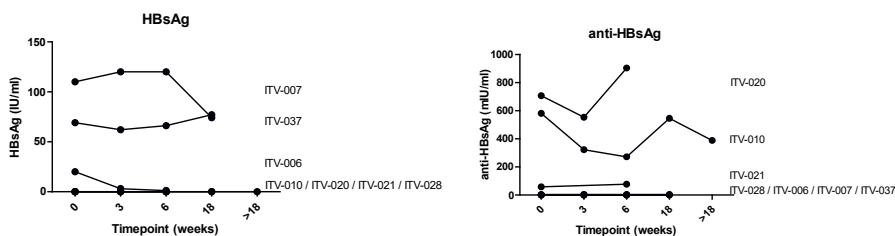
Supplementary Figure S8. CTA and HBV-specific peptide stimulation induces IL2 production in PBMC of HCC patients.

Peptide-specific induction of IL2 production was measured after re-stimulation of expanded PBMCs of 8 HCC patients prior to local ablative treatment (t=0) and at the indicated weeks after intervention. Heatmaps depict the fold changes for production of IL2 in the peptide stimulated condition compared to the solvent-containing medium condition. Peptides with a ≥ 2 fold change were determined to have evoked a peptide-specific response and are depicted as such (color-coded legend). Annotation above the heat map indicates the etiology of HCC, AFP levels before treatment and the treatment (RFA or TACE) that patients received.



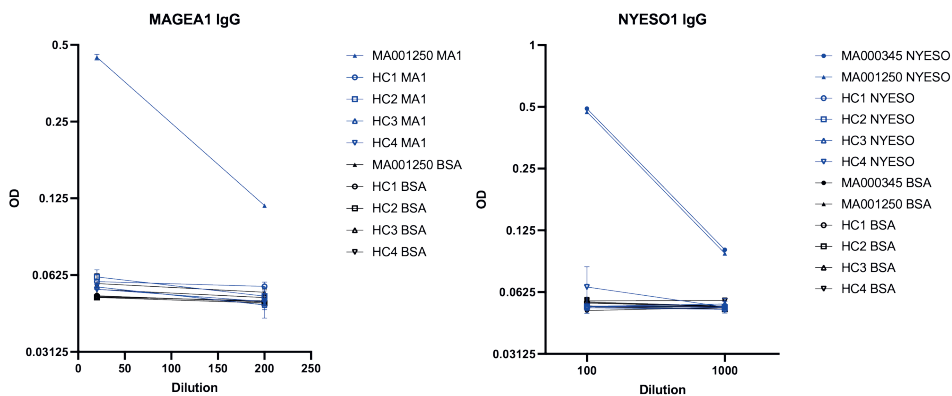
Supplementary Figure S9. CTA and HBV-specific peptide stimulation induces TNF α production in PBMC of HCC patients.

Peptide-specific induction of TNF α production was measured after re-stimulation of expanded PBMCs of 8 HCC patients prior to local ablative treatment (t=0) and at the indicated weeks after intervention. Heatmaps depict the fold changes for production of TNF α in the peptide stimulated condition compared to the solvent-containing medium condition. Peptides with a ≥ 2 fold change were determined to have evoked a peptide-specific response and are depicted as such (color-coded legend). Annotation above the heat map indicates the etiology of HCC, AFP levels before treatment and the treatment (RFA or TACE) that patients received.



Supplementary Figure S10. HBsAg and anti-HBsAg kinetics in response to local ablative therapy.

Plasma levels of HBsAg (left) and anti-HBsAg (right) prior to treatment and at several time points after intervention for HCC patients with an HBV infection that is chronic (ITV-006, ITV-007, ITV-037) or resolved (ITV-010, ITV-020, ITV-021, ITV-028).



Supplementary Figure S11. MAGEA1 and NYESO1 IgG responses in positive sera and healthy controls.

MAGEA1 and NYESO1 IgG responses were measured in 2 positive control sera and 4 healthy control plasma samples by indirect ELISA. The two positive control sera samples were sera of melanoma patients containing MAGEA1 and/or NYESO1-specific IgG antibodies. ELISA plates were coated with human recombinant full length CTA protein or bovine serum albumin (BSA), and after incubation with positive controls' serum or healthy controls' plasma, CTA-specific IgG was detected by anti-human IgG-HRP.

Protein Sequences

Protein sequences used for generation of codon-optimized mRNAs used in the CTA-specific T-cell proliferation assays.

MAGEA1

MSLEQRSLHCKPEEALAQQEALGLVCVQAATSSSSPLVLGTLEEVPAGSTDPQPSPQGASAFPTTIN
FTRQRQPSEGSSSREEEGPSTSCILESIFRAVITKKVADLVGFLLLKYRAREPVTKAEMLESVIKYNKYHCF
PEIFGKASESLQLVFGIDVKEADPTGHSYVLVTCGLSYDGLLDGNQIMPKTGFLIIVLMIAMEGGHAP
EEEIWEELSVMVEVYDGREHSAYGEPKLLTQDLVQEKYLEYRQVPDSDPARYEFLWGPRLAETSIVVK
LEYVIKVSARVRRFFPSLREAAALREEEEGV

MAGEA9

MSLEQRSPHCKPDEDLAQGEDLGLMGAQEPTGEEETTSSSDSKEEEVSAAGSSSPQSPQGGASSS
ISVYYTLWSQFDEGSSSQEEEEPSSSDPAQLFQMFQALKLVAELVHFLHXYRVEKVPVTKAEMLESVI
KNYKRYFPVIFGKASEFMQVIFGTDVKEVDPAGHSYILVTALGLSCDSMLGDGHSMPKAALLIIVLGVILTK
DNCAPEEVIWEALSVMGVVYVYVKEHMFYGEPRKLLTQDWVQENYLEYRQVPDSDPAHYEFLWGSKAHA
ETSYEKVINYLVMNLNAREPICYPSLYEEVLGEEQEGV

MAGEB2

MPRGQKSKLRAREKRRKARDETRGLNVPQVTEAEEEEAPCCSSSVSGGAASSSPAAGIPQEPQRAPTT
AAAAAAGVSSTKSKKGAKSHQGEKNASSSQASTSTKSPSEDPLTRKSGSLVQFLLYKYKIKKSVTKGEML
KIVGKRFRHFPEILKASEGLSVVFGLELNKVNPNNGHTYTFIDKVDLTDEESLLSSWDFPRRLLMPLLG
VIFLNGNSATEEEIWEFLNMLGVYDGEHSVFGEPWKLITKDLVQEKYLEYKQVPSSDPPRFQFLWGPR
AYAETSKMKVLEFLAKVNGTTPCAFPTHYEEALKDEEKAGV

MAGEC1
⁹³⁴⁻¹¹⁴²

MLTNVISRYTGYFPVIFRKAREFIEILFGISLREVDPPDSYVFNLTDLTSEGCLSDEQGMNQNRLLILLSI
IFIKGTYASEEVIWDVLSGIGVRAGREHFAGFEPRELLTKVWVQEHYLEYREVPNSSPPRYEFLWGPRAS
EVIKRKKVVEFLAMLKNTVPITFPSSYKDALKDVEERAQAIIDTDDSTATESASSVMSPSPFSSE

MAGEC2

MPPVPGVPFRNVDNDSPTSVELEDWVDAQHPTDEEEEEASSASSTLYLVFSPSSFSTSSSLILGGPEE
EEVPSGVIPNLTESIPSSPPQGPQGPSQSPLSCCSSFSWSSFSEESSQKGEDTGTCCQLPDSESSF
TYTLDEKVAELVEFLLKYEAEPPVTEAEMLMIVIKYKDYFPVILKRAREFMELLFGLALIEVGPDPHFCVF
ANTVGLTDEGSDDEGMPENSLIIILSVIFIKGNCASEEVIWEVLNAVGVYAGREHFVYGEPRELLTKV
WVQGHYLEYREVPHSSPPYYEFLWGPRAHSESIKKKVLFLAKLNNTVPSSFPSWYKDALKDVEERVQ
ATIDTADDATVMASELSVMSSNVSFSE

PAGE1

MGFLRRLIYRRRPMIYVESSESSDEQPDEVESPTQSQDSTPAEEREDEGASAAQGQPEADSQELVQP
KTGCELGDGPDTKRVCLRNNEEQMKLPAEGPEPEADSQEQVHPKTGCERGDGPDVQELGLPNPEEVKTP
EEDEGQSQP

SSX2

MNGDDAFARRPTVGAQIPEKIQAFAFDDIAKYFSKEEWEKMKASEKIFVYMKRKYEAMTKLGFKATLPP
FMCNKRAEDFQGNLDNDPNRGNQVERPQMTFGRLQGISPIMPKKPAEEGNDSEEVPEASGPQN
DGKELCPPGKPTTSEKIHRSRGPKRGEHAWTHRLRERKQLVIYEEISDPEEDDE

Luciferase

MRTENGSYFHNPGTEPLTVATLGDVIAETAHKYPGRVAVRSVHEDLTITYEELLNQADSLGCALRAQGF
QKGDRLGLWTHNCIGWVVCVGAARAGLISVLVNPVYEKAELSFINKTKLGLMIGDTLNN

Patient allocation

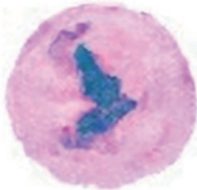
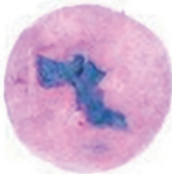
Due to a limited number of PBMCs and HLA-type restriction, not all patients could be included into every experiment. First, eight patients were selected to be included into the peptide assay, based on their HLA-types. If sufficient PBMCs remained, these patients were also included into phenotyping ($\geq 5 \times 10^6$) and proliferation ($\geq 20 \times 10^6$) experiments. Only patients with an HLA-A*02 phenotype were included in the dextramer stainings. Three proliferation assays could not be performed due to an insufficient number of cultured B cell blasts (ITV-015, ITV-028 and ITV-032). All patients were included in the humoral response experiment, except for 5 patients of whom only one time point was collected (ITV-001, ITV-018, ITV-035, ITV-036 and ITV-038).

REFERENCES

1. Gamadia LE, Rentenaar RJ, Baars PA, et al. Differentiation of cytomegalovirus-specific CD8(+) T cells in healthy and immunosuppressed virus carriers. *Blood*. 2001;98(3):754-61.
2. Ottaviani S, Zhang Y, Boon T, et al. A MAGE-1 antigenic peptide recognized by human cytolytic T lymphocytes on HLA-A2 tumor cells. *Cancer Immunol Immunother*. 2005;54(12):1214-20.
3. Oehlrich N, Devitt G, Linnebacher M, et al. Generation of RAGE-1 and MAGE-9 peptide-specific cytotoxic T-lymphocyte lines for transfer in patients with renal cell carcinoma. *Int J Cancer*. 2005;117(2):256-64.
4. Barnea E, Beer I, Patoka R, et al. Analysis of endogenous peptides bound by soluble MHC class I molecules: a novel approach for identifying tumor-specific antigens. *Eur J Immunol*. 2002;32(1):213-22.
5. Tyler EM, Jungbluth AA, Gnjatich S, et al. Cancer-testis antigen 7 expression and immune responses following allogeneic stem cell transplantation for multiple myeloma. *Cancer Immunol Res*. 2014;2(6):547-58.
6. Zhou G, Sprengers D, Boor PPC, et al. Antibodies Against Immune Checkpoint Molecules Restore Functions of Tumor-Infiltrating T Cells in Hepatocellular Carcinomas. *Gastroenterology*. 2017;153(4):1107-19 e10.
7. Chen JL, Dunbar PR, Gileadi U, et al. Identification of NY-ESO-1 peptide analogues capable of improved stimulation of tumor-reactive CTL. *J Immunol*. 2000;165(2):948-55.
8. Smith HA, McNeel DG. Vaccines targeting the cancer-testis antigen SSX-2 elicit HLA-A2 epitope-specific cytolytic T cells. *J Immunother*. 2011;34(8):569-80.
9. Sawada Y, Sakai M, Yoshikawa T, et al. A glypican-3-derived peptide vaccine against hepatocellular carcinoma. *Oncoimmunology*. 2012;1(8):1448-50.
10. Tsuchiya N, Yoshikawa T, Fujinami N, et al. Immunological efficacy of glypican-3 peptide vaccine in patients with advanced hepatocellular carcinoma. *Oncoimmunology*. 2017;6(10):e1346764.
11. Chaux P, Luiten R, Demotte N, et al. Identification of five MAGE-A1 epitopes recognized by cytolytic T lymphocytes obtained by in vitro stimulation with dendritic cells transduced with MAGE-A1. *J Immunol*. 1999;163(5):2928-36.
12. Celis E, Fikes J, Wentworth P, et al. Identification of potential CTL epitopes of tumor-associated antigen MAGE-1 for five common HLA-A alleles. *Mol Immunol*. 1994;31(18):1423-30.
13. Luiten R, van der Bruggen P. A MAGE-A1 peptide is recognized on HLA-B7 human tumors by cytolytic T lymphocytes. *Tissue Antigens*. 2000;55(2):149-52.
14. Huang LQ, Brasseur F, Serrano A, et al. Cytolytic T lymphocytes recognize an antigen encoded by MAGE-A10 on a human melanoma. *J Immunol*. 1999;162(11):6849-54.
15. Bertoni R, Sidney J, Fowler P, et al. Human histocompatibility leukocyte antigen-binding supermotifs predict broadly cross-reactive cytotoxic T lymphocyte responses in patients with acute hepatitis. *J Clin Invest*. 1997;100(3):503-13.
16. Tan AT, Sodsai P, Chia A, et al. Immunoprevalence and immunodominance of HLA-Cw*0801-restricted T cell response targeting the hepatitis B virus envelope transmembrane region. *J Virol*. 2014;88(2):1332-41.
17. Lee HG, Lim JS, Lee KY, et al. Peptide-specific CTL induction in HBV-seropositive PBMC by stimulation with peptides in vitro: novel epitopes identified from chronic carriers. *Virus Res*. 1997;50(2):185-94.
18. Depla E, Van der Aa A, Livingston BD, et al. Rational design of a multi-epitope vaccine encoding T-lymphocyte epitopes for treatment of chronic hepatitis B virus infections. *J Virol*. 2008;82(1):435-50.
19. Desmond CP, Gaudieri S, James IR, et al. Viral adaptation to host immune responses occurs in chronic hepatitis B virus (HBV) infection, and adaptation is greatest in HBV e antigen-negative disease. *J Virol*. 2012;86(2):1181-92.
20. van der Burg SH, Vissers MJ, Brandt RM, et al. Immunogenicity of peptides bound to MHC class I molecules depends on the MHC-peptide complex stability. *J Immunol*. 1996;156(9):3308-14.

21. Gehring AJ, Ho ZZ, Tan AT, et al. Profile of tumor antigen-specific CD8 T cells in patients with hepatitis B virus-related hepatocellular carcinoma. *Gastroenterology*. 2009;137(2):682-90.
22. Ding FX, Wang F, Lu YM, et al. Multiepitope peptide-loaded virus-like particles as a vaccine against hepatitis B virus-related hepatocellular carcinoma. *Hepatology*. 2009;49(5):1492-502.
23. Miyara M, Yoshioka Y, Kitoh A, et al. Functional delineation and differentiation dynamics of human CD4+ T cells expressing the FoxP3 transcription factor. *Immunity*. 2009;30(6):899-911.

CHAPTER 6



LOW-DOSE CYCLOPHOSPHAMIDE DEPLETES CIRCULATING NAIVE AND ACTIVATED REGULATORY T CELLS IN MALIGNANT PLEURAL MESOTHELIOMA PATIENTS SYNERGISTICALLY TREATED WITH DENDRITIC CELL- BASED IMMUNOTHERAPY

Low-dose cyclophosphamide depletes circulating naive and activated regulatory T cells in malignant pleural mesothelioma patients synergistically treated with dendritic cell-based immunotherapy

L. Noordam, M.E.H. Kaijen-Lambers, K. Bezemer, R. Cornelissen, A.P.W.M. Maat, H.C. Hoogsteden, J.G.J.V. Aerts, R.W. Hendriks, J.P.J.J. Hegmans, H. Vroman

Oncolmmunology, Jul 2018, Vol. 7, No. 12: e1474318

This chapter has been published in Oncolmmunology.

Rationale

Regulatory T cells (Treg) play a pivotal role in the immunosuppressive tumor micro-environment in cancer, including mesothelioma. Recently, the combination of autologous tumor lysate-pulsed dendritic cells (DC) and metronomic cyclophosphamide (mCTX) was reported as a feasible and well-tolerated treatment in malignant pleural mesothelioma patients and further as a method to reduce circulating Tregs.

Objectives

The aim of this study was to establish the immunological effects of mCTX alone and in combination with DC-based immunotherapy on circulating Treg and other T cell subsets in mesothelioma patients.

Methods

Ten patients received mCTX and DC-based immunotherapy after chemotherapy (n=5) or chemotherapy and debulking surgery (n=5). Peripheral blood mononuclear cells before, during and after treatment were analyzed for various Treg and other lymphocyte subsets by flow cytometry.

Results

After one week treatment with mCTX, both activated FoxP3^{hi} and naïve CD45RA⁺ Tregs were effectively decreased in all patients. In addition, a shift from naïve and central memory towards effector memory and effector T cells was observed. Survival analysis showed that overall Treg levels before treatment were not correlated with survival, however, nTreg levels before treatment were positively correlated with survival. After completion of mCTX and DC-based immunotherapy treatment, all cell subsets returned to baseline levels, except for the proportions of proliferating EM CD8 T cells, which increased.

Conclusions

mCTX treatment effectively reduced the proportions of circulating Tregs, both aTregs and nTregs, thereby favoring EM T cell subsets in mesothelioma patients. Interestingly, baseline levels of nTregs were positively correlated to overall survival upon complete treatment.

INTRODUCTION

Malignant pleural mesothelioma (MPM) is a rare but aggressive form of cancer most often caused by asbestos fiber inhalation. The incidence of MPM is rising,^{1, 2} and the prognosis is infaust; with the best standard of care, antifolate and platinum combination chemotherapy, overall survival is 13.3 months.³ In the last ten years no major breakthroughs have been reported and consequently, this systemic therapy has remained unchanged.³ Recently, addition of bevacizumab to the chemotherapy-backbone showed a positive effect on survival.⁴ Extensive investigation of the effects of implementation of radiotherapy and/or debulking surgery in standard treatment revealed variable success, but only when applied to select patient subgroups.^{1, 5-7}

Complementary to the current standard anti-cancer treatment options, immunotherapy is gaining momentum.⁸⁻¹⁰ The potential of cancer immunotherapy lies in the ability of the immune system to recognize tumor cells, without harming healthy tissue. There are various methods to either induce or enhance an anti-tumor immune response, including adoptive transfer of immune cells, peptide or tumor cell vaccines and immune checkpoint blockade.¹⁰ Recently, there have been major leaps in development of blocking the immunosuppressive tumor microenvironment (TME) by checkpoint inhibitors.¹¹⁻¹⁵ Importantly, for immunotherapy, including checkpoint inhibition, to become successful, tumor recognition by the immune system is necessary.¹⁶ For an effective anti-tumor immune response, both a CD4 and CD8 T cell response is required, which can be enhanced by immune checkpoint blockade.¹⁷ By loading them *ex vivo* with tumor antigens, they can be used as cellular immune therapy. DC-based immunotherapy is, in contrast to other immunotherapies including adoptive T cell transfer and peptide-based vaccines, not human lymphocyte antigen (HLA)-restricted and can induce an immune response to a wide array of antigens. In a recent meta-analysis, it was shown that cellular immunotherapy seems to be more effective than tumor vaccines in non-small cell lung carcinoma (NSCLC).¹⁸ Furthermore, in an earlier phase I clinical trial with MPM patients DC-based immunotherapy, in which DCs were loaded with autologous tumor lysate, has been proven safe, feasible and capable of inducing an anti-tumor response, which was detectable in peripheral blood of patients.¹⁹

Aside from inhibitory receptor expression, efficacy of immunotherapy can also be hampered by the immunosuppressive TME induced by the tumor²⁰. In particular, the tumor affects regulatory T cell (Treg) function, quenches pro-inflammatory signals and inhibits antigen presentation,^{21, 22} all of which ultimately prevent successful execution of antitumor immune responses. As illustrated by the study of Bjoern, *et al.*,²³ melanoma patients treated with DC vaccination and low-dose interleukin 2 (IL-2) that progressed under this therapy had significantly higher levels of CD25^{high} CD4 T cells than patients with stable disease. Miyara, *et al.*²⁴ have shown that the classically defined Treg population of FoxP3⁺ CD4 T cells, comprise three functionally different subpopulations: suppressive naïve Tregs (nTreg; CD45RA⁺FoxP3^{med}), activated Tregs (aTreg; CD45RA⁻FoxP3^{hi}) and the cytokine-secreting activated T cells (aTcell; CD45RA⁻FoxP3^{med}). Santegoets, *et al.*²⁵ showed that the frequency of aTregs and proliferating Ki67⁺ FoxP3⁺CD25⁺CD127^{low} Tregs prior to treatment were associated with worse survival in recurrent ovarium carcinoma patients

undergoing chemo-immunotherapeutic treatment, whilst frequencies of classically defined Tregs prior to treatment were not associated with survival. In mesothelioma, Tregs contribute to an impaired T cell function^{26, 27} and are associated with tumor progression and poor prognosis.²⁸ Low-dose (metronomic) cyclophosphamide (mCTX) regimens have beneficial immunomodulatory effects by inducing Treg apoptosis or by reducing their functionality.²⁹⁻³² In mice we have previously shown that mCTX induced beneficial immunomodulatory effects, by decreasing the Tregs numbers and thereby improving CD8 T cell function.³³ It is unknown what the effects of debulking surgery and mCTX are on the different subpopulations of Tregs.

To improve DC-based immunotherapy, the immunosuppressive TME, specifically Tregs, was targeted by mCTX to the treatment in a phase I/II clinical trial.³⁴ This therapy has also been proven safe, feasible and moreover, effective in depleting Tregs. Radiographic disease control was obtained in 8 out of 10 patients and the median overall survival was 26 months.³⁴

The aim of this study was to determine whether mCTX treatment, has beneficial effects on subpopulations of circulating Tregs or other peripheral blood mononuclear cell subsets that could explain the enhanced survival observed in MPM patients treated with DC/mCTX-based immunotherapy. To this end, an in depth immunological analysis was performed on peripheral blood of patients included in a phase I/II clinical trial.³⁴

RESULTS

Patient characteristics and toxicity

Ten patients with MPM suitable for extended pleurectomy/decortication (P/D) and a stable disease or response after an antifolate-based regimen of chemotherapy were enrolled in this study between August 2009 and October 2011. The DC/mCTX treatment was preceded by P/D in five of the ten patients (**Figure 1**); all patients completed the full treatment schedule and were available for immunological

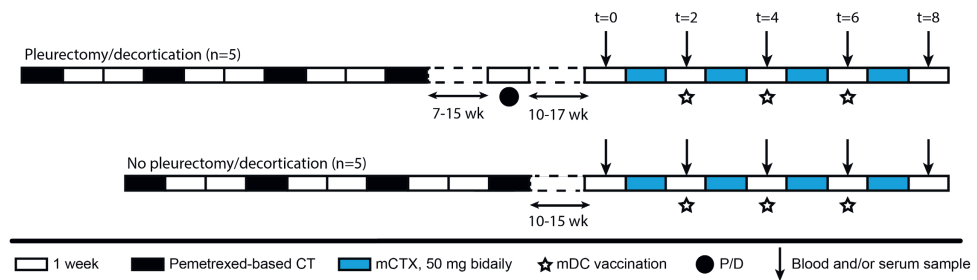


Figure 1. Schematic overview of the clinical trial.

Patients were included if they had partial response or stable disease after pemetrexed-based chemotherapy. Five patients underwent additional P/D 7-15 weeks after chemotherapy. DC/mCTX therapy started 10-17 weeks after either the last chemotherapeutic treatment or P/D. Blood samples were obtained at t=0 (baseline); t=2 (mCTX); t=4; t=6; t=8 (2 wk after DC/mCTX therapy).

analysis. Patient characteristics, safety and toxicity data, as well as clinical response were previously reported.³⁴ There was no significant difference in survival between patients that did or did not undergo the P/D (data not shown). To establish the effect of P/D on T cells, peripheral blood mononuclear cells (PBMC) obtained at t=0 were compared between the P/D group and the no P/D group by flow cytometry. The gating strategy for characterizing nTregs and aTregs using CD45RA and FoxP3, as well as the differentiation status for CD4 and CD8 T cell subpopulations, using CD45RA and CCR7 to distinguish between naïve (CD45RA⁺CCR7⁺), central memory (CM; CD45RA⁻CCR7⁺), effector memory (EM; CD45RA⁻CCR7⁻) and effector (EMRA; CD45RA⁺CCR7⁻) populations was performed according **Supplementary Figure S1**.²⁴

Within the circulating T cell compartment, there is a trend to an increase in T cells and a decrease in monocytes in P/D patients, however these changes were not significant, and neither were changes in other T cell subsets, including Tregs (**Supplementary Figure S2A** and **S2B**). In addition, no significant differences were found in the proportions of total CD4 and CD8 T cells, B cells, natural killer (NK) cells, NK T cells, $\gamma\delta$ T cells and monocytes and IFN γ -producing or Granzyme B (GrB) containing T cells (**Supplementary Figure S2C**).

Thus, in peripheral blood of the P/D group all measured circulating immune subsets were comparable to mesothelioma patients without debulking surgery and for further analyses data from P/D and no P/D patients were pooled.

mCTX treatment affects both aTregs and nTregs, while increasing effector memory populations

To determine the effect of mCTX on circulating Tregs, and other T cells subsets, PBMCs obtained at t=0 and t=2 weeks were analyzed by flow cytometry. Compared with nTregs, the aTregs showed higher expression of CCR4, CTLA-4 and Ki67, confirming their active and immunosuppressive state (**Supplementary Figure S3A**).

After two weeks (with one week of mCTX treatment; **Figure 1**), total T cells and CD4 T cells decreased upon mCTX treatment, whereas CD8 T cells increased and both the proportions of nTregs and aTregs (as percentage of total CD4 T cells) were significantly decreased (**Figures 2A-B**). Within the FoxP3⁻ CD4 T cells and CD8 T cells the naïve and central memory subsets decreased, while the effector subsets increased (**Figure 2C-D**). The percentages of proliferating FoxP3⁻CD4 T cells significantly increased in all subsets, except for the TEMRA subset (**Figure 2E**). In the circulating CD8 T cells an increase in proliferation was observed in all subsets, except for the CM subset (**Figure 2E**). In addition, even though the percentage of both Treg populations decreased, the percentage of proliferating nTregs increased upon treatment with mCTX, while the percentage of proliferating aTregs did not change (**Figure 2E**). Also the CTLA4 expression increased in the nTregs, however, in the aTregs the expression of CTLA4 decreased (**Figure 2F**). The proportions of IFN γ -producing and GrB-containing CD4 and CD8 T cells seemed to increase, although not significantly (**Figure 2G**). Correlation analysis indicated that the change IFN γ -producing and GrB-containing CD4 T cells and the GrB-containing CD8 T cells induced by mCTX might inversely correlate with the change in Tregs (**Supplementary Figures S4**), however,

this correlation was not significant. The proportions of B cells, NK cells, NKT cells and monocytes (as percentage of total PBMCs), did not change upon mCTX treatment, the proportions of $\gamma\delta$ T cells slightly increased (**Supplementary Figure S5**).

From these findings, we conclude that mCTX effectively reduced the proportions of both nTregs and aTregs within the CD4 T cell population, with a decreased CTLA4 expression in aTregs and an increased expression in nTregs. In addition, within the total population of T cells the proportions of CD4 T cells decreased and CD8 T cells increased, a shift was observed from the naïve and CM subsets to the EM and TEMRA subsets and the majority of circulating CD4 and CD8 T cell subsets had an increased proliferation.

DC/mCTX-based immunotherapy increased proliferation of CM CD8 T cells

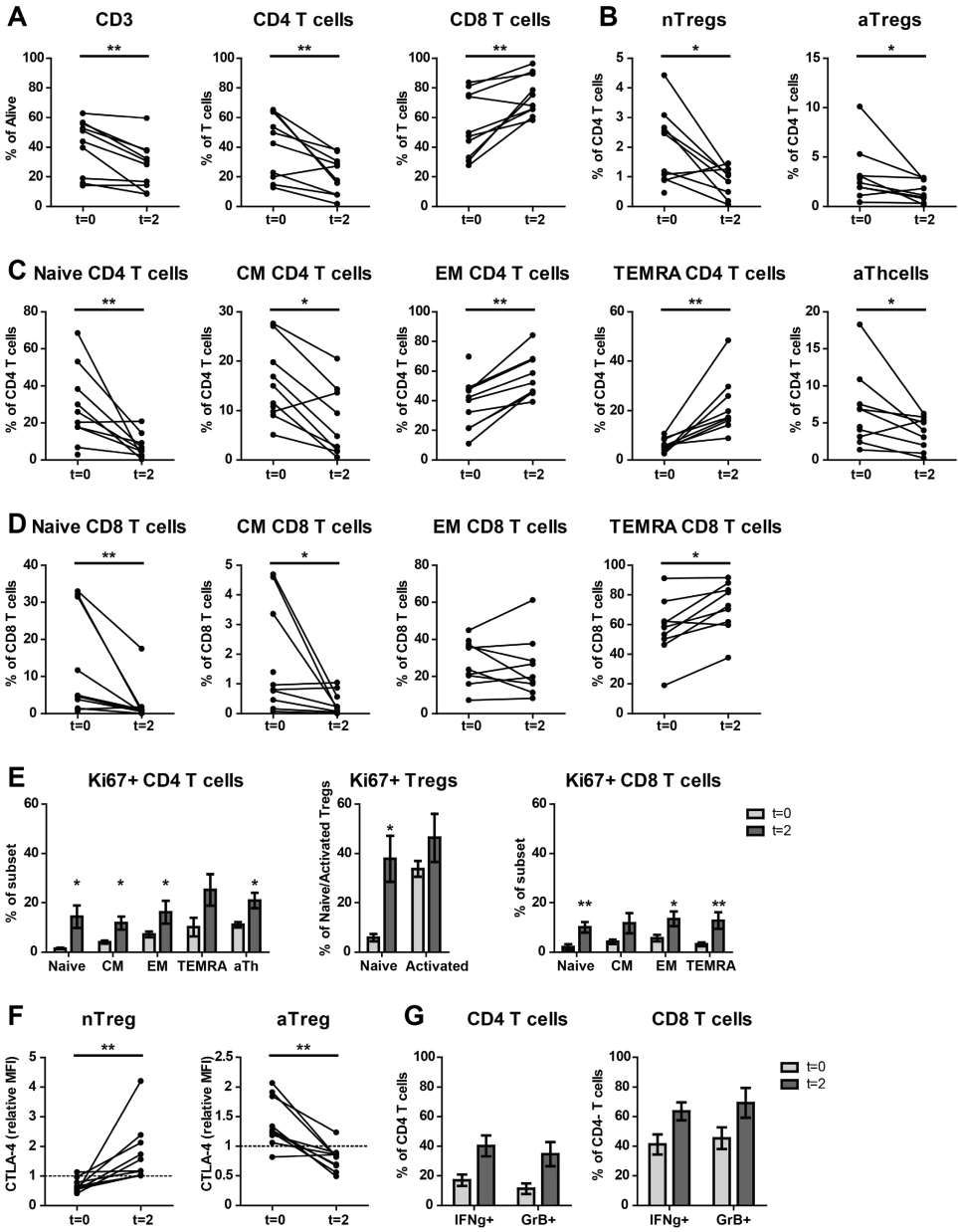
To examine the effect of combined DC/mCTX-based immunotherapy on T cells, flowcytometric analysis of PBMCs obtained at t=0 were compared with those of t=8, corresponding to the time point after completion of DC/mCTX-based immunotherapy (**Figure 1**).

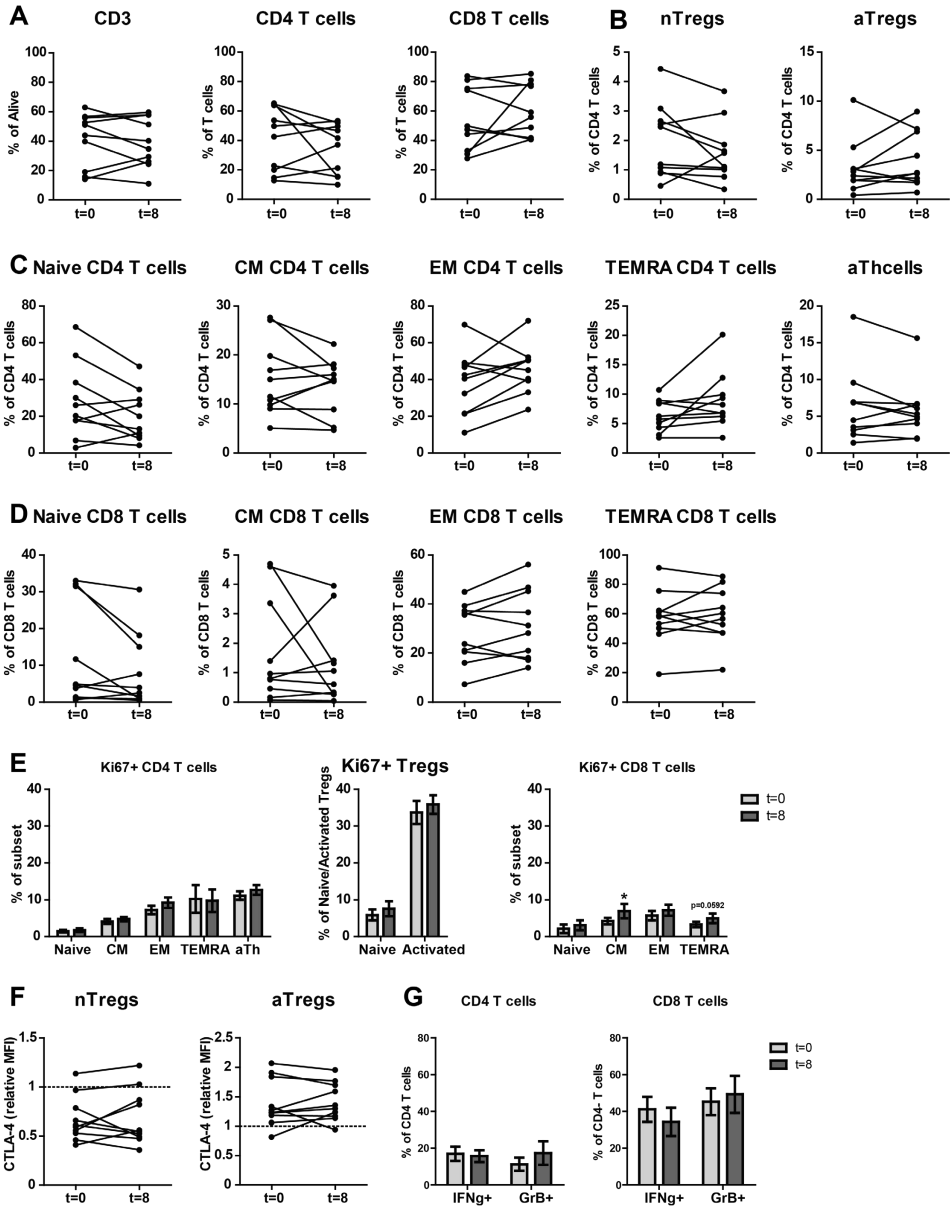
Whereas after one week of mCTX percentages of total T cells and CD4 T cells were decreased and CD8 T cells were increased, these percentages returned to baseline after the complete treatment (**Figure 3A**). Also, Treg levels and all differentiated T cell subsets (**Figure 3B-D**) returned back to their levels before therapy. At t=8, also the percentages of CD4 T cell subsets, and proliferating nTregs were comparable to baseline, nevertheless, the percentages of proliferating CM CD8 T cells were significantly increased and the TEMRA CD8 T cell population showed a trend towards an increase (**Figure 3E**). The CTLA4 expression in both nTregs and aTregs were comparable to baseline (**Figure 3F**), as were the percentages of IFN γ -

Figure 2. Both aTregs and nTregs, and other naïve cell subsets decreased upon mCTX administration, meanwhile the percentages of proliferating T cells increased. ►

To determine the effect of mCTX administration on activated and naïve Tregs, and other T cell populations, flowcytometric analysis was performed on PBMCs obtained at t=0 and t=2, and thereby comparing baseline proportions with the proportions after mCTX administration. To determine IFN γ -production, T cells were stimulated 4hrs with PMA/ionomycin in the presence of monensin. **A.** The proportion of CD3 T cells decreased significantly upon mCTX treatment, as did CD4 T cells. The percentage of CD8 T cells increased significantly. **B.** Both percentages of naïve and activated Tregs decreased significantly. **C.** The percentages of naïve, CM and activated CD4 T cells decreased significantly, while the percentages of EM and TEMRA CD4 T cells increased significantly upon mCTX treatment. **D.** The percentages of naïve and CM CD8 T cells decreased significantly, while the percentages of TEMRA CD8 T cells increased significantly upon mCTX treatment. The percentage of EM CD8 T cells did not change. **E.** Upon treatment with mCTX the percentages of proliferating CD4 T cells increased in the naïve, CM, EM and activated CD4 T cells subset, but not in the TEMRA subset. The percentage of proliferating nTregs increased, but not of aTregs. In CD8 T cells, the naïve, EM and TEMRA cells had increased proliferation, but not the CM subset. **F.** CTLA4 expression in nTregs and aTregs. The dashed line represents the MFI (mean fluorescence intensity) of CTLA4 in a healthy individual. The MFI of CTLA4 increased significantly in nTregs and decreased significantly in aTregs upon treatment with mCTX. **G.** The proportions of IFN γ -producing CD4 and CD8 T cells did not change significantly, neither did the percentage of GrB+ CD4 and CD8 T cells.

Results represent mean \pm Standard Error of the Mean (SEM). *p < 0.05, **p > 0.01 (Wilcoxon matched-pairs signed rank test), differences were considered significant when p < 0.05.





◀ **Figure 3. After completion of DC/mCTX-based immunotherapy, all Treg and other T cell populations were returned to baseline levels, the percentage of proliferating CM CD8 T was increased compared to baseline.**

To determine the effects of DC/mCTX-based immunotherapy, flowcytometric analysis of PBMCs obtained at t=0 (baseline) and t=8 (after completing DC/mCTX-based immunotherapy) were compared. To determine IFN γ -production, T cells were stimulated 4hrs with PMA/ionomycin in the presence of monensin. **A.** The proportion of CD3, CD4 and CD8 T cells after DC/mCTX-based immunotherapy were comparable to baseline. **B.** The percentages of nTregs and aTregs did not change significantly. **C.** The percentages of naïve, CM, EM, TEMRA and activated CD4 T cells did not change significantly. **D.** Neither did the different subsets in CD8 T cells; naïve, CM, EM and TEMRA. **E.** Upon treatment with DC/mCTX-based immunotherapy the percentages of proliferating CD4 T cells did not change in the different subsets; naïve, CM, EM, TEMRA and activated. Neither did the proportion of proliferating nTregs and aTregs. In CD8 T cells the proportion of proliferating cells was higher in the CM subset and there was a trend towards more proliferating TEMRA. In the naïve and EM subset the proportion of proliferating cells was equal before and after DC/mCTX-based immunotherapy. **F.** The proportions of IFN γ -producing CD4 and CD8 T cells did not change significantly, neither did the percentage of GrB+ CD4 and CD8 T cells.

Results represent mean \pm Standard Error of the Mean (SEM). *p < 0.05 (Wilcoxon matched-pairs signed rank test), differences were considered significant when p < 0.05.

producing and GrB-containing CD4 and CD8 T cells (**Figure 3G**) and the proportions of B cell, NK cell, NKT cell, $\gamma\delta$ T cell and monocytes (from total PBMC) (**Supplementary Figure S6**).

In conclusion, after completed DC/mCTX-based immunotherapy at t=8, all immune cell subsets, including Tregs, returned to baseline. Only the CM CD8 T cell subset showed an increased proportion of proliferating cells compared to baseline.

Correlation of pre-treatment proportions of Treg subsets with overall survival

To determine whether the proportions of Tregs before treatment (at t=0) were correlated with survival in MPM patients treated with DC/mCTX-based immunotherapy, linear regression analyses were performed. The pre-treatment percentage of total Tregs (nTregs and aTregs), did not show a correlation with survival (**Figure 4A**). Subsequently, the same analysis was performed for aTregs and nTregs separately. Interestingly, the pre-treatment percentage of nTregs correlated positively with survival, whereas the percentage of aTregs did not show any correlation (**Figure 4A**). On the basis of the positive correlation of nTregs and overall survival, two patient clusters could be distinguished: six patients with low proportions of nTregs and a low overall survival, and four patients with high pre-treatment nTreg proportions and a relatively high overall survival. For these groups – patients with a pre-treatment nTreg percentage below 2% of total CD4 T cells (n=5; range 0.46%-1.19%) and higher than 2% of CD4 T cells (n=5; range 2.46%-4.43%) – a survival analysis was performed. This confirmed that proportions of nTregs above 2% of total CD4 T cells were associated with a higher overall survival (**Figure 4B**).

Thus, we concluded that in mesothelioma patients treated with DC/mCTX-based immunotherapy, the pretreatment percentage of circulating nTregs had a positive correlation with overall survival.

DISCUSSION

The primary aims of this study were to determine the immunological effects of mCTX and the effects of DC/mCTX based therapy specifically on subpopulations of Tregs and other immune cell subsets in peripheral blood of mesothelioma patients. Patients with partial response (PR) or stable disease (SD) after standard chemotherapeutic treatment were included in this study. As we have previously shown,³⁴ mCTX effectively reduced the number of FoxP3⁺CD25⁺CD127^{low} CD4 T cells. In this study, we showed that both the nTreg and aTreg subsets were reduced by mCTX treatment, and that pre-treatment proportions of nTregs positively correlated with survival. P/D had no effect on nTregs or aTregs, nor on other circulating lymphocyte and monocyte subsets. Total Tregs and aTregs were not correlated with survival. At t=2, after mCTX treatment, FoxP3⁻ CD4 T cells were also decreased in quantity, while CD8 T cells increased and a shift from naïve to effector T cell populations was observed. Other lymphocyte and monocyte subsets were not affected. At t=8, after completion of DC/mCTX therapy, all examined cell subsets returned to the patients' baseline levels before the therapy, with the exception of proliferating CM CD8 T cells. We found an increase in the proportions of these cells, which were not increased by mCTX treatment alone, indicating that these CD8 T cells started proliferating upon the DC vaccinations.

A key factor for inducing an effective immune response is an immune-stimulatory environment. In mesothelioma, Tregs are a major contributor to creating an immunosuppressive environment.^{26, 27} To reduce the number of Tregs in mesothelioma patients, debulking surgery and mCTX administration were investigated. It is hypothesized that debulking surgery can reduce Tregs locally by decreasing the tumor load and mCTX systemically by directly targeting Tregs.³⁰ In NSCLC, circulating Treg levels in thoracotomy patients were reduced up until postoperative day (POD) 30 and had normalized at POD 90.³⁵ In another study in NSCLC patients, circulating Treg levels were also reduced 1-3 months after pneumectomy or lobectomy.³⁶ In contrast to these studies, in our study the Treg levels in blood were not significantly different between the P/D and no P/D groups three months after surgery. However, we analyzed only a limited number of patients, we could not study the effect of P/D on Tregs within the TME, preoperative data were not available and the P/D patients were at least three months after P/D. This could indicate that mCTX might be an effective treatment strategy to reduce Tregs in both of these groups.

Administration of mCTX transiently depleted Tregs, as has been shown before.³⁰ However, to the best of our knowledge, we are the first to show that both naïve and activated Tregs are depleted. In addition, upon mCTX the CTLA4 expression was reduced specifically on aTregs. Conflicting results have been published about the effect of mCTX on the suppressive capacity of Tregs; in metastasized breast cancer patients 50 mg cyclophosphamide daily for three months resulted in an initial Treg reduction but a preservation of their suppressive function.³⁷ Another study in end stage cancer patients treated with 50 mg cyclophosphamide twice daily, one week on and one week off for one month, also found a selective reduction of Tregs, but also a suppression of their inhibitory functions.³⁰ Since we observed a downregulation of CTLA4 in aTregs, but an upregulation in nTregs, these inconsistent results could be explained by a subset dependent effect of mCTX. Another explanation could be the dosing schedule of

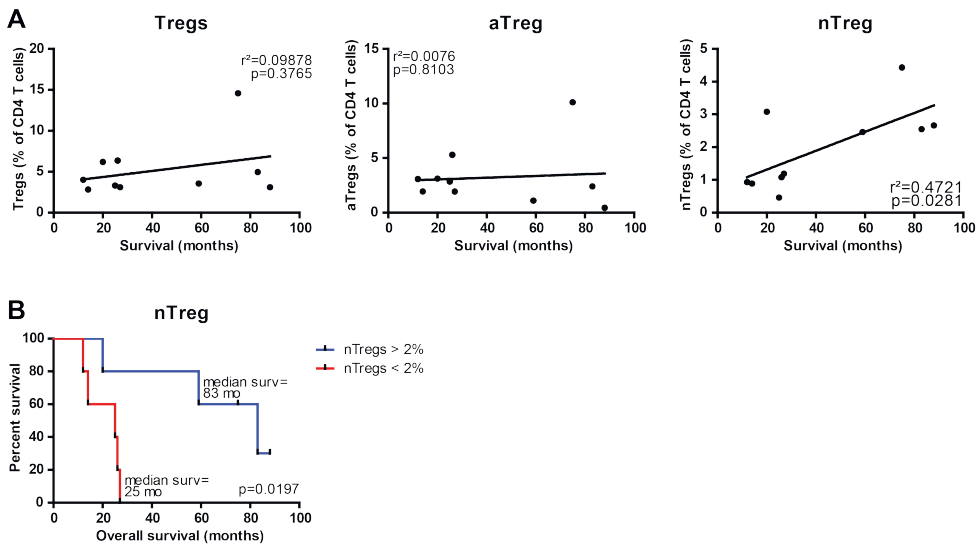


Figure 4. Pretreatment frequencies of nTregs correlated with overall survival in mesothelioma patients treated with DC/mCTX-based immunotherapy.

A. To determine whether pretreatment frequencies of total Tregs (the percentage of nTregs and aTregs of total CD4 T cells), aTregs or nTregs correlated with survival in mesothelioma patients treated with DC/mCTX-based immunotherapy, linear regression was performed. No significant correlation was observed between total Tregs (A, left) or aTregs (A, middle) and survival. Linear regression showed a significant positive correlation between pretreatment nTreg frequencies and survival (A, left). **B.** To determine whether patients with lower pretreatment nTreg frequencies (below 2% of total CD4 T cells, $n=5$) had a different survival from patients with higher nTreg frequencies (above 2% of total CD4 T cells, $n=5$), survival analysis was performed. Patients with a nTreg percentage above 2% of CD4 T cells, had a better overall survival.

Statistical analysis was performed by log-rank (Mantel-Cox) testing, and differences were considered significant when $p < 0.05$.

cyclophosphamide,³⁸ in a murine model cyclophosphamide treatments with drug free intervals of 6, 9 and 12 days were tested and only the 6 day drug free interval showed induction of tumor specific CD8 T cells. It is hypothesized that if the interval is too short, activated CD8 T cells and NK cells can also be depleted, but if the interval is too long, the cells could acquire drug resistance and the therapy would lose its effect.³⁹

Complementary to the decrease of CTLA4 in aTregs, and indicative of reduced immune suppression, we detected a shift from naïve and CM subsets towards effector memory and effector subsets. The previously mentioned clinical studies by Ghiringhelli, *et al.*³⁰ and Ge, *et al.*³⁷, also described an increase in effector T cells upon mCTX treatment. In animal models skewing towards a Th1 profile with increased type I interferons and IL-2 upon mCTX treatment was observed,^{40, 41} which could correspond to the increase in IFN γ + CD4 and CD8 T cells observed in this study. The IL-2 secretion by Th1 cells could induce proliferative expansion of CD8 T cells,⁴¹ which could have led to the increased effector T cells.

In addition, these cells could be enhanced by the decrease of Treg mediated immune suppression.³⁹ And lastly, a cytokine storm and thereafter homeostatic proliferation, could be caused by the lympho-depletion due to the mCTX treatment.⁴² This would be in concordance with the increased proportion of proliferating naïve Tregs, CD4 T cells and CD8 T cells. No change was observed in the proportions of B cells, NK cells, $\gamma\delta$ T cells and monocytes. Comparable results have been reported in other studies.^{37, 43}

The analysis of Tregs showed that pretreatment circulating Treg levels did not correlate with survival when patients were treated with DC/mCTX based immunotherapy. In fact, the patient with the highest proportion of both nTregs and aTregs had a survival of more than 6 years after diagnosis and is still alive at the time of writing. Survival analysis and correlation of pretreatment percentages of the two Treg subsets with overall survival rate, showed that patients with higher percentages of nTregs had a better survival. nTregs differentiate into aTregs upon T-cell receptor stimulation by antigen recognition,^{24, 44, 45} which could imply that patients having a relatively high percentage of peripheral nTregs have less tumor-specific Tregs. Due to their naïve phenotype, these nTregs are inefficient in infiltrating the tumor,⁴⁶ as is also illustrated by their low CCR4 expression, and thus these cells cannot exert immunosuppressive activity. Therefore, immunotherapy might be more effective in these patients, which is a possible explanation for this counterintuitive finding. Moreover, Treg diversity, including the pool of nTregs, is controlled by homeostasis,⁴⁴ thus having a higher percentage of nTregs might indicate a healthier immune system.

However, from this study alone we cannot deduce whether patients with a higher percentage of nTregs have a better survival due to the mCTX or the DC-based immunotherapy, the combination therapy or have an initial better survival. In contrast to our study, Kwa, *et al.*,⁴⁷ found that elevated baseline levels of nTregs were a negative predictive factor for survival in metastatic breast cancer patients treated with exemestane and mCTX. However, Kwa, *et al.* used a different definition of nTregs (CD4+CD45RO-FoxP3+Helios+) and the mCTX treatment was combined with hormone therapy instead of immunotherapy, which might have resulted in a different outcome. In addition, they did not establish an effect of mCTX alone on either memory or naïve Tregs, so it cannot be excluded that the observed effects were caused by the combination of mCTX and hormone therapy, which possibly increases Tregs and their function.⁴⁸

In light of the recent developments in the tumor immunology field, the approved checkpoint inhibitors, against CTLA-4 or PD-(L)1,^{15, 49, 50} or anti-CCR4 antibodies to inhibit aTregs,^{51, 52} could be interesting methods to reduce the immunosuppressive TME as a synergistic addition to DC-based immunotherapy in mesothelioma, instead of or complementary to surgery and mCTX.

Our study has several limitations. First, to make the autologous tumor lysate used to pulse the DCs with, in the non-P/D group only patients that had sufficient amounts of tumor cells in the pleural fluid were included. For the P/D group, patients had to be fit enough to be able to undergo surgery. Both of these factors might have caused a selection bias. In addition, this study was exploratory and only ten patients were enrolled in this study, which might not be enough to objectify smaller differences and

establish significant results and thus larger patient groups are needed to validate findings in this study. For example, the positive correlation between higher pretreatment levels of nTregs and overall survival should be validated in a larger patient cohort.

In summary, in this small patient cohort DC/mCTX-based immunotherapy in mesothelioma patients seems to improve survival;³⁴ this therapy simultaneously countered tumor-induced immune suppression and induced a distinct adaptive immune response. Based on these results and the improved overall survival compared to DC-based immunotherapy alone,¹⁹ mCTX seems to add to solely DC-based immunotherapy in mesothelioma patients with stable disease after the standard chemotherapy regimen, and seems to specifically benefit patients with a high pretreatment level of nTregs. It would be very interesting to explore synergistic therapies to reduce immunosuppression, such as checkpoint inhibitors, to complement DC/mCTX-based immunotherapy.

MATERIALS AND METHODS

Study design

The institutional ethical committee of the Erasmus MC (MEC-2008-109) and the Central Committee on Research involving Human Subjects (CCMO; NL24050-000-08) as defined by the WMO (Medical Research Involving Human Subjects Act) approved the phase I study.³⁴ Procedures followed were in accordance with the ethical standards of these committees on human experimentation and with the Helsinki Declaration of 1975. The study is registered at <http://www.clinicaltrials.gov> with identifier NCT01241682.

Patients and treatment

An extensive description of the patient eligibility and treatment is given by Cornelissen, *et al.*³⁴ In short, patients with mesothelioma suitable for P/D and partial response (PR) or stable disease (SD) after standard chemotherapeutic treatment were included. Before inclusion a delayed type hypersensitivity (DTH) test with tetanus toxoid as a positive control and saline as a negative was performed to confirm immunological competence. DC-based immunotherapy in combination with mCTX was planned 8 to 10 weeks after completion of chemotherapy (n=5) or chemotherapy and P/D (n=5). Patients received at least three vaccinations consisting of 50×10^6 mature DC (mDC) pulsed with autologous tumor lysate with a 2-week interval, every immunization one-third of the dosage was administered intradermally in the forearm and two-thirds was administered intravenously. Patients were treated with 50 mg tablet twice daily of CTX (Endoxan; Baxter B.V., Utrecht, The Netherlands) for a week, followed by a week interval in which the vaccination was administered, starting a week before the first vaccination and ending one week after the third vaccination. The treatment schedule is depicted in **Figure 1**.

Survival data were determined on March 1st, 2018. Blood and serum samples were obtained before immunotherapy treatment initiation (t=0), just before administration of the vaccinations (t=2, t=4 and t=6), two weeks after the third vaccination (t=8), and three months after the third vaccination (t=18), as illustrated in **Figure 1**. Peripheral blood mononuclear cells (PBMC) were isolated using Ficoll density

gradient centrifugation, cryopreserved in 50% RPMI-1640 medium (Gibco Life Technologies), 40% Fetal Calf Serum (FCS), and 10% DMSO and stored in liquid nitrogen until use. Serum samples were stored at -80°C until use.

Immunological evaluation

Flowcytometric analysis

Flow cytometric analyses of Tregs was based on markers that differentiate between activated and naïve Tregs, as previously described by Miyara, *et al.*²⁴ and Santegoets, *et al.*²⁵. Cryopreserved PBMCs were thawed and washed twice in cold PBS. Dead cells were stained using LIVE/DEAD Fixable Aqua Dead Cell Stain (Invitrogen life technologies, Cat# L34957). Antibodies used in stainings are specified in **Supplementary Table S1** ("Treg" and "Immune Subsets (IS)" panel). The eBioscience FoxP3/Transcription factor staining buffer kit (eBioscience, Cat# 00-5521-00) was used for fixation and permeabilization of cells in the Treg panel for detection of FoxP3, Ki67 and CTLA-4, cells in the IS panel were not fixated and permeabilized. Cells were measured on the LSR-II flow cytometer (BD Biosciences) and analyzed using FlowJo software (version 10.1r5, FlowJo). All populations with less than 100 cells were excluded for further analysis (Ki67 and CTLA4 expression and CD4 T cell differentiation). Since experiments were performed on several days, expression of CTLA-4 in nTregs and aTregs (**Figure 2F** and **3F**) was normalized to the expression of CTLA-4 in those respective populations in a healthy individual that was included in every experiment, the dashed line in the figures represents the MFI of CTLA-4 in the nTreg (left panel) and aTreg (right panel) population of the healthy individual.

Effector T cell responses

The cryopreserved PBMCs obtained at t=0 (all patients), t=2 (4 patients; 2-3 and 9-10), t=4 (all patients), t=6 (9 patients; 1-7 and 9-10) and t=8 (7 patients; 2, 4-8 and 10) were thawed and per sample 1×10^6 PBMCs were stimulated with phorbol myristate acetate (PMA; Sigma-Aldrich) and ionomycin (Sigma-Aldrich) in the presence of Golgistop (BD Biosciences) in RPMI supplemented with 10% pooled human AB serum (Human Culture Medium; HCM) at 37°C for 4 hours. Following the stimulation, cells were stained using LIVE/DEAD Fixable Aqua Dead Cell Stain and antibodies that are specified in **Supplementary Table S1** ("Cytokines" panel). IFN γ and GrB were detected following fixation and permeabilization using 2% paraformaldehyde (PFA) in PBS and subsequently 0.5% saponin in PBS. Cells were measured on the LSR-II flow cytometer (BD Biosciences) and analyzed using FlowJo software (version 10.1r5, FlowJo).

Statistical analysis

Statistical calculations were performed using GraphPad Prism (version 6.0c for Mac OS X, GraphPad Software, La Jolla California USA). For unpaired samples, the Mann Whitney test was used and for paired samples the Wilcoxon matched paired test was used, as indicated in the figures. There was no correction performed for multiple testing. For survival analysis the Mantel-Cox log-rank test was used. Statistical significance was established at the $p < 0.05$ level, and analysis was two-sided.

REFERENCES

1. Raja S, Murthy SC, Mason DP. Malignant pleural mesothelioma. *Curr Oncol Rep* 2011; 13:259-64.
2. Robinson BM. Malignant pleural mesothelioma: an epidemiological perspective. *Ann Cardiothorac Surg* 2012; 1:491-6.
3. Yap TA, Aerts JG, Popat S, Fennell DA. Novel insights into mesothelioma biology and implications for therapy. *Nat Rev Cancer* 2017; 17:475-88.
4. Zalcman G, Mazieres J, Margery J, Greillier L, Audigier-Valette C, Moro-Sibilot D, Molinier O, Corre R, Monnet I, Gounant V, et al. Bevacizumab for newly diagnosed pleural mesothelioma in the Mesothelioma Avastin Cisplatin Pemetrexed Study (MAPS): a randomised, controlled, open-label, phase 3 trial. *Lancet* 2016; 387:1405-14.
5. Haas AR, Sterman DH. Malignant pleural mesothelioma: update on treatment options with a focus on novel therapies. *Clin Chest Med* 2013; 34:99-111.
6. Vogelzang NJ, Rusthoven JJ, Symanowski J, Denham C, Kaukel E, Ruffie P, Gatzemeier U, Boyer M, Emri S, Manegold C, et al. Phase III study of pemetrexed in combination with cisplatin versus cisplatin alone in patients with malignant pleural mesothelioma. *Journal of clinical oncology : official journal of the American Society of Clinical Oncology* 2003; 21:2636-44.
7. Treasure T, Lang-Lazdunski L, Waller D, Bliss JM, Tan C, Entwisle J, Snee M, O'Brien M, Thomas G, Senan S, et al. Extra-pleural pneumonectomy versus no extra-pleural pneumonectomy for patients with malignant pleural mesothelioma: clinical outcomes of the Mesothelioma and Radical Surgery (MARS) randomised feasibility study. *Lancet Oncol* 2011; 12:763-72.
8. Coulie PG, Van den Eynde BJ, van der Bruggen P, Boon T. Tumour antigens recognized by T lymphocytes: at the core of cancer immunotherapy. *Nature reviews Cancer* 2014; 14:135-46.
9. van der Burg SH, Arens R, Ossendorp F, van Hall T, Melief CJ. Vaccines for established cancer: overcoming the challenges posed by immune evasion. *Nature reviews Cancer* 2016; 16:219-33.
10. Lievense LA, Sterman DH, Cornelissen R, Aerts JG. Checkpoint Blockade in Lung Cancer and Mesothelioma. *Am J Respir Crit Care Med* 2017.
11. Borghaei H, Paz-Ares L, Horn L, Spigel DR, Steins M, Ready NE, Chow LQ, Vokes EE, Felip E, Holgado E, et al. Nivolumab versus Docetaxel in Advanced Nonsquamous Non-Small-Cell Lung Cancer. *N Engl J Med* 2015; 373:1627-39.
12. Brahmer J, Reckamp KL, Baas P, Crino L, Eberhardt WE, Poddubskaya E, Antonia S, Pluzanski A, Vokes EE, Holgado E, et al. Nivolumab versus Docetaxel in Advanced Squamous-Cell Non-Small-Cell Lung Cancer. *N Engl J Med* 2015; 373:123-35.
13. Motzer RJ, Escudier B, McDermott DF, George S, Hammers HJ, Srinivas S, Tykodi SS, Sosman JA, Procopio G, Plimack ER, et al. Nivolumab versus Everolimus in Advanced Renal-Cell Carcinoma. *N Engl J Med* 2015; 373:1803-13.
14. Reck M, Rodriguez-Abreu D, Robinson AG, Hui R, Czoszi T, Fulop A, Gottfried M, Peled N, Tafreshi A, Cuffe S, et al. Pembrolizumab versus Chemotherapy for PD-L1-Positive Non-Small-Cell Lung Cancer. *N Engl J Med* 2016; 375:1823-33.
15. Maverakis E, Cornelius LA, Bowen GM, Phan T, Patel FB, Fitzmaurice S, He Y, Burrall B, Duong C, Kloxin AM, et al. Metastatic melanoma - a review of current and future treatment options. *Acta Derm Venereol* 2015; 95:516-24.
16. Housseau F, Llosa NJ. Immune checkpoint blockade in microsatellite instable colorectal cancers: Back to the clinic. *Oncoimmunology* 2015; 4:e1008858.
17. Dobrzanski MJ. Expanding roles for CD4 T cells and their subpopulations in tumor immunity and therapy. *Front Oncol* 2013; 3:63.

18. Dammeijer F, Lievense LA, Veerman GD, Hoogsteden HC, Hegmans JP, Arends LR, Aerts JG. Efficacy of Tumor Vaccines and Cellular Immunotherapies in Non-Small-Cell Lung Cancer: A Systematic Review and Meta-Analysis. *J Clin Oncol* 2016; 34:3204-12.
19. Hegmans JP, Veltman JD, Lambers ME, de Vries IJ, Figdor CG, Hendriks RW, Hoogsteden HC, Lambrecht BN, Aerts JG. Consolidative dendritic cell-based immunotherapy elicits cytotoxicity against malignant mesothelioma. *Am J Respir Crit Care Med* 2010; 181:1383-90.
20. Hegmans JP, Aerts JG. Immunomodulation in cancer. *Curr Opin Pharmacol* 2014; 17:17-21.
21. Drake CG, Jaffee E, Pardoll DM. Mechanisms of immune evasion by tumors. *Advances in immunology* 2006; 90:51-81.22. V i n a y DS, Ryan EP, Pawelec G, Talib WH, Stagg J, Elkord E, Lichtor T, Decker WK, Whelan RL, Kumara HM, et al. Immune evasion in cancer: Mechanistic basis and therapeutic strategies. *Seminars in cancer biology* 2015; 35 Suppl:S185-98.
23. Bjoern J, Brimnes MK, Andersen MH, Thor Straten P, Svane IM. Changes in peripheral blood level of regulatory T cells in patients with malignant melanoma during treatment with dendritic cell vaccination and low-dose IL-2. *Scand J Immunol* 2011; 73:222-33.
24. Miyara M, Yoshioka Y, Kitoh A, Shima T, Wing K, Niwa A, Parizot C, Taflin C, Heike T, Valeyre D, et al. Functional delineation and differentiation dynamics of human CD4+ T cells expressing the FoxP3 transcription factor. *Immunity* 2009; 30:899-911.
25. Santegoets SJ, Dijkgraaf EM, Battaglia A, Beckhove P, Britten CM, Gallimore A, Godkin A, Gouttefangeas C, de Gruijl TD, Koenen HJ, et al. Monitoring regulatory T cells in clinical samples: consensus on an essential marker set and gating strategy for regulatory T cell analysis by flow cytometry. *Cancer immunology, immunotherapy : CII* 2015; 64:1271-86.
26. Hegmans JP, Hemmes A, Hammad H, Boon L, Hoogsteden HC, Lambrecht BN. Mesothelioma environment comprises cytokines and T-regulatory cells that suppress immune responses. *The European respiratory journal* 2006; 27:1086-95.
27. Ireland DJ, Kissick HT, Beilharz MW. The Role of Regulatory T Cells in Mesothelioma. *Cancer microenvironment : official journal of the International Cancer Microenvironment Society* 2012; 5:165-72.
28. McCoy MJ, Nowak AK, van der Most RG, Dick IM, Lake RA. Peripheral CD8(+) T cell proliferation is prognostic for patients with advanced thoracic malignancies. *Cancer immunology, immunotherapy : CII* 2013; 62:529-39.
29. Motoyoshi Y, Kaminoda K, Saitoh O, Hamasaki K, Nakao K, Ishii N, Nagayama Y, Eguchi K. Different mechanisms for anti-tumor effects of low- and high-dose cyclophosphamide. *Oncol Rep* 2006; 16:141-6.30. Ghiringhelli F, Menard C, Puig PE, Ladoire S, Roux S, Martin F, Solary E, Le Cesne A, Zitvogel L, Chauffert B. Metronomic cyclophosphamide regimen selectively depletes CD4+CD25+ regulatory T cells and restores T and NK effector functions in end stage cancer patients. *Cancer immunology, immunotherapy : CII* 2007; 56:641-8.
31. Kan S, Hazama S, Maeda K, Inoue Y, Homma S, Koido S, Okamoto M, Oka M. Suppressive effects of cyclophosphamide and gemcitabine on regulatory T-cell induction in vitro. *Anticancer Res* 2012; 32:5363-9.
32. Heylmann D, Bauer M, Becker H, van Gool S, Bacher N, Steinbrink K, Kaina B. Human CD4+CD25+ regulatory T cells are sensitive to low dose cyclophosphamide: implications for the immune response. *PLoS one* 2013; 8:e83384.
33. Veltman JD, Lambers ME, van Nimwegen M, de Jong S, Hendriks RW, Hoogsteden HC, Aerts JG, Hegmans JP. Low-dose cyclophosphamide synergizes with dendritic cell-based immunotherapy in antitumor activity. *J Biomed Biotechnol* 2010; 2010:798467.
34. Cornelissen R, Hegmans JP, Maat AP, Kaijen-Lambers M, Bezemer K, Hendriks RW, Hoogsteden HC, Aerts JG. Extended Tumor Control after Dendritic Cell Vaccination with Low-Dose Cyclophosphamide as Adjuvant Treatment in Patients with Malignant Pleural Mesothelioma. *Am J Respir Crit Care Med* 2016; 193:1023-31.

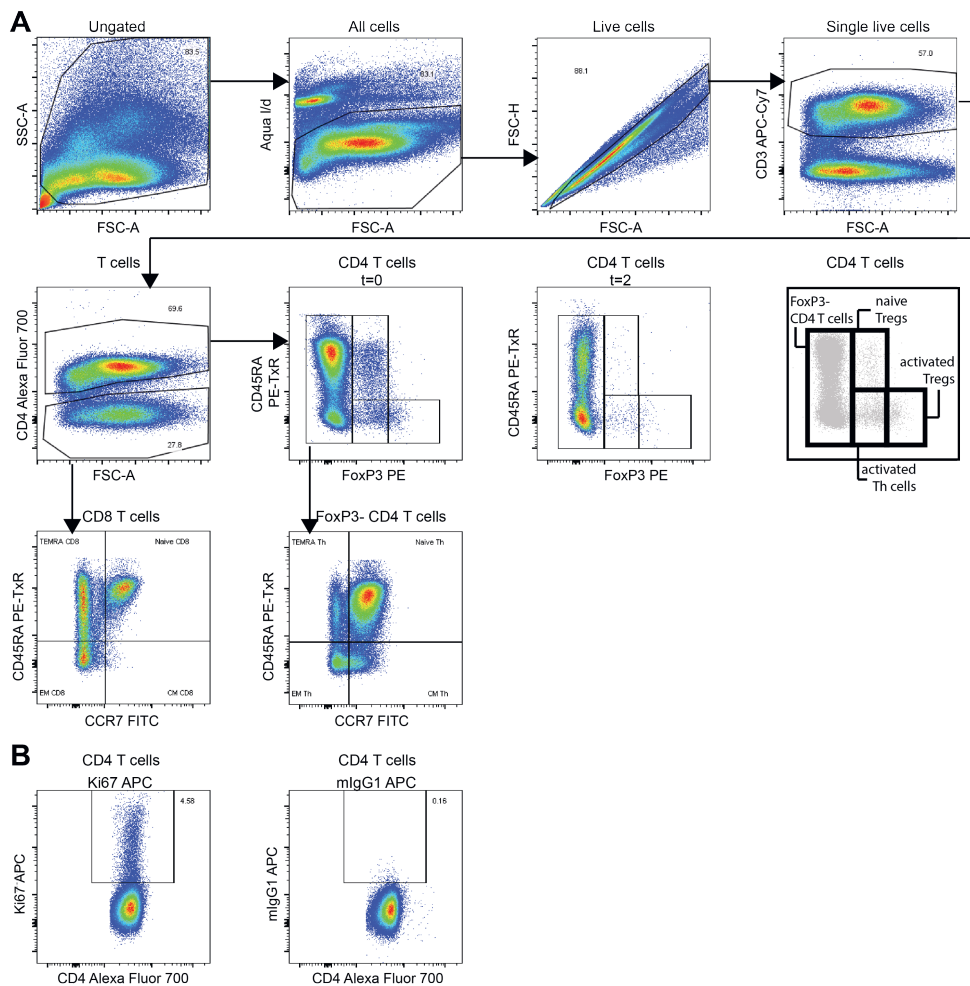
35. Zhang S, Pan SB, Lyu QH, Wu P, Qin GM, Wang Q, He ZL, He XM, Wu M, Chen G. Postoperative Regulatory T-Cells and Natural Killer Cells in Stage I Nonsmall Cell Lung Cancer Underwent Video-assisted Thoracoscopic Lobectomy or Thoracotomy. *Chin Med J (Engl)* 2015; 128:1502-9.
36. Chen C, Chen D, Zhang Y, Chen Z, Zhu W, Zhang B, Wang Z, Le H. Changes of CD4+CD25+FOXP3+ and CD8+CD28-regulatory T cells in non-small cell lung cancer patients undergoing surgery. *Int Immunopharmacol* 2014; 18:255-61.
37. Ge Y, Domschke C, Stoiber N, Schott S, Heil J, Rom J, Blumenstein M, Thum J, Sohn C, Schneeweiss A, et al. Metronomic cyclophosphamide treatment in metastasized breast cancer patients: immunological effects and clinical outcome. *Cancer Immunol Immunother* 2012; 61:353-62.
38. Wu J, Waxman DJ. Metronomic cyclophosphamide schedule-dependence of innate immune cell recruitment and tumor regression in an implanted glioma model. *Cancer Lett* 2014; 353:272-80.
39. Madondo MT, Quinn M, Plebanski M. Low dose cyclophosphamide: Mechanisms of T cell modulation. *Cancer Treat Rev* 2016; 42:3-9.
40. Matar P, Rozados VR, Gervasoni SI, Scharovsky GO. Th2/Th1 switch induced by a single low dose of cyclophosphamide in a rat metastatic lymphoma model. *Cancer Immunol Immunother* 2002; 50:588-96.
41. Schiavoni G, Mattei F, Di Pucchio T, Santini SM, Bracci L, Belardelli F, Proietti E. Cyclophosphamide induces type I interferon and augments the number of CD44(hi) T lymphocytes in mice: implications for strategies of chemoimmunotherapy of cancer. *Blood* 2000; 95:2024-30.
42. Bracci L, Moschella F, Sestili P, La Sorsa V, Valentini M, Canini I, Baccarini S, Maccari S, Ramoni C, Belardelli F, et al. Cyclophosphamide enhances the antitumor efficacy of adoptively transferred immune cells through the induction of cytokine expression, B-cell and T-cell homeostatic proliferation, and specific tumor infiltration. *Clin Cancer Res* 2007; 13:644-53.
43. Podrazil M, Horvath R, Becht E, Rozkova D, Bilkova P, Sochorova K, Hromadkova H, Kayserova J, Vavrova K, Lastovicka J, et al. Phase I/II clinical trial of dendritic-cell based immunotherapy (DCVAC/PCa) combined with chemotherapy in patients with metastatic, castration-resistant prostate cancer. *Oncotarget* 2015; 6:18192-205.
44. Liston A, Gray DH. Homeostatic control of regulatory T cell diversity. *Nat Rev Immunol* 2014; 14:154-65.
45. Booth NJ, McQuaid AJ, Sobande T, Kissane S, Agius E, Jackson SE, Salmon M, Falciani F, Yong K, Rustin MH, et al. Different proliferative potential and migratory characteristics of human CD4+ regulatory T cells that express either CD45RA or CD45RO. *J Immunol* 2010; 184:4317-26.
46. Wang C, Lee JH, Kim CH. Optimal population of FoxP3+ T cells in tumors requires an antigen priming-dependent trafficking receptor switch. *PloS one* 2012; 7:e30793.47. Kwa M, Li X, Novik Y, Oratz R, Jhaveri K, Wu J, Gu P, Meyers M, Muggia F, Speyer J, et al. Serial immunological parameters in a phase II trial of exemestane and low-dose oral cyclophosphamide in advanced hormone receptor-positive breast cancer. *Breast Cancer Res Treat* 2018; 168:57-67.
48. Prieto GA, Rosenstein Y. Oestradiol potentiates the suppressive function of human CD4 CD25 regulatory T cells by promoting their proliferation. *Immunology* 2006; 118:58-65.
49. Sundar R, Cho BC, Brahmer JR, Soo RA. Nivolumab in NSCLC: latest evidence and clinical potential. *Therapeutic advances in medical oncology* 2015; 7:85-96.
50. Johnson DB, Peng C, Sosman JA. Nivolumab in melanoma: latest evidence and clinical potential. *Therapeutic advances in medical oncology* 2015; 7:97-106.
51. Sugiyama D, Nishikawa H, Maeda Y, Nishioka M, Tanemura A, Katayama I, Ezoe S, Kanakura Y, Sato E, Fukumori Y, et al. Anti-CCR4 mAb selectively depletes effector-type FoxP3+CD4+ regulatory T cells, evoking antitumor immune responses in humans. *Proc Natl Acad Sci U S A* 2013; 110:17945-50.

52. Kurose K, Ohue Y, Sato E, Yamauchi A, Eikawa S, Isobe M, Nishio Y, Uenaka A, Oka M, Nakayama E. Increase in activated Treg in TIL in lung cancer and in vitro depletion of Treg by ADCC using an antihuman CCR4 mAb (KM2760). *J Thorac Oncol* 2015; 10:74-83.

Supplementary Table S1. Antibodies used for flowcytometry

Marker	Clone	Conjugate	Company	Cat#	Used in panel
CCR4	1G1	BV605	BD Biosciences	562906	Treg
CCR7	150503	FITC	R&D Systems	FAB197F-100	Treg
CD3	UCHT1	APC-eFluor780	eBioscience	47-0038-42	Treg, IS
CD3	UCHT1	PE-CF594	BD Biosciences	562280	Cytokines
CD4	RPA-T4	AlexaFluor 700	eBioscience	56-0049-42	Treg, IS
CD4	SK3	PE-Cy7	BD Biosciences	557852	Cytokines
CD8	RPA-T8	V450	BD Biosciences	560347	IS
CD8	RPA-T8	APC	eBioscience	17-0088-42	Cytokines
CD11c	B-ly6	PE	BD Biosciences	555392	IS
CD14	61D3	FITC	eBioscience	11-0149-42	IS
CD16	3G8	PerCP-Cy5.5	BD Biosciences	338440	IS
CD19	J3-119	ECD	Beckman Coulter	A07770	IS
CD25	M-A251	PE-Cy7	BD Biosciences	557741	Treg
CD45RA	MEM-56	PE-TexasRed	Invitrogen Life Technologies	MHCD45RA17	Treg
CD56	B159	PE-Cy7	BD Biosciences	557747	IS
CD127	HIL-7R-M21	V450	BD Biosciences	560823	Treg
CTLA-4	14D3	PerCP-eFluor710	eBioscience	46-1529-42	Treg
FoxP3	236A/E7	PE	eBioscience	12-4777-42	Treg
GranzymeB	GB12	PE	Caltag laboratories	MHGB04	Cytokines
IFN γ	4S.B3	PerCP-Cy5.5	eBioscience	45-7319-42	Cytokines
Ki67	20Raj1	APC	eBioscience	17-5699-42	Treg
TCR $\gamma\delta$	B1	APC	BD Biosciences	555718	IS

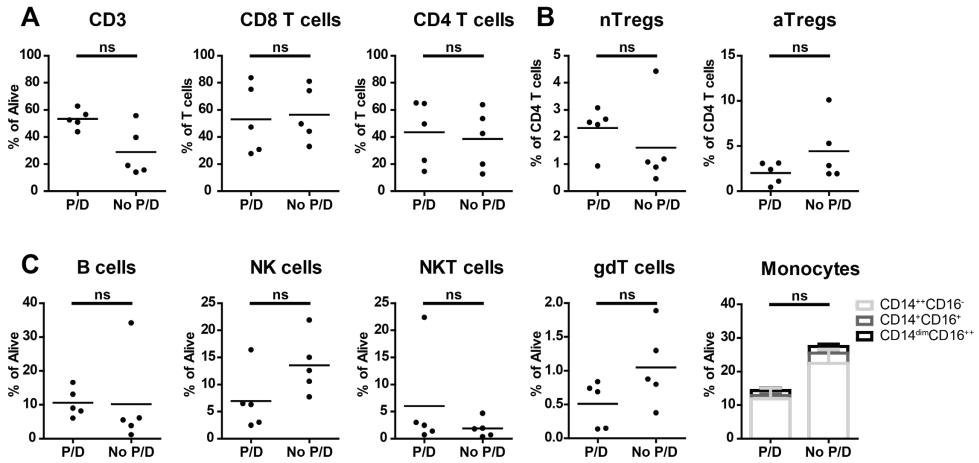
Abbreviations: IS, immune subsets



Supplementary Figure S1. Gating strategy of Tregs.

To characterize Tregs and the CD4 and CD8 T cell subsets, the following gating strategy was used. **A**. First the debris was gated out based on FSC, SSC. Then live cells were selected based on aqua I/d staining and consecutively single cells were selected based on FSC-H and FSC-A. Out of the single live cells the T cells were gated, based on CD3 expression. Then, CD4 T cells were gated upon CD4 expression and the negative population was considered CD8 T cells. The CD4 T cells were then analyzed for CD45RA and FoxP3 expression; in which we gated for FoxP3- CD4 T cells, nTregs (CD45RA+FoxP3med), aTregs (CD45RA-FoxP3hi) and aThcells (CD45RA-FoxP3med). Lastly, both FoxP3- CD4 T cells and CD8 T cells were plotted using CD45RA and CCR7, resulting in the naïve (CD45RA+CCR7+, CM (CD45RA-CCR7+), EM (CD45RA-CCR7-) and TEMRA (CD45RA+CCR7-) subpopulations. **B** The gate for Ki67+ cells was set using a mlgG1 isotype control.

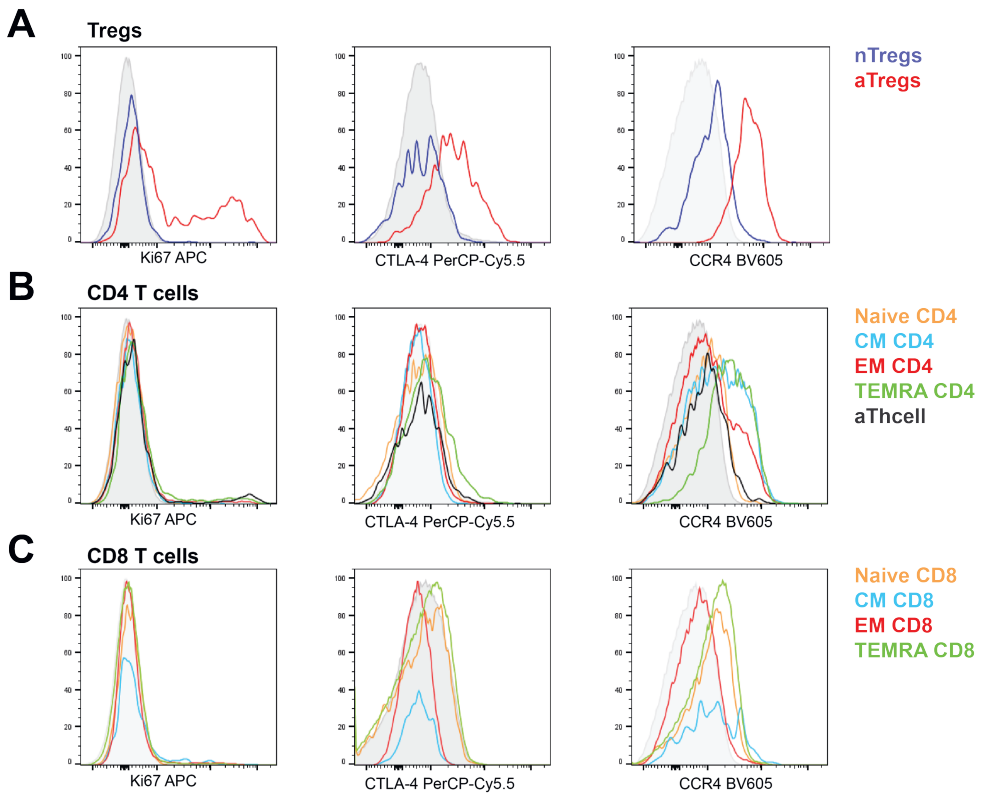
Representative patient is shown (MM02-2).



Supplementary Figure S2. No differences in T cell and other immune cell subsets between P/D and no P/D patients.

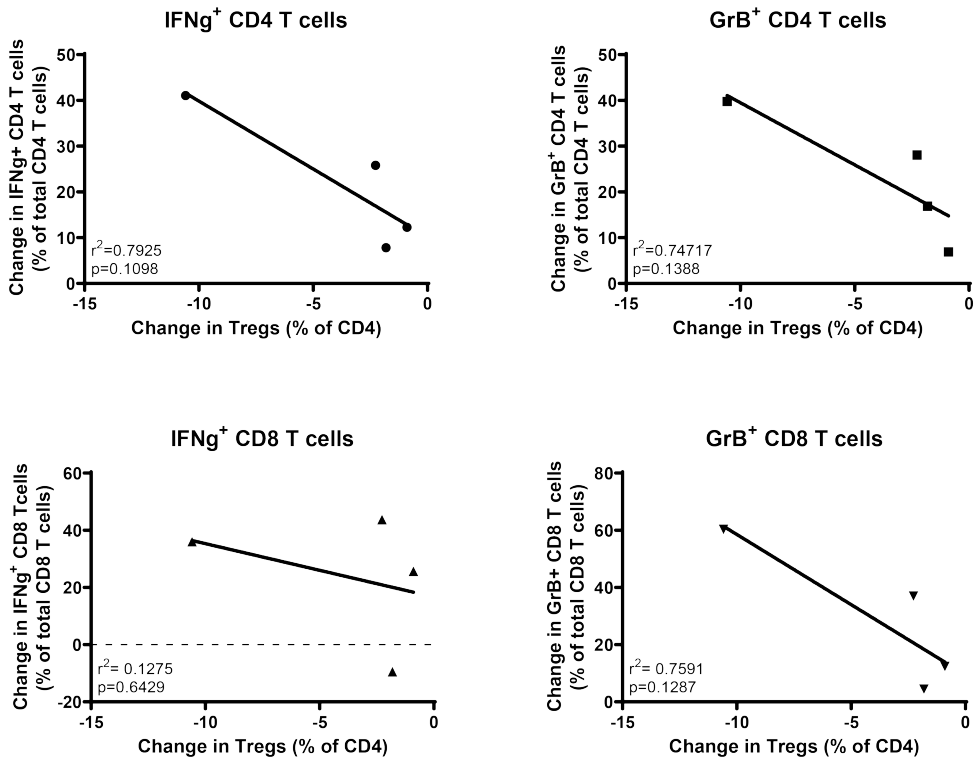
Before DC/mCTX immunotherapy, 5 patients were treated with pleurectomy/decortication (P/D) to reduce tumor load and thereby immunosuppressive regulatory T cells (Tregs). To evaluate the effects on Treg and T cell constitution and proliferation, PBMCs, obtained at $t=0$ were phenotyped using flowcytometry to determine the proportions of different T cell populations, B cells, NK cells, NKT cells, $\gamma\delta$ T cells and monocytes. **A.** Total T cells, CD4 and CD8 T cells were comparable between P/D and no P/D patients. **B.** The proportion of the two Treg subsets did not differ significantly between the P/D and the non P/D group. **C.** None of the other cell populations (B cells, NK cells, NKT cells, $\gamma\delta$ T cells and monocytes) were significantly different between the P/D and the no P/D group.

Results represent mean \pm Standard Error of the Mean (SEM) ($n=5$, per group), ns = not significant (Mann-Whitney U test).



Supplementary Figure S3 - Expression of Ki67, CTLA-4 and CCR4 within the different subsets of Tregs.

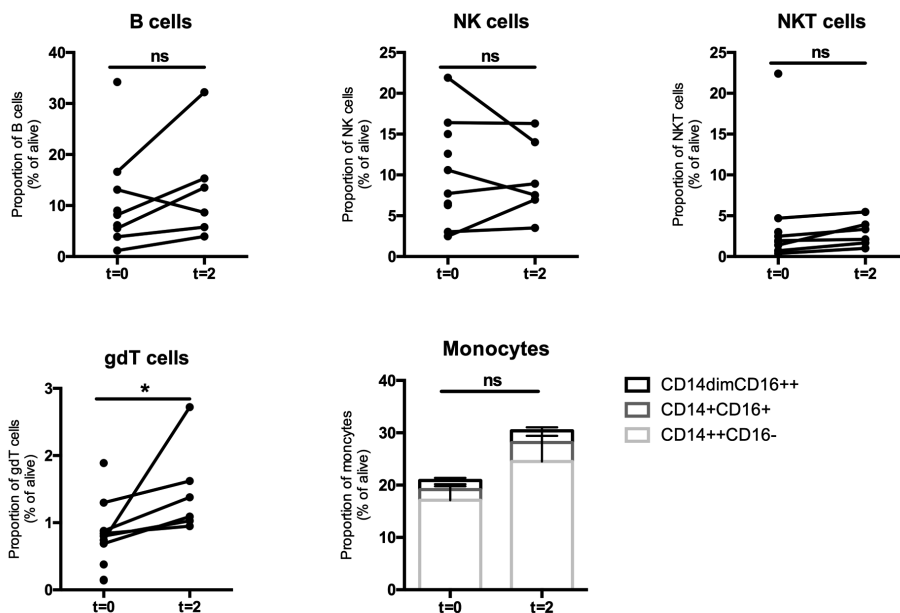
The expression of Ki67, CTLA-4 and CCR4 are highest within the activated Tregs, confirming their activated and immunosuppressive status. **A.** Naïve and activated Tregs were gated according to Supplementary Figure 1, populations are shown in a representative patient (MM02_7) at t=0. nTregs are depicted in blue, aTregs in red, and in grey the isotype control is shown (Ki67 APC, CCR4 BV605) or the expression in the total T cell population (CTLA-4 PerCP-Cy5.5). Expression of the proliferation marker Ki67 (left), the immune checkpoint CTLA-4 (middle) and the chemokine receptor CCR4 (right) within the two subsets of Tregs, all showed high expression within the aTregs (red) and low expression in nTregs (blue). **B.** The expression of Ki67, CTLA-4 and CCR4 were also analyzed for the subpopulations of FoxP3+ CD4 T cells and FoxP3+ aThcells. Ki67 expression is low in all subsets, and highest in aThcells (black). CTLA-4 expression is low in all subsets, highest in TEMRA C4 T cells (green) and CCR4 is expressed on TEMRA (green), CM (blue) and EM (red) CD4 T cells. **C.** In CD8 T cells the expression of Ki67 and CTLA-4 is low in all subsets, CCR4 is expressed on naïve (orange), CM (blue) and TEMRA (green) CD8 T cells.



Supplementary Figure S4. The change in IFN γ -producing and GrB-containing T cells possibly inversely correlates with the change in Tregs.

To determine whether the increase in IFN-producing and GrB-containing CD4+ and CD8+ T cells upon treatment with mCTX correlated with the decrease in Tregs (aTregs + nTregs as proportion of CD4 T cells) upon treatment with mCTX, linear regression was performed. For this, we correlated the differences between t=0 and t=2 between the different cell populations. For this analysis, only four datapoints were available, which showed that IFN-producing CD4+ T cells and GrB-containing CD4+ and CD8+ T cells seemed to correlate with the decrease in Tregs, however, these correlations are non-significant.

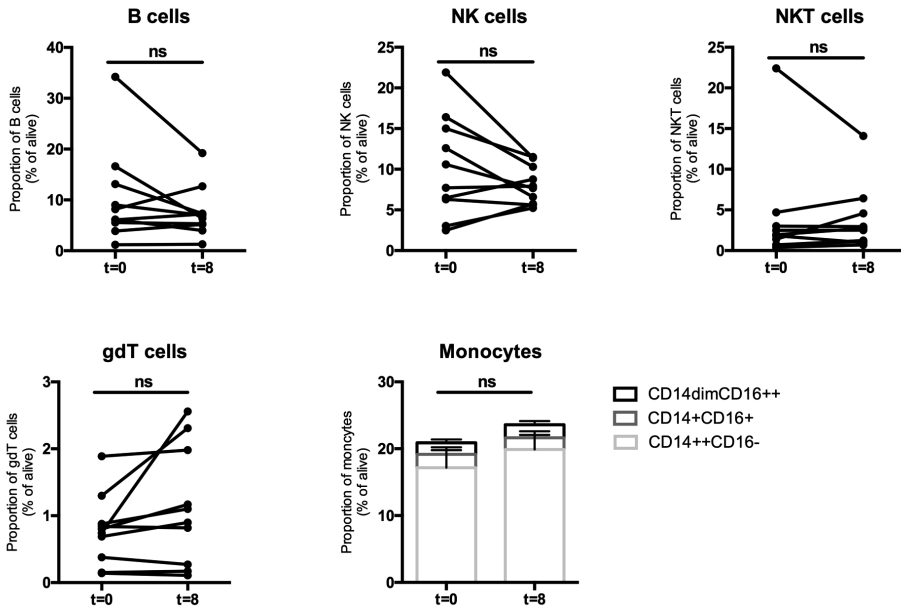
Statistical analysis was performed by log-rank (Mantel-Cox) testing, and differences were considered significant when $p < 0.05$.



Supplementary Figure S5. mCTX does not affect B/NK/NKT cells and monocytes, it increases the proportion of gdT cells.

To determine the effect of mCTX administration on B cells, NK cells, NKT cells, $\gamma\delta$ T cells and monocytes, flowcytometric analysis was performed on PBMCs obtained at t=0 and t=2, and thereby comparing baseline proportions with the proportions after mCTX administration. The percentage of B cells, NK cells, NKT cells and monocytes did not change upon mCTX treatment, the percentage of $\gamma\delta$ T cells increased.

Results represent mean \pm Standard Error of the Mean (SEM). *P<0.05, and ns = not significant (Wilcoxon matched-pairs signed rank test).

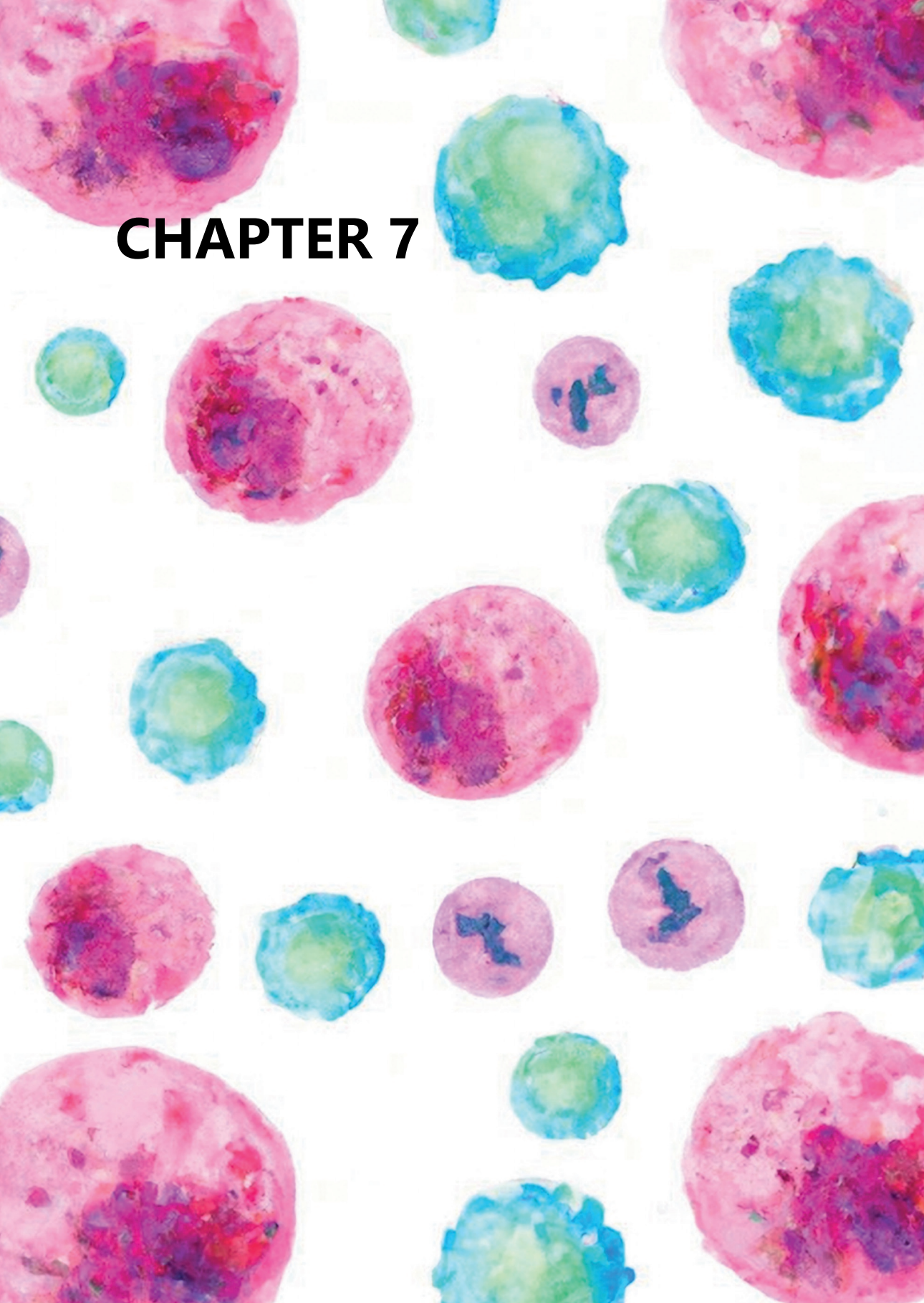


Supplementary Figure S6. DC/mCTX-based immunotherapy does not change proportions of B/ NK/NKT/gdT cells and monocytes.

To determine the effects of DC/mCTX-based immunotherapy on B cells, NK cells, NKT cells, $\gamma\delta$ T cells and monocytes, flowcytometric analysis of PBMCs obtained at t=0 (baseline) and t=8 (after completing DC/mCTX-based immunotherapy) were compared. Changes in immune cell subsets were not significant.

Results represent mean \pm Standard Error of the Mean (SEM). ns = not significant (Wilcoxon matched-pairs signed rank test).

CHAPTER 7



SUMMARY AND DISCUSSION

The aim of this thesis was to explore several methods to improve the results of cancer (immuno)therapy. It has been consistently shown consistently that there is no “one-size-fits-all” cancer therapy. Immune checkpoint blockade has shown the most progress, and has led to promising long-term responses, but it fails either directly or after development of treatment resistance, in the majority of patients.¹ The tumor cells employ different mechanisms to evade the immune system, many have been characterized, and more continue to be revealed. By elucidating and co-targeting these mechanisms of resistance, or by preventing these mechanisms of resistance to come into effect, treatments can be tailored to improve clinical outcomes.

In this context it is important to refer to Chen and Mellman, who have introduced the cancer immunity cycle, which envisions that anti-tumor T-cell responses progress through seven steps.² All seven of these steps can be targeted to improve the anti-tumor immune response (**Figure 1**). The mechanisms employed by the tumor also come into play in this cycle, for example, the expression of inhibitory checkpoint receptors inhibits both priming and activation of T-cells and killing of cancer cells. This proposed classification of anti-cancer immunity provides a convenient framework for discussing the

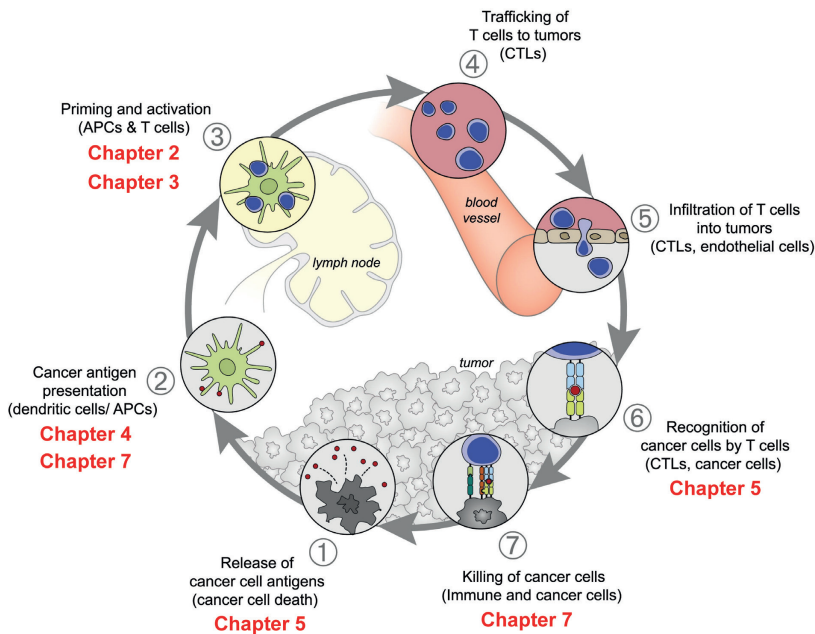


Figure 1. The Cancer Immunity Cycle.

Overview of the induction and maintenance of an anti-tumor immune response, a cyclic process which can amplify itself, leading to a broadened and intensified T cell response. The cycle includes 7 steps, the steps investigated in this thesis are indicated per chapter (in red) and described in the text.

APC, antigen presenting cell; CTL, cytotoxic T lymphocyte.

Adapted from Chen and Mellman²

results that were obtained in this thesis; five out of the seven steps postulated by Chen and Mellman have been explored. In this discussion, the results obtained from our studies are discussed in the context of this cycle.

Release of cancer cell antigens

The first step of any adaptive immune response is the presentation of antigens to the immune system. In many histological types of cancer, it has been implied that treatment with chemotherapy, radiation therapy and targeted therapies induce the release of tumor associated antigens (TAAs).³ Moreover, the immune composition is a major predictive factor in the response of patients to both conventional and targeted antitumor therapy,⁴ and in turn, these agents also modulate the composition and functionality of the immune cells infiltrating the tumor, and thereby influence the outcome.⁵ In hepatocellular carcinoma (HCC) it has been hypothesized that cancer cells release tumor antigens upon treatment with either radiofrequency ablation (RFA) or trans-arterial chemo-embolization (TACE),^{6, 7} and it has been shown that combination treatment of subtotal RFA or TACE with tremelimumab (anti-cytotoxic T-lymphocyte associated protein 4 [CTLA4]) led to increased intratumoral CD8 T-cell infiltration.⁸ In **Chapter 5** we determined peripheral immune cell responses upon RFA and TACE therapy in HCC patients. Although we could detect both B and T-cell responses, we could not establish a correlation between these peripheral immune responses and the local therapies. However, we did find increased expression of CD137 on TAA-specific T-cells upon RFA/TACE. A possible interpretation would be that the TAA-specific T-cells migrate to the tumor and do not reside in the periphery, hampering their detection. As we did not perform tumor biopsies, we cannot dismiss this possibility. Future research may focus on determining an increase of TAA-specific tumor-infiltrating lymphocytes (TIL) to evaluate local ablation as a feasible therapy to stimulate the release of cancer cell antigens.

Cancer antigen presentation

In the absence of efficient loading of antigen presenting cells by endogenous cancer antigens, exogenous sources of these antigens may prove useful to elicit anticancer immunity. Most attempts regarding cancer antigen presentation have involved therapeutic vaccines, as they can be easily deployed and have been successful historically in combating microbial and viral infections.⁹ As mentioned previously, they have mostly led to minimal anticancer immune responses, with the exception of the preventive human papillomavirus (HPV) vaccination,¹⁰ and they are limited on multiple factors. First, as historically vaccines were used to prevent microbial infections, there was a general lack of understanding on how to achieve potent CD8 T-cell responses. Secondly, the immunosuppressive tumor micro-environment may dampen a successfully established anti-tumor T-cell response, and therefore the effects of successful vaccinations may be obscured. Moreover, appropriate tumor antigens need to be identified, and it also needs to be established how to best deliver them to patients.

In **Chapter 4** we aimed to identify tumor antigens expressed in HCC that can be used for therapeutic vaccination, but that could also be conceivably used for therapeutic targeting of cancer in any other way

(e.g. for targeting cancer ablating radionuclides to tumors). Here we identified 12 cancer-testis antigens (CTAs) expressed in approximately 80% of HCC patients, which individually are expressed in at least 10% of HCC patients. Most patients expressed more than one CTA, allowing for targeting of multiple CTAs per patient. This increases the chance of inducing a sufficiently robust T-cell response. Moreover, several of these CTAs, such as the melanoma-associated antigen (MAGE)-family members, testis-specific Y-encoded protein (TSPY) and cancer antigen 1 (CAGE1), are functionally involved in tumorigenesis and cancer progression by modulating gene expression, regulating mitosis and tumorigenic signaling.^{11, 12} Involvement of these CTAs in cancer progression may prevent antigen loss upon therapeutic targeting.⁹ ¹³ Recently, however, the focus has been on neo-antigens, as these are mutated, non-self antigens and are therefore thought to induce more robust immune responses. These antigens vary from patient to patient and may even be heterogeneously expressed within a single tumor. Additionally, expression of these neo-antigens does not assure their immunogenicity. The use of intact proteins, or full-length ribonucleic acid (RNA) that are translated into intact proteins, may mitigate this issue. There are also other strategies, amongst which is adoptive transfer of antigen-loaded dendritic cells (DC), described in **Chapter 6**. An advantage of the latter approach is that, as for this study the DCs were loaded with autologous tumor lysate, there is no requirement for knowing the exact tumor antigens. Therapeutic DC vaccinations however, need to be produced for each patient individually. This is a very laborious process, hampering implementation outside the setting of clinical studies. Moreover, the availability of autologous tumor material is a limitation for some patients, making it not universally applicable. Nevertheless, this approach turned out to be feasible and led to remarkable outcomes, with two patients still being alive after six years (**Chapter 6**). To overcome the limitation of available autologous tumor material, the use of a lysate derived of six allogeneic mesothelioma cell lines has been tested and was shown to be successful, as it led to both immunological and clinical responses.¹⁴

Priming and activation

Even if specific antigens can be adequately presented to the immune system, clinically relevant immunity requires effective stimulation of the effector lymphocytes. Priming and activation of tumor-specific T-cells is the presumed main mechanism of action for anti-CTLA-4 antibodies and can be enhanced in a multitude of ways.¹⁵ Antibodies targeting co-stimulatory molecules, such as agonistic anti-CD137, anti-glucocorticoid-induced tumor necrosis factor receptor [TNFR]-related protein (GITR) and anti-CD27 are thought to act mainly via this mechanism.¹⁶⁻¹⁸ During antigen presentation in lymphoid organs, these monoclonal antibodies (mAb) either reverse the inhibition of T-cell responses or stimulate the T-cells, and thus promote T-cell responses. In **Chapter 2** multiple checkpoint inhibitors (CPI) were assessed in the context of liver metastases of colorectal cancer (LM-CRC). Programmed death protein 1 (PD-1) and programmed death-ligand 1 (PD-L1) blocking antibodies were previously proven unsuccessful in colorectal carcinoma (CRC) patients, however, the role of immune checkpoint pathways in LM-CRC had not been studied yet. Intratumoral CD4 and CD8 T-cells showed increased expression of checkpoint receptors compared to CD4 and CD8 T-cells in blood and tumor-free liver tissues, suggesting these

molecules play a role in intra-tumoral immune suppression. Moreover, CD8 T-cells density was higher in LM-CRC than primary CRC. The differences between mismatch repair (MMR)-proficient LM-CRC and MMR-proficient CRC are to some extent comparable of those found by Llosa, et al., comparing MMR-proficient and MMR-deficient primary CRC.¹⁹ As patients with MMR-deficient CRC respond better to CPI compared to MMR-proficient CRC, these difference may indicate that LM-CRC are suitable for treatment with CPIs. In vitro anti-tumor TIL responses were most robustly enhanced by anti-lymphocyte-activation gene 3 (LAG3), suggesting that this might be the most promising CPI in treatment of LM-CRC.

In **Chapter 3** we investigated the possibilities of the bispecific mAb CD137xPD-L1 to activate tumor derived T-cells. Similarly to the antagonistic CTLA-4 mAb ipilimumab, the agonistic CD137 mAb urelumab was accompanied with significant immune-related toxicities. These toxicities were thought to be caused by a lack of selectivity, as both ipilimumab and urelumab cause general, non-specific T-cell activation.²⁰⁻²² Urelumab is a strong agonistic mAb that does not rely on Fc gamma receptor (FcγR-) mediated crosslinking to stimulate T-cells. The dependency on crosslinking is a hallmark of the human TNFR family, in which three receptor units bind to a single homotrimeric ligand. Generally two or more of these ligand-receptor complexes need to cluster on the cell membrane to induce sufficient receptor signaling.²³ The observed hepatotoxicity in patients treated with urelumab may have been caused by the interaction of this mAb with FcγRIIB expressed by liver sinusoidal endothelial cells, macrophages and dendritic cells, which led to superactivation of hepatic T-cells.^{24, 25} In this chapter, we have used Fc-silenced antibodies to abrogate such interactions. The CD137xPD-L1 Biclonic is designed to promote target-mediated clustering of CD137. In theory, in the absence of PD-L1, minimal clustering should occur and therefore immune activation via CD137 will be limited. However, in the presence of PD-L1, crosslinking will induce CD137 activated signaling. As CD137 clustering and signal induction by this Biclonic is dependent on PD-L1, which is overexpressed in the tumor micro-environment, toxicities outside of the tumor micro-environment should be limited. It has also been shown that the PD1/PDL1 pathway is pivotal in tumor-draining lymph nodes.^{26, 27} As such, this bispecific CD137xPD-L1 Ab may also play a role in T-cell activation and priming in the lymph nodes. Nevertheless, this therapy will also have an effect on the last step of the cancer immunity cycle, "killing of cancer cells", and will be discussed further in that paragraph.

Recognition of cancer cells by T-cells

Even in the presence of effective stimulation of anti-cancer T lymphocytes, a lack of cancer cell recognition by the thus-activated immune compartment can become a rate limiting step for effective treatment. In **Chapter 5** we tested the ability of the immune system to recognize the CTAs identified in **Chapter 4**. Expression of tumor antigens at protein or RNA level does not assure the ability of T-cells to recognize these tumor antigens. As such, we determined the immunogenicity of the CTAs included in this panel. Several of them have previously been proven immunogenic, in both HCC and other types of cancers. In HCC patients both cellular and humoral responses have already been identified against several of these antigens. MAGE-A1-, MAGE-A10-, MAGE-C2- and New York Esophageal Squamous Cell

Carcinoma-1 (NY-ESO-1)-specific CD8+ T-cells²⁸⁻³³ and TSPY-specific IgG³⁴ have been detected. We are the first to demonstrate MAGE-A9, MAGE-B2, MAGE-C1 and PAGE family member 1 (PAGE1)-specific CD8+ T-cells in HCC patients, and we confirmed presence of MAGE-A1 and MAGE-C2-specific CD8+ T-cells. Previously, only MAGEC2 and NYESO1-specific CD4+ T-cells have been demonstrated.^{28, 31} In this chapter we additionally demonstrated the reactivity of CD4+ T-cells against all previously mentioned CTAs, which are required for a functional antitumor CD8+ T-cell response. Recently also their direct anti-tumor potency was demonstrated, as well as their role in directed a sustained anti-tumor response.³⁵ Additionally, the identified humoral responses are an extra indication for the immunogenicity of these CTAs. Taken together these CTAs seem promising candidates for cancer (immuno)therapy and should be explored in future studies.

Killing of cancer cells

In **Chapter 6** several of the vaccinated patients with malignant pleural mesothelioma had a long disease-free survival, whereas the median survival of mesothelioma patients is 11 months. This insinuates vaccination therapies have a great potential in inducing anti-tumor immune responses and killing of cancer cells, and thus, as an additional tool in cancer immunotherapy. However, patient numbers were small and no control group was included. Furthermore, there was no direct demonstration of either anti-tumor immune responses, or killing of tumor cells by the vaccination. Recently, tumor organoids have become a method to analyze and demonstrate the direct ability of T-cells to kill (autologous) tumor cells.³⁶ In recent mice studies it has not only been shown that tumor-specific T-cells are capable of killing tumor cells, but that the immunogenicity and epitope spreading of this process has been established as well.^{37, 38} Addition of immune checkpoint inhibitors, in particular bispecific antibodies, could further enhance tumor cell lysis. The CD137xPD-L1 Biclonic used in **Chapter 3** may function as a bridge between PD-L1 expressing tumor cells or intra-tumoral APCs and CD137 expressing T-cells, which could lead to increased killing of tumor cells or antigen-presentation to T-cells, respectively. Future research should elucidate whether the CTA-specific T-cells identified in **Chapter 5**, are capable of eliminating the cancer cells and create an immunogenic environment, completing the cycle.

Identification of patients at risk

These days patient stratification is considered to be an important element to achieve better clinical outcome and to avoid unnecessary side effects. We found that expression of the CTAs identified in **Chapter 4** in adjacent macroscopically tumor-free liver, correlates with tumor recurrence in HCC patients that underwent curative surgery; likely due to occult metastasis during the time of recurrence. This further emphasizes the relevance of these CTAs and opens new doors in the selection of patients eligible for (neo-)adjuvant treatment.

Final consideration

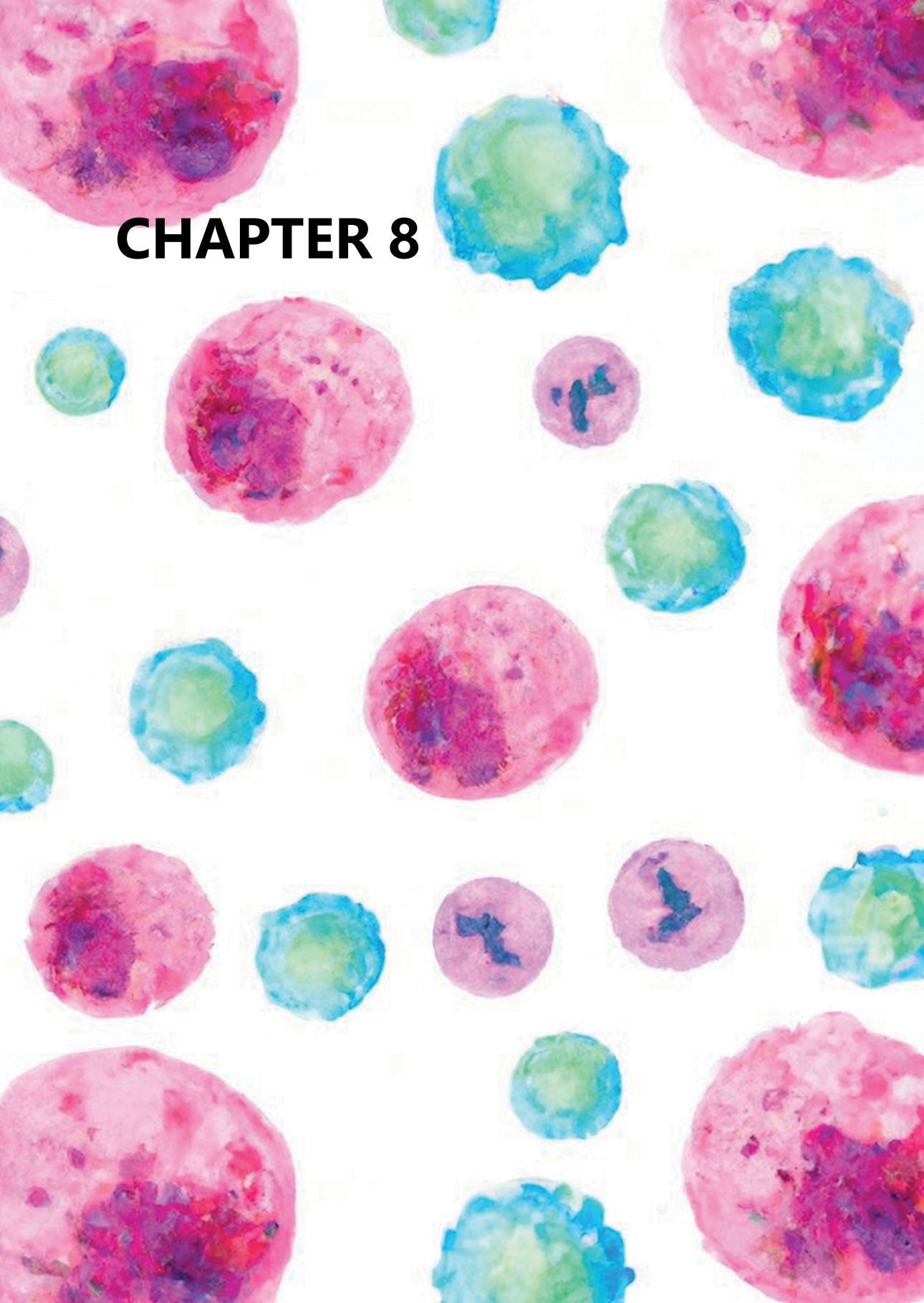
Using the cancer immunity cycle of Chen and Mellman as a framework to categorize the studies in this thesis, we have furthered insight into the anti-cancer immune response and provided foundations for further research to develop rational approaches aimed at employing immunity towards improved treatment of cancer.

REFERENCES

1. Fares CM, Van Allen EM, Drake CG, et al. Mechanisms of Resistance to Immune Checkpoint Blockade: Why Does Checkpoint Inhibitor Immunotherapy Not Work for All Patients? *Am Soc Clin Oncol Educ Book*. 2019;39:147-64.
2. Chen DS, Mellman I. Oncology meets immunology: the cancer-immunity cycle. *Immunity*. 2013;39(1):1-10.
3. Galluzzi L, Buque A, Kepp O, et al. Immunological Effects of Conventional Chemotherapy and Targeted Anticancer Agents. *Cancer Cell*. 2015;28(6):690-714.
4. Fridman WH, Pages F, Sautes-Fridman C, et al. The immune contexture in human tumours: impact on clinical outcome. *Nat Rev Cancer*. 2012;12(4):298-306.
5. Senovilla L, Vacchelli E, Galon J, et al. Trial watch: Prognostic and predictive value of the immune infiltrate in cancer. *Oncoimmunology*. 2012;1(8):1323-43.
6. Mizukoshi E, Yamashita T, Arai K, et al. Enhancement of tumor-associated antigen-specific T-cell responses by radiofrequency ablation of hepatocellular carcinoma. *Hepatology*. 2013;57(4):1448-57.
7. Mizukoshi E, Nakamoto Y, Arai K, et al. Enhancement of tumor-specific T-cell responses by transcatheter arterial embolization with dendritic cell infusion for hepatocellular carcinoma. *Int J Cancer*. 2010;126(9):2164-74.
8. Duffy AG, Ulahannan SV, Makorova-Rusher O, et al. Tremelimumab in combination with ablation in patients with advanced hepatocellular carcinoma. *J Hepatol*. 2017;66(3):545-51.
9. Palucka K, Banchereau J. Dendritic-cell-based therapeutic cancer vaccines. *Immunity*. 2013;39(1):38-48.
10. Drolet M, Benard E, Perez N, et al. Population-level impact and herd effects following the introduction of human papillomavirus vaccination programmes: updated systematic review and meta-analysis. *Lancet*. 2019;394(10197):497-509.
11. Gjerstorff MF, Andersen MH, Ditzel HJ. Oncogenic cancer/testis antigens: prime candidates for immunotherapy. *Oncotarget*. 2015;6(18):15772-87.
12. Whitehurst AW. Cause and consequence of cancer/testis antigen activation in cancer. *Annu Rev Pharmacol Toxicol*. 2014;54:251-72.
13. Maxfield KE, Taus PJ, Corcoran K, et al. Comprehensive functional characterization of cancer-testis antigens defines obligate participation in multiple hallmarks of cancer. *Nat Commun*. 2015;6:8840.
14. Aerts J, de Goeje PL, Cornelissen R, et al. Autologous Dendritic Cells Pulsed with Allogeneic Tumor Cell Lysate in Mesothelioma: From Mouse to Human. *Clin Cancer Res*. 2018;24(4):766-76.
15. Qureshi OS, Zheng Y, Nakamura K, et al. Trans-endocytosis of CD80 and CD86: a molecular basis for the cell-extrinsic function of CTLA-4. *Science*. 2011;332(6029):600-3.
16. Dharmadhikari B, Wu M, Abdullah NS, et al. CD137 and CD137L signals are main drivers of type 1, cell-mediated immune responses. *Oncoimmunology*. 2016;5(4):e1113367.
17. van de Ven K, Borst J. Targeting the T-cell costimulatory CD27/CD70 pathway in cancer immunotherapy: rationale and potential. *Immunotherapy*. 2015;7(6):655-67.
18. Sabharwal SS, Rosen DB, Grein J, et al. GITR Agonism Enhances Cellular Metabolism to Support CD8(+) T-cell Proliferation and Effector Cytokine Production in a Mouse Tumor Model. *Cancer Immunol Res*. 2018;6(10):1199-211.
19. Llosa NJ, Cruise M, Tam A, et al. The vigorous immune microenvironment of microsatellite instable colon cancer is balanced by multiple counter-inhibitory checkpoints. *Cancer Discov*. 2015;5(1):43-51.
20. Segal NH, Logan TF, Hodi FS, et al. Results from an Integrated Safety Analysis of Urelumab, an Agonist Anti-CD137 Monoclonal Antibody. *Clin Cancer Res*. 2017;23(8):1929-36.

21. Chester C, Sanmamed MF, Wang J, et al. Immunotherapy targeting 4-1BB: mechanistic rationale, clinical results, and future strategies. *Blood*. 2018;131(1):49-57.
22. Hodi FS, O'Day SJ, McDermott DF, et al. Improved survival with ipilimumab in patients with metastatic melanoma. *N Engl J Med*. 2010;363(8):711-23.
23. Wajant H. Principles of antibody-mediated TNF receptor activation. *Cell Death Differ*. 2015;22(11):1727-41.
24. Qi X, Li F, Wu Y, et al. Optimization of 4-1BB antibody for cancer immunotherapy by balancing agonistic strength with FcγR affinity. *Nat Commun*. 2019;10(1):2141.
25. Claus C, Ferrara C, Xu W, et al. Tumor-targeted 4-1BB agonists for combination with T-cell bispecific antibodies as off-the-shelf therapy. *Sci Transl Med*. 2019;11(496).
26. Fransen MF, Schoonderwoerd M, Knopf P, et al. Tumor-draining lymph nodes are pivotal in PD-1/PD-L1 checkpoint therapy. *JCI Insight*. 2018;3(23).
27. Dammeijer F, van Gulijk M, Mulder EE, et al. The PD-1/PD-L1-Checkpoint Restrains T-cell Immunity in Tumor-Draining Lymph Nodes. *Cancer Cell*. 2020.
28. Korangy F, Ormandy LA, Bleck JS, et al. Spontaneous tumor-specific humoral and cellular immune responses to NY-ESO-1 in hepatocellular carcinoma. *Clin Cancer Res*. 2004;10(13):4332-41.
29. Flecken T, Schmidt N, Hild S, et al. Immunodominance and functional alterations of tumor-associated antigen-specific CD8⁺ T-cell responses in hepatocellular carcinoma. *Hepatology*. 2014;59(4):1415-26.
30. Bricard G, Bouzourene H, Martinet O, et al. Naturally acquired MAGE-A10- and SSX-2-specific CD8⁺ T-cell responses in patients with hepatocellular carcinoma. *J Immunol*. 2005;174(3):1709-16.
31. Zhou G, Sprengers D, Boor PPC, et al. Antibodies Against Immune Checkpoint Molecules Restore Functions of Tumor-Infiltrating T-cells in Hepatocellular Carcinomas. *Gastroenterology*. 2017;153(4):1107-19 e10.
32. Shang XY, Chen HS, Zhang HG, et al. The spontaneous CD8⁺ T-cell response to HLA-A2-restricted NY-ESO-1b peptide in hepatocellular carcinoma patients. *Clin Cancer Res*. 2004;10(20):6946-55.
33. Inada Y, Mizukoshi E, Seike T, et al. Characteristics of Immune Response to Tumor-Associated Antigens and Immune Cell Profile in Patients With Hepatocellular Carcinoma. *Hepatology*. 2019;69(2):653-65.
34. Yin YH, Li YY, Qiao H, et al. TSPY is a cancer testis antigen expressed in human hepatocellular carcinoma. *Br J Cancer*. 2005;93(4):458-63.
35. Tay RE, Richardson EK, Toh HC. Revisiting the role of CD4(+) T-cells in cancer immunotherapy-new insights into old paradigms. *Cancer Gene Ther*. 2020.
36. Dijkstra KK, Cattaneo CM, Weeber F, et al. Generation of Tumor-Reactive T-cells by Co-culture of Peripheral Blood Lymphocytes and Tumor Organoids. *Cell*. 2018;174(6):1586-98 e12.
37. Jaime-Sanchez P, Uranga-Murillo I, Aguilo N, et al. Cell death induced by cytotoxic CD8(+) T-cells is immunogenic and primes caspase-3-dependent spread immunity against endogenous tumor antigens. *J Immunother Cancer*. 2020;8(1).
38. Minute L, Teixeira A, Sanchez-Paulete AR, et al. Cellular cytotoxicity is a form of immunogenic cell death. *J Immunother Cancer*. 2020;8(1).

CHAPTER 8



NEDERLANDSE SAMENVATTING

HOOFDSTUK 8

Het overkoepelende doel van deze dissertatie was om de behandeling van kanker te verbeteren door middel van manipulatie van het immuun systeem. Er zijn verschillende manieren onderzocht, en die worden hieronder besproken.

Een van de manieren om gebruik te maken van het immuunsysteem om tumorgroei te controleren, is stimulatie van anti-tumor T-cellen middels zogenoemde "immune checkpoint inhibitors" (ICPI) of "immune checkpoint stimulators" (ICPS). ICPIs blokkeren remmende receptoren op T-cellen, terwijl ICPS stimulerende receptoren op T-cellen activeren. In **hoofdstuk 2** vonden we een toegenomen aantal cytotoxische T-cellen, antigen presenterende cellen en inhiberende receptoren op intra-tumorale T-cellen in "mismatch repair" (MMR)-proficiënte levermetastasen van colorectaal carcinoom (LM-CRC), dit kan betekenen dat de intra-tumorale T-cellen van MMR-proficiënte LM-CRC gevoeliger zijn voor ICPI in vergelijking met MMR-proficiënte primair colorectaal carcinoom (CRC). Blokkering van de inhiberende receptoren "lymphocyte-activation gene 3 (LAG3) en "programmed death-ligand 1" (PD-L1) bevorderden beide de *ex vivo* capaciteiten van intra-tumorale T-cellen van MMR-proficiënte LM-CRC. Deze twee pathways zijn van potentieel belang in immuno-therapeutische behandeling van LM-CRC. Klinische studies moeten uitwijzen of deze hypothese correct is. In **hoofdstuk 3**, in een proof-of-concept studie, werd gevonden dat het Biclonaal antilichaam CD137xPD-L1 in staat is om proliferatie en cytokine productie van humane intra-tumorale T-cellen te stimuleren. De CD137 arm op zichzelf was niet in staat om intra-tumorale T-cellen te stimuleren. De PD-L1 arm is nodig voor effectiviteit en zorgt, voor specificiteit en concentratie van het antilichaam ter plaatse van de tumor, waar PD-L1 is opgereguleerd.

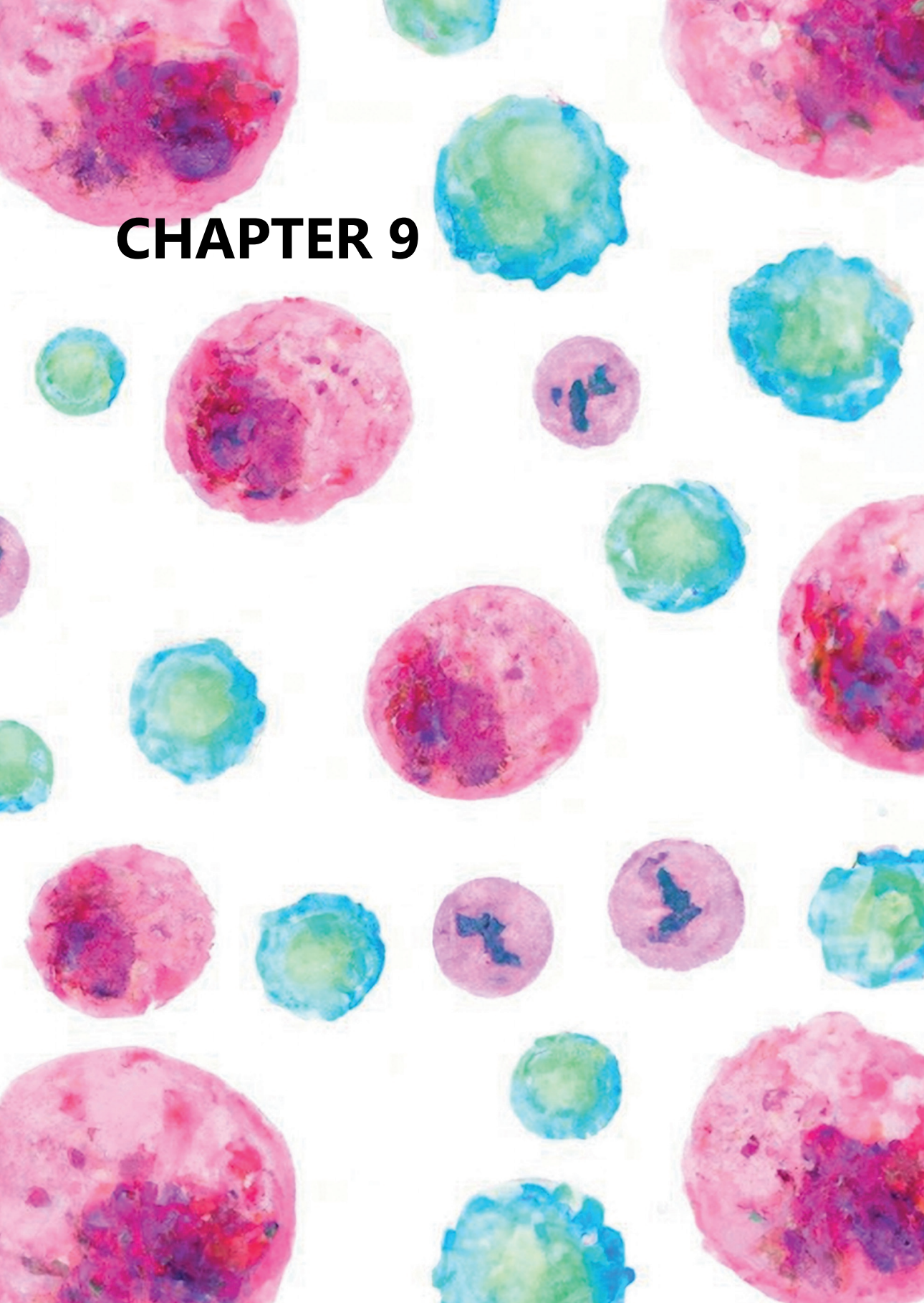
Een tweede aanpak is om de systemische anti-tumor T-cel respons te stimuleren. Een van de manieren om dit te doen is middels vaccinatie, hiervoor is het nodig om antigenen te identificeren die selectief in de tumor tot expressie komen en niet in andere gezonde weefsels. Zo wordt auto-immuniteit voorkomen en kunnen potente anti-tumor T-cellen worden gegenereerd, aangezien T-cel receptoren voor zelf-antigenen negatief worden geselecteerd in de thymus. In **hoofdstuk 4** werd een panel van 12 zogenoemde tumor-antigenen samengesteld, deze tumor-antigenen komen tot expressie in tumoren van bijna 80% van de hepatocellulair carcinoom (HCC) patiënten. Tegen onze verwachting in, werden deze tumor-antigenen ook gevonden in tumor vrije levers van deze patiënten. Patiënten met expressie van tumor-antigenen in de macroscopisch tumor vrije lever hadden vaker terugkeer van kanker na een met opzet curatieve resectie en overleden ook vaker ten gevolge van HCC. Dit insinueert dat expressie van deze tumor-antigenen in tumor vrije lever is een indicatie van de aanwezigheid van micro-metastasen. Hiervan kan gebruik gemaakt worden voor het selecteren van patiënten die in aanmerking zouden moeten komen voor adjuvante therapie, middels immuuntherapie gericht op deze tumor-antigenen, andere (immuun)therapeutische strategieën, of een combinatie hiervan.

Vervolgens hebben we in **hoofdstuk 5** laten zien dat de tumor-antigenen geïdentificeerd in **hoofdstuk 4** immunogeen zijn. We hebben proliferatie van helper en cytotoxische T-cellen, humorale responsen en cytokine productie in respons op deze tumor-antigenen aangetoond. Vaccins gebaseerd op deze tumor-antigenen zouden dus pre-existente tumor-specifieke immuniteit kunnen boosten, en zo mogelijk de

micro-metastasen benoemd in **hoofdstuk 4** bestrijden, of therapeutische effectiviteit van ICPI in HCC patiënten verbeteren.

Een andere manier om de effectiviteit van therapeutische kanker vaccinaties (of systemische anti-tumor immuun responsen in het algemeen) kan worden verbeterd door immuunsuppressie te verminderen. In **hoofdstuk 6** werd het effect van lage-dosis cyclophosphamide op circulerende aantallen regulatoire T-cellen geëvalueerd. De patiënten geïncludeerd in deze studie werden behandeld middels zowel dendritische cel therapie en lage-dosis cyclophosphamide. De overleving van de patiënten leek verbeterd, de frequentie circulerende regulatoire T-cellen nam af en een adaptieve immuun respons werd geïnduceerd. De lage-dosis cyclophosphamide leek een toegevoegd effect te hebben op de overleving en immuun respons in vergelijking met dendritische cel therapie alleen. Met name patiënten met een hoge frequentie van een specifieke subset regulatoire T-cellen (nTregs) leken voordeel te hebben van deze therapie. De effectiviteit van deze therapie kan mogelijk nog verder worden verbeterd door combinatie met bijvoorbeeld ICPI of ICPS.

CHAPTER 9



APPENDICES

Abbreviations

Word of thanks

List of Publications

PhD Portfolio

Curriculum Vitae

The background of the page is a white surface covered with numerous watercolor-style circular shapes. These shapes are scattered across the page and vary in size. The colors used are primarily shades of pink, light blue, and light green. Some of the larger pink circles have darker, more saturated purple or magenta areas in the center, giving them a textured, layered appearance. The blue and green circles are more uniform in color but also show some soft, blended edges characteristic of watercolor painting. The overall effect is a soft, artistic, and somewhat abstract pattern.

CHAPTER 9

ABBREVIATIONS

7AAD	7-aminoactinomycin D
Ab	Antibody
AFP	Alpha-fetoprotein
APC	Antigen-presenting cell
aTh	Activated T helper cell
aTreg	Activated regulatory T cell
BCLC	Barcelona clinic liver cancer
BSA	Bovine serum albumin
BSC	Best supportive care
BTLA	B and T lymphocyte attenuator
CAGE1	Cancer antigen 1
CCL20	MIP3a
CCR7	C-C chemokine receptor 7
CD134	OX40
CD137	4-1BB
CD40L	CD40 ligand
CEA	Carcinoembryonic antigen
CFSE	Carboxyfluorescein succinimidyl ester
CI	Confidence interval
CM	Central memory
CMV	Cytomegalovirus
CpG ODN	CpG oligodeoxynucleotides
CRC	Colorectal carcinoma
CT	Computed tomography
CT47A1	Cancer/testis antigen family 47 member A1
CTA	Cancer testis antigen
CTAG1B	Cancer/testis antigen 1B
CTL	Cytotoxic T lymphocytes
CTLA-4	Cytotoxic T-lymphocyte-associated protein-4
CXCL10	IP10
Cyp-B	Cyclophorin B
DC	Dendritic cell
DTH	Delayed type hypersensitivity
EDTA	Ethylenediaminetetraacetic acid
eGFP	Enhanced green fluorescent protein
ELISA	Enzyme-linked immunosorbent assay
EM	Effector memory
FCS	Fetal calf serum
FDA	Food and Drug administration
FFPE	Formalin-fixed paraffin-embedded
GITR	Glucocorticoid-induced TNFR-related protein
GM-CSF	Granulocyte-macrophage colony-stimulating factor
GPC3	Glypican3
GrB	Granzyme B

HBsAg	Hepatitis B surface antigen
HBV	Hepatitis B virus
HCC	Hepatocellular carcinoma
HLA	Human leukocyte antigens
HNSCC	Head and neck squamous cell carcinoma
HPA	Human protein atlas
HPV	Human papilloma virus
HR	Hazard ratio
hTERT	Human telomerase reverse transcriptase
IBD	Inflammatory bowel disease
ICPI	Immune checkpoint inhibition
IDO	Indoleamine 2,3-dioxygenase
IFN- γ	Interferon gamma
Ig	Immunoglobulin
IHC	Immunohistochemistry
IL	Interleukin
IMDM	Isocove's modified Dulbecco's medium
LAG3	Lymphocyte-activation gene 3
LM-CRC	Liver metastasis of colorectal carcinoma
mAb	Monoclonal antibody
MAGE	Melanoma associated antigen
mCTX	metronomic cyclophosphamide
mDC	myeloid dendritic cell
MDSC	Myeloid derived suppressor cell
MEM NEAA	Minimum essential medium non-essential amino acids
MFI	mean fluorescence intensity
MHC	Major histocompatibility complex
MMR	Mismatch repair
MPM	Malignant pleural mesothelioma
mRNA	Messenger ribonucleic acid
MRP3	Multiresistance protein 3
NASH	Non-alcoholic steatohepatitis
NCD	non-communicable disease
NK	Natural killer
NSCLC	Non-small cell lung cancer
nTreg	Naïve regulatory T cell
NY-ESO-1	New York esophageal squamous cell carcinoma 1
OD	Optical density
P/D	Pleurectomy/decortication
PAGE1	PAGE family member 1
PALGA	Dutch nationwide pathology archives
PAP	Prostate acid phosphatase
PBMC	Peripheral blood mononuclear cells
PBS	Phosphate-buffered saline

PCR	Polymerase chain reaction
PD-1	Programmed death receptor 1
PD-L1	Programmed death ligand 1
PD-L2	Programmed death ligand 2
PM-CRC	Peritoneal metastasis of colorectal carcinoma
RCC	Renal cell carcinoma
RFA	Radiofrequency ablation
RNA	ribonucleic acid
RNF17	Ring finger protein 17
RNF43	Ring finger protein 43
RSV	Respiratory syncytial virus
RT	Room temperature
SART	Squamous cell carcinoma antigen recognized by T cells
SEB	Staphylococcal endotoxin B
SLCO6A1	Solute carrier organic anion transporter family member 6A1
SLP	synthetic long peptide
SSX2	Synovial sarcoma, X breakpoint 2
TAA	Tumor-associated antigen
TACE	Transarterial chemo-embolization
TCR	T-cell receptor
TEMRA	Effector memory T-cells re-expressing CD45RA
TFL	Tumor-free liver
Th	T helper
TIL	Tumor-infiltrating lymphocytes
TIM3	T-cell immunoglobulin and mucin-domain containing 3
TLR	Toll-like receptor
TMA	Tissue microarray
TMB	Tumor mutational burden
TME	Tumor microenvironment
TNF	Tumor necrosis factor
TNFR	Tumor necrosis factor receptor
TOMM34	Translocase of outer mitochondrial membrane 34
Treg	Regulatory T cell
TSPY1	Testis-specific Y-encoded protein 1
VEGF(R)	Vascular endothelial growth factor (receptor)
WT1	Wilms tumor protein



CHAPTER 9
WORD OF THANKS

Dear supervisors, committee members,
colleagues, collaborators, roomies, family, friends
and Anton,

In the past few years, I have been working
with wonderful people, without whom this thesis
would not have been the same. Words cannot
express my gratitude for your help during my
PhD. From guidance and feedback, to providing me
with your knowledge, expertise, materials and
sometimes much needed mental support. You made
the late nights and weekends processing patient
materials significantly more fun and without
you the endless PCRs would have been even
more endless.

I had an unforgettable time, thanks to the
ramen quest (we found a winner 😊), sushi
nights, coffee and high tea dates, Halloween
parties, the Oktoberfest, Mario Party,

Bonaparte (& sourz), pub quizzes, and many other dinner parties and nights out, which kept my spirits high!

This endeavor would not have been possible without all of you, thank you!!

- Lisanne

The background of the page is a white surface decorated with numerous watercolor-style circular shapes. These shapes are scattered across the page and vary in size. The colors used are primarily shades of pink, light blue, and light green. Some of the larger pink circles have darker, more saturated areas of purple and red, giving them a textured, layered appearance. The blue and green circles are more uniform in color but also show some soft, blended edges characteristic of watercolor painting.

CHAPTER 9

LIST OF PUBLICATIONS

Noordam L, de Beijer MTA, Mancham S, Vogler I, Boor PPC, de Ruiter V, Luijten R, IJzermans JNM, Sahin U, Bruno MJ, Sprengers D, Buschow SI*, Kwekkeboom J*. Systemic T-cell and humoral responses against cancer testis antigens in hepatocellular carcinoma patients. *Oncoimmunology*. 2022 Oct 5; 11(1): 2131096.

Duizendstra AA, van der Grift MV, Boor PPC, **Noordam L**, de Knecht RJ, Peppelenbosch MP, Betjes MGH, Litjens NHR, Kwekkeboom J. Current tolerance-associated peripheral blood gene expression profiles after liver transplantation are influenced by immunosuppressive drugs and prior cytomegalovirus infection. *Frontiers Immunology*. 2022 Jan 11;12:738837.

Xu Y*, Carrascosa LC*, Yeung YA, Chu ML, Yang W, Djuretic I, Pappas DC, Zeytounian J, Ge Z, de Ruiter V, Starbeck-Miller GR, Patterson J, Rigas D, Chen SH, Kraynov E, Boor PP, **Noordam L**, Doukas M, Tsao D, IJzermans JN, Guo J, Grünhagen DJ, Erdmann J, Verheij J, van Royen ME, Doornebosch PG, Feldman R, Park T, Mahmoudi S, Dorywalska M, Ni I, Chin SM, Mistry T, Mosyak L, Lin L, Ching KA, Lindquist KC, Ji C, Londono LM, Kuang B, Rickert R, Kwekkeboom J, Sprengers D, Huang TH, Chaparro-Riggers J. An Engineered IL15 Cytokine Mutein Fused to an Anti-PD1 Improves Intratumoral T-cell Function and Antitumor Immunity. *Cancer Immunol Res*. 2021 Oct;9(10):1141-1157. doi: 10.1158/2326-6066.CIR-21-0058. Epub 2021 Aug 10.

Noordam L, Ge Z, Öztürk H, Doukas M, Mancham S, Boor PPC, Campos Carrascosa L, Zhou G, van den Bosch TPP, Pan Q, IJzermans JNM, Bruno MJ, Sprengers D, Kwekkeboom J. Expression of Cancer Testis Antigens in Tumor-Adjacent Normal Liver Is Associated with Post-Resection Recurrence of Hepatocellular Carcinoma. *Cancers (Basel)*. 2021 May 20;13(10):2499. doi: 10.3390/cancers13102499.

Ge Z, Helmijr JCA, Jansen MPH, Boor PPC, **Noordam L**, Peppelenbosch M, Kwekkeboom J, Kraan J, Sprengers D. Detection of oncogenic mutations in paired circulating tumor DNA and circulating tumor cells in patients with hepatocellular carcinoma. *Transl Oncol*. 2021 Jul;14(7):101073. doi: 10.1016/j.tranon.2021.101073. Epub 2021 Apr 26.

Ge Z, Zhou G, Campos Carrascosa L, Gausvik E, Boor PPC, **Noordam L**, Doukas M, Polak WG, Terkivatan T, Pan Q, Takkenberg RB, Verheij J, Erdmann JI, IJzermans JNM, Peppelenbosch MP, Kraan J, Kwekkeboom J, Sprengers D. TIGIT and PD1 Co-blockade Restores ex vivo Functions of Human Tumor-Infiltrating CD8+ T Cells in Hepatocellular Carcinoma. *Cell Mol Gastroenterol Hepatol*. 2021;12(2):443-464. doi: 10.1016/j.jcmgh.2021.03.003. Epub 2021 Mar 27.

Zhang R, **Noordam L**, Ou X, Ma B, Li Y, Das P, Shi S, Liu J, Wang L, Li P, Verstegen MMA, Reddy DS, van der Laan LJW, Peppelenbosch MP, Kwekkeboom J, Smits R, Pan Q. The biological process of lysine-tRNA charging is therapeutically targetable in liver cancer. *Liver Int*. 2021 Jan;41(1):206-219. doi: 10.1111/liv.14692. Epub 2020 Oct 20.

Liu J, Li P, Wang L, Li M, Ge Z, **Noordam L**, Lieshout R, Verstegen MMA, Ma B, Su J, Yang Q, Zhang R, Zhou G, Carrascosa LC, Sprengers D, IJzermans JNM, Smits R, Kwekkeboom J, van der Laan LJW, Peppelenbosch MP, Pan Q, Cao W. Cancer-Associated Fibroblasts Provide a Stromal Niche for Liver Cancer Organoids That Confers Trophic Effects and Therapy Resistance. *Cell Mol Gastroenterol Hepatol*. 2021;11(2):407-431. doi: 10.1016/j.jcmgh.2020.09.003. Epub 2020 Sep 12.

Campos Carrascosa L, van Beek AA, de Ruiter V, Doukas M, Wei J, Fisher RS, Ching K, Yang W, van Loon K, Poor PPC, Rakke YS, **Noordam L**, Doorneboch P, Grunhagen D, Verhoef K, Polak WG, IJzermans JNM, Ni I, Yeung YA, Salek-Ardakani S, Sprengers D, Kwekkeboom J. FcγRIIB engagement drives agonistic activity of Fc-engineered αOX40 antibody to stimulate human tumor-infiltrating T cells. *J Immunother Cancer*. 2020 Sep;8(2):e000816.

Cao W, Li M*, Liu J*, Zhang S, **Noordam L**, Verstegen MMA, Wang L, Ma B, Li S, Wang W, Bolkestein M, Doukas M, Chen K, Ma Z, Bruno M, Sprengers D, Kwekkeboom J, van der Laan LJW, Smits R, Peppelenbosch MP, Pan Q. LGR5 marks targetable tumor-initiating cells in mouse liver cancer. *Nat Commun*. 2020 Apr 23;11(1):1961. doi: 10.1038/s41467-020-15846-0.

Zhou G, Sprengers D, Mancham S, Erkens R, Boor PPC, van Beek AA, Doukas M, **Noordam L**, Campos Carrascosa L, de Ruiter V, van Leeuwen RWF, Polak WG, de Jonge J, Groot Koerkamp B, van Rosmalen B, van Gulik TM, Verheij J, IJzermans JNM, Bruno MJ, Kwekkeboom J. Reduction of immunosuppressive tumor microenvironment in cholangiocarcinoma by ex vivo targeting immune checkpoint molecules. *J Hepatol*. 2019 Oct;71(4):753-762. doi: 10.1016/j.jhep.2019.05.026. Epub 2019 Jun 11.

van Beek AA, Zhou G, Doukas M, Boor PPC, **Noordam L**, Mancham S, Campos Carrascosa L, van der Heide-Mulder M, Polak WG, IJzermans JNM, Pan Q, Heirman C, Mahne A, Bucktrout SL, Bruno MJ, Sprengers D, Kwekkeboom J. GITR ligation enhances functionality of tumor-infiltrating T cells in hepatocellular carcinoma. *Int J Cancer*. 2019 Aug 15;145(4):1111-1124. doi: 10.1002/ijc.32181. Epub 2019 Feb 27.

Noordam L, Kwekkeboom J, de Man RA, Sprengers D. Immunotherapie en het hepatocellulair carcinoom. *Ned Tijdschr Oncol*, Sept 2018, Vol. 15, No. 6: 210–17

Noordam L, Kaijen MEH, Bezemer K, Cornelissen R, Maat LAPWM, Hoogsteden HC, Aerts JGJV, Hendriks RW, Hegmans JPJJ, Vroman H. Low-dose cyclophosphamide depletes circulating naïve and activated regulatory T cells in malignant pleural mesothelioma patients synergistically treated with dendritic cell-based immunotherapy. *Oncoimmunology*. 2018 Jul 30;7(12):e1474318. doi: 10.1080/2162402X.2018.1474318. eCollection 2018.

Zhou G, **Noordam L**, Sprengers D, Doukas M, Boor PPC, van Beek AA, Erkens R, Mancham S, Grünhagen D, Menon AG, Lange JF, Burger PJWA, Brandt A, Galjart B, Verhoef C, Kwekkeboom J, Bruno MJ. Blockade of LAG3 enhances responses of tumor-infiltrating T cells in mismatch repair-proficient liver metastases of colorectal cancer. *Oncoimmunology*. 2018 Apr 25;7(7):e1448332. doi: 10.1080/2162402X.2018.1448332. eCollection 2018.

*These authors contributed equally to this work

The background of the page is a white surface covered with numerous watercolor-style circular shapes. These shapes are rendered in various shades of pink, magenta, blue, and green, with some overlapping and blending into each other. The colors are soft and painterly, creating a textured, artistic effect. The shapes vary in size and are scattered across the page, with some appearing more prominent than others.

CHAPTER 9

PHD PORTFOLIO

PhD Candidate: Lisanne Noordam

Erasmus MC Department: Gastroenterology and Hepatology

PhD Period: April 2016 – October 2020

Promotor: Prof. Dr. Marco J. Bruno

Copromotor: Dr. Jaap Kwekkeboom

PhD Training

Seminars

Weekly Gastroenterology and Hepatology Seminars 2016-2020 (Attending: 10,1 ECTS, Presenting: 2,3 ECTS)

Weekly Research Group Meetings 2016-2020 (Attending 10,1 ECTS, Presenting: 5,1 ECTS)

Weely Tumor Immunology Platform 2016-2020 (Attending 10,1 ECTS, Presenting 1,1 ECTS)

Courses and Workshops

Survival Analysis, Erasmus MC, 2016 (0,6 ECTS)

Scientific Integrity, Erasmus MC, 2017 (0,3 ECTS)

BROK (Basic course Rules and Organisation for Clinical Researchers), Erasmus MC, 2017 (1,5 ECTS)

Basic Course on R, Erasmus MC, 2018 (1,1 ECTS)

Basic and Translational Oncology, 2018 (1,8 ECTS)

National & International Scientific Meetings

Dutch Tumor Immunology Meeting, 2017 (0,6 ECTS)

Symposium "Current and Future Perspectives in Primary Liver Tumors", 2017 (0,6 ECTS)

Erasmus MC Cancer Institute Research Day, 2017 – Oral Presentation (1,0 ECTS)

17th CIMT (Cancer Immunotherapy) Annual Meeting, 2019 (0,9 ECTS)

MACS Immuno-Oncology Day, 2020 (0,3 ECTS)

International Liver Congress, 2020 – Oral Presentation (1,2 ECTS)

Honors and Prizes

Full Bursary-Young Investigator Award, EASL, Digital ILC, 2020

Supervising Junior Lab Members

Hadiye Ozturk, Master Student Medicine, Research Internship 2017 (6,0 ECTS)

Thijs Schrama, Master Student Infection & Immunity, Research Internship 2019 (7,4 ECTS)

Memberships

Dutch Society for Immunology (NVVI)

The European Association for the Study of the Liver (EASL)

Nederlandse vereniging voor Hepatologie (NVH)

The background of the page is a white surface covered with numerous watercolor-style circular shapes. These shapes are rendered in shades of pink, magenta, blue, and green, with some overlapping and blending of colors. The shapes vary in size and intensity, creating a vibrant, abstract pattern.

CHAPTER 9

Curriculum Vitae

Lisanne Noordam was born on August 29th 1992 in the Hague, the Netherlands and grew up in 's-Gravenzande. After completing her secondary education at the Interconfessionele Scholengroep Westland in 's-Gravenzande in 2009, she started her Medical degree in 2009 at the Erasmus Medical Center in Rotterdam. During her Bachelor degree, which she obtained in 2012, she started with the Master of Research in Infection & Immunity at the same university. Both her internships for the Research Master were performed at the Department of Pulmonary Medicine in the group of by Dr. Joost Hegmans. In these internships, she studied the adaptive immune cell response after dendritic cell-based immunotherapy combined with low dose cyclophosphamide in advanced malignant pleural mesothelioma patients. This led to the publication of her first paper in 2017 and a Research Master's degree with Honours in August 2016. Simultaneously, she started with the Master of Medicine in 2012, which she completed in April 2016. In April 2016 she started her PhD project under supervision of Dr. Jaap Kwekkeboom and Prof. Dr. Marco Bruno in the Department of Gastroenterology and Hepatology, Erasmus Medical Center Rotterdam. She focused her research on various aspects of cancer immunotherapy. The results of this Phd project are described in this thesis. In October 2020 Lisanne started her residency in Pathology at the Erasmus Medical Center in Rotterdam.



